Biological and Medical Physics, Biomedical Engineering

Sharon Gerecht
Editor

Biophysical Regulation of Vascular Differentiation and Assembly

Springer

Biophysical Regulation of Vascular Differentiation and Assembly

BIOLOGICAL AND MEDICAL PHYSICS, BIOMEDICAL ENGINEERING

The fields of biological and medical physics and biomedical engineering are broad, multidisciplinary and dynamic. They lie at the crossroads of frontier research in physics, biology, chemistry, and medicine. The Biological and Medical Physics, Biomedical Engineering Series is intended to be comprehensive, covering a broad range of topics important to the study of the physical, chemical and biological sciences. Its goal is to provide scientists and engineers with textbooks, monographs, and reference works to address the growing need for information.

Books in the series emphasize established and emergent areas of science includingmolecular,membrane, and mathematical biophysics; photosynthetic energy harvesting and conversion; information processing; physical principles of genetics; sensory communications; automata networks, neural networks, and cellular automata. Equally important will be coverage of applied aspects of biological and medical physics and biomedical engineering such as molecular electronic components and devices, biosensors, medicine, imaging, physical principles of renewable energy production, advanced prostheses, and environmental control and engineering.

For further volumes:
http/www.springer.com/series/3740

Sharon Gerecht
Editor

Biophysical Regulation of Vascular Differentiation and Assembly

Springer

Editor
Sharon Gerecht
Department of Chemical and Biomolecular Engineering
Johns Hopkins Physical Sciences-Oncology Center
Institute for NanoBioTechnology
Johns Hopkins University
Baltimore, MD 21218, USA
gerecht@jhu.edu

ISBN 978-1-4419-7834-9 e-ISBN 978-1-4419-7835-6
DOI 10.1007/978-1-4419-7835-6
Springer New York Dordrecht Heidelberg London

Preface

I am pleased to present this book, *Biophysical Regulation of Vascular Differentiation and Assembly* in the series *Biological and Medical Physics, Biomedical Engineering*.

The ability to grow stem cells in the laboratory and to guide their maturation to functional cells allows us to study the underlying mechanisms that govern vasculature differentiation and assembly in health and disease. Accumulating evidence suggests that early stages of vascular growth are exquisitely tuned by biophysical cues from the microenvironment, yet the scientific understanding of such cellular environments is still in its infancy. Comprehending these processes sufficiently to manipulate them would pave the way to controlling blood vessel growth in therapeutic applications. This book assembles the works and views of experts from various disciplines to provide a unique perspective on how different aspects of microenvironment regulate the differentiation and assembly of the vasculature. In particular, it describes recent efforts to exploit modern engineering techniques to study and manipulate various biophysical cues.

The book opens with a description of the emergence of blood and blood vessels during development; understanding their emergence increases our understanding of postnatal and disease processes (*Sills and Hirschi)*. The following chapters describe the critical role of the three-dimensional extracellular matrix milieu in controlling tube morphogenesis and stabilization (*Davis, Stratman, and Sacharidou*), in directing vascular differentiation of human embryonic stem cells (*Kraehenbuehl, Aday, and Ferreira*), in affecting the intra- and extracellular microrheology of endothelial cells (*Fraley, Hale, Bloom, Celedon, Lee, and Wirtz*), and in modulating blood vessel formation through biophysical cues (*Critser and Yoder*). The book then details the hypoxic regulation of vascular remodeling through the mediation of hypoxia-inducible factor 1 (*Sarkar and Semenza*), in the context of the three-dimensional extracellular matrix during development and regeneration (*Abaci, Hanjaya-Putra, and Gerecht*), and as one of the complex microenvironmental factors in tumor angiogenesis (*Infanger, Pathi, and Fischbach*). The final chapters consider the design of biologically inspired culture systems to control multiple microenvironmental factors during differentiation (*Freytes and Vunjak-Novakovic*), with a focus on understanding the effects of hemodynamic forces and their application to vascular graft engineering (*Diop and Li*).

This book provides an interdisciplinary view of vasculature regulation by various biophysical cues and presents recent advances in measuring and controlling such parameters. I hope it will inspire life scientists, biophysicists, and engineers to pursue unconventional approaches to answering fundamental questions in vascular differentiation and assembly.

I am grateful to all of the authors for their excellent contributions and thank Springer for implementing this project; especially, I want to thank Christopher Coughlin, the publishing editor of the book, for initiating and supporting this project and Ho Ying Fan for his excellent production work.

Baltimore, 2010 Sharon Gerecht

Contents

Contributors

Hasan E. Abaci
Department of Chemical and Biomolecular Engineering, Johns Hopkins University, Baltimore, MD 21218, USA
and
Johns Hopkins Physical Sciences-Oncology Center, Johns Hopkins University, Baltimore, MD 21218, USA
and
Institute for NanoBioTechnology, Johns Hopkins University, Baltimore, MD 21218, USA

Sezin Aday
Department of Chemical Engineering, Massachusetts Institute of Technology, Cambridge, MA 02139, USA
and
Biocant, Centro de Inovação em Biotecnologia, 3060-197 Cantanhede, Portugal;
Center of Neurosciences and Cell Biology,
University of Coimbra, 3004-517, Coimbra, Portugal

Ryan J. Bloom
Department of Chemical and Biomolecular Engineering, The Johns Hopkins University, Baltimore; MD 21218, USA

Alfredo Celedon
Johns Hopkins Physical Sciences-Oncology Center, The Johns Hopkins University, Baltimore, MD 21218, USA
and
Department of Mechanical Engineering, Pontificia Universidad Católica de Chile, P.O. Box 306, Santiago 6904411, Chile

Paul J. Critser
Herman B Wells Center for Pediatric Research, Department of Pediatrics, Indiana University School of Medicine, Indianapolis, IN, USA

George E. Davis
Department of Medical Pharmacology and Physiology,
University of Missouri School of Medicine MA415 Medical Sciences Building,
Columbia; MO 65212, USA
and
Department of Pathology and Anatomical Sciences, University of Missouri
School of Medicine, Columbia, MO 65212, USA
and
Dalton Cardiovascular Sciences Center, Columbia, MO 65212, USA

Rokhaya Diop
Department of Bioengineering, University of California, B108A Stanley Hall,
Berkeley, CA 94720-1762, USA

Lino S. Ferreira
Biocant, Centro de Inovação em Biotecnologia, 3060-197 Cantanhede, Portugal;
Center of Neurosciences and Cell Biology, University of Coimbra, 3004-517
Coimbra, Portugal

Claudia Fischbach
Department of Biomedical Engineering, Cornell University, 157 Weill Hall,
Ithaca, NY 14853, USA

Stephanie I. Fraley
Department of Chemical and Biomolecular Engineering, The Johns Hopkins
University, Baltimore, MD 21218, USA
and
Johns Hopkins Physical Sciences-Oncology Center, The Johns Hopkins University,
Baltimore; MD 21218, USA

Donald O. Freytes
Department of Biomedical Engineering, Columbia University, 622 west 168th Street,
Vanderbilt Clinic, room 12-234, New York, NY 10032, USA

Sharon Gerecht
Department of Chemical and Biomolecular Engineering, Johns Hopkins Physical
Sciences-Oncology Center, Institute for NanoBioTechnology, Johns Hopkins
University, Baltimore, MD 21218, USA

Christopher M. Hale
Department of Chemical and Biomolecular Engineering,
The Johns Hopkins University, Baltimore, MD 21218, USA
and
Johns Hopkins Physical Sciences-Oncology Center, The Johns Hopkins University,
Baltimore, MD 21218, USA

Donny Hanjaya-Putra
Department of Chemical and Biomolecular Engineering, Johns Hopkins University, Baltimore, MD 21218, USA
and
Johns Hopkins Physical Sciences-Oncology Center, Johns Hopkins University, Baltimore, MD 21218, USA
and
Institute for NanoBioTechnology, Johns Hopkins University, Baltimore, MD 21218, USA

Karen K. Hirschi
Interdisciplinary Program in Cell and Molecular Biology, Department of Molecular and Cellular Biology, Baylor College of Medicine, One Baylor Plaza, Rm N1020, Houston, TX 77030, USA
and
Department of Pediatrics, Baylor College of Medicine, Houston, TX 77030, USA
and
Center for Cell and Gene Therapy, Baylor College of Medicine, Houston, TX 77030, USA
and
Children's Nutrition Research Center, Baylor College of Medicine, Houston, TX 77030, USA

David W. Infanger
Department of Biomedical Engineering, Cornell University, 157 Weill Hall, Ithaca, NY 14853, USA

Thomas P. Kraehenbuehl
Department of Chemical Engineering, Massachusetts Institute of Technology, Cambridge, MA 02139, USA

Jerry S.H. Lee
Department of Chemical and Biomolecular Engineering, The Johns Hopkins University, Baltimore, MD 21218, USA
and
Center for Strategic Scientific Initiatives, Office of the Director, National Cancer Institute, National Institutes of Health, Bethesda, MD 20892, USA

Song Li
Department of Bioengineering, University of California, B108A Stanley Hall, Berkeley, CA 94720-1762, USA

Siddharth P. Pathi
Department of Biomedical Engineering, Cornell University, 157 Weill Hall, Ithaca, NY 14853, USA

Anastasia Sacharidou
Department of Medical Pharmacology, University of Missouri
School of Medicine, Columbia, MO 65212, USA
and
Dalton Cardiovascular Sciences Center, University of Missouri
School of Medicine, Columbia, MO 65212, USA

Kakali Sarkar
Vascular Program, Institute for Cell Engineering, The Johns Hopkins University
School of Medicine, 733 North Broadway, Baltimore, MD 21205, USA
and
Department of Medicine, The Johns Hopkins University School of Medicine,
Baltimore, MD, USA

Gregg L. Semenza
Vascular Program, Institute for Cell Engineering, The Johns Hopkins University
School of Medicine, 733 North Broadway, Baltimore, MD 21205, USA
and
Department of Medicine, The Johns Hopkins University School of Medicine,
733 North Broadway, Baltimore, MD 21205 USA
and
McKusick-Nathans Institute of Genetic Medicine, The Johns Hopkins University
School of Medicine, 733 North Broadway, Baltimore, MD 21205 USA
and
Departments of Pediatrics, Oncology, Radiation Oncology, and Biological
Chemistry, The Johns Hopkins University School of Medicine The Johns Hopkins
University School of Medicine, 733 North Broadway, Baltimore, MD 21205, USA

Tiffany M. Sills
Interdisciplinary Program in Cell and Molecular Biology, Department of Molecular
and Cellular Biology, Baylor College of Medicine, One Baylor Plaza, Rm N1020,
Houston, TX 77030, USA
and
Department of Pediatrics, Baylor College of Medicine, Houston, TX 77030, USA
and
Center for Cell and Gene Therapy,Baylor College of Medicine,
Houston, TX 77030, USA
and
Children's Nutrition Research Center, Baylor College of Medicine,
Houston, TX 77030, USA

Amber N. Stratman
Department of Medical Pharmacology, University of Missouri School of Medicine,
Columbia, MO 65212, USA
and
Dalton Cardiovascular Sciences Center, University of Missouri School of Medicine,
Columbia, MO 65212, USA

Gordana Vunjak-Novakovic
Department of Biomedical Engineering, Columbia University,
622 west 168th Street, Vanderbilt Clinic, Room 12-234, New York,
NY 10032, USA

Denis Wirtz
Department of Chemical and Biomolecular Engineering, The Johns Hopkins University, Baltimore, MD 21218, USA
and
Johns Hopkins Physical Sciences-Oncology Center, The Johns Hopkins University, Baltimore, MD 21218, USA

Mervin C. Yoder
Department of Pediatrics, Indiana University School of Medicine,
1044 West Walnut Street, R4-W125A, Indianapolis, IN, 46202, USA
and
Herman B Wells Center for Pediatric Research, Indiana University School of Medicine, Indianapolis, IN, USA
and
Department of Biochemistry and Molecular Biology, Indiana University School of Medicine, Indianapolis, IN, USA

Chapter 1
The Emergence of Blood and Blood Vessels in the Embryo and Its Relevance to Postnatal Biology and Disease

Tiffany M. Sills and Karen K. Hirschi

1.1 Introduction

Emergence of vascular endothelial cells and blood cells occurs within a similar time frame in mammals, and the vascular and hematopoietic systems continue to develop in parallel throughout embryogenesis. There are several specialized centers of hematopoietic activity in the developing embryo, including the yolk sac, aorta-gonad-mesonephros (AGM) region, fetal liver, and fetal bone marrow (where hematopoietic activity persists after birth). Elegant in vivo experiments and localization studies have shown that specialized endothelial cells residing within the yolk sac and AGM have the ability to give rise to (and/or support the maturation of) hematopoietic stem cells (HSC) and hematopoietic progenitors (HP). Whether similar vascular microenvironments (niches) exist within fetal liver and fetal bone marrow remains to be defined; however, sinusoidal endothelium within adult bone marrow is known to similarly support HSC/HP activity. Other recent studies in embryonic stem cell models (mouse and human) have further demonstrated that endothelial cells function as precursors of HSC/HP in vitro. All of these observations collectively confirm the century-old speculation of the existence of hemogenic endothelial cells and their pivotal role in hematopoiesis. It remains critical to define the phenotype and regulation of the subset of specialized vascular endothelium with hemogenic function within the embryo, and determine whether an adult counterpart exists. It would also be imperative to determine the relationship of the putative postnatal hemogenic endothelial cells to vascular and hematopoietic progenitors in the adult, and investigate whether postnatal blood and vascular disease states are mediated by aberrant hemogenic endothelial cell function. Only in so doing, can we then determine the usefulness of hemogenic endothelial cells in therapeutic applications.

K.K. Hirschi (✉)
Interdisciplinary Program in Cell and Molecular Biology, Departments of Pediatrics and of Molecular and Cellular Biology, Center for Cell and Gene Therapy and Children's Nutrition Research Center, Baylor College of Medicine, One Baylor Plaza, Room N1020, Houston, TX 77030, USA
e-mail: khirschi@bcm.tmc.edu

S. Gerecht (ed.), *Biophysical Regulation of Vascular Differentiation and Assembly*, Biological and Medical Physics, Biomedical Engineering,
DOI 10.1007/978-1-4419-7835-6_1,

1.2 Concepts in Development of Blood and Blood Vessels

In mammals, the development of blood and blood vessels is highly interdependent. Genetic manipulation studies in multiple model systems have revealed that blood does not form in the absence of vasculature [1, 2], and the vasculature does not remodel in the absence of blood circulation [3]. Interestingly, the biomechanical forces exerted by blood circulation upon the onset of cardiovascular function also regulate developmental hematopoiesis [4]. In addition to the concurrent developmental timelines of these systems, blood and blood vessels work in concert to deliver oxygen and nutrients, remove metabolic waste, and distribute circulating effectors and cells to all tissues of the developing organism. In order to more fully understand the dependency of one system on the other, we first briefly overview the development of each system separately and then discuss a putative cellular link between the two, via hemogenic endothelium, with a focus on development in the mouse model system.

1.2.1 Embryonic Vasculogenesis

Embryonic vasculogenesis is the de novo differentiation of endothelial cells and formation of blood vessels within the developing yolk sac and embryo. After gastrulation in the murine yolk sac, the visceral endoderm induces adjacent mesodermal progenitors to differentiate into endothelial cells, which first emerge in blood islands at E7.25 near the placental cone. Newly formed endothelial cells coalesce to form the primary vascular plexus, which is established throughout the entire yolk sac tissue by E8.0. Over the next 36 h (until E9.5), the yolk sac plexus is remodeled into a differentiated vascular network by both molecular signaling and hemodynamic forces generated at the onset of cardiac function, which begins ~E8.25 (7–8 somites). Vasculogenesis also occurs within the embryo proper, leading to the formation of early vessels including the paired dorsal aorta by E8.0, which fuse by E9.0 to supply the backbone for angiogenic sprouting and branching of most of the remaining major embryonic vessels. The embryonic vitelline and umbilical vessels also develop concurrently with the aorta and connect to the yolk sac and placenta, respectively. Throughout gestation such early vessels will remodel by angiogenic sprouting and pruning, while also connecting to vasculogenic regions of new vessel formation.

Remodeling of the vascular network also involves "specification" (or specialization) of primordial (or primitive) endothelial cells into phenotypically and functionally distinct endothelial cells that line arterial, venous, and lymphatic vessels. While VEGF-A signaling is required for global vascular development, it appears that VEGF-A-induced Notch signaling promotes arterial specification, and the orphan nuclear receptor COUP-TFII acts to negatively regulate Notch function in presumptive venous endothelial cells. In fact, loss of COUP-TFII results in venous structures

acquiring arterial-like properties including expression of components of the Notch signaling pathway and appearance of hematopoietic cell clusters in vessel lumens [5]. The homeobox gene Prox1 has been shown to be required for both initiation and maintenance of lymphatic vessel endothelial cells, which arise from a subset of the venous endothelium [6–8]. Other factors and pathways involved in arterial/venous/lymphatic specification include angiopoietin and the hedgehog signaling pathway, which function coordinately to control the endothelial cell migration and cell–cell association (reviewed in detail in [9]). Sufficient evidence has established that physiologic influences secondary to blood flow also play a role in the final composition of blood vessels within the circulatory system (reviewed recently in [10]). Furthermore, studies of the ligand/receptor pair ephrin-B2 and Eph-B4 suggest that there may be some genetic determination of arterial/venous specification prior to angiogenesis [11]. Thus, subsets of endothelium could, in fact, be specified genetically prior to extrinsic signaling, perhaps even shaping their locations within the developing vascular plexus.

Another type of endothelium that is formed during embryonic vascular remodeling is hemogenic endothelium that has the capacity to give rise to multilineage blood cell progenitors and contribute to definitive hematopoiesis. Whether hemogenic endothelium is genetically "predetermined," or specialized in response to soluble and mechanical factors is not yet clearly defined. This population of cells, and its relevance to hematopoiesis in the embryo and adult, is further discussed later in this chapter.

1.2.2 Embryonic Hematopoiesis

The formation of blood, or hematopoiesis, is a critical process during embryogenesis and throughout postnatal life, as is vasculogenesis. During mammalian development, hematopoiesis occurs in two distinctly different stages, termed primitive and definitive hematopoiesis (timeline summarized in Fig. 1.1). In mice, the first wave of primitive hematopoiesis occurs ~E7.25 when primitive (nucleated) erythroblasts arise in blood islands of the yolk sac in close proximity to primordial (nonspecialized) endothelial cells. The second wave of blood formation in the developing embryo, definitive hematopoiesis, leads to the formation of all cell types of the blood lineage (erythroid, myeloid, and lymphoid). The generation of multilineage progenitors occurs in the extraembryonic yolk sac at ~E8.25 [12–14] and within several intraembryonic tissues, the first of which is the AGM region beginning at ~E10.5 [13, 15, 16].

In the AGM, emergence of clusters of blood cells within the lumen of the aorta marks the initiation of hematopoietic activity in this area. Further examination reveals that the emerging intra-aortic cell clusters are bound by tight junctions to the underlying endothelium [17, 18]. These AGM-derived HSC/HP are proposed to then seed and proliferate in the fetal liver at ~E14.5 before taking up residence in fetal bone marrow at ~E17.5. Whether multilineage HSC/PC emerge independently

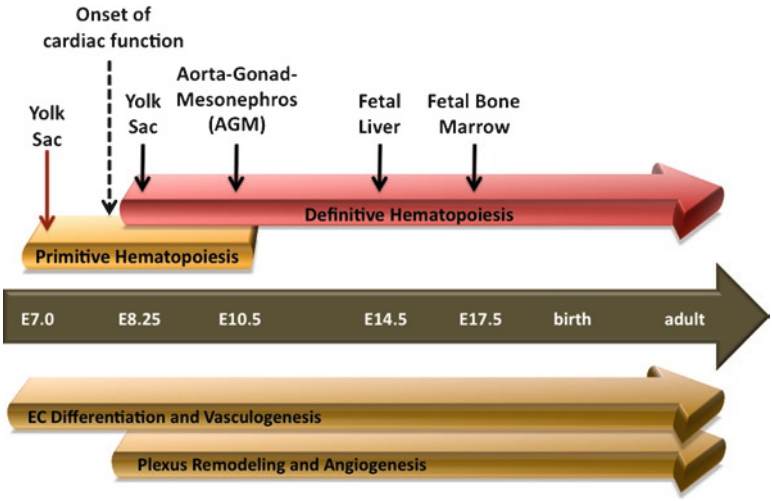

Fig. 1.1 Timeline reflecting the parallel development of endothelium and blood at the major sites of hematopoietic activity in the developing murine embryo. *Mustard bar* and *red arrow* above timeline represent the two waves of hematopoiesis during embryonic development, while *copper arrows* below represent primary vascular phenomena. Spatial locations of all phenomena are denoted by *black arrows*, and *dotted arrow* indicates initiation of cardiac function in the murine embryo

within fetal liver and bone marrow, and perhaps from hemogenic endothelium, is not yet known. It is well documented, however, that quiescent HSC reside predominantly within bone marrow postnatally, and various physiologic, pathologic, and pharmacologic events induce a cycling (proliferative) phenotype that gives rise to all blood lineages throughout postnatal life.

1.2.3 Historical Observations of the Lineage Relationship of Endothelium and Blood

The lineage connection between blood and endothelial cells during embryonic development has been heavily debated for more than 100 years. Their coincident temporal and physical emergence during embryogenesis has led to two hypotheses: (1) blood cells arise from specialized (hemogenic) endothelial cells and (2) blood and endothelial cells arise from the same progenitor, referred to as a "hemangioblast." We will briefly recount the historical observations that led to these hypotheses and review the current evidence for each in the field.

Seminal work by Florence Sabin in the 1920s [19], studying the chick yolk sac, describes blood islands as structures in which hematopoietic cells are anchored to, and derived from, surrounding endothelium. Specifically, she wrote:

> Red blood-corpuscles can be seen to grow from the endothelial lining of blood-vessels. They may develop from little masses of the original angioblasts, which become partially separated by the liquefaction of cytoplasm around them. Such a mass of cells becomes a blood-island by having haemoglobin develop within the cells. The color of haemoglobin can be detected in the living cells earlier than I have been able to fix and stain it. Again an endothelial cell of a blood-vessel will divide so that one daughter cell projects into the lumen. This cell becomes filled with basophilic granules and develops haemoglobin. It is then a unicellular blood-island. It divides and the mass is increased also by the addition of other cells, which differentiate from the endothelium in the neighborhood and creep along the wall to join the first cell. These cells soon form a yellow syncytial mass projecting into the lumen of the vessel. At this stage the islands have a smooth, sharp contour. As they develop, cells begin to round up on their surface until the whole mass comes to look like a mulberry and then the red cells break free from the mass and float away in the blood-plasma [19].

Soon afterwards, observations by others including P.D.F. Murray in 1932 [20] spawned the definition of the "hemangioblast," a progenitor cell with the capability to give rise to both endothelial and HSC. This describes a separate, distinct phenomenon of a grouping of progenitor cells where those along the periphery become primitive endothelial cells and the inner cells remain free to differentiate into primitive blood. In attempting to clarify the differences among angioblasts, blood islands, and hemangioblasts, he wrote the following:

> The "angioblasts" are masses of cells or single cells formed from the mesenchyme, from which develop the endothelial vessels containing plasma and the blood islands; the blood islands proper are the groups of cells or single cells derived directly from the "angioblasts," which persist attached to the endothelial walls, and whose component cells, when separated from one another by the dissolution of the blood islands, become the primitive blood cells. Such a distinction is justified, for "angioblasts" and blood islands are two distinct developmental stages differing from one another in prospective significance and in structural relationships. To "angioblast," however, I prefer the term "haemangioblast." This expresses the fact that both endothelium and blood develop from the solid mass, whereas the term "angioblast" strictly refers only to the vessels, i.e., to the endothelium [20].

Even in this instance, Murray describes a "hemangioblast" as a tissue mass that gives rise to both endothelium and blood, not necessarily a progenitor that generates two distinct lineages, hematopoietic and endothelial cells. However, by the 1980s, the term "hemangioblast" had come to be used to describe such a bipotent cell, which was presumed to be generated in the primitive streak and exist transiently for establishment of the blood and vascular systems. While there is some evidence for a multipotent Brachyury^{+}Flk-1^{+} progenitor involved in primitive hematopoiesis in the yolk sac, indirect tracking of this cell type reveals that it also generates vascular smooth muscle cells therein [21]; thus, it is not truly bipotent. Furthermore, there remains minimal data supporting a direct role for this type of cell in intraembryonic definitive hematopoiesis [21, 22]. In contrast, there is evidence that endothelial and hematopoietic cell lineages are independently fated during gastrulation, even during primitive hematopoiesis in the yolk sac [23].

Regardless of this debate, which appears to be relevant to only primitive hematopoiesis, it is now generally accepted that definitive blood cells arise from hemogenic endothelium, and that even "hemangioblast-derived" blood cells are

produced via an endothelial-intermediate [24]. Therefore, definitive hematopoiesis cannot occur in the absence of proper vascular development, which is why there is no generation of definitive blood cells in experimental animal models with defective endothelial cell development [1, 2].

1.3 Review of Hemogenic Endothelium Function During Embryogenesis

1.3.1 Yolk Sac

The embryonic yolk sac is the first site of definitive hematopoiesis. It has been extensively studied with regard to early development of both endothelial and blood cells due to its structural simplicity, accessibility for dynamic imaging, and ease of cell isolation there from, relative to the embryo proper. Previous work in our laboratory, exploiting the Hoechst dye-efflux property (side population or SP phenotype) attributed to adult bone marrow HSC, revealed that hemogenic endothelial cells also exhibit dye-efflux properties relative to non-blood-forming endothelial cells within the developing embryo, presumably due to overexpression of multidrug-resistant pumps such as ABCG2 [25, 26]. We further characterized these cells phenotypically by fluorescence-activated cell sorting (FACS) analysis and functionally on a clonal level using in vitro assays, and found them to be Flk-1^{+}cKit^{+}CD31^{+}VE-Cad$^{+/-}$CD45^{-} SP cells [14, 27]. We also found that retinoic acid signaling is critical for their specification [14].

Other groups have shown that expression of CD41, an earlier marker of hematopoietic potential than CD45, is restricted to intraluminal cells in yolk sack vascular channels. Using Tie2, Flk1/VEGFR2, and CD41 to discriminate different cell types, it was shown that a Tie2^{+}Flk^{dim}CD41^{-} population, after coculture on murine OP9 bone marrow stromal cells, could give rise to endothelial-like structures or hematopoietic colonies. The hematopoietic colonies contained cells that gained expression of CD41 after coculture [28]. CD41 expression may also bias progenitors to certain hematopoietic lineages depending on the tissue in which these cells reside [29].

1.3.2 Aorto-Gonado-Mesonephros Region

The murine AGM region is regarded as the first site of intraembryonic definitive hematopoiesis, and thus has been the target of substantial study regarding hemogenic endothelium. Earlier studies in this region were largely carried out using avian and transgenic mouse models, FACS sorting, and culturing of wild-type cells/tissues [15, 30–32]. While they revealed some insights into the relationship

between endothelium and blood, significant questions remained about the immediate precursor to definitive blood cell types. VE-cadherin-Cre lineage-tracing models have more recently been used to demonstrate that multilineage hematopoietic cells have an endothelial cell origin. These studies also suggested that the Runx1 transcription factor plays an important role in mediating the endothelial-to-hematopoietic cell transition [33, 34]. Other studies involving live imaging of AGM explants from Sca-1:GFP and CD41-YFP mice have shown emergence of presumptive HSC/HP directly from the mouse aortic wall [35].

A summary of published murine markers of endothelial cells, hemogenic endothelial cells, and hematopoietic stem/progenitor cells of yolk sac and AGM tissues are shown in Fig. 1.2. Hemogenic endothelial cells are localized in the E11.5 AGM in situ via immunofluorescent costaining of endothelial cell marker VE-cadherin and hematopoietic stem/progenitor marker cKit (Fig. 1.3). While the formation and function of hemogenic endothelium has been most thoroughly studied in avian, zebrafish, and murine models, limited human embryonic studies have revealed similar cell populations, exhibiting similar functions, during the equivalent time course in human embryos [36–41].

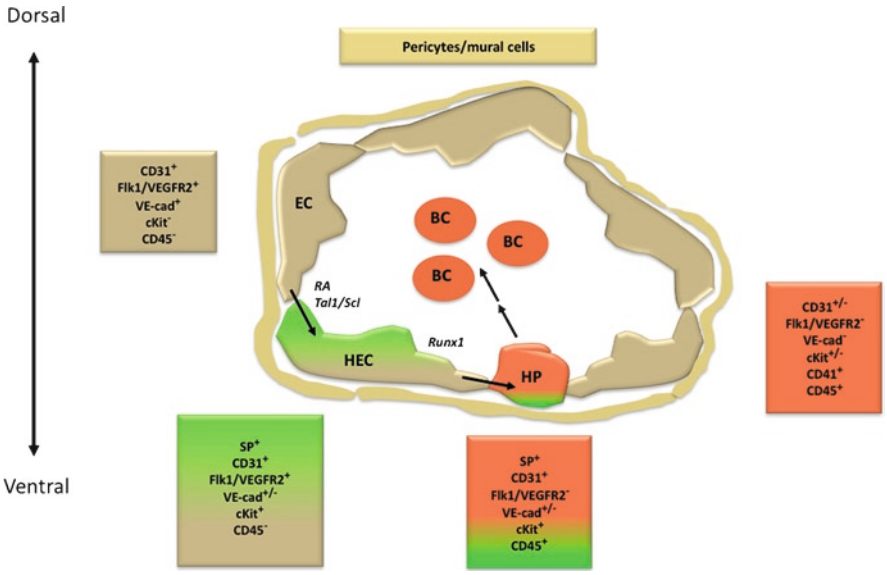

Fig. 1.2 Schematic representation of primitive endothelium, hemogenic endothelium, hematopoietic progenitors, and differentiated blood cells within the context of the developing aorta at E10.5. Adjacent color-matched columns list murine phenotypic markers for each subset of cells, and italicized words represent transcription factors placed at arrows where this signaling exerts its effect in specification of HEC and blood. *EC* endothelial cell; *HEC* hemogenic endothelial cell; *HP* hematopoietic progenitors; *BC* blood cell

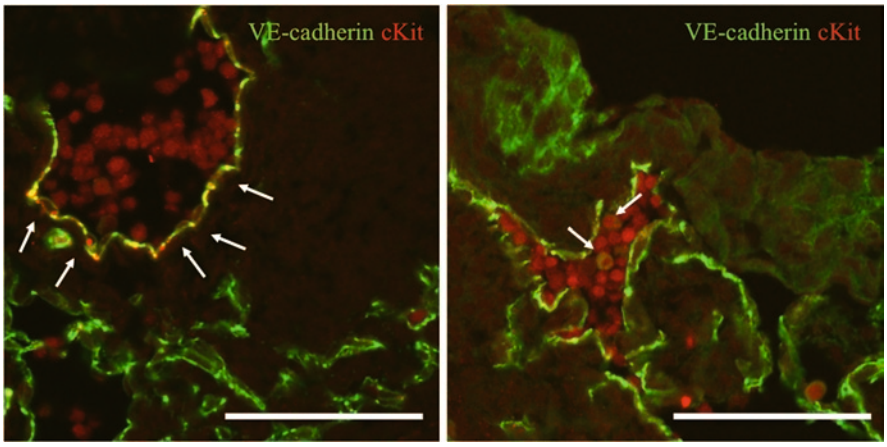

Fig. 1.3 Immunofluorescent staining of E11.5 aorta and associated vasculature reveals coexpression of endothelial and stem cell markers used to isolate hemogenic endothelium. (*Left panel*) Areas of aortic wall with coexpression of VE-cadherin (*green*) and cKit (*red*) (indicated with *white arrows*) with blood cells in close approximation. (*Right panel*) VE-cadherin$^+$ (*green*)/cKit$^+$ (*red*) cells in E11.5 vessel lumen (indicated by *white arrows*), likely representative of blood cells derived from endothelial precursors which subsequently entered embryonic circulation. Scale bar = 100 μm

1.3.3 Stem Cell Models of Vascular and Blood Cell Development

In addition to the characterization of developmental vasculogenesis and hematopoiesis in avian, murine, and human embryonic models, work using both mouse and human embryonic stem (ES) cells further established an endothelial-intermediate in blood cell development. By examining the expression of various hematopoietic factors in spontaneously differentiating embryoid bodies by RT-PCR and evaluating the kinetics of precursor development, it was determined that blood progenitors are derived from mouse ES cells in a temporal order similar to that exhibited in the murine embryo. More specifically, primitive erythroid progenitors arise at day 4 of embryoid body formation, 24 h before definitive erythroid and macrophage development, followed by neutrophils/macrophage differentiation at day 6, production of multilineage progenitors at day 8, and finally mast cell differentiation at day 10 [42, 43].

Embryoid bodies also give rise to endothelial cells during this same time frame, as Flk-1$^+$CD31$^+$ cells appeared as early as day 4 of embryoid body formation, and expression of additional endothelial markers Tie-1, Tie-2, and VE-cadherin occurs by day 5. Furthermore, it was shown that embryoid bodies differentiated to the point of vascular-like structures at day 11 often contained definitive hematopoietic precursors [44], providing more evidence of the intimate relationship between endothelial and vascular development. Recent studies in mouse ES cells have established the roles of BMP4 and Wnt3a in hematopoietic differentiation through the induction of *HoxB4* and *Cdx4* [45, 46].

As in the murine ES cell model, human ES cell differentiation has also successfully modeled mammalian endothelial-hematopoietic development of the early embryo. Human ES cell differentiation has provided evidence of mesodermal-hemato-endothelial colonies that exhibit striking morphological resemblance to clusters of cells of the human yolk sac during primitive hematopoiesis. Continued culturing of these colonies leads to emergence of cells with HSC and HP characteristics. Cells isolated from human embryoid bodies at days 9 and 10 of spontaneous differentiation exhibit an embryonic endothelial cell phenotype ($CD31^+/CD34^+$ or $VE\text{-}Cad^+/CD45^-$) that give rise to $CD45^+$ erythroid/myeloid cells and $CD56^+$ Natural Killer (NK) cells [47–50].

Although cells with hematopoietic phenotypic characteristics, and in vitro colony forming ability, are generated from ES cell differentiation systems, clear demonstration that they, indeed, represent adult-type HSC/HP has been hampered by lack of their successful transplantation into irradiated adult hosts. Nonetheless, several groups have shown that expression of factors thought to be involved in embryonic HSC maturation in vivo significantly improves engraftment of ES-derived HSC/HP [48, 51, 52]. In addition, both murine ES cell-derived $Flk\text{-}1^+$ and mesodermal cells have recently been used to track the formation of nonadherent $CD41^+$ and $CD45^+$ blood cells from sheets of cells expressing canonical endothelial markers and exhibiting endothelial cell morphology in vitro by time-lapse imaging [53]. In this system, it was also established that Tal1/Scl is necessary for the formation of hemogenic endothelial cells from blast colonies [24].

1.3.4 Phenotype and Origin of HSC in the Adult

Adult bone marrow HSC are among the most well-characterized stem cells in terms of cell phenotype and in vivo function. A variety of different techniques exist to isolate these cells from their bone marrow niche, including FACS based on cell surface marker expression and/or dye-efflux properties (SP phenotype). Presently, HSC are regularly and consistently purified from whole bone marrow as the $cKit^+$, $Sca\text{-}1^+$ and blood lineage $marker^-$ (also referred to as Lin^-; blood cell lineage markers include CD4, CD8, B220, Mac-1, Gr-1, and Ter119) or "KSL" fraction, the Hoechst dye-effluxing side population (SP) fraction, or a combination of both SP and KSL (termed SP-KSL or "SParKLS") [54–56]. Furthermore, we are learning much more about the microenvironment (niche, discussed below) in which the HSC reside from in vivo imaging and molecular regulation studies. However, there is relatively little known about the origin of HSC in adult bone marrow. Thus, despite the fact that there is increasing evidence from animal and stem cell culture studies indicating that HSC and definitive blood cell lineages arise from the endothelium during embryonic development, there is no proven counterpart in the adult. Thus, the origin of the adult HSC, and its lineage relationship to the vasculature, is not clear.

1.3.5 Vascular Niche for Adult HSC

Adult HSC are known to exist in a quiescent, nondividing state awaiting local and/or systemic signals to cycle and mobilize, as necessary. While significant evidence establishes a role for osteoblasts and an endosteal HSC niche in adult bone marrow [57, 58], immunofluorescence analysis for the SLAM family of receptors revealed that the majority of $CD150^{+}CD48^{-}CD41^{-}$ HSC are intimately associated with the fenestrated endothelium of sinusoidal bone marrow and spleen [59], emphasizing an important relationship between HSC and specialized endothelium.

Supportive of the in vivo localization studies, ex vivo culture of primary endothelial cells from adult bone marrow and embryonic yolk sac or AGM region reveal their ability to promote or maintain adult bone marrow/HSC phenotype, expansion, differentiation, and in vivo repopulating ability [60–62]. Furthermore, bone marrow endothelial cells constitutively express several cytokines and adhesion molecules important for mobilization, homing and engraftment of HSC, as well as other blood progenitors [63, 64]. Hence, HSC residing in this vascular niche would be well maintained, and available to respond quickly to perturbations in hematopoietic homeostasis and begin proliferation and differentiation, as needed. Interestingly, even endothelium isolated from adult nonhematopoietic tissues such as brain, heart, liver, and lung are supportive of HSC maintenance and repopulating function, but kidney endothelium decreased these processes [65].

1.4 Future Directions

1.4.1 Potential Relationship of Hemogenic Endothelial Cells to Postnatal Vascular and Hematopoietic Progenitors?

While there exists a growing body of literature focusing on the role of specialized endothelium in the support and maintenance of HSC in the adult bone marrow niche, there is little discussion regarding the possibility of this endothelium (or any other in the adult murine and human systems) contributing to de novo HSC/HP generation. As hemogenic endothelium has been proven a major source of blood production during embryonic development, it is reasonable to postulate that this phenomenon could be contributing to the pool of HSC/HP in mature bone marrow as a naturally occurring process. While current dogma stipulates that the long-term HSC provide a sufficient reservoir for blood production throughout the course of adult life, it would not be surprising if the supporting endothelium, closely associated with HSC in the niche, also contributed to maintenance of the HSC pool in a manner similar to their initial production of cells with similar function during embryonic development.

Similarly, it is possible that certain pathologic states or toxicities result in gene expression changes causing some injured adult endothelium to revert to a state in which it produces HSC and/or HP. A 2002 study by Montfort et al. showed that

donor-derived vessel grafts protected hosts from lethal irradiation via production of donor hematopoietic cells over a 50-day time course [66]. While the tissue harvesting procedure and subsequent implantation into the kidney could have caused numerous changes in gene expression and molecular signaling, this validates the notion of differentiated cells residing in the vasculature have the ability to produce blood. Possibly, there are idiopathic myeloproliferative disorders (MPD) resulting from aberrant production of blood from the vasculature, which until recently would not have been considered a potential source for such cases. Interestingly, several studies of blood malignancies have shown that the same chromosomal translocations/deletions present in hematopoietic cells are present in at least some marrow-derived endothelial cells and can contribute to both malignant angiogenesis and hematopoiesis [67–71]. Further investigation may reveal a host of previously unknown targets for hematologic malignancies and disorders refractive to current therapies.

Endothelial progenitor cells (EPC) are broadly classified as nonendothelial cells that can give rise to vascular cells in vitro and contribute to blood vessel formation in vivo. First isolated from human peripheral blood as $CD34^+$ cells (and as either $CD34^+$ or Flk-1^+ circulating cells in mice) [72], EPC show great therapeutic promise for repair of vascular injury and regenerative therapies. While there remains much debate about the origin and phenotype of, and interrelationship among, all vascular progenitor cell populations, there is evidence that vascular progenitors can arise from within, or around, the vasculature of specific tissues (reviewed recently in [73]). There is also evidence that EPC can be generated directly from HSC and perhaps other hematopoietic cell types (i.e., myeloid progenitors) (reviewed most recently in [74–76]).

Therefore, it is confusing to sort out the lineage interrelationship(s) between the vascular and hematopoietic systems in the adult. If EPC are derived from the vasculature, they may have very little association with the hematopoietic system expect for the fact that they circulate within peripheral blood. However, if EPC are derived from a hemogenic endothelial cell type that persists in adults, then perhaps they can be thought of as specialized hematopoietic progenitors that retain vascular potential. Although this latter hypothesis can be supported by many published studies, it does not account for the fact that transplanted HSC can also give rise to EPC and endothelial cells. Thus, important questions remain to be answered regarding the existence of hemogenic endothelium in the adult, the origin of both HSC and EPC from embryogenesis throughout adulthood, as well as their lineage relationship(s) (postulated interrelationships are summarized in Fig. 1.4).

1.4.2 Therapeutic Applications for Hemogenic Endothelium

As the role of hemogenic endothelium in blood production has been established, at least in the embryo and stem cell culture systems, it is reasonable to hypothesize that under certain circumstances, adult endothelium may contribute, or be altered

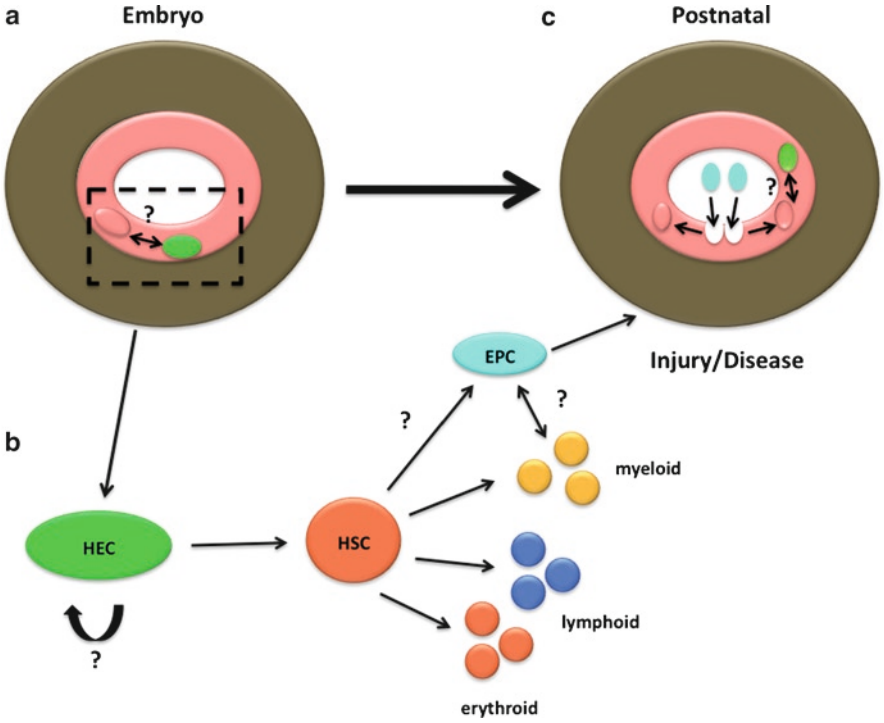

Fig. 1.4 Proposed "circulatory loop" of hemogenic endothelium, HSC, and EPC. (**a**) Representation of endothelial subset becoming specified as hemogenic endothelial cells, which give rise to HSC/progenitors within YS and AGM region. (**b**) Simplified schematic of definitive hematopoiesis beginning with HEC in the embryo, generating HSC that then produce the full complement of blood lineages. (**c**) Circulating EPC mobilizing to endothelium in response to injury or disease, leading to integration into vasculature and replacement of damaged EC. *Question marks* denote current areas of uncertainty in these processes

to contribute, to HSC repopulation and/or EPC generation. Many groups are working to understand the properties of "stemness" and using this knowledge to dedifferentiate somatic cell types into induced pluripotent stem (iPS) cells [77–80]. In the case of endothelium, perhaps induction of some primordial state could allow generation of functional hemogenic endothelium for the production of HSC and/or EPC in vitro or in vivo.

The ability to generate HSC/HP from isogenic endothelium would be particularly useful in the setting of bone marrow diseases and blood cancers. Numerous hematologic malignancies and MPD necessitate depletion of the bone marrow through radiation and/or chemotherapy; afterward, individuals most often rely on allogenic bone marrow transplants to repopulate the full complement of blood components. Advances in medical science to reprogram adult endothelium (or EPC) to a hemogenic phenotype could be used to generate new, adult-type definitive HSC and progenitors in vivo. This would eliminate complications such as lack of suitable

donors, graft vs. host disease, graft rejection, and risks associated with the procedure. A major caveat is that the endothelium would have to be screened to ensure that the defect originally causing the malignancy is not present; otherwise, such measures would likely recapitulate the initial disease state. To this end, a recent study by Ye et al. showed that iPS cells derived from $CD34^+$ blood cells from patients with MPD maintain the pathologic phenotype of the patient source upon redifferentiation [81]. Hence, while the utility of inducing blood-forming endothelium in the adult system is apparent, there are many areas of uncertainty that must be more thoroughly investigated before deeming this a practical therapeutic option.

1.4.3 Conclusions

Overlapping development of the vascular and hematopoietic systems reflects a unique interdependence between these earliest-functioning organ systems during embryogenesis. Furthermore, identification of endothelial cells as a major source of hematopoiesis during embryogenesis provides insight into the signaling hierarchy required for initial HSC emergence within vertebrate systems. Gaining further understanding of the complex processes leading to specification and regulated function of hemogenic endothelium, as well as determining whether these processes are relevant in the adult, may enable us to target therapeutic and regenerative medicine strategies to better treat vascular and hematologic pathologies.

Acknowledgments The authors would like thank Dr. Sharon Gerecht for the opportunity to contribute to this book and additional reviewers for critiques of the manuscript.

References

1. Shalaby, F., et al., *Failure of blood-island formation and vasculogenesis in Flk-1-deficient mice.* Nature, 1995. 376(6535): p. 62–6.
2. Shalaby, F., et al., *A requirement for Flk1 in primitive and definitive hematopoiesis and vasculogenesis.* Cell, 1997. 89(6): p. 981–90.
3. Lucitti, J.L., et al., *Vascular remodeling of the mouse yolk sac requires hemodynamic force.* Development, 2007. 134(18): p. 3317–26.
4. Adamo, L., et al., *Biomechanical forces promote embryonic haematopoiesis.* Nature, 2009. 459(7250): p. 1131–5.
5. You, L.R., et al., *Suppression of Notch signalling by the COUP-TFII transcription factor regulates vein identity.* Nature, 2005. 435(7038): p. 98–104.
6. Wigle, J.T. and G. Oliver, *Prox1 function is required for the development of the murine lymphatic system.* Cell, 1999. 98(6): p. 769–78.
7. Wigle, J.T., et al., *An essential role for Prox1 in the induction of the lymphatic endothelial cell phenotype.* EMBO J, 2002. 21(7): p. 1505–13.
8. Johnson, N.C., et al., *Lymphatic endothelial cell identity is reversible and its maintenance requires Prox1 activity.* Genes Dev, 2008. 22(23): p. 3282–91.

9. Harvey, N.L. and G. Oliver, *Choose your fate: artery, vein or lymphatic vessel?* Curr Opin Genet Dev, 2004. 14(5): p. 499–505.
10. Culver, J.C. and M.E. Dickinson, *The effects of hemodynamic force on embryonic development.* Microcirculation, 2010. 17(3): p. 164–78.
11. Wang, H.U., Z.F. Chen, and D.J. Anderson, *Molecular distinction and angiogenic interaction between embryonic arteries and veins revealed by ephrin-B2 and its receptor Eph-B4.* Cell, 1998. 93(5): p. 741–53.
12. Palis, J., et al., *Development of erythroid and myeloid progenitors in the yolk sac and embryo proper of the mouse.* Development, 1999. 126(22): p. 5073–84.
13. Cumano, A., F. Dieterlen-Lievre, and I. Godin, *Lymphoid potential, probed before circulation in mouse, is restricted to caudal intraembryonic splanchnopleura.* Cell, 1996. 86(6): p. 907–16.
14. Goldie, L.C., et al., *Cell signaling directing the formation and function of hemogenic endothelium during murine embryogenesis.* Blood, 2008. 112(8): p. 3194–204.
15. Medvinsky, A. and E. Dzierzak, *Definitive hematopoiesis is autonomously initiated by the AGM region.* Cell, 1996. 86(6): p. 897–906.
16. Muller, A.M., et al., *Development of hematopoietic stem cell activity in the mouse embryo.* Immunity, 1994. 1(4): p. 291–301.
17. North, T., et al., *Cbfa2 is required for the formation of intra-aortic hematopoietic clusters.* Development, 1999. 126(11): p. 2563–75.
18. Marshall, C.J. and A.J. Thrasher, *The embryonic origins of human haematopoiesis.* Br J Haematol, 2001. 112(4): p. 838–50.
19. Sabin, F.R., *Preliminary note on the differentiation of angioblasts and the method by which they produce blood-vessels, blood-plasma and red blood-cells as seen in the living chick. 1917.* J Hematother Stem Cell Res, 2002. 11(1): p. 5–7.
20. Murray, P.D.F., *The development in vitro of the blood of the early chick embryo.* Proc R Soc Lond B Biol Sci, Containing Papers of a Biological Character, 1932. 111(773): p. 497–521.
21. Huber, T.L., et al., *Haemangioblast commitment is initiated in the primitive streak of the mouse embryo.* Nature, 2004. 432(7017): p. 625–30.
22. Choi, K., et al., *A common precursor for hematopoietic and endothelial cells.* Development, 1998. 125(4): p. 725–32.
23. Kinder, S.J., et al., *The orderly allocation of mesodermal cells to the extraembryonic structures and the anteroposterior axis during gastrulation of the mouse embryo.* Development, 1999. 126(21): p. 4691–701.
24. Lancrin, C., et al., *The haemangioblast generates haematopoietic cells through a haemogenic endothelium stage.* Nature, 2009. 457(7231): p. 892–5.
25. Zhou, S., et al., *The ABC transporter Bcrp1/ABCG2 is expressed in a wide variety of stem cells and is a molecular determinant of the side-population phenotype.* Nat Med, 2001. 7(9): p. 1028–34.
26. Zhou, S., et al., *Bcrp1 gene expression is required for normal numbers of side population stem cells in mice, and confers relative protection to mitoxantrone in hematopoietic cells in vivo.* Proc Natl Acad Sci USA, 2002. 99(19): p. 12339–44.
27. Nadin, B.M., M.A. Goodell, and K.K. Hirschi, *Phenotype and hematopoietic potential of side population cells throughout embryonic development.* Blood, 2003. 102(7): p. 2436–43.
28. Li, W., et al., *Endothelial cells in the early murine yolk sac give rise to CD41-expressing hematopoietic cells.* Stem Cells Dev, 2005. 14(1): p. 44–54.
29. Hashimoto, K., et al., *Distinct hemogenic potential of endothelial cells and CD41+ cells in mouse embryos.* Dev Growth Differ, 2007. 49(4): p. 287–300.
30. de Bruijn, M.F., et al., *Hematopoietic stem cells localize to the endothelial cell layer in the midgestation mouse aorta.* Immunity, 2002. 16(5): p. 673–83.
31. Hirai, H., et al., *Hemogenic and nonhemogenic endothelium can be distinguished by the activity of fetal liver kinase (Flk)-1 promoter/enhancer during mouse embryogenesis.* Blood, 2003. 101(3): p. 886–93.
32. Fraser, S.T., et al., *Definitive hematopoietic commitment within the embryonic vascular endothelial-cadherin(+) population.* Exp Hematol, 2002. 30(9): p. 1070–8.

33. Zovein, A.C., et al., *Fate tracing reveals the endothelial origin of hematopoietic stem cells.* Cell Stem Cell, 2008. 3(6): p. 625–36.
34. Chen, M.J., et al., *Runx1 is required for the endothelial to haematopoietic cell transition but not thereafter.* Nature, 2009. 457(7231): p. 887–91.
35. Boisset, J.C., et al., *In vivo imaging of haematopoietic cells emerging from the mouse aortic endothelium.* Nature, 2010. 464(7285): p. 116–20.
36. Labastie, M.-C., et al., *Molecular identity of hematopoietic precursor cells emerging in the human embryo.* Blood, 1998. 92(10): p. 3624–35.
37. Oberlin, E., et al., *Blood-forming potential of vascular endothelium in the human embryo.* Development, 2002. 129(17): p. 4147–57.
38. Peault, B., E. Oberlin, and M. Tavian, *Emergence of hematopoietic stem cells in the human embryo.* C R Biol, 2002. 325(10): p. 1021–6.
39. Tavian, M., et al., *Aorta-associated CD34+ hematopoietic cells in the early human embryo.* Blood, 1996. 87(1): p. 67–72.
40. Tavian, M., M.F. Hallais, and B. Peault, *Emergence of intraembryonic hematopoietic precursors in the pre-liver human embryo.* Development, 1999. 126(4): p. 793–803.
41. Tavian, M., et al., *The human embryo, but not its yolk sac, generates lympho-myeloid stem cells: mapping multipotent hematopoietic cell fate in intraembryonic mesoderm.* Immunity, 2001. 15(3): p. 487–95.
42. Keller, G., et al., *Hematopoietic commitment during embryonic stem cell differentiation in culture.* Mol Cell Biol, 1993. 13(1): p. 473–86.
43. Wiles, M.V. and G. Keller, *Multiple hematopoietic lineages develop from embryonic stem (ES) cells in culture.* Development, 1991. 111(2): p. 259–67.
44. Vittet, D., et al., *Embryonic stem cells differentiate in vitro to endothelial cells through successive maturation steps.* Blood, 1996. 88(9): p. 3424–31.
45. Lengerke, C., et al., *BMP and Wnt specify hematopoietic fate by activation of the Cdx-Hox pathway.* Cell Stem Cell, 2008. 2(1): p. 72–82.
46. Lengerke, C., et al., *The cdx-hox pathway in hematopoietic stem cell formation from embryonic stem cells.* Ann NY Acad Sci, 2007. 1106: p. 197–208.
47. Wang, L., et al., *Endothelial and hematopoietic cell fate of human embryonic stem cells originates from primitive endothelium with hemangioblastic properties.* Immunity, 2004. 21(1): p. 31–41.
48. Wang, Y., et al., *Embryonic stem cell-derived hematopoietic stem cells.* Proc Natl Acad Sci USA, 2005. 102(52): p. 19081–6.
49. Zambidis, E.T., et al., *Blood-forming endothelium in human ontogeny: lessons from in utero development and embryonic stem cell culture.* Trends Cardiovasc Med, 2006. 16(3): p. 95–101.
50. Zambidis, E.T., et al., *Hematopoietic differentiation of human embryonic stem cells progresses through sequential hematoendothelial, primitive, and definitive stages resembling human yolk sac development.* Blood, 2005. 106(3): p. 860–70.
51. Kyba, M., R.C. Perlingeiro, and G.Q. Daley, *HoxB4 confers definitive lymphoid-myeloid engraftment potential on embryonic stem cell and yolk sac hematopoietic progenitors.* Cell, 2002. 109(1): p. 29–37.
52. Kyba, M., et al., *Enhanced hematopoietic differentiation of embryonic stem cells conditionally expressing Stat5.* Proc Natl Acad Sci USA, 2003. 100(90001): p. 11904–10.
53. Eilken, H.M., S. Nishikawa, and T. Schroeder, *Continuous single-cell imaging of blood generation from haemogenic endothelium.* Nature, 2009. 457(7231): p. 896–900.
54. Okada, S., et al., *In vivo and in vitro stem cell function of c-kit- and Sca-1-positive murine hematopoietic cells.* Blood, 1992. 80(12): p. 3044–50.
55. Goodell, M.A., et al., *Isolation and functional properties of murine hematopoietic stem cells that are replicating in vivo.* J Exp Med, 1996. 183(4): p. 1797–806.
56. Lin, K.K. and M.A. Goodell, *Purification of Hematopoietic Stem Cells Using the Side Population*, In: *Methods in Enzymology*, edited by L. Irina Klimanskaya and Robert Lanza. 2006, Academic Press, New York, NY, p. 255–64.
57. Zhang, J., et al., *Identification of the haematopoietic stem cell niche and control of the niche size.* Nature, 2003. 425(6960): p. 836–41.

58. Calvi, L.M., et al., *Osteoblastic cells regulate the haematopoietic stem cell niche.* Nature, 2003. 425(6960): p. 841–6.
59. Kiel, M.J., et al., *SLAM family receptors distinguish hematopoietic stem and progenitor cells and reveal endothelial niches for stem cells.* Cell, 2005. 121(7): p. 1109–21.
60. Ohneda, O., et al., *Hematopoietic stem cell maintenance and differentiation are supported by embryonic aorta-gonad-mesonephros region-derived endothelium.* Blood, 1998. 92(3): p. 908–19.
61. Li, W., et al., *Primary endothelial cells isolated from the yolk sac and para-aortic splanchnopleura support the expansion of adult marrow stem cells in vitro.* Blood, 2003. 102(13): p. 4345–53.
62. Rafii, S., et al., *Human bone marrow microvascular endothelial cells support long-term proliferation and differentiation of myeloid and megakaryocytic progenitors.* Blood, 1995. 86(9): p. 3353–63.
63. Sipkins, D.A., et al., *In vivo imaging of specialized bone marrow endothelial microdomains for tumour engraftment.* Nature, 2005. 435(7044): p. 969–73.
64. Avecilla, S.T., et al., *Chemokine-mediated interaction of hematopoietic progenitors with the bone marrow vascular niche is required for thrombopoiesis.* Nat Med, 2004. 10(1): p. 64–71.
65. Li, W., et al., *Hematopoietic stem cell repopulating ability can be maintained in vitro by some primary endothelial cells.* Exp Hematol, 2004. 32(12): p. 1226–37.
66. Montfort, M.J., et al., *Adult blood vessels restore host hematopoiesis following lethal irradiation.* Exp Hematol, 2002. 30(8): p. 950–6.
67. Gunsilius, E., et al., *Evidence from a leukaemia model for maintenance of vascular endothelium by bone-marrow-derived endothelial cells.* Lancet, 2000. 355(9216): p. 1688–91.
68. Della Porta, M.G., et al., *Immunophenotypic, cytogenetic and functional characterization of circulating endothelial cells in myelodysplastic syndromes.* Leukemia, 2008. 22(3): p. 530–7.
69. Rigolin, G.M., et al., *Neoplastic circulating endothelial cells in multiple myeloma with 13q14 deletion.* Blood, 2006. 107(6): p. 2531–5.
70. Streubel, B., et al., *Lymphoma-specific genetic aberrations in microvascular endothelial cells in B-cell lymphomas.* N Engl J Med, 2004. 351(3): p. 250–9.
71. Wu, J., et al., *Dominant contribution of malignant endothelial cells to endotheliopoiesis in chronic myeloid leukemia.* Exp Hematol, 2009. 37(1): p. 87–91.
72. Asahara, T., et al., *Isolation of putative progenitor endothelial cells for angiogenesis.* Science, 1997. 275(5302): p. 964–7.
73. Tilki, D., et al., *Emerging biology of vascular wall progenitor cells in health and disease.* Trends Mol Med, 2009. 15(11): p. 501–9.
74. Chao, H. and K.K. Hirschi, *Hemato-vascular origins of endothelial progenitor cells?* Microvasc Res, 2010. 79(3): p. 169–73.
75. Hirschi, K.K., D.A. Ingram, and M.C. Yoder, *Assessing identity, phenotype, and fate of endothelial progenitor cells.* Arterioscler Thromb Vasc Biol, 2008. 28(9): p. 1584–95.
76. Steinmetz, M., G. Nickenig, and N. Werner, *Endothelial-regenerating cells: an expanding universe.* Hypertension, 2010. 55(3): p. 593–9.
77. Takahashi, K. and S. Yamanaka, *Induction of pluripotent stem cells from mouse embryonic and adult fibroblast cultures by defined factors.* Cell, 2006. 126(4): p. 663–76.
78. Wernig, M., et al., *In vitro reprogramming of fibroblasts into a pluripotent ES-cell-like state.* Nature, 2007. 448(7151): p. 318–24.
79. Takahashi, K., et al., *Induction of pluripotent stem cells from fibroblast cultures.* Nat Protoc, 2007. 2(12): p. 3081–9.
80. Okita, K., T. Ichisaka, and S. Yamanaka, *Generation of germline-competent induced pluripotent stem cells.* Nature, 2007. 448(7151): p. 313–7.
81. Ye, Z., et al., *Human-induced pluripotent stem cells from blood cells of healthy donors and patients with acquired blood disorders.* Blood, 2009. 114(27): p. 5473–80.

Chapter 2
Molecular Control of Vascular Tube Morphogenesis and Stabilization: Regulation by Extracellular Matrix, Matrix Metalloproteinases, and Endothelial Cell–Pericyte Interactions

George E. Davis, Amber N. Stratman, and Anastasia Sacharidou

2.1 Introduction

Considerable progress has been made in our understanding of molecular events underlying the development of the vasculature and how it is regulated in postnatal life, particularly in the context of tissue injury and tumorigenesis [1, 17, 28, 49]. A key point is that the major advances in the field appear to be directly related *to our understanding of basic events* that control these processes such as cell survival, proliferation, migration, invasion, and morphogenesis. Also, it should be pointed out that both in vitro and in vivo studies have played major roles in advancing this understanding, and *it remains essential that both types of approaches are utilized* to approach the complexities inherent in the developing and postnatal vasculature.

The molecular control of the vasculature is affected by many factors and signals, and in this chapter, we focus on the influence of extracellular matrix (ECM), matrix metalloproteinases (MMPs), and endothelial cell (EC)–pericyte interactions in controlling vascular development and postnatal vascularization events. In general terms, the ECM is a fundamental regulator of vascularization in that it presents a physical scaffold containing adhesive and growth factor modulatory signals that are necessary for blood vessels to form and mature [24, 26, 51, 72]. Vascular cell recognition of ECM occurs through a variety of receptors including both integrin and nonintegrin adhesion receptors [24, 51, 83], and these mediate the complex signals

G.E. Davis (✉)
Department of Medical Pharmacology and Physiology, University of Missouri School of Medicine MA415 Medical Sciences Building, Columbia, MO 65212, USA
and
Department of Pathology and Anatomical Sciences, University of Missouri School of Medicine, Columbia, MO 65212, USA
and
Dalton Cardiovascular Sciences Center, Columbia, MO 65212, USA
e-mail: davisgeo@health.missouri.edu

S. Gerecht (ed.), *Biophysical Regulation of Vascular Differentiation and Assembly*, Biological and Medical Physics, Biomedical Engineering,
DOI 10.1007/978-1-4419-7835-6_2,

that are delivered. There is considerable evidence that ECM can provide both stimulatory and inhibitory signals [24, 26], and thus, the ECM composition, the vascular cell types, and the biological context of the signaling dictate the cellular response that occurs. An important regulator of ECM structure and function are MMPs, which can not only degrade matrix components [25, 26, 41, 46] but can also release liberate factors such as cytokines from these matrices to affect vascular cell behavior. Within the vascular wall, homotypic interactions between ECs [31] and heterotypic interactions of ECs and mural cells affect ECM production and deposition, [81] as well as its ability to be degraded by MMPs [77]. Many new studies are now focused on such interactions to understand how mural cells affect EC behavior during development and under various disease conditions [1, 5, 42, 50, 81]. In this chapter, we review past and present work that addresses mechanisms by which ECM, MMPs, and EC–pericyte interactions influence vascular tube assembly and remodeling, tube stabilization, and vascular regression to control tissue vascularization in normal versus disease states.

2.2 Concepts in Vascular Tube Morphogenesis in 3D Extracellular Matrices

2.2.1 Extracellular Matrix and Vascular Morphogenesis

A critical regulator of vascular morphogenesis is the ECM, which serves as a physical, mechanical, and agonistic substrate to affect survival, motility, invasion, and morphogenic events of both endothelial cells (ECs) and mural cells, including pericytes and vascular smooth muscle cells [1, 24, 26, 51, 72]. Interestingly, different types of ECM have opposite effects depending on the biologic context with evidence for promorphogenic and proregressive activities [24, 26]. Also, certain ECM environments may present quiescence signals to vascular cells that play an important role in vascular stabilization. Alterations in the ECM through proteolysis or conformational changes are known to generate matricryptic sites, which activate cells, and thus, the ECM is a critical regulator of how cells perceive their environment and sense an injurious stimulus [21, 29]. Furthermore, the ECM is a scaffold that possesses adhesive signals for cells by binding to both integrin and nonintegrin surface receptors, and it also binds and presents specific growth factors to cells [24, 51, 52]. Also, the ECM modulates the activation of specific growth factors and, thus, can modulate growth factor action to affect the vasculature [52]. Also, it is clear that cosignaling between integrins and growth factor receptors is a critical regulator of vascularization events both during development and in postnatal life. The ECM is also mechanosensitive and responds to mechanical forces generated by cells that exert tensional forces on this matrix. A key mechanosensitive ECM component is fibronectin, which contains matricryptic sites that affect its self-assembly, particularly its III-I domain [39, 69, 85, 89]. Interestingly, this domain is exposed in instances where

fibronectin is absorbed to surfaces such as cell surfaces or ECM [29, 85] and appears to be particularly exposed when cells exert mechanical force on fibronectin through integrin-based interactions [89]. This facilitates fibronectin binding to itself, which promotes a self-assembly reaction (i.e., including disulfide exchange to form covalent bonds between fibronectin molecules) necessary to form an insoluble matrix [69]. Since fibronectin is one of the few ECM proteins with clear mechanosensitive domains, it suggests that fibronectin may play a particularly important role in ECM assembly events that depend on mechanical forces such as those observed during vascular morphogenic events in a variety of contexts [81, 90].

2.2.2 Differential Effects of ECM Components on Vascular Tube Morphogenesis

Certain ECM components are potent stimulators of vascular tube morphogenesis, while others appear inhibitory. Interestingly, collagen type I, the most abundant ECM component particularly in adult animals, is a potent stimulator of vascular tube morphogenesis in 3D matrices [24, 86]. An accumulating view is that fibrillar collagen matrices are potent ECM agonists for these events. Another strong ECM agonist for EC tube morphogenesis is fibrin [70], a provisional matrix component that is deposited along with fibronectin during tissue injury [24]. Interestingly, the collagen-binding integrins $\alpha 2\beta 1$ and $\alpha 1\beta 1$ have been shown to control EC tube morphogenic events in vitro and in vivo in collagenous matrices [9, 22, 24, 79], while the fibrin/fibronectin-binding integrins $\alpha v\beta 3$ and $\alpha 5\beta 1$ have been shown to control tube morphogenesis in fibrin matrices [9, 10]. Because of the strong promorphogenic influence of collagen and fibrin matrices, these have been predominantly used to establish 3D EC tube morphogenic models [58, 70] that have strongly enhanced our knowledge concerning the molecular basis for EC tubulogenesis, sprouting, and tube maturation events. Overall, the ECM and integrin data strongly suggests that vascular tube morphogenesis is connected to integrin-mediated recognition of different promorphogenic ECM components and that multiple members of the integrin family can participate in stimulating EC tubulogenesis in 3D matrix environments [24]. It does not appear that any particular integrin family member is special with respect to its ability to affect tube morphogenesis, and their influence is dictated by the ECM environment in which the morphogenic process takes place. In contrast, it appears that laminin-rich matrices are likely to present inhibitory signals to endothelial cells to interfere with morphogenic events [24, 26, 63]. As blood vessels mature, laminin matrix deposits as a component of the vascular basement membrane matrix, an assembly event that is strongly enhanced by EC–pericyte interactions in 3D matrices [81]. Vascular basement membrane assembly generally is thought to be a tube maturation stimulus, and hence, decreased morphogenesis is coincident with its appearance around the ablumenal surface of EC-lined tubes. This point needs to be investigated in more detail, but early information suggests that some laminin isoforms have inhibitory activity toward ECs during morphogenic events [63].

The vasculature appears to predominantly express laminin-8 (α4, β1, γ1), laminin-9 (α4, β2, γ1), laminin-10 (α5, β1, γ1), and laminin-11 (α5, β2, γ1) isoforms [24, 44, 68]. Previously and more recently, we have reported that these subunits are differentially expressed by both ECs and pericytes during vascular tube morphogenesis and maturation events [11, 81]. The biological role of each isoform has not yet been elucidated in sufficient detail during these processes.

One critical aspect that similarly has not been investigated in sufficient detail is the nature of the embryonic ECM environment where vascular development takes place [26, 51]. It is clear that there is much less fibrillar collagen during development, while the matrices are known to be rich in glycosaminoglycans, such as hyaluronic acid, proteoglycans, and fibronectin. It appears that developing embryos strongly depend on the presence of fibronectin (perhaps its importance relates to its mechanosensitive ability to self-assemble) [51]. Fibronectin knockout mice show severe defects in vascular development along with other abnormalities [6, 36]. Fibronectin is also alternatively spliced, and several splice isoforms (IIIA and IIIB) appear to play a critical functional role to promote vascular tube assembly and maturation during development [6]. One of the problems with investigating such issues in more molecular detail is that there currently are no 3D systems available that mimic an embryonic ECM environment, an important future direction for in vitro model development using vascular or other cell types.

2.3 Review of Work

2.3.1 Molecular Events Regulating Vascular Tube Morphogenesis and EC Sprouting in 3D Matrices

A major effort of our laboratory has been to elucidate the molecular and signaling requirements for ECs to form tube networks when suspended within 3D matrices and to sprout and form tubes from a monolayer surface into 3D matrices [24, 28, 53]. To this end, we have developed 3D matrix microassay systems to assess both of these phenomena in assays that mimic vasculogenesis and angiogenic sprouting events using either collagen or fibrin matrices [58]. Other laboratories have developed related systems to investigate these events [3, 70]. The majority of our work has focused on a model that mimics embryonic vasculogenesis, whereby human ECs are seeded as single cells within a 3D matrix [22, 58]. Using appropriate media conditions, ECs undergo dramatic morphologic changes that lead to the development of interconnecting networks of EC-lined tubes (Fig. 2.1). In Fig. 2.1a, two ECs are observed in a time-lapse series to form intracellular vacuoles, which fuse within each cell, and then through exocytic events, the two cells then interconnect to form early multicellular lumen and tube structures. There is no intermixing of cytoplasmic contents when this occurs, so the tube consists of adjacent ECs, which interact through cell–cell adhesive contacts. In addition, the ECs are attached to the ECM to form the wall of a lumenal space and need to maintain these adhesive contacts (i.e., both

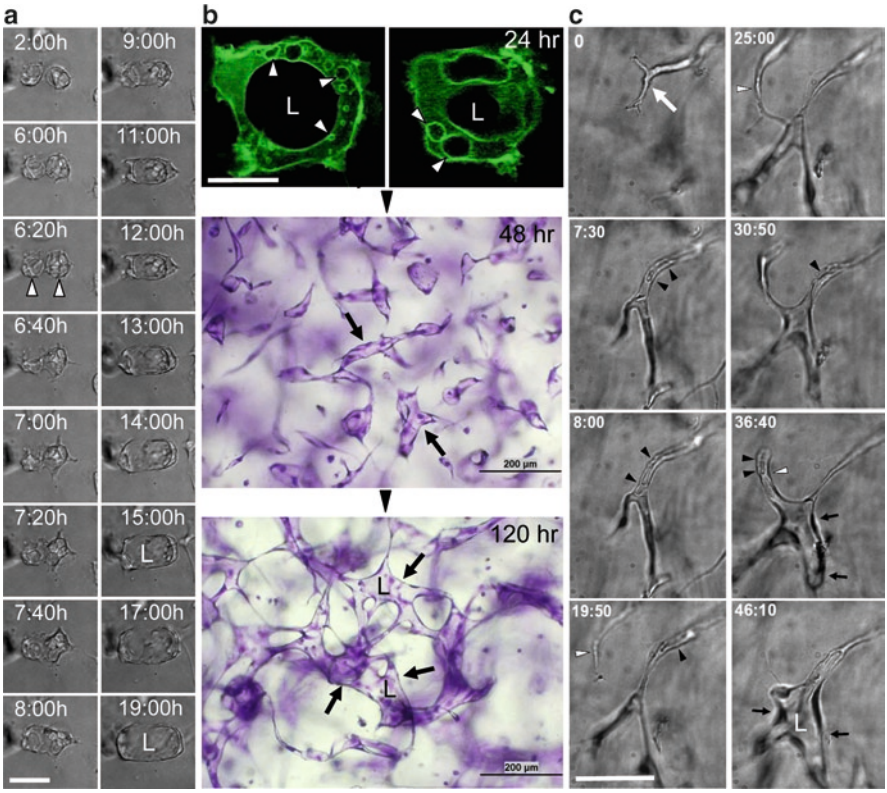

Fig. 2.1 Temporal analysis of endothelial tube formation events in 3D collagen matrices during vasculogenesis and angiogenic sprouting. (**a**) A time-lapse series is shown whereby two ECs are shown to form intracellular vacuoles that eventually coalesce inside each cell and then following cell–cell contact with the neighboring cells form a lumenal space in between the two cells. Vacuole fusion events are observed while they are contacting each other. L indicates EC lumen; *arrowheads* indicate vacuolating ECs. *Bar* equals 25 μm. (**b**) Confocal images of ECs expressing GFP-Rac1 fusion proteins that label intracellular vacuoles, the developing lumenal membrane as well as the plasma membrane during lumen formation events at 24 h of culture. *Upper panels* – L indicates EC lumenal space and *arrowheads* indicate intracellular vacuoles. *Bar* equals 20 μm. Over time ECs form inconnecting networks of tubes, which are illustrated using fixed and toluidine-blue stained cultures. *Arrows* indicate tube structures; L indicate EC lumen; *Bar* equals 200 μm. (**c**) EC sprouting was stimulated by the combination of sphingosine-1-phosphate (1 mM) and SDF-1α (200 ng/ml), which were mixed in the collagen matrix. A time-lapse series (over a 46 h period) was taken beneath the surface of the monolayer to examine sprouting events and lumen development in assays mimicking angiogenesis. *White arrow* and *arrowheads* indicate EC tip cells that are sprouting through the 3D collagen matrices; *black arrowheads* indicate intracellular vacuoles that are observed particularly in ECs directly trailing tip cells; *black arrows* indicate the cell border of EC tubes; L indicates EC lumen. *Bar* equals 50 μm

cell–ECM and cell–cell adhesion) to remain stable on this lumenal wall. Intracellular vacuoles can be observed to form through integrin- and cytoskeletal-dependent pinocytic events, and these vacuoles are targeted to a pericentrosomal location in a polarized fashion and then move to fuse with the developing lumenal membrane as

shown in Fig. 2.1b (upper panel) [8, 22, 28, 55]. In Fig. 2.1b, intracellular vacuoles are strongly labeled with a GFP-Rac1 construct [8]. We have previously observed labeling of intracellular vacuoles with GFP-Rac1, GFP-Cdc42, and GFP-RalA [8, 28]. This GFP-Cdc42 was expressed using an EC-specific promoter in zebrafish, revealing that intracellular vacuoles are observed and participate in the lumen formation process of intersegmental vessels during vascular development [55].

Both Cdc42 and Rac1 are required for intracellular vacuole formation as well as EC lumen and tube formation [8, 28, 57]. We have performed these experiments using either dominant negative mutants of Cdc42 and Rac1 or specific siRNAs to these GTPases. Developing multicellular lumenal structures then interconnect into more extensive networks over time (Fig. 2.1b, middle and lower panels). Using an angiogenic sprouting model [9, 58], time-lapse images are shown, which reveal how invading ECs interact, develop intracellular vacuoles, and migrate toward each other to form multicellular lumen and tube structures over time (Fig. 2.1c).

After much effort over many years, we have elucidated molecular requirements and signaling pathways that underlie the ability of human ECs to form lumen and tube structures in 3D matrices [8, 23, 24, 27]. Most of our studies have focused on collagen matrices, and thus, a major requirement for these events is the α2β1 integrin, a collagen-binding integrin [22]. Blocking antibodies directed to α2β1 markedly block lumen formation as do α2 integrin subunit siRNAs. Interestingly, blocking antibodies directed to many other integrin subunits, including α5β1, a fibronectin receptor, have no effect in this system. Also, considerable work has shown that the α2β1 integrin is important for vascularization events in vivo and in both developmental and postnatal life contexts [75, 79]. In contrast, when our studies utilized fibrin matrices, we identified that both αvβ3 and α5β1 were required for EC lumen and tube formation [10], while α2β1 was not shown to be involved. Importantly, both of these integrins have been shown to be involved during vessel formation in development and in postnatal mice [51, 83]. Thus, an important point is that the in vitro models of our laboratory and others accurately predicted the in vivo findings made by other groups. Another key point is that the in vitro model systems demonstrated first that multiple integrin chains can be utilized by ECs to regulate tube morphogenesis, and there is little evidence to suggest that any particular integrin is unique or special in this property to regulate the morphogenic cascade necessary to form new blood vessels. The role of particular integrins in morphogenesis appears to be directly linked to the ECM environment (and the predominant ECM components) that is in contact with the ECs.

2.3.2 Functional Role of the Rho GTPases, Cdc42 and Rac1, and the Effectors, Pak2 and Pak4, in EC Tube Morphogenesis

An important question raised by the above studies is which downstream signaling pathways are activated by integrins to control these morphogenic processes. Integrins have been known to activate Rho GTPases among other molecules [43]

such as a variety of kinases, including Src and focal adhesion kinase [24, 51]. Our laboratory reported that Cdc42 was a critical GTPase controlling EC lumen formation [8]. This was also the first report from any system implicating Cdc42 and tube formation. Subsequent studies have revealed that Cdc42 is a critical regulator of lumen formation from both ECs and epithelial cells [8, 23, 57, 59, 67, 74]. We reported a role for Rac1 in EC tubulogenesis [8, 57], while RhoA had no influence on these events. Both Cdc42 and Rac1 were shown to be activated during the morphogenic cascade in 3D collagen matrices [57, 74]. To address the question of downstream effectors that are responsible for the influence of Cdc42 and Rac1, we screened a series of known effectors using siRNA treatment of ECs. Major blocking phenotypes were observed using siRNAs to p21-activated kinase (Pak)-2 and Pak-4 [57]. Both EC tube formation and EC sprouting into 3D collagen matrices were markedly inhibited by these siRNAs. We also demonstrated that a time course of Pak-2 and Pak-4 activation, as indicated by phosphorylation, directly correlated with the EC lumen formation process [57]. It was further demonstrated that activated Pak-2 and Pak-4 could be demonstrated to be associated with activated Cdc42 during these events [57]. Expression of a dominant negative mutant of either Pak-2 or Pak-4 was shown to completely inhibit EC lumen formation [57]. Interestingly, both Cdc42 and Rac1 are able to activate Pak-2, while Cdc42 selectively activates Pak-4 [16, 38]. Recent experiments have revealed important roles for both Pak-2 and Pak-4 during vascular development [38, 62, 84], which again corroborate the in vitro findings.

2.3.3 Functional Role for PKCε and Src in EC Tube Morphogenesis and Subsequent Pak Activation Events

Other known kinases that are activated by cell–ECM interactions include protein kinase C isoforms and Src family kinases. In our studies of EC lumen formation in 3D collagen matrices, we have shown that PKCε, but not PKCα or PKCδ, is involved in the process [57, 59]. siRNA suppression experiments or expression of dominant negative mutants of PKCε blocks lumen formation and downstream Src and Pak activation [59]. Interestingly, increased expression of PKCε strongly stimulates EC lumen and tube formation as well as both increased Src, Pak-2, and Pak-4 phosphorylation events that directly correlate with its morphogenic influence [59]. Our studies indicate that PKCε is upstream of Src activation, while Src activation is upstream of Pak activation [59]. Blockade of Src kinases by siRNA suppression, increased expression of the Src inhibitor CSK (i.e., C-terminal Src kinase), or treatment with chemical inhibitors (e.g., PP2) completely interferes with EC tube formation. Expression of a dominant negative Csk construct strongly increased lumen formation, again suggesting a positive role for Src in EC lumen formation [59]. Interestingly, Src and Pak kinases are known to activate Raf kinases to affect processes such as cell survival that has previously been shown to influence angiogenesis in vivo [2], and we have recently shown that they are required for

EC lumen formation [59]. Mouse knockout of B-Raf shows an embryonic lethal phenotype that is due to vascular abnormalities [37]. Of great interest is that we have shown that Raf kinase activation (of both C-Raf and B-Raf) occurs downstream of Src and Pak activation and controls EC tube morphogenic events along with survival [59]. This is accompanied by Erk1/2 activation, which also directly correlates with the ability of these ECs to form tube networks. Interestingly, expression of a phosphatase, MKP-3, with selectivity for phospho-Erk1/2, markedly decreases Erk phosphorylation and strongly blocks lumen formation [59]. A dominant negative MEK kinase inhibitor also abrogates lumen formation and Erk1/2 phosphorylation events. What is interesting about these results is that a known pathway to regulate both proliferation and survival is utilized by ECs to regulate a separate tubulogenic pathway in 3D matrices. In our systems, there is little to no evidence for proliferation during these processes, so the signaling cascade appears particularly focused on tube morphogenesis [28]. Overall, this morphogenic pathway is coupled to cytoskeletal signaling (i.e., PKC, Src, Pak), survival (i.e., Raf), and transcriptional events (i.e., Erk) to coordinately control this process [28, 57, 59]. Also, it is likely that these kinases are not limited to affecting only one of these critical functions during these events.

2.3.4 Cdc42 Coupling to Cell Polarity Pathways Controls EC Lumen and Tube Formation

A major function of Cdc42 is its ability to affect cell polarity signaling by interfacing with the polarity proteins, Par6, Par3, and atypical PKC isoforms [34, 65]. Cell polarity signaling controls directional cell motility that involves Cdc42 [34]. In fact, active Cdc42 (i.e., Cdc42-GTP) binds directly to Par6, which then couples to Par3, a scaffold protein that also interacts with atypical protein kinase C isoforms such as PKCζ [65]. We have recently reported that Cdc42-dependent EC lumen and tube formation is dependent on Par6b, Par3, and PKCζ [57]. Thus, this work reveals a fundamental role for Cdc42-dependent polarity signaling in EC tubulogenesis. Par3 is known to interact with a number of other cell surface proteins including members of the junction adhesion molecule (Jam) family (i.e., Jam-A, Jam-B, and Jam-C) [32, 33]. Our most recent work has revealed that JamB and Jam-C associate with Par3 in ECs to control EC lumen formation in 3D collagen matrices [74]. Furthermore, these Jam proteins coassemble into a defined EC lumen signaling complex consisting of α2β1, MT1-MMP, Jam-C, Jam-B, Par3, Par6b, and Cdc42-GTP that is responsible for the ability of ECs to form tubes in 3D collagen matrices [74] (see later on). Disruption of any member of this complex markedly interferes with the ability of ECs to form tubes [74]. These lumen signaling complexes are also directly coupled to the kinase cascade discussed earlier including PKCε, Src, Pak, Raf, and Erk 1/2, since blockade of these complexes completely interferes with the downstream kinase signaling necessary to regulate vascular tube morphogenesis [74]. Cdc42 and Par3 have also been shown to control lumen formation in

epithelial cells, and a recent study has shown that Par3 and β1 integrins coregulate arteriolar lumen formation in vivo using a conditional β1 integrin subunit knockout mouse system [93]. Thus, the latter work again confirms our prior conclusions obtained in vitro, showing that β1 integrins, Cdc42, and polarity proteins control the lumen and tube formation process in 3D matrix environments [28, 57, 74].

2.3.5 Critical Functional Role for MT1-MMP in EC Lumen and Tube Formation in 3D Collagen Matrices

Matrix metalloproteinases (MMPs) are a family of zinc-dependent metalloendopeptidases that degrade a variety of substrates to affect the vasculature and other tissues [25, 41]. Their targets include the ECM, cytokines, and cell surface receptors to affect vascularization as well as many other cellular responses [25, 41]. Our work and that of others have demonstrated a role for MT1-MMP (i.e., MMP-14) in EC morphogenic events in 3D matrix environments [19, 77, 82]. MT1-MMP is a transmembrane protein, and its cell surface expression is required for it to perform the localized ECM degradation necessary to control cell movement in 3D matrices. MT2-MMP is also able to participate in these types of events, while the function of MT3-MMP is less clear, although several studies show that it is does not play a major role. Mouse knockout of MT1-MMP is compatible with embryogenesis, but the mice are small and fall ill and die within a month or two after birth [91]. Attempts to induce angiogenesis in these mice reveal that these responses do not occur [91]. Furthermore, aortic ring assays in 3D collagen matrices show no sprouting in either 3D collagen or fibrin matrices using MT1-MMP knockout tissues compared to control [19]. Thus, this work demonstrates an important role for MT1-MMP in vascular morphogenic events in 3D matrices and during in vivo angiogenic responses.

To elucidate the molecular mechanisms by which MT1-MMP controls vascular morphogenesis as well as cellular invasive events, our laboratory has examined this question using models of vasculogenesis and angiogenesis [9, 77, 82]. We have utilized protein and chemical MMP inhibitors, as well as siRNA suppression approaches. In our initial studies, we demonstrated that EC sprouting in response to sphingosine-1-phosphate (incorporated into the collagen matrices) was blocked by the broad-spectrum inhibitor, GM6001, as well as tissue inhibitor of metalloproteinase (TIMP)-2, TIMP-3, and TIMP-4, but not TIMP-1 (Fig. 2.2a) [9]. Interestingly, MT-MMPs are insensitive to TIMP-1, but the other inhibitors utilized will block their activity. When EC lumen and tube formation assays were performed, GM6001, TIMP-2, TIMP-3, and TIMP-4 blocked completely, while TIMP-1 had no influence. One important distinction among the TIMPs is that TIMP-3 is able to block not only the activity of MT-MMPs but also that of many members of the ADAM family of cell-surface-expressed metalloproteinases [7]. To functionally dissect EC surface-expressed metalloproteinases that are relevant during EC sprouting and lumen formation, we performed siRNA suppression analysis. Our results suggest that the

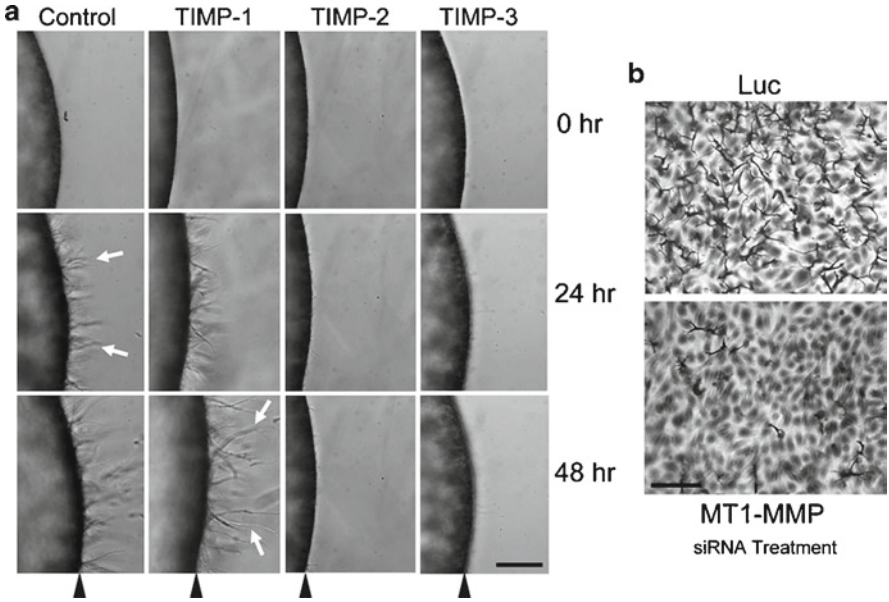

Fig. 2.2 MT1-MMP plays a critical role in EC sprouting in 3D collagen matrices from a monolayer surface in assays that mimic angiogenesis. (**a**) A time-lapse series was performed of EC sprouting viewed from the side into 3D collagen matrices where either no addition or recombinant TIMPs were added. Sphingosine-1-phosphate (1 μM) was added to the collagen matrix. *Arrowhead* indicates EC monolayer surface; *arrows* indicate EC sprouts. TIMP-2 and TIMP-3 block sprouting in an equivalent manner, while TIMP-1 has no blocking influence relative to the control. *Bar* equals 100 μm. (**b**) An siRNA suppression experiment was performed to examine the influence of an MT1-MMP siRNA versus a luciferase control. Sprouting assays were performed using the treated cells, and the latter were seeded on collagen matrices containing 1 μM sphingosine-1-phosphate. Cultures were fixed, stained, and photographed after 24 h. *Bar* equals 100 μm

dominant metalloproteinase controlling these events is MT1-MMP (Fig. 2.2b), with a lesser influence of MT2-MMP during both sprouting and lumen formation [77, 82]. We observed a partial blocking effect of ADAM-15 siRNA knockdown in EC sprouting assays using stromal-derived factor-1α as the invasion stimulus [77]. We did not observe an effect of either MT3-MMP or ADAM-17 siRNAs in our assays [77], although a recent study using a similar system has revealed a potential role for ADAM-17 in modulating the invasion response [60]. The fact that TIMP-2 and TIMP-4 have dramatic blocking effects on both sprouting and lumen formation is more supportive of a major role for MT-MMPs rather than ADAMs, since there is currently no evidence to suggest that they can block ADAM proteinases [7].

A further important experiment that demonstrates a role for MT1-MMP during EC tubulogenesis showed that increased expression of MT1-MMP using viral vectors leads to marked increases in lumen formation that depends on its MMP catalytic domain [82]. Furthermore, addition of GM6001 to block MT1-MMP completely

inhibits the stimulatory influence of the recombinant protein. In support of this result is that a catalytically dead full-length MT1-MMP construct (EA mutant) has no ability to stimulate EC lumen formation [82], while interestingly, it does not exert an inhibitory influence. In very recent experiments, we have further shown that increasing the expression of wild-type, full-length MT1-MMP increases both the rate and extent of EC lumen formation in 3D collagen matrices [74]. Of great interest is that we have created a construct that appears to be a dominant negative mutant of MT1-MMP in this system where we mutated the active site and at the same time deleted its cytoplasmic tail [74]. When expressed in ECs, the cells are completely unable to make lumens in 3D collagen matrices. An additional finding is that expression of wild-type MT1-MMP without its cytoplasmic tail markedly stimulates the rate and extent of EC lumen formation compared to full-length wild-type MT1-MMP expression [74]. A number of studies suggest that its cytoplasmic tail plays a role in endocytic recycling, and thus, deleting the tail increases cell surface expression, which in our case, leads to additional increases in EC lumen formation events. Overall, these results demonstrate that MT1-MMP is a major regulator of EC lumen and tube formation and that it works closely in conjunction with the $\alpha 2\beta 1$ integrin as well as Cdc42 and Rac1 to control this process.

2.3.6 MT1-MMP-Dependent EC Lumen and Tube Formation Leads to the Formation of a Network of Physical Spaces Within the ECM Termed Vascular Guidance Tunnels

During the course of the above studies, we made the novel observation that during EC lumen and tube formation, ECs are also creating a network of physical spaces, which we term vascular guidance tunnels. These form as a result of MT1-MMP-mediated proteolysis of collagen matrices [82]. In every instance that has been examined, there is a direct relationship between EC tube formation and the formation of vascular guidance tunnels [82]. The tunnels were first detected by staining the collagen type I matrix with a monoclonal antibody that recognizes native type I collagen and not denatured collagen (which is generated at 37°C when it is cut with mammalian collagenases). The lumen and tube formation creates an extensive interconnecting network of these tunnel spaces within the 3D collagen matrices [82]. To further prove that these represent physical spaces in the ECM, they were microinjected with silicone oil [82]. Dramatic filling of networks was demonstrated showing that EC tube formation leads to the formation of interconnecting vascular guidance tunnel spaces. We further showed that the ECs produced twice as many tunnel spaces than were occupied by EC-lined tubes [82], raising the interesting possibility that vessel remodeling could occur through these preformed physical tunnel spaces. Although MT1-MMP was required for the formation of vascular guidance tunnel formation, once they were formed, blockade of MT1-MMP did not affect the ability of ECs to migrate within the spaces [82]. Thus, EC migration events, which are necessary for EC tube formation, are completely inhibited in 3D

collagen matrices if MT1-MMP is blocked from the beginning of culture. However, once vascular guidance tunnels have formed through MT1-MMP-mediated events, ECs are then able to migrate within these physical spaces in an MMP-independent manner [82]. Thus, vascular guidance tunnel spaces are similar to 2D matrix surfaces where EC motility is insensitive to MT1-MMP inhibition (siRNA or inhibitors) [82]. We also observed that while the creation of vascular guidance tunnels by ECs requires the α2β1 integrin, a native collagen-binding integrin, the motility of ECs within MT1-MMP-generated tunnels was not sensitive to inhibition with anti-α2 integrin subunit blocking antibodies. In contrast, EC motility was blocked using anti-αv subunit blocking antibodies [82], which are known to bind cryptic RGD sites that are present within unfolded collagen molecules following proteolysis [29] (an event that controls the generation of the tunnel spaces).

Another important finding from this work is that inhibitors of EC lumen and tube formation including anti-α2 and anti-β1 integrin blocking antibodies, chemical inhibitors of PKC and Src, as well as MT1-MMP inhibitors, completely abrogate the formation of vascular guidance tunnels [82]. Thus, the formation of EC tubes is an obligate step in the formation of vascular guidance tunnels, and thus, these processes are directly linked in some fundamental manner. Several critical questions arise from these studies including how the lumen and tube formation processes are functionally connected with the cell surface proteolytic machinery to create vascular guidance tunnels. Also, what is the functional purpose of vascular guidance tunnels during vascular tube assembly? Very recent work described below provides some insights into these questions.

2.3.7 Cdc42 and MT1-MMP Are Functionally Interdependent Signaling Molecules, Which Are Components of an EC Lumen Signaling Complex That Controls EC Tubulogenesis in 3D Extracellular Matrices

Several new findings begin to shed light into how Cdc42-dependent signaling events, which activate kinase cascades and interact with cell polarity machinery (i.e., Par3, Par6, atypical PKC), intersect with MT1-MMP proteolysis to create EC lumens, tubes, and vascular guidance tunnels [57, 59, 74, 82]. One important point to be made is that the EC lumen and tube formation is a 3D matrix-specific process [27], in that tubulogenesis does not occur on a 2D matrix surface. In contrast, EC motility can occur quite readily on a 2D matrix surface, while it also occurs in 3D matrices, but in a manner that depends on MT1-MMP proteolytic events. Importantly, MT1-MMP activity is not required for EC motility on a 2D matrix surface as discussed above. With this introduction, our new findings show that blockade of MT1-MMP activity using siRNA suppression or MT1-MMP inhibitors leads to marked interference with Cdc42 activation (a critical step necessary for activation of effectors such as Pak2, Pak4, and Par6 that lead to EC tubulogenesis) in 3D collagen matrices [74]. However, this blockade of MT1-MMP does not affect

Cdc42 activation of ECs when they are seeded on 2D collagen surfaces, and coincidently, their motility is also not affected [74]. Expression of the dominant negative MT1-MMP construct also markedly blocks lumen formation and Cdc42 activation [74]. Interestingly, the activation of RhoA, which is not involved in EC lumen and tube formation, is not affected by blockade of Cdc42 or MT1-MMP, nor is it affected by 2D vs. 3D collagen matrices. These results show that MT1-MMP activity is directly coupled to Cdc42 activation in 3D, but not 2D matrices, to control the tube formation process [74]. The reverse is also true, in that, blockade of Cdc42 using siRNA suppression leads to marked decreases in vascular guidance tunnel formation, a consequence of inactivation of MT1-MMP-dependent proteolysis [74]. Thus, this work suggests a new hypothesis, which states that Cdc42 and MT1-MMP are interdependent signaling molecules that control vascular morphogenic events specifically in a 3D matrix environment.

2.3.8 Definition of an EC Lumen Signaling Complex That Controls Vascular Tube Morphogenesis

In order to explain how Cdc42 and MT1-MMP regulate each other during vascular morphogenesis, we wondered if they might be coassociated in a multimolecular complex. During our analysis of Cdc42 activation, we utilized Pak-beads, a specific adsorbant for Cdc42-GTP and Rac1-GTP (the beads do not bind the GDP-bound GTPases or RhoA-GTP). Eluates from these beads, in addition to revealing the presence of Cdc42-GTP, also contained MT1-MMP, the α2β1 integrin, Jam-C, Jam-B, Par3, and Par6b [74] (Fig. 2.3a). We also S-epitope tagged Cdc42, MT1-MMP, and Jam-B, and in all cases, we were able to demonstrate the coassociation of these molecules that constitute the definition of an EC lumen signaling complex in 3D collagen matrices [74]. Each of the molecules is required for lumen formation and disruption of each member leads to blockade of this process [74]. Our evidence suggests that MT1-MMP and α2β1 integrin are tightly associated and that they interact together with Jam-C. SiRNA suppression of either component eliminates their binding to Jam-C and dissociates them from the signaling complex. This suggests that MT1-MMP and α2β1 are interdependent molecules. This makes considerable sense since they both bind to collagen triple helices to perform their functions. Jam-C shows affinity for Jam-B, and together, they bind through their cytoplasmic tails to Par3, a scaffolding protein with affinity for both Par6 and atypical PKC isoforms, such as PKCζ. Par6 binds Cdc42-GTP to complete the signaling complex. The lumen signaling complex then activates the kinase signaling cascade involving PKCε, Src, Pak-2, Pak-4, B-Raf, C-Raf, and Erk1/2 that we have recently identified [74] (Fig. 2.3a). What is particularly interesting is that any situation in which MT1-MMP cannot be cocaptured with Cdc42 is not compatible with the ability of ECs to form tube structures in 3D collagen matrices [74]. Thus, siRNA suppression of any of the components in between MT1-MMP and Cdc42 leads to complete blockade of EC lumen and tube formation. What is intriguing is that these findings indicate that

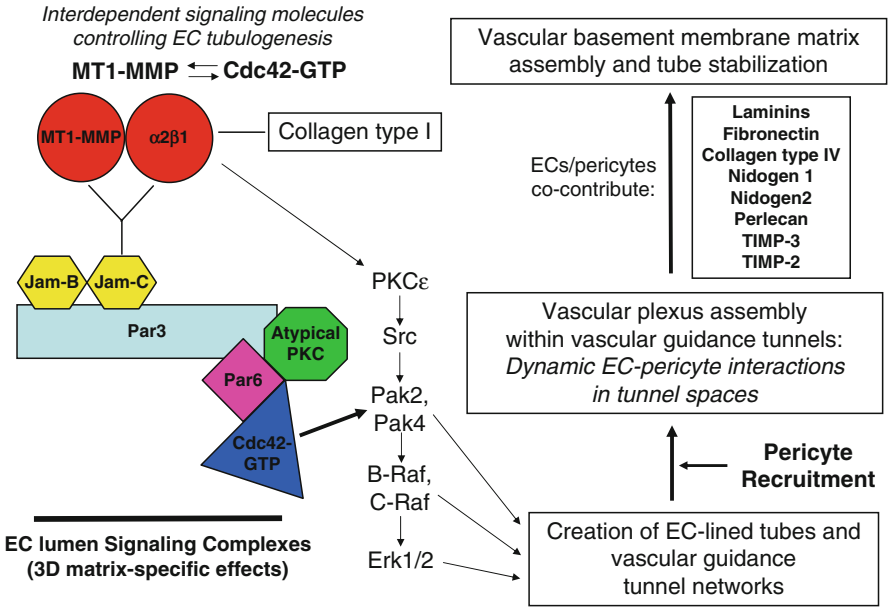

Fig. 2.3 Schematic diagram demonstrates EC lumen signaling complexes, which control EC lumen and tube formation events that allow pericyte recruitment, vascular basement membrane matrix assembly, and tube stabilization in 3D matrices. Cdc42 and MT-MMP are shown to be interdependent molecules that affect each other selectively in 3D matrices. They coassemble through the indicated EC lumen signaling complex, which activates a morphogenic and kinase signaling cascade, leading to tube formation as well as vascular guidance tunnel formation (processes dependent on both Cdc42 and MT1-MMP). Pericytes are recruited into vascular guidance tunnels and through dynamic cell–cell interactions and motility events along the ablumenal EC tube surface lead to the deposition of vascular basement membrane matrices. Both ECs and pericytes cocontribute the indicated basement membrane matrix and MMP inhibitors, which control these events to stimulate vascular tube maturation and stability

a physical interaction between these components is necessary for this process to occur within 3D matrices. It is interesting to speculate that the tensional forces inherent in the linkage between the ECM, EC surface, and underlying cytoskeleton during EC tube morphogenesis are such that a strong physical complex of proteins is necessary to compartmentalize the signaling events necessary to accomplish the appropriate cell shape changes for tube formation and maintenance.

Of particular importance to this lumen signaling complex is the necessity to bridge MT1-MMP together with Cdc42-GTP, and the molecules that control this interaction are α2β1, Jam-C, Jam-B, Par3, and Par6 [74] (Fig. 2.3). Using an epitope-tagged MT1-MMP, we demonstrate that α2β1 binds to MT1-MMP even if Jam-C is knocked down. Interestingly, siRNA suppression of Par3 allows us to detect Jam-B, Jam-C, MT1-MMP, and α2β1 complexes, but this is not compatible with tube formation, since Cdc42 and MT1-MMP are physically disconnected. Knockdown of Jam-C eliminates the binding of epitope-tagged Jam-B to MT1-MMP

and α2β1, showing that Jam-C is present between these molecules. Epitope-tagged Jam-B is unable to bind MT1-MMP when either Jam-C or α2β1 is knocked down, and it is also unable to bind α2β1 when either Jam-C or MT1-MMP is knocked down. Thus, MT1-MMP and α2β1 are interdependent in these complexes such that they are unable to connect to Jam-C and Jam-B unless they are interacting [74]. In each case, these experiments were performed from lysates of ECs undergoing tube formation in 3D collagen matrices [74]. Expression of cytoplasmic tail deleted forms of either Jam-B or Jam-C completely inhibits EC lumen formation and Cdc42 activation as well. This work indicates that interactions between Jam-B and Jam-C with Par3 are necessary for this process. A matter of great interest to us is to determine the identity of the Cdc42 guanine exchange factor (GEF) that is responsible for Cdc42 activation during these events. Also, we wish to determine how this Cdc42 GEF interacts with the EC lumen signaling complex, since we hypothesize that it shows affinity for one of the components within the complex. In conclusion, our data define an EC lumen signaling complex that is responsible for human ECs to form lumen and tube structures in a 3D matrix environment [74] (Fig. 2.3). Considerable future work is necessary to identify other components of this signaling complex as well as to identify both positive and negative regulators of the complex, which modulate these processes.

2.3.9 Critical Role for MMPs in the Molecular Control of Vascular Tube Regression Responses in 3D Collagen Matrices

A critically important direction of research is to understand how blood vessels regress under physiologic and pathophysiologic situations. Physiologic regression occurs with hyaloid vessels in the developing eye, during the menstrual cycle in both the endometrium and ovaries, and during vascular remodeling events in development [25]. Pathophysiologic regression characteristically occurs during wound repair and during processes such as hypertension and diabetes where vessel densities can decrease particularly in the distal limbs. Also, there have been considerable efforts to induce vascular tube regression responses in the context of the tumor vasculature by disrupting VEGF and PDGF signaling [14]. An important point here is that it is critical to understand how vascular regression is controlled at the molecular level in much the same way that the studies described earlier have been performed to determine how blood vessels form.

A variety of past and recent studies have identified MMPs that regulate vascular tube regression events [30, 76, 92]. A number of years ago, we identified the secreted MMPs, MMP-1 and MMP-10, as being involved in vascular tube regression responses in vitro [25, 26, 30, 76] We showed that these enzymes were secreted as proenzymes and that they need to be activated by serine proteases, such as plasminogen/plasmin and plasma kallikrein, to cause vascular tube collapse and regression [76]. Disruption of their activity by TIMP-1 (which blocks both MMP-1

and MMP-10) or blockade of serine protease activity leads to inhibition of the MMP-1- and MMP-10-dependent regression response. Other studies using the aortic ring model reached similar conclusions with the exception that MT1-MMP was also found to be involved in both tube formation and regression [4]. We also identified ADAM-15 as being involved in the vascular regression response in a manner similar to that of MMP-1 and MMP-10 [77]. Interestingly, siRNA suppression of either MMP-1 or MMP-10 did not affect tube formation but markedly blocked tube regression following addition of plasminogen or plasma kallikrein to the serum-free media system [76]. Interestingly, a mouse knockout of histone deacetylase 7 (HDAC7) caused a vascular hemorrhage phenotype in vivo during vascular development, which led to embryonic lethality [18]. siRNA suppression of HDAC7 resulted in marked increases in MMP-10 and marked decreases in TIMP-1 expression, which led to the vascular developmental regression phenomenon [18].

Of great interest is that the MMP-1 and MMP-10 regression phenomena are strongly abrogated in our in vitro model when pericytes are added along with the ECs [77]. Pericyte recruitment to the tubes occurs, and they become much more resistant to pro-regressive stimuli. Thus, our model mimics that observed in vivo where EC tubes without pericytes are much more susceptible to regression [5, 12, 13]. Interestingly, tumor vessels have associated pericytes, but the interactions are abnormal. In this case, despite these abnormalities, the tumor vessels persist, which may relate to the fact that many aggressive tumors overproduce TIMP-1 [87], which can interfere with the MMP-1 and MMP-10-dependent regression system [25]. We also observed that EC–pericyte interactions upregulate the production of EC TIMP-2 and pericyte TIMP-3, which together control how EC–pericyte interactions protect against pro-regressive MMP-1 and MMP-10 and also ADAM-15 [77]. Pericytes are a rich source of TIMP-3 [77], which is interesting because of its ECM-binding ability (i.e., ability to bind cell surfaces and basement membrane matrices) and its dual ability to inhibit soluble and membrane MMPs as well as membrane ADAM proteinases [7]. In addition to interfering with pro-regressive stimuli, TIMP-3 and TIMP-2 block MT1-MMP to interfere with further EC tube formation. Thus, these TIMPs contribute to vascular tube stabilization by inhibiting both vascular tube regression phenomena as well as further vascular tube morphogenesis. In further support of their latter influence, both TIMP-2 and TIMP-3 are also antagonists of VEGFR2 signaling [71, 80], a critical promorphogenic signaling receptor.

One of the very interesting questions for future work is to assess in more functional detail how MMPs and TIMPs interface with other key vascular regression factors such as soluble VEGFR1. Administration of this soluble VEGF antagonist leads to vascular regression in many instances including tumor vessels [66]. Also, elevated levels of this antagonist along with other soluble receptors are observed in women with preeclampsia where placental vascular insufficiency is a pathogenic feature. There are multiple VEGFR1 splice variants known that act as “VEGF traps,” and the question concerning the functional roles of these variants is fascinating since they vary in their C-terminal sequences [78]. It is interesting to speculate that these C-terminal sequences may confer specific targeting sequences for extracellular

molecules such as ECM or cell surfaces to affect function. Of interest is whether any of these "VEGF traps" are MMP targets and whether vascular regression could be affected by release of such traps. Also, VEGF itself is known to be cleaved by MMP-3 [61] (related to MMP-10), which may make it more susceptible to inhibition by VEGFR1 isoforms. Clearly, this direction of research is important for future work to further our understanding of how vascular regression is regulated at a molecular level.

2.3.10 Critical Functional Role for EC-Generated Vascular Guidance Tunnels During Blood Vessel Assembly in 3D Matrices

As shown in Fig. 2.3, ECs utilize a lumen signaling complex to form tubes in 3D matrices while at the same time generating networks of vascular guidance tunnel spaces. ECs are able to migrate through these spaces in an MMP-independent manner. We have also shown that ECs can regrow within these spaces following tube collapse. EC-lined tubes were treated with thrombin, which reversibly causes tube collapse, leaving rounded up ECs within tunnel spaces [82]. After inhibition of thrombin with the thrombin inhibitor hirudin, the ECs regrow within tunnels to reassemble the collapsed tube [82]. Thus, preexisting tunnel spaces are matrix conduits that allow for rearrangement of tubes and migration of ECs, and thus, they are used for tube remodeling events. In early vascular development, there is considerable evidence for dramatic tube network remodeling that occurs following the onset of flow [20, 64, 73], and we hypothesize that this is possible in large part due to the presence of vascular guidance tunnels, which allows ECs to rapidly rearrange to accommodate the flows and pressure forces that are applied to the network. Also, at this stage of development, the ECM is likely to be elastic, and thus, the forces generated may be able to expand lumen or tunnel width by mechanical distension. We have also shown that groups of cells comprising a tube structure can migrate together through tunnel spaces to move and connect with adjacent EC tubes to regulate such vascular remodeling events [82]. As mentioned earlier, the EC lumen and tube formation process generates more vascular guidance tunnels than those that are utilized at any given time, which further suggests that this occurs to accommodate the necessary vascular remodeling events involved in generating a proper microcirculatory network.

Also, vascular guidance tunnels are important to consider in the context of vascular tube regression and regrowth of vessels. One of the ways to eliminate the possibility of vascular regrowth following regression events would be to induce regression of not only vascular tubes but also vascular guidance tunnels. In fact, the MMP-1 and MMP-10 regression mechanism discussed earlier does cause collapse of both structures. The presence of pericytes, which blocks the regression event, can thus protect not only the vascular tube structure but also the integrity of the vascular guidance tunnels. Of interest here is that tumor vessels are highly resistant

to vascular regression due to their production of regression inhibitors such as TIMP-1. Again, TIMP-1 is capable of protecting both the vessels and tunnel spaces. Also, when tumors are treated with vascular regression agents such as VEGF or VEGFR2 antagonists, vessels regress, but they can rapidly regrow (following withdrawal of the regression agent) in a similar fashion to recapitulate the original pattern of vessels [66]. This appears to occur through vascular guidance tunnels that were generated during initial tumor vessel formation. So, an important therapeutic consideration here would be to devise approaches to induce both vessel and vascular guidance tunnel regression. In this way, vessel regrowth is less likely to occur, allowing a better therapeutic opportunity to treat the tumors, their vascular supplies, and existing matrix conduits, which facilitate vascular regrowth.

It is also important to consider how events such as arteriovenous identity might be regulated by vascular guidance tunnels. The tunnels represent a 2D matrix surface in a 3D matrix environment [82]. There is important data showing that ephrinB2 (an arterial marker) and EphB4 (a venous marker) represent a repulsive signaling pair, which appears early in development to control the development of A-V identity [40]. These repulsive interactions allow differential cell sorting, and early in development, ECs expressing these markers are intermixed, but over time, they sort out and become segregated to either the arterial or venous side [40, 47, 56]. They also appear to sort very early even at the level of initial cardinal vein formation due to sprouting from the developing aorta. This process is very analogous to what has been described for lymphatic sprouting and development from the cardinal vein [88]. Notch signaling appears to control this phenomenon, and when overactive Notch-4 is produced in ECs, venous ECs inappropriately express ephrinB2, and this contributes to the development of arteriovenous malformations [56]. Of great interest is that many of these lesions will regress following withdrawal of the overactive Notch4. The important point to be made is that the repulsive ephrinB2–EphB4 interactions are occurring within vascular guidance tunnels (formed as a result of EC tube assembly) and that the ability to sort following such interactions requires the ability of ECs to move around on 2D matrices at the vessel wall surface. Also, the interactions are secondary to ECs contacting each other.

However, the concept of vascular guidance tunnels extends to recruitment and sorting of mural cells within the vessel wall as well. EphrinB2 is also expressed on vascular smooth muscle cells with selectivity in arteries, so similar repulsive interactions are likely to control this cell distribution as well [35]. What is interesting here is that this type of interaction would require that mural cell recruitment to EC-lined tubes and within vascular tunnel spaces occurs in a polarized fashion exclusively on the EC ablumenal surface. In fact, we have recently discovered that this is precisely what occurs during pericyte recruitment to EC-lined tubes. They are recruited within vascular guidance tunnels and are localized only on the EC tube ablumenal surface [81]. Thus, mural cells could sort through not only repulsive interactions with each other but also secondary to repulsive interactions with ECs. The vascular guidance tunnel matrix conduit is a critical ECM structure that is necessary for EC–EC, mural cell–mural cell, and EC–mural cell interactions to occur and to also allow for motility events required for proper sorting. In support

of this possibility is the fact that ECs and mural cells are highly dynamic during vascular tube assembly, and in fact, we have recently shown that both ECs and pericytes are rapidly migrating in the ECM as well as within vascular guidance tunnels during tube coassembly and maturation events [81]. Also, ECs have been shown by a number of groups to be rapidly migrating in vivo during vascular development to regulate both tube assembly and vascular remodeling [20, 64].

2.3.11 *Pericyte Recruitment to Vascular Guidance Tunnels Induces Vascular Tube Stabilization*

Many studies indicate that microvessels covered with pericytes are not only more stable to pro-regressive stimuli but they also show reduced vascular permeability indicative of tube stabilization. Different vascular beds have varying pericyte numbers covering capillary networks, although many have approximately 20–25% coverage of pericytes relative to ECs. Individual pericytes can span to touch multiple ECs, which resemble other types of supporting cells such as glia in the nervous system interacting with multiple neurons. Tissues such as the central nervous system including the retina have a very high pericyte to EC ratio, which approaches 1:1. Thus, these interactions account in part for the blood–brain barrier with strongly increased permeability barrier functions relative to other vascular beds. Considerable work suggests that the high VEGF environment of tumors is one reason why pericyte coverage is decreased compared to normal vascular beds [42, 54]. Treatment with VEGF antagonists has led to the finding that pericyte coverage increases, which results in improved microcirculatory function (i.e., vascular normalization) [54]. This approach has represented a new strategy to improve drug delivery into the tumor microenvironment, since poor perfusion exists due to the abnormal microcirculatory network that is present.

2.3.12 *Molecular Mechanisms Underlying Why Pericytes Are Able to Stabilize EC-Lined Tube Networks*

A major question that has not been sufficiently addressed is why pericyte coverage stabilizes vessels and what their functions are when they arrive at the EC ablumenal surface. To address this question, we have established novel EC–pericyte coculture models in 3D collagen matrices. We have developed systems using either bovine retinal pericytes or human brain pericytes. In each case, the pericyte populations express the pericyte markers, NG2 proteoglycan, 3G5 ganglioside, smooth muscle actin and desmin. Perhaps the most important function of pericytes is to recruit to microvascular capillary beds. Using our model of EC vasculogenic tube assembly, we have developed a system whereby we randomly mix together ECs and pericytes

at a 5:1 or 5:1.25 ratio (i.e., 20–25% pericytes compared to 100% of ECs). Remarkably, the ECs form tube networks, and then, pericytes are recruited to these tubes [81] (Fig. 2.4). This ratio of ECs to pericytes is particularly optimal, and the reasons for this are currently not clear. It may be that too many pericytes (through their production of TIMP-3) [77] interfere with morphogenesis by inhibiting MT1-MMP-dependent signaling, or that they are physically in the way and counteract

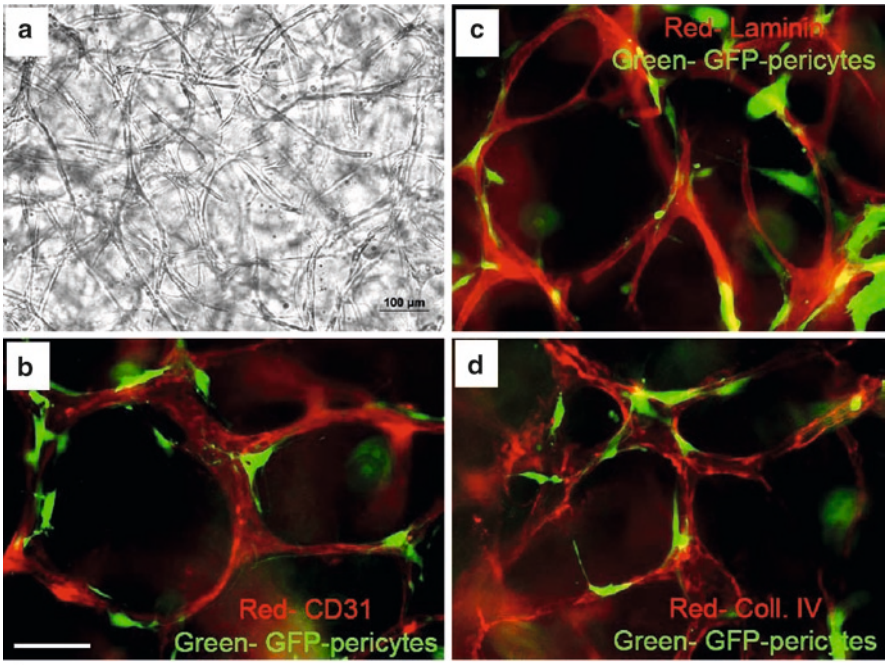

Fig. 2.4 EC–pericyte tube coassembly in 3D collagen matrices leads to vascular basement membrane matrix deposition and tube stabilization. ECs were cocultured with bovine retinal pericytes (20% pericytes relative to 100% ECs) in 3D collagen matrices, and after 5 days of culture, the cells were fixed and photographed (**a**) or were processed for immunofluorescence microscopy. The pericytes were labeled with GFP, while the ECs and extracellular matrix were stained with the indicated antibodies. Fluorescent images were overlaid to assess the relationship of the ECs and matrices with the presence of pericytes. (**b**) CD31 staining to detect EC-lined tubes. *Bar* equals 50 µm. (**c**) Laminin and (**d**) collagen type IV staining to detect vascular basement membrane matrix assembly. In the latter two cases, no detergent was utilized so that only extracellular antigens would be detected. (**e**) RT-PCR and Western blot analyses of EC-only versus EC–pericyte cocultures demonstrate marked changes in integrin and basement membrane matrix protein expressed during this process

the ability of ECs to find their neighbors to properly form multicellular tubes. It is clear that too many pericytes can disrupt EC–pericyte tube coassembly.

We further made the observation that EC tubes from EC-only cultures eventually become much wider than EC tubes from EC–pericyte cocultures. We examined this issue over time and observed that vascular diameters reached a range of 20–25 μm in EC–pericyte cocultures, which are vessel diameters observed in vivo during vasculogenesis, while in EC-only cultures, diameters can reach 80–100 μm over a 5-day period [81]. Thus, pericytes have a marked ability to negatively regulate vascular tube diameters, which may have to do with the induction of TIMP-2 and TIMP-3. As discussed earlier, they are induced in EC–pericyte cocultures [77] and can inhibit and restrict EC lumen diameters. A number of studies indicate that vascular diameters are greater when pericyte recruitment is reduced or when ECM components such as fibronectin are knocked out of ECs during vasculogenesis in vivo [6, 36].

The mechanisms whereby pericytes are recruited to EC-lined tubes remain unclear, although the literature supports the idea that PDGF plays a role [5, 15, 48]. In fact, in ongoing studies of our laboratory, it is clear that about one half of pericyte recruitment to EC-lined tubes can be blocked by PDGF-BB antagonists. This finding is consistent with the work showing that EC-specific knockout of PDGF-BB leads to about a 50% decrease in pericyte coverage of vessels [15]. Of interest is that these mice show primary defects in microvessel beds (where pericyte coverage is present), while larger vessels are much less affected. This microvascular deficiency phenotype manifests particularly in the kidney and central nervous system, which strongly resembles that observed in diabetic microangiopathy [15]. Loss of pericytes is a major pathogenic cause of this type of microvascular disease [45]. It is important to further understand the signaling mechanisms that underlie pericyte recruitment to EC-lined tubes to both identify other factors that regulate this recruitment and understand how pericytes invade 3D matrices to recruit to these tubes. This is currently a major research direction of our laboratory.

2.3.13 Pericyte Recruitment to EC-Lined Tubes Stimulates ECM Remodeling Events and Vascular Basement Membrane Matrix Assembly

Using our new model of EC–pericyte tube coassembly, we sought to identify how pericytes contribute to vascular tube maturation and stabilization events. At different time points of tube coassembly, we performed transmission electron microscopy and immunofluorescence microscopy to examine if basement membrane matrix assembly was affected [81]. In Fig. 2.4b, we show immunostaining for the EC marker CD31, while the pericytes stably express green fluorescent protein (GFP). This image shows EC tube networks that have associated pericytes at day 5 of culture. We also show a light microscopy image of the coculture system in Fig. 2.4a. As shown in Fig. 2.4c, d, there is marked deposition of laminin and collagen type IV,

two critical basement membrane matrix components. In addition, we have recently reported that fibronectin, nidogen-1, nidogen-2, and perlecan were also deposited around EC-lined tubes only when pericytes were cocultured with ECs [81] (Fig. 2.4e). Also, we demonstrated that basement membrane matrices were observed by transmission electron microscopy only when EC–pericytes were cocultured [81], and we have never observed basement membrane deposition in the absence of pericytes in electron microscopic studies over many years. Furthermore, we confirmed our results in vivo and demonstrated that pericyte recruitment to developing quail EC tubes directly correlates with vascular basement membrane assembly at day 7 of embryonic development [81]. Prior to pericyte recruitment, no vascular basement membranes around EC tubes were observed in vivo [81].

To perform the immunostaining experiments, we utilized detergent-free conditions so that we examine only ECM that is deposited extracellularly [81] and not intracellular ECM molecules. We utilized this approach in our in vitro 3D cultures and also stained an in vivo tissue, the quail chorioallantoic membrane, in the same manner [81]. This is a key point because we have shown that extracellular deposition of vascular basement membrane matrix is markedly stimulated by pericyte recruitment [81]. Although increased production of individual basement membrane components was observed, this upregulation was not as marked as that observed in the immunostaining experiments. We utilized our human EC and bovine pericyte coculture system to determine which cell type produces particular ECM components over time to regulate basement membrane matrix assembly (using species-specific RT-PCR primer sets) [81]. Major findings were that ECs increased the production of fibronectin selectively in the presence of pericytes (and not in their absence) and that nidogen-1 was induced in pericytes that occurred selectively in the presence of ECs [81]. We also observed induction of particular laminin isoforms as well as perlecan at the mRNA level, which occurred through EC–pericyte interactions. Thus, EC–pericyte contacts during tube coassembly events affected mRNA and protein levels for key basement membrane matrix molecules [81]. Interestingly, both fibronectin and nidogen-1 are known to bridge key molecules that compose the basement membrane matrix [24, 68]. Fibronectin shows affinity for collagen type IV and perlecan, while nidogen-1 binds collagen type IV and laminin isoforms. It is possible that these ECM components initiate a nidus that leads to the assembly of the insoluble matrix surrounding the EC-lined tubes that controls basement membrane deposition as observed by electron microscopy. Most ECM proteins have self-assembly functions, but they need to interact with another to create the complex meshwork that is characteristic of fully assembled basement membrane matrices. It is also intriguing that collagen type IV, which is a fundamental basement membrane component that is greatly responsible for its structural integrity, shows affinity for both fibronectin and nidogen-1, which are selectively affected by EC–pericyte interactions [81].

One question that is of great interest is how continuous basement membrane assembly is accomplished along EC-lined tubes despite the fact that pericytes are only one fifth to one fourth of the total number of ECs. We believe that this occurs because of the motility of pericytes along the ablumenal EC tube surface, which

scan along the tubes to stimulate the deposition of the basement membrane in a continuous manner [81]. Furthermore, the movement of both pericytes and ECs along each other within vascular guidance tunnels will almost certainly exert mechanical stress on the newly deposited ECM to facilitate basement membrane assembly. Thus, it is intriguing that fibronectin, a mechanosensitive ECM component and whose assembly is facilitated by cell-exerted tensional forces, is a critical protein that only strongly deposits around EC-lined tubes when pericytes are present along the tube surface [81]. Another interesting possibility is that the presence of pericytes along the EC ablumenal surface (and in a polarized fashion) [81] may stimulate the directional secretion and deposition of basement membrane components from both cell types toward the other. Thus, both mechanical forces and vectorial secretion mechanisms might play a fundamental role in how pericyte recruitment to EC-lined tubes leads to vascular basement membrane matrix assembly, a major step toward further tube maturation and stabilization. As discussed above, the deposition of laminin isoforms may represent stimuli for ECs to stop undergoing morphogenesis to become a stable tube structure with a quiescent layer of ECs. Another molecule, TIMP-3, whose deposition in the basement membrane would lead to a similar phenotype, binds basement membrane perlecan as well as other components to suppress vascular morphogenesis [77]. The role of these individual components as well as the questions raised above need to be investigated in more detail in future studies.

2.3.14 Critical Functional Role for Fibronectin Matrix Assembly During Vascular Development

A series of studies indicate that fibronectin gene knockouts result in an embryonic lethal phenotype during vasculogenesis [36, 51]. Also, evidence has been presented that fibronectin alternative splicing (IIIA and IIIB isoforms) is important during these events [6]. Further work will be necessary to elucidate why these particular fibronectin isoforms are playing a role during these processes. Vessel diameters from these animals are extremely wide, which as discussed above may be secondary to defects in proper EC–pericyte interactions that result from abnormal basement membrane formation or reduced adhesiveness to these remodeled, but abnormal matrices. Also, EC-specific knockout of the α5 integrin also shows phenotypes that are manifested in a wider vessel phenotype, which appears to be further enhanced by knockout of αv integrins, another class of fibronectin receptors [51].

Since we observed strong fibronectin upregulation in ECs as well as deposition selectively in EC–pericyte cocultures, we performed additional experiments to determine if fibronectin matrix assembly affected EC tube maturation events in this system. We incorporated a 70 kDa N-terminal fragment of fibronectin, which is known to block fibronectin matrix assembly [89], to assess if it had any influence during these events. Our work shows that disruption of fibronectin matrix assembly affects EC tube width by significantly increasing it [81], suggesting that deposited

fibronectin may play a role in restricting vascular tube diameter. Interestingly, this treatment also markedly disrupted collagen type IV matrix deposition [81] and had a lesser influence on laminin assembly. In support of these findings are experiments showing that selective blockade of EC α5β1 integrin, a fibronectin receptor, also significantly increases vascular tube width in the EC–pericyte cocultures, but not in the EC-only cultures, where this receptor appears to play minor role [81].

2.3.15 *Important Functional Role for Collagen Type IV in EC–Pericyte Tube Coassembly and Maturation Events*

In addition to the critical roles for fibronectin and nidogen-1 as bridging proteins for ECM assembly, collagen type IV is another key basement membrane component with affinity for both of these bridging molecules. Interestingly, pericyte-induced fibronectin assembly around developing tubes appears to be involved in collagen type IV assembly [81]. To assess which cell types contributed the collagen type IV that was deposited extracellularly during these events, we performed siRNA suppression experiments revealing that ECs were the predominant source of collagen type IV [81]. Knockdown of collagen type IV in ECs strongly decreased collagen type IV assembly around tubes, and this resulted again in increased vascular tube width, an indicator of dysfunctional interactions between ECs and pericytes [81]. Knockdown of collagen type IV in pericytes had lesser but nonetheless significant inhibitory effects on both collagen type IV deposition and vessel tube width [81], suggesting that both ECs and pericytes contribute collagen type IV during basement membrane assembly.

2.3.16 *Pericyte TIMP-3 Contributes to Vascular Basement Membrane Matrix Assembly by Increasing Collagen Type IV Deposition or Stability*

Another contributing role of pericytes during this process is the delivery of TIMP-3, a basement membrane- and ECM-binding protein. As discussed earlier, TIMP-3 plays a critical role in pericyte-induced tube stabilization by blocking MMP-1, MMP-10, and ADAM-15, which promote vascular regression events, as well as by inhibiting further morphogenic events by blocking MT1-MMP [77]. In this new work, we show that TIMP-3 plays yet another role by facilitating collagen type IV assembly in EC–pericyte cocultures. siRNA suppression of pericyte TIMP-3 results in markedly decreased collagen type IV assembly [81], which may be due to less deposition or increased turnover due to lack of inhibition of MT1-MMP (which degrades type IV collagen). With decreased collagen type IV assembly around EC tubes, there was a significant increase in vessel diameter [81]. Thus, collagen

type IV assembly may be a primary determinant of vascular tube diameter. It is particularly intriguing to again consider the fact that EC-only tubes, which are not surrounded by basement membranes, become very wide during morphogenic events, suggesting a lack of inhibitory signals. In contrast, EC–pericyte coassembled tubes are much narrower, suggesting that these inhibitory signals are present as a result of basement membrane assembly and signals are delivered to the ECs to suppress further morphogenesis and promote maturation. The marked differences in vessel diameter in these two situations demonstrate functional evidence for both the production and deposition of basement membrane matrices and also reveal that ECs recognize the proteins and respond by restricting tube diameter. Decreased vessel diameter and tube network areas are measurements that reflect the ability of pericytes to negatively regulate vascular tube morphogenesis while preventing pro-regressive stimuli from acting. Thus, EC tube diameter is also an important indicator of dysfunctional EC–pericyte interactions that lead to a variety of vessel abnormalities (which frequently show increased vessel diameter). In addition, it is well known that basement membranes can facilitate cell polarity functions by enhancing cell–cell contacts mediated through junctional contacts, such as through adherens and tight junctional proteins. Although, the EC apical membrane domain has been difficult to define in molecular terms, clear evidence of EC polarization in our coculture model is the deposition of basement membrane matrices specifically to the ablumenal surface and the prior recruitment of pericytes to the same ablumenal membranes [81].

2.3.17 Specific Upregulation of EC and Pericyte Integrins Recognizing Basement Membrane Matrices During EC–Pericyte Tube Coassembly in 3D Collagen Matrices

Again using our coculture system with human ECs and bovine pericytes, we assessed how EC vs. pericyte integrins were regulated during this process. We assessed mRNA levels and performed function blocking experiments with anti-integrin monoclonal antibodies. As discussed above, blocking antibodies to the $\alpha5\beta1$ integrin had function blocking effects that selectively occurred in the EC–pericyte cocultures, but not in EC-only cultures [81]. Interestingly, the EC $\alpha5$ integrin subunit was induced at the mRNA level in EC–pericyte cocultures, but not in EC-only cultures where it was downregulated. An important theme which emerged from these studies is that integrins, which recognize the newly remodeled ECM assembling between ECs and pericytes, were induced, while others that recognized collagen type I matrices, such as the $\alpha2$ integrin subunit from ECs, were downregulated [81] (Fig. 2.4e). Thus, as basement membranes assemble around EC tubes, the direct interaction of ECs with collagen type I decreases, while their contact with basement membrane matrices increases. Concomitantly, we observed increases in the expression of integrin $\alpha5$, $\alpha3$, and $\alpha6$ from ECs, which can recognize fibronectin, nidogens, and laminin isoforms,

while α5, α3, α6, and α1 integrin subunits were increased from pericytes, which recognize fibronectin, nidogens, laminin isoforms, and collagen type IV [81]. We also observed functional effects of these integrins, since blocking antibodies to the α5, α3, α6, and α1 integrin all caused abnormalities in the tube maturation process by significantly increasing tube width [81]. None of these antibodies has any influence on EC-only cultures, which are solely dependent on the collagen-binding integrin α2β1 [81]. These data strongly indicate that the purpose of the multiple β1 integrins on the EC cell surface is to recognize key ECM components that they encounter at different stages of the tube morphogenic and maturation process. When they are exposed to collagen type I matrices, which serve as a strong agonist for tubulogenesis, they utilize collagen-binding integrins such as α2β1. However, when EC-lined tubes attract pericytes, ECM remodeling occurs that induces deposition of basement membrane matrices that are recognized by different sets of integrins such as α5β1 (a fibronectin receptor), α3β1 (a nidogen and laminin isoform receptor), α6β1 (a laminin isoform receptor), and α1β1 (a collagen type IV, collagen type I, and laminin receptor) [81]. Interestingly, α1β1 appears to be predominantly pericyte-derived during the EC–pericyte tube coassembly process, and thus, the effects of blocking antibodies that have been observed may be due to an inhibitory influence on pericyte recognition of basement membrane matrices during these events [81]. Also, the EC-dependence on α2β1, which is continuously observed over time in EC-only cultures, is lost with time in EC–pericyte cocultures as basement membrane matrix assembly occurs and exposure of ECs to collagen type I is strongly diminished. In conclusion, our findings show that EC–pericyte interactions control vascular basement membrane matrix assembly and that concomitant changes in EC and pericyte integrins occur to recognize this newly remodeled matrix to facilitate further tube maturation and stabilization events.

2.4 Future Directions

It is clear that major advances have occurred over the past two decades in elucidating the molecular mechanisms that underlie the ability of vessels to form, mature, and regress. In our view, it is this type of mechanistic research that will most likely lead to the generation of novel therapeutic strategies to manipulate blood vessels in the context of disease. It is also critical that both in vitro and in vivo approaches be continued and appreciated by individuals who focus on either side of these strategies. As in vitro models and experimental strategies have evolved, it is more and more evident that very rapid advances are occurring in this area. Particular assay systems have repeatedly been shown to accurately reflect the biology of developing and postnatal vessels in vivo, and thus, these systems represent a critical experimental approach to rapidly advance the field.

In terms of key future directions, it is clear that more cytokine and growth factor research is necessary, since the angiogenic cytokines that have been described to date are insufficient to explain many aspects of these processes. Another major area

of interest is how ECM binds to particular cytokines to regulate their function and how regression phenomena might be caused by perturbations in these types of interactions. This could apply to either stimulatory or inhibitory cytokine regulators. Thus, how cytokine receptor signaling interfaces with integrin signaling remains a direction of major importance. Another important concept that needs to be stressed is that molecules (cytokines, MMPs, ECM) work together in groups, and it is critical to understand how such signals integrate to provide the biological responses that are observed. The single molecule analysis that is inherent to many studies can be quite misleading in terms of our understanding of complex biological events. Systems approaches (i.e., DNA microarray, miRNA regulation, and proteomic approaches), which are difficult to perform well, are particularly important directions in future work to identify key new signaling pathways that regulate vascularization responses and to assess how these are altered in vascular disease.

Acknowledgments This work was supported by NIH grants HL79460, HL59373, and HL87308 to G.E. Davis. A.N. Stratman was supported by a AHA predoctoral fellowship #09PRE2140028.

References

1. Adams RH, Alitalo K (2007) Molecular regulation of angiogenesis and lymphangiogenesis. Nature Reviews 8(6): 464–478.
2. Alavi A, Hood JD, Frausto R, Stupack DG, Cheresh DA (2003) Role of Raf in vascular protection from distinct apoptotic stimuli. Science (New York, NY) 301(5629): 94–96.
3. Aplin AC, Fogel E, Zorzi P, Nicosia RF (2008) The aortic ring model of angiogenesis. Methods in Enzymology 443: 119–136.
4. Aplin AC, Zhu WH, Fogel E, Nicosia RF (2009) Vascular regression and survival are differentially regulated by MT1-MMP and TIMPs in the aortic ring model of angiogenesis. American Journal of Physiology 297(2): C471–C480.
5. Armulik A, Abramsson A, Betsholtz C (2005) Endothelial/pericyte interactions. Circulation Research 97(6): 512–523.
6. Astrof S, Crowley D, Hynes RO (2007) Multiple cardiovascular defects caused by the absence of alternatively spliced segments of fibronectin. Developmental Biology 311(1): 11–24.
7. Baker AH, Edwards DR, Murphy G (2002) Metalloproteinase inhibitors: biological actions and therapeutic opportunities. Journal of Cell Science 115(Pt 19): 3719–3727.
8. Bayless KJ, Davis GE (2002) The Cdc42 and Rac1 GTPases are required for capillary lumen formation in three-dimensional extracellular matrices. Journal of Cell Science 115(Pt 6): 1123–1136.
9. Bayless KJ, Davis GE (2003) Sphingosine-1-phosphate markedly induces matrix metalloproteinase and integrin-dependent human endothelial cell invasion and lumen formation in three-dimensional collagen and fibrin matrices. Biochemical and Biophysical Research Communications 312(4): 903–913.
10. Bayless KJ, Salazar R, Davis GE (2000) RGD-dependent vacuolation and lumen formation observed during endothelial cell morphogenesis in three-dimensional fibrin matrices involves the alpha(v)beta(3) and alpha(5)beta(1) integrins. The American Journal of Pathology 156(5): 1673–1683.
11. Bell SE, Mavila A, Salazar R, Bayless KJ, Kanagala S et al. (2001) Differential gene expression during capillary morphogenesis in 3D collagen matrices: regulated expression of genes involved in basement membrane matrix assembly, cell cycle progression, cellular differentiation and G-protein signaling. Journal of Cell Science 114(Pt 15): 2755–2773.

12. Benjamin LE, Hemo I, Keshet E (1998) A plasticity window for blood vessel remodelling is defined by pericyte coverage of the preformed endothelial network and is regulated by PDGF-B and VEGF. Development 125(9): 1591–1598.
13. Benjamin LE, Golijanin D, Itin A, Pode D, Keshet E (1999) Selective ablation of immature blood vessels in established human tumors follows vascular endothelial growth factor withdrawal. The Journal of Clinical Investigation 103(2): 159–165.
14. Bergers G, Song S, Meyer-Morse N, Bergsland E, Hanahan D (2003) Benefits of targeting both pericytes and endothelial cells in the tumor vasculature with kinase inhibitors. The Journal of Clinical Investigation 111(9): 1287–1295.
15. Bjarnegard M, Enge M, Norlin J, Gustafsdottir S, Fredriksson S et al. (2004) Endothelium-specific ablation of PDGFB leads to pericyte loss and glomerular, cardiac and placental abnormalities. Development 131(8): 1847–1857.
16. Bokoch GM (2003) Biology of the p21-activated kinases. Annual Review of Biochemistry 72: 743–781.
17. Carmeliet P (2005) Angiogenesis in life, disease and medicine. Nature 438(7070): 932–936.
18. Chang S, Young BD, Li S, Qi X, Richardson JA et al. (2006) Histone deacetylase 7 maintains vascular integrity by repressing matrix metalloproteinase 10. Cell 126(2): 321–334.
19. Chun TH, Sabeh F, Ota I, Murphy H, McDonagh KT et al. (2004) MT1-MMP-dependent neovessel formation within the confines of the three-dimensional extracellular matrix. The Journal of Cell Biology 167(4): 757–767.
20. Czirok A, Zamir EA, Szabo A, Little CD (2008) Multicellular sprouting during vasculogenesis. Current Topics in Developmental Biology 81: 269–289.
21. Davis GE (2010) Matricryptic sites control tissue injury responses in the cardiovascular system: relationships to pattern recognition receptor regulated events. Journal of Molecular and Cellular Cardiology 48(3): 454–460.
22. Davis GE, Camarillo CW (1996) An alpha 2 beta 1 integrin-dependent pinocytic mechanism involving intracellular vacuole formation and coalescence regulates capillary lumen and tube formation in three-dimensional collagen matrix. Experimental Cell Research 224(1): 39–51.
23. Davis GE, Bayless KJ (2003) An integrin and Rho GTPase-dependent pinocytic vacuole mechanism controls capillary lumen formation in collagen and fibrin matrices. Microcirculation 10(1): 27–44.
24. Davis GE, Senger DR (2005) Endothelial extracellular matrix: biosynthesis, remodeling, and functions during vascular morphogenesis and neovessel stabilization. Circulation Research 97(11): 1093–1107.
25. Davis GE, Saunders WB (2006) Molecular balance of capillary tube formation versus regression in wound repair: role of matrix metalloproteinases and their inhibitors. The Journal of Investigative Dermatology. Symposium Proceedings 11(1): 44–56.
26. Davis GE, Senger DR (2008) Extracellular matrix mediates a molecular balance between vascular morphogenesis and regression. Current Opinion in Hematology 15(3): 197–203.
27. Davis GE, Bayless KJ, Mavila A (2002) Molecular basis of endothelial cell morphogenesis in three-dimensional extracellular matrices. The Anatomical Record 268(3): 252–275.
28. Davis GE, Koh W, Stratman AN (2007) Mechanisms controlling human endothelial lumen formation and tube assembly in three-dimensional extracellular matrices. Birth Defects Research. Part C, Embryo Today 81(4): 270–285.
29. Davis GE, Bayless KJ, Davis MJ, Meininger GA (2000) Regulation of tissue injury responses by the exposure of matricryptic sites within extracellular matrix molecules. The American journal of pathology 156(5): 1489–1498.
30. Davis GE, Pintar Allen KA, Salazar R, Maxwell SA (2001) Matrix metalloproteinase-1 and -9 activation by plasmin regulates a novel endothelial cell-mediated mechanism of collagen gel contraction and capillary tube regression in three-dimensional collagen matrices. Journal of Cell Science 114(Pt 5): 917–930.
31. Dejana E, Tournier-Lasserve E, Weinstein BM (2009) The control of vascular integrity by endothelial cell junctions: molecular basis and pathological implications. Developmental Cell 16(2): 209–221.

32. Ebnet K, Suzuki A, Ohno S, Vestweber D (2004) Junctional adhesion molecules (JAMs): more molecules with dual functions? Journal of Cell Science 117(Pt 1): 19–29.
33. Ebnet K, Aurrand-Lions M, Kuhn A, Kiefer F, Butz S et al. (2003) The junctional adhesion molecule (JAM) family members JAM-2 and JAM-3 associate with the cell polarity protein PAR-3: a possible role for JAMs in endothelial cell polarity. Journal of Cell Science 116(Pt 19): 3879–3891.
34. Etienne-Manneville S, Hall A (2003) Cdc42 regulates GSK-3beta and adenomatous polyposis coli to control cell polarity. Nature 421(6924): 753–756.
35. Foo SS, Turner CJ, Adams S, Compagni A, Aubyn D et al. (2006) Ephrin-B2 controls cell motility and adhesion during blood-vessel-wall assembly. Cell 124(1): 161–173.
36. Francis SE, Goh KL, Hodivala-Dilke K, Bader BL, Stark M et al. (2002) Central roles of alpha5beta1 integrin and fibronectin in vascular development in mouse embryos and embryoid bodies. Arteriosclerosis, Thrombosis, and Vascular Biology 22(6): 927–933.
37. Galabova-Kovacs G, Matzen D, Piazzolla D, Meissl K, Plyushch T et al. (2006) Essential role of B-Raf in ERK activation during extraembryonic development. Proceedings of the National Academy of Sciences of the United States of America 103(5): 1325–1330.
38. Galan Moya EM, Le Guelte A, Gavard J (2009) PAKing up to the endothelium. Cellular Signalling 21(12): 1727–1737.
39. Gao M, Craig D, Lequin O, Campbell ID, Vogel V et al. (2003) Structure and functional significance of mechanically unfolded fibronectin type III1 intermediates. Proceedings of the National Academy of Sciences of the United States of America 100(25): 14784–14789.
40. Gerety SS, Anderson DJ (2002) Cardiovascular ephrinB2 function is essential for embryonic angiogenesis. Development 129(6): 1397–1410.
41. Gill SE, Parks WC (2008) Metalloproteinases and their inhibitors: regulators of wound healing. The International Journal of Biochemistry & Cell Biology 40(6–7): 1334–1347.
42. Greenberg JI, Shields DJ, Barillas SG, Acevedo LM, Murphy E et al. (2008) A role for VEGF as a negative regulator of pericyte function and vessel maturation. Nature 456(7223): 809–813.
43. Hall A (2005) Rho GTPases and the control of cell behaviour. Biochemical Society Transactions 33(Pt 5): 891–895.
44. Hallmann R, Horn N, Selg M, Wendler O, Pausch F et al. (2005) Expression and function of laminins in the embryonic and mature vasculature. Physiological Reviews 85(3): 979–1000.
45. Hammes HP (2005) Pericytes and the pathogenesis of diabetic retinopathy. Hormone and Metabolic Research 37 Suppl 1: 39–43.
46. Handsley MM, Edwards DR (2005) Metalloproteinases and their inhibitors in tumor angiogenesis. International Journal of Cancer 115(6): 849–860.
47. Herbert SP, Huisken J, Kim TN, Feldman ME, Houseman BT et al. (2009) Arterial-venous segregation by selective cell sprouting: an alternative mode of blood vessel formation. Science (New York, NY) 326(5950): 294–298.
48. Hirschi KK, Rohovsky SA, D'Amore PA (1998) PDGF, TGF-beta, and heterotypic cell-cell interactions mediate endothelial cell-induced recruitment of 10T1/2 cells and their differentiation to a smooth muscle fate. The Journal of Cell Biology 141(3): 805–814.
49. Holderfield MT, Hughes CC (2008) Crosstalk between vascular endothelial growth factor, notch, and transforming growth factor-beta in vascular morphogenesis. Circulation Research 102(6): 637–652.
50. Hughes CC (2008) Endothelial-stromal interactions in angiogenesis. Current Opinion in Hematology 15(3): 204–209.
51. Hynes RO (2007) Cell-matrix adhesion in vascular development. Journal of Thrombosis and Haemostasis 5 Suppl 1: 32–40.
52. Hynes RO (2009) The extracellular matrix: not just pretty fibrils. Science (New York, NY) 326(5957): 1216–1219.
53. Iruela-Arispe ML, Davis GE (2009) Cellular and molecular mechanisms of vascular lumen formation. Developmental Cell 16(2): 222–231.
54. Jain RK (2005) Normalization of tumor vasculature: an emerging concept in antiangiogenic therapy. Science (New York, NY) 307(5706): 58–62.

55. Kamei M, Saunders WB, Bayless KJ, Dye L, Davis GE et al. (2006) Endothelial tubes assemble from intracellular vacuoles in vivo. Nature 442(7101): 453–456.
56. Kim YH, Hu H, Guevara-Gallardo S, Lam MT, Fong SY et al. (2008) Artery and vein size is balanced by Notch and ephrin B2/EphB4 during angiogenesis. Development 135(22): 3755–3764.
57. Koh W, Mahan RD, Davis GE (2008a) Cdc42- and Rac1-mediated endothelial lumen formation requires Pak2, Pak4 and Par3, and PKC-dependent signaling. Journal of Cell Science 121(Pt 7): 989–1001.
58. Koh W, Stratman AN, Sacharidou A, Davis GE (2008b) In vitro three dimensional collagen matrix models of endothelial lumen formation during vasculogenesis and angiogenesis. Methods in Enzymology 443: 83–101.
59. Koh W, Sachidanandam K, Stratman AN, Sacharidou A, Mayo AM et al. (2009) Formation of endothelial lumens requires a coordinated PKC{epsilon}-, Src-, Pak- and Raf-kinase-dependent signaling cascade downstream of Cdc42 activation. Journal of Cell Science 122(Pt 11): 1812–1822.
60. Kwak HI, Mendoza EA, Bayless KJ (2009) ADAM17 co-purifies with TIMP-3 and modulates endothelial invasion responses in three-dimensional collagen matrices. Matrix Biology 28(8): 470–479.
61. Lee S, Jilani SM, Nikolova GV, Carpizo D, Iruela-Arispe ML (2005) Processing of VEGF-A by matrix metalloproteinases regulates bioavailability and vascular patterning in tumors. The Journal of Cell Biology 169(4): 681–691.
62. Liu J, Fraser SD, Faloon PW, Rollins EL, Vom Berg J et al. (2007) A betaPix Pak2a signaling pathway regulates cerebral vascular stability in zebrafish. Proceedings of the National Academy of Sciences of the United States of America 104(35): 13990–13995.
63. Liu Y, Senger DR (2004) Matrix-specific activation of Src and Rho initiates capillary morphogenesis of endothelial cells. FASEB J 18(3): 457–468.
64. Lucitti JL, Jones EA, Huang C, Chen J, Fraser SE et al. (2007) Vascular remodeling of the mouse yolk sac requires hemodynamic force. Development 134(18): 3317–3326.
65. Macara IG (2004) Par proteins: partners in polarization. Current Biology 14(4): R160–R162.
66. Mancuso MR, Davis R, Norberg SM, O'Brien S, Sennino B et al. (2006) Rapid vascular regrowth in tumors after reversal of VEGF inhibition. The Journal of Clinical Investigation 116(10): 2610–2621.
67. Martin-Belmonte F, Gassama A, Datta A, Yu W, Rescher U et al. (2007) PTEN-mediated apical segregation of phosphoinositides controls epithelial morphogenesis through Cdc42. Cell 128(2): 383–397.
68. Miner JH, Yurchenco PD (2004) Laminin functions in tissue morphogenesis. Annual Review of Cell and Developmental Biology 20: 255–284.
69. Morla A, Ruoslahti E (1992) A fibronectin self-assembly site involved in fibronectin matrix assembly: reconstruction in a synthetic peptide. The Journal of Cell Biology 118(2): 421–429.
70. Nakatsu MN, Hughes CC (2008) An optimized three-dimensional in vitro model for the analysis of angiogenesis. Methods in Enzymology 443: 65–82.
71. Qi JH, Ebrahem Q, Moore N, Murphy G, Claesson-Welsh L et al. (2003) A novel function for tissue inhibitor of metalloproteinases-3 (TIMP3): inhibition of angiogenesis by blockage of VEGF binding to VEGF receptor-2. Nature Medicine 9(4): 407–415.
72. Rhodes JM, Simons M (2007) The extracellular matrix and blood vessel formation: not just a scaffold. Journal of Cellular and Molecular Medicine 11(2): 176–205.
73. Rupp PA, Czirok A, Little CD (2003) Novel approaches for the study of vascular assembly and morphogenesis in avian embryos. Trends in Cardiovascular Medicine 13(7): 283–288.
74. Sacharidou A, Koh W, Stratman AN, Mayo AM, Fisher KE et al. (2010) Endothelial lumen signaling complexes control 3D matrix-specific tubulogenesis through interdependent Cdc42- and MT1-MMP-mediated events. Blood 115(25): 5259–5269.
75. San Antonio JD, Zoeller JJ, Habursky K, Turner K, Pimtong W et al. (2009) A key role for the integrin alpha2beta1 in experimental and developmental angiogenesis. The American Journal of Pathology 175(3): 1338–1347.

76. Saunders WB, Bayless KJ, Davis GE (2005) MMP-1 activation by serine proteases and MMP-10 induces human capillary tubular network collapse and regression in 3D collagen matrices. Journal of Cell Science 118(Pt 10): 2325–2340.
77. Saunders WB, Bohnsack BL, Faske JB, Anthis NJ, Bayless KJ et al. (2006) Coregulation of vascular tube stabilization by endothelial cell TIMP-2 and pericyte TIMP-3. The Journal of Cell Biology 175(1): 179–191.
78. Sela S, Itin A, Natanson-Yaron S, Greenfield C, Goldman-Wohl D et al. (2008) A novel human-specific soluble vascular endothelial growth factor receptor 1: cell-type-specific splicing and implications to vascular endothelial growth factor homeostasis and preeclampsia. Circulation Research 102(12): 1566–1574.
79. Senger DR, Claffey KP, Benes JE, Perruzzi CA, Sergiou AP et al. (1997) Angiogenesis promoted by vascular endothelial growth factor: regulation through alpha1beta1 and alpha2beta1 integrins. Proceedings of the National Academy of Sciences of the United States of America 94(25): 13612–13617.
80. Seo DW, Li H, Guedez L, Wingfield PT, Diaz T et al. (2003) TIMP-2 mediated inhibition of angiogenesis: an MMP-independent mechanism. Cell 114(2): 171–180.
81. Stratman AN, Malotte KM, Mahan RD, Davis MJ, Davis GE (2009a) Pericyte recruitment during vasculogenic tube assembly stimulates endothelial basement membrane matrix formation. Blood 114(24): 5091–5101.
82. Stratman AN, Saunders WB, Sacharidou A, Koh W, Fisher KE et al. (2009b) Endothelial cell lumen and vascular guidance tunnel formation requires MT1-MMP-dependent proteolysis in 3-dimensional collagen matrices. Blood 114(2): 237–247.
83. Stupack DG, Cheresh DA (2004) Integrins and angiogenesis. Current Topics in Developmental Biology 64: 207–238.
84. Tian Y, Lei L, Cammarano M, Nekrasova T, Minden A (2009) Essential role for the Pak4 protein kinase in extraembryonic tissue development and vessel formation. Mechanisms of Development 126(8–9): 710–720.
85. Vogel V (2006) Mechanotransduction involving multimodular proteins: converting force into biochemical signals. Annual Review of Biophysics and Biomolecular Structure 35: 459–488.
86. Whelan MC, Senger DR (2003) Collagen I initiates endothelial cell morphogenesis by inducing actin polymerization through suppression of cyclic AMP and protein kinase A. The Journal of Biological Chemistry 278(1): 327–334.
87. Wurtz SO, Schrohl AS, Sorensen NM, Lademann U, Christensen IJ et al. (2005) Tissue inhibitor of metalloproteinases-1 in breast cancer. Endocrine-Related Cancer 12(2): 215–227.
88. Yaniv K, Isogai S, Castranova D, Dye L, Hitomi J et al. (2006) Live imaging of lymphatic development in the zebrafish. Nature Medicine 12(6): 711–716.
89. Zhong C, Chrzanowska-Wodnicka M, Brown J, Shaub A, Belkin AM et al. (1998) Rho-mediated contractility exposes a cryptic site in fibronectin and induces fibronectin matrix assembly. The Journal of Cell Biology 141(2): 539–551.
90. Zhou X, Rowe RG, Hiraoka N, George JP, Wirtz D et al. (2008) Fibronectin fibrillogenesis regulates three-dimensional neovessel formation. Genes & Development 22(9): 1231–1243.
91. Zhou Z, Apte SS, Soininen R, Cao R, Baaklini GY et al. (2000) Impaired endochondral ossification and angiogenesis in mice deficient in membrane-type matrix metalloproteinase I. Proceedings of the National Academy of Sciences of the United States of America 97(8): 4052–4057.
92. Zhu WH, Guo X, Villaschi S, Francesco Nicosia R (2000) Regulation of vascular growth and regression by matrix metalloproteinases in the rat aorta model of angiogenesis. Laboratory Investigation 80(4): 545–555.
93. Zovein AC, Alfonso Luque A, Turlo KA, Hofmann JJ, Yee KM et al. (2010) β1 integrin establishes endothelial cell polarity and arteriolar lumen formation via a Par3-dependent mechanism. Developmental Cell 18: 39–51.

Chapter 3
Scaffolding for Three-Dimensional Embryonic Vasculogenesis

Thomas P. Kraehenbuehl, Sezin Aday, and Lino S. Ferreira

3.1 Introduction

Human embryonic stem cells (hESCs) derived from the inner cell mass of blastocysts are an unlimited source of vascular cells and represent a potent model system for studying early vasculogenesis [1, 2]. These cells could help identify cues directing undifferentiated hESCs along vascular lineages and understand the de novo formation of vascular networks in vitro and in vivo. Early endothelial progenitor cells isolated from differentiating hESCs have been shown to give rise to the cell types involved in blood vessels, i.e. endothelial and smooth muscle cells [3]. These cells are very promising for the revascularization of ischemic tissues such as ischemic leg, chronic wounds, and infarcted heart [4, 5, 84].

Vasculogenesis is defined as the differentiation of endothelial precursor cells, also known as angioblasts, into endothelial cells (ECs) in combination with the formation of primitive vascular networks [6]. The key steps in vasculogenesis during embryo development are (1) establishment of the angioblasts from mesoderm, (2) assembly of angioblasts into vascular structures, (3) formation of vascular lumens, and (4) organization of continuous vascular networks. Vasculogenesis occurs at two distinct embryonic locations during development: the extraembryonic and intraembryonic tissues [2, 6]. The vascular precursor cells that contribute to the primary vascular plexus are initially scattered throughout the mesoderm and assemble either at the location where they arise or, following migration, at the location of the developing vessel.

The mechanisms characterizing vasculogenesis are dynamic processes modulated by the cell–extracellular matrix (ECM) and cell–cell interactions in the presence of growth factors and morphogens [6]. The ECM plays a crucial role in embryonic vasculogenesis [7, 8]. Complex spatiotemporal interaction of inductive and repressive

L.S. Ferreira (✉)
Biocant, Centro de Inovação em Biotecnologia, 3060-197 Cantanhede, Portugal
and
Center of Neurosciences and Cell Biology, University of Coimbra, 3004-517 Coimbra, Portugal
e-mail: lino@biocant.pt

S. Gerecht (ed.), *Biophysical Regulation of Vascular Differentiation and Assembly*, Biological and Medical Physics, Biomedical Engineering,
DOI 10.1007/978-1-4419-7835-6_3,

signals from ECM is critical for vascular morphogenesis. To mimic the 3D architecture and biological role of the ECM, we and others have developed biomaterial scaffolds, which can be modulated to drive the differentiation of hESCs toward vascular cells [9–11]. These tissue-engineered constructs can add value to drug discovery and help understand developmental biology better by elucidating biophysical and biochemical factors governing vascular tissue-specific development.

In this chapter, we give an overview on the following: (1) developmental cues for directed differentiation of hESCs into vascular cells, (2) 3D vascular differentiation in embryoid bodies (EBs), (3) preparation of 3D scaffolds for the vascular differentiation of hESCs, and (4) the most significant studies combining scaffolding and hESCs for development of vascular-like tissue.

3.2 Developmental Cues for hESC Differentiation into Vascular Cells

Vasculogenesis is initiated by the establishment of the angioblasts from mesoderm [2]. The angioblasts undergo sequential maturation to express a set of typical endothelial markers including VEGFR-2, CD31, vascular endothelial (VE)–cadherin, Tie-1, and Tie-2. The endocardium and great vessels are the first endothelial structures formed in the embryo during development (see [2, 12] for a review). Some of these steps have been reproduced and identified in the hESC differentiation system [13, 14]. A recent study has reported that hESC-derived hemangioblast (a precursor of endothelial and hematopoietic cells) expresses KDR and develops within 72–96 h of EB differentiation, the stage during which KDR and CD117 are expressed on distinct populations, prior to the expression of CD31 and CD34. These human hemangioblasts generate distinct blast colonies that display hematopoietic and endothelial potential [13].

The presentation of spatially and temporally orchestrated soluble and insoluble factors directs vascular differentiation of hESCs [15–18]. Directed vascular differentiation of hESCs has been reported when different soluble growth factors/inhibitors in combination or alone were used including VEGF, PDGF, TGF-β1, activin A, bone morphogenetic protein 4 (BMP4), basic fibroblast growth factor (bFGF, also known as FGF2), and dickkopf homolog 1 (DKK1, WNT inhibitor) [3, 17, 19–21]. Other factors have been identified to be necessary for vasculogenesis in mice, but their role in the differentiation of hESCs remains to be elucidated (see [2] for a review). In general, the protocols involve several steps and the isolation of precursor cells at various differentiation levels [3, 15–17, 21]. Typically, the use of only one factor is insufficient to efficiently drive the differentiation of hESCs into vascular cells. Some factors induce the differentiation of hESCs into mesoderm lineage, including BMP-4 and activin [22]. hESCs treated with BMP-4 for 7 days induce mesoderm differentiation [22]. Others have an important role in endothelial commitment, including VEGF and bFGF [3, 21]. hESCs treated with $VEGF_{165}$ for more than 10 days highly coexpress CD34 and the $VEGF_{165}$ receptor

KDR, indicating that these cells have vasculogenic potential. In addition, hESCs seeded on collagen IV-coated culture dishes and treated with $VEGF_{165}$ differentiate partially into endothelial cells [17]. DKK1 is an important regulator of cardiovascular lineages, thus affecting the differentiation into endothelial and smooth muscle cells [3]. Finally, PDGF and TGF-β1 induce the differentiation of hESCs into smooth muscle cells [17, 21].

ECM components have also an important effect in embryonic vasculogenesis. Fibronectin is the earliest and most abundantly expressed ECM molecule in the embryo [23]. Studies in mice indicate that fibronectins are essential for vascular morphogenesis but are dispensable for specification of vascular cells [24]. Studies in vitro indicate that the formation of vascular networks is defective in fibronectin-null mouse EBs and that α5 integrin subunit is important for blood vessel development in mouse embryos [23]. It is unclear whether the role of fibronectin is similar in the vascular differentiation of hESCs.

To isolate vascular progenitor cells from phenotypically different cells, several methods were shown to be useful, including magnetic beads, fluorescence-activated cell sorting (FACS), or mechanical separation, resulting in highly purified vascular progenitor cells (>90%, $CD31^+$, $CD34^+$) [15, 18, 21]. The isolation of vascular progenitor cells by expression of CD34 or KDR/Flk-1 was reported to yield both endothelial and smooth muscle cells within ~10 days upon selection, in some cases with addition of VEGF (endothelial cells) or PDGF (smooth muscle cells) [3, 21]. In contrast, the selection by CD31 expression resulted in endothelial cells [15]. The markers used for characterization of the developed cells have been recently reviewed [18, 25, 26].

3.3 EBs as a 3D Embryonic Vasculogenic Model

EBs recapitulate many aspects of human embryonic development. They have been used to study not only the earliest stages of endothelial specification but also later stages related to the formation of primitive vasculature [2, 27]. The vascular differentiation of human EBs occurs by the sequential upregulation of the endothelial markers VE-CAD, CD34, and PECAM1, reaching expression peaks between 13th and 15th days [15, 18, 21]. Gene array analysis also demonstrated that temporal gene expression changes in EBs correlate substantially with human embryonic hematopoietic and endothelial differentiation data [28]. Therefore, this 3D system recapitulates in many aspects the in vivo vasculogenesis and can be used to investigate the process of blood vessel development.

Several methods have been used to obtain EBs from hESCs, including (1) liquid suspension culture in bacterial-grade dishes, (2) culture in methylcellulose (MC) semisolid media, and (3) hanging drop. Low-adhesion polystyrene dishes have often been used to favor cell aggregation and EB formation [21]. However, since the number and size of EBs differ, the obtained EBs are typically heterogeneous in number and size. Hematopoietic and endothelial cells have been efficiently

generated using EBs formed by a MC approach [29]. However, this technique has shown disadvantages such as limited mass transfer and handling difficulties. The hanging-drop approach has been used to obtain EBs with controllable size [30]. Although this method has been widely used to generate a broad spectrum of cell types including smooth muscle and hematopoietic cells, the limited volume (less than 50 μl) and difficulty in exchanging small volume of medium led researchers to develop alternative approaches.

Microscale engineering approaches are a powerful tool for controlling EB size and the cellular microenvironment. Microfabrication techniques and microcontact printing have been used to obtain EBs with uniform size for high throughput screening [31, 32]. In addition, the formation of controllable size EBs in a robust and scalable manner has been achieved by a centrifugal forced-aggregation technique developed in combination with a centrifugal extraction (spin-in, spin-out, SISO) approach [20, 33].

The vascular differentiation of EBs is affected by different factors such as input hESC composition, input colony size, EB size, composition of culture media (soluble factors), cell–cell and cell–ECM interactions [34]. Successful induction of EBs into mesoderm and cardiac lineages has been observed for EBs with large diameter when they were generated from Gata6/Pax6 (endoderm-biased) input hESCs. Interestingly, a recent study has demonstrated that endothelial cell differentiation increased in smaller EBs (150 μm in diameter) [35]. EB-size mediated differentiation was driven by differential expression of WNTs, particularly noncanonical WNT pathway. The higher expression of WNT5a in smaller EBs enhanced endothelial cell differentiation [35]. Interestingly, the results of the study seem to indicate that as the size of the EBs increase with culture time, there is a downregulation of WNT5a and an upregulation of WNT11 that favor a cardiac differentiation [35].

The agglomeration of EBs at later stages of differentiation has negative effects on cell differentiation. Typically, large EBs have high probability to exhibit necrotic cell areas [36]. Bioreactors can be used to generate scalable quantities of EBs, prevent EB agglomeration, facilitate process control strategies, and simplify the cell differentiation process. The ability to measure and control culture conditions in stirred-suspension bioreactors is a valuable tool for understanding and optimizing delivery profiles of exogenous factors that affect ES cell differentiation [37]. Spinner flasks and rotating cell culture systems (RCCS) developed by NASA have been used to produce large numbers of EBs for vascular differentiation [36, 38]. In the spinner flasks, impeller type and speed (shear stress) are the main parameters that affect EB size and homogeneity [38–40]. The RCCS are geometrically designed to enable efficient gas exchange and to confer a very low shear environment [36]. Quantification of cell density at day 28 of differentiation revealed that cell density was approximately three times higher in the bioreactor than on the static culture system.

EBs comprise multiple cells having cell–cell interactions that may be important for the vasculogenesis program. However, the complexity of the EBs can also be a disadvantage, since the diffusive transport of inductive factors may be impaired by the multiple layers of cells and basement membranes. This may hamper the

interpretation of the results. It has been shown that during the initial days of EB differentiation, ECM proteins are deposited on the EB exterior [41]. This shell consists of a superficial outer ECM layer formed by collagen type I, a squamous cell layer bound by E-cadherin, and an underlying basement membrane formed primarily by collagen type IV and laminin. Disruption of the basement membrane by either inhibiting its formation with noggin or permeabilizing it with collagenase, resulted in recovery of diffusive transport [41].

EBs cultured in suspension differentiate spontaneously into the three germ layers of the embryo including ectoderm, endoderm, and mesoderm, which makes it difficult to control their differentiation into vascular cells. For example, between 2 and 10% of cells in EBs can be isolated as endothelial cells or endothelial progenitor cells after 10–13 days of differentiation [15, 21]. Recently, we have reported a strategy to control the vasculogenic program of EBs by the incorporation of particulate growth factor-delivery vehicles in EBs [20]. This approach increased the growth factor concentration within the EBs and likely extended the duration of exposure of cells to the growth factors, which otherwise tend to have short half-lives. The results showed that the incorporation of these particles had a minimal effect on cell viability and proliferation but a large impact on differentiation [20]. In some cases, the effect on vascular differentiation of particles containing growth factors (VEGF, or PlGF, or bFGF) was superior to that observed by exposing EBs to large extrinsic doses of the same growth factors [20]. The vascular induction was superior when microparticles-containing PlGF were used. Concomitantly, the use of microparticle-containing factors reduced the differentiation of hESCs toward ectoderm and endoderm germ layers.

Although EBs recapitulate in many aspects the embryonic vasculogenesis, it is likely that complex processes that might involve extrinsic factors and high structural organization may be underrepresented. For example, although the differentiation of hESCs into ECs is reproduced, the subsequent differentiation into arterial, vein, or brain endothelial cells is typically difficult to observe. Furthermore, the vascular development in EBs progresses in the absence of blood flow, and this aspect may be important for certain studies as flow induces shear stress, which might influence remodeling of the vascular system [42]. Another drawback is that the vascular organization in individual EBs is much more variable compared with the precise vascular patterning in embryos [14]. Therefore, the use of 3D scaffolds, which are able to confer a higher level of tissue organization and in some cases having mechanical properties that resemble the ones found in blood vessels, might be an important tool to address some of these issues.

3.4 Scaffolds for Vascular Differentiation

In nature, tissue development is driven by cell–cell contacts and cell–matrix interactions. A complex interplay of ECM signals drives undifferentiated or progenitor cells along tissue-specific lineages [43]. It is crucial for vascular scaffold design to

identify the spatiotemporal signals of natural ECM required for vasculogenesis. Several vascular key factors have been identified as being able to trigger vascular differentiation in 3D environments, including mechanical properties (elasticity etc.), and, as mentioned in previous sections, the kinetic pattern of soluble and immobilized factors (growth factors, cell adhesion ligands, etc.). Several of these biophysical and biochemical factors have been incorporated into 3D biomaterial scaffolds to develop vascular constructs. The ideal scaffold for vascular differentiation should provide (1) the mechanical environment similar to the natural vascular environment in terms of elasticity, compressibility, viscoelasticity, tensile strength, and failure strain, (2) a degradation rate that matches the rate of newly forming vascular tissue, (3) a pattern of insoluble signals such as cell adhesion ligands displayed in a time-dependent manner to drive the undifferentiated cells through several stages of maturation, and (4) temporally and spatially controlled release of differentiation stage-specific factors, such as growth factors and/or hormones (Fig. 3.1).

Recent studies have indicated that cell growth, self-renewal, and differentiation can be induced by above-mentioned biochemical and biophysical inputs to the cells [44–46]. Both, natural and synthetic matrices have been applied to direct differentiation of hESCs. While *natural* materials have many advantages in displaying biological signals to direct the stem cell fate, it is relatively difficult to control their biophysical and biochemical properties without losing their 3D structure or bioactivity. In contrast, *synthetic* materials allow for better control over biophysical and biochemical properties, and degradation profile. These materials can incorporate

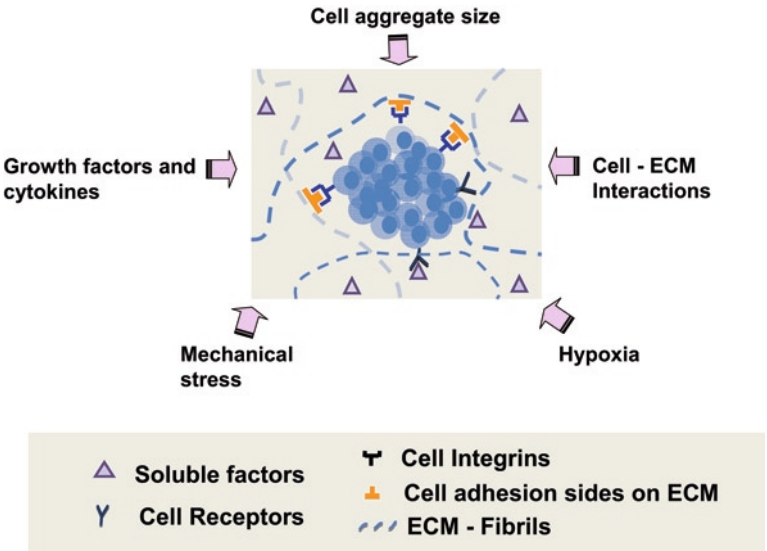

Fig. 3.1 Elements provided by the scaffold that might enhance vasculogenesis. The scaffold can provide a pattern of insoluble and soluble factors that are able to drive the differentiation of hESCs or hESC-derived progenitor cells, might prevent agglomeration of the cells, and might induce hypoxia and mechanical stress

growth factors, cytokines, peptides, and other ligands at a density not amenable for natural materials [47]. For example, 3D networks of nanofibers formed by the self-assembly of peptide amphiphilic molecules present a higher density of neurite-promoting laminin epitope IKVAV than laminin [47].

3.4.1 General Considerations About Structure and Bioactivity of Scaffolds

Materials with variable physicochemical properties can be used to prepare scaffolds with the ability to drive the differentiation of hESCs. These materials have been fabricated into hydrogels, fibrous, or porous scaffolds. Hydrogels are a class of biomaterial scaffolds that store large amounts of water, resembling soft biological tissue [48, 49]. These hydrogels are cross-linked by hydrophilic polymer chains of natural or synthetic origin. Among commonly used *natural* hydrogels for encapsulation of hESC are collagen, fibrin, hyaluronic acid (HA), alginate, dextran, or chitosan, whereas a major class of *synthetic* hydrogels are built from polyethylene glycol (PEG). hESCs have been encapsulated through various approaches, including ionic cross-linking (alginate, dextran, chitosan, HA, etc.) or photopolymerization (PEG with acrylate or methacrylate groups). These gels degrade by enzymatic reaction triggered by the encapsulated cells (collagen, fibrin, HA, dextran, chitosan; MMP-cross-linked PEG) or by slow dissolution (alginate).

One of the main disadvantages of synthetic hydrogels is their lack of bioactivity. To overcome this hurdle, researchers modulated synthetic hydrogels with specific bioactive molecules identified in natural matrices. These biomolecules can be incorporated into the scaffolds by different means including (1) physical immobilization, (2) chemical immobilization, and (3) incorporation into micro- and nanoparticles that are physically immobilized in the scaffold (Fig. 3.2). In the physical immobilization approach, the biomolecule is mixed with a polymer solution that is cross-linked by the effect of light, pH, temperature, or other means, resulting in a 3D scaffold with the immobilized biomolecule. This approach can be easily implemented for hydrogel-based scaffolds, and the release of the biomolecule is controlled by varying the cross-linking density [50, 51].

To extend the delivery of biomolecules, they can be incorporated into micro- or nanoparticles, which are then immobilized in the scaffold (Fig. 3.2). These micro or nanoparticles can be prepared from different polymers including alginate, HA, chitosan, and poly(D, L-lacticglycolic acid) (PLGA), among others. PLGA is very often used, since it is biocompatible, biodegradable, easily processed, and has been approved by FDA for drug-delivery use [52, 53]. In addition, it is possible to obtain PLGA copolymers with variable physicochemical properties (variable molecular weight, copolymer composition, crystallinity), which can be used to design micro- and nanoparticles with variable release properties. PLGA copolymer undergoes degradation (hydrolytic and enzymatic) in physiologic conditions through cleavage

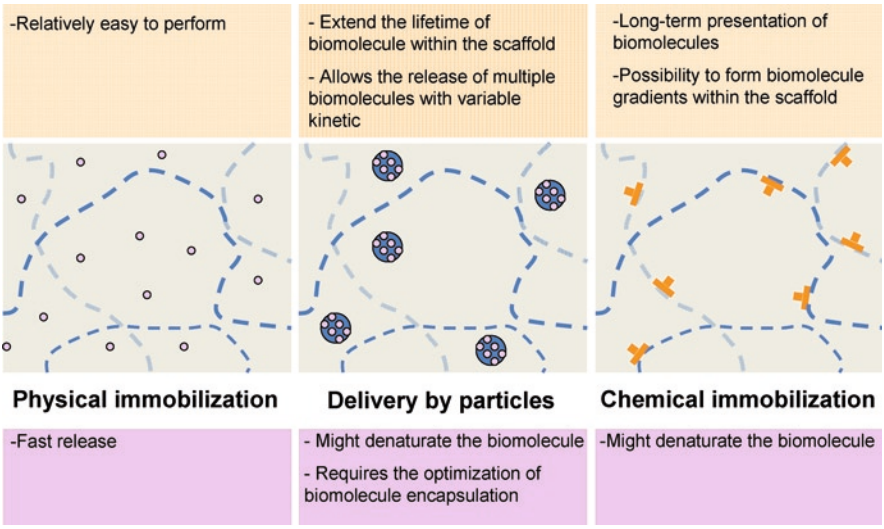

Fig. 3.2 Strategies to incorporate biomolecules into 3D scaffolds. Biomolecules can be incorporated by (1) physical immobilization, (2) chemical immobilization, and (3) incorporation into micro- and nanoparticles that are physically immobilized in the scaffold

of its backbone ester linkages. A number of techniques can be used to encapsulate the biomolecules within the micro- or nanoparticles, and the choice depends on the release profile required and the type of biomolecules used [53].

A third approach to incorporate the biomolecules in the scaffold is by chemical immobilization (Fig. 3.2). This approach is recommended for the immobilization of cell-adhesion peptides or to allow a stable, long-term presentation of growth factors. This approach can be used to present the biomolecules uniformly throughout the bulk of the material at the same or variable concentration (i.e. gradients). Several functional groups in the amino acids of biomolecules can be used for the immobilization including amine, hydroxyl, carboxyl, and thiol groups [54].

Several types of biomolecules have been immobilized in scaffolds to drive the differentiation of hESCs. For example, RGD-peptides have been chemically immobilized into synthetic PEG-hydrogels to support the attachment of hESC-derived committed chondrogenic cells [55]. Cells in the RGD-modified PEG-hydrogels demonstrated higher amounts of cartilage-specific markers, on both the gene and the protein level. Similarly, RGD-adhesion ligands have been covalently immobilized in dextran-based hydrogels and VEGF physically immobilized in PLGA microparticles to induce the vascular differentiation of hESCs [10].

Morphological elements of natural matrices have been reproduced by nanotechnologies to guide the differentiation of hESCs. The fibrillar structure of collagen and fibrin can be reproduced by electrospinning, a process involving the extrusion of a charged polymer. The resulting fibres can have a diameter at the nanometer scale. These fibers have not only been reported to support hESC's self-renewal capacity [56] but also directed differentiation into neuronal progenitor cells [57]. However, a major limitation of these nanofiber-based scaffolds is the limited cell infiltration. Other

nanotechnology approaches have been used to capture the complexity of ECM and control the behavior of hESCs. An example is substrate nanotopography, which can alter morpohology and proliferation of hESCs in vitro via contact guidance [58]. Fibronectin-coated poly(dimethyl siloxane) substrates applied with line grating (600 nm ridges with 600 nm spacing and 600 ± 150 nm feature height) contributed to hESC alignment and elongation, altered organization of cytoskeletal components including actin, vimentin, and α-tubulin, and reduced proliferation [58].

An alternative to hydrogel and nanofiber-based scaffolds is macroporous scaffolds. These scaffolds can form interconnected porous networks, which enable cellular infiltration, and control of cellular alignment. Poly(glycolic acid) (PGA), poly(L-lactic acid) (PLLA), and the copolymer PLGA have been extensively used [9, 59]. Most of these macroporous scaffolds are formed by salt leaching (size of salt particles defined pore size), porogen melting, or sintering. The degradation is triggered by hydrolysis due to the presence of ester bonds [53].

3.4.2 Natural Scaffolds for Vascular Differentiation

Several scaffolds based on natural polymers have been proposed to support 3D vasculogenesis of hESCs, including alginate, dextran, hyaluronic acid (HA), agarose, and collagen. Alginate is a hydrophilic, linear polysaccharide copolymer derived from seaweeds, consisting of (1–4)-linked β-D-mannuronic acid (M) and α-L-guluronic acid (G) monomers. In the presence of a divalent cation such as Ca^{2+}, Ba^{2+}, or Sr^{2+}, it forms an ionically cross-linked hydrogel [60, 61]. The mechanical properties and pore size can be altered by varying the ratio of the copolymers, as well as the molecular weight of the polymer chains. Alginate scaffolds with ~90% porosity, interconnecting pore structure, and pore diameters between 50 and 200 μm (average pore diameter of 100 μm) have been reported [62]. The Young's modulus was assessed to be in a range of 500–1,136 kPa (dry state) [60, 62]. The hydrophilic nature of the alginate material enables rapid wetting of the scaffolds by the culture medium, which is relevant for rapid cell adherence and initial cell survival. The degradation of alginate is not triggered by cells, but by slow, uncontrolled dissolution. The embedded cells can be released from the scaffold by adding gentle agents to disrupt the ionic bonds of the alginate [63].

Enhanced vasculogenesis was demonstrated when undifferentiated hESCs were seeded into 3D alginate scaffolds [60]. EBs formed within the scaffold pores within 48 h. At 30 days after seeding, the scaffold-borne hESCs displayed a significantly higher fraction of $CD34^+$ cells (1.7-fold) than EBs cultured in static conditions or STLV bioreactors. The enhanced vasculogenesis process in the 3D alginate matrix might be due to its ability to control the EBs at a certain size (from 250 to 900 μm in diameter after 1 month of culture), while EBs grown in suspension typically aggregate forming millimeter structures [60]. In fact, recent data indicate that small EBs tend to differentiate at higher levels into vascular cells than large EBs [35]. Another explanation for the enhanced vasculogenesis is considering that the interaction of the EBs with the matrix favored vasculogenesis. However, this seems

unlikely, since alginate is known to discourage protein adsorption due to its hydrophilic character [64]. A final explanation is to consider that the physical confinement of the EBs in the alginate and consequent mechanical stress favored the vasculogenic process [36]. Further research is needed to clarify this issue.

Dextran-based hydrogels have been also proposed as a 3D scaffold for vasculogenesis. These hydrogels are cell nonadhesive materials, which enable to tailor the scaffold with vasculogenic factors [65, 66]. Dextran-based hydrogels can be photopolymerized and degraded by dextranases [10, 67]. Pore sizes in the range of 0.035–210 μm have been reported [68], depending on the cross-linking density of the network. The Young's modulus was assessed to be between 2 and 5 kPa [10].

Enhanced vasculogenesis was demonstrated when undifferentiated hESC aggregates were encapsulated for 10 days in a dextran-based hydrogel [10] (Fig. 3.3). The gels were modified with fibronectin-derived RGD ligands, since fibronectin is the earliest and most abundantly expressed ECM molecule during embryonic vasculogenesis [23]. In addition to the cell adhesion ligand, soluble factors were incorporated into the dextran matrix, using VEGF-loaded PLGA microparticles. Remarkably, the fraction of encapsulated cells expressing VEGF receptor KDR/Flk-1, a vascular marker, was increased ~20-fold as compared to spontaneously differentiated EB [10] (Table 3.1). The incorporation of 0.5 mM RGD, but not 5 mM RGD, in the hydrogel network reduced the expression of KDR/Flk-1 marker as compared to cells encapsulated in the hydrogel without this epitope [10]. Curiously, the incorporation of VEGF-loaded microparticles within the dextran-based hydrogel did not increase the expression of KDR/Flk-1 marker in the hESC aggregates in a statistically significant manner for any concentration of VEGF released (Table 3.1).

The vasculogenic induction mediated by dextran-based hydrogels is poorly understood. Increased vasculogenesis in dextran-based hydrogel could be due to high levels of hypoxia in the encapsulated cells. It is known that VEGF is significantly upregulated in response to hypoxia via activation of hypoxia inducible factors (HIFs), which bind to the hypoxia-response element in the VEGF promoter [69]. However, HIF-1α expression was not statistically significant in hESC aggregates encapsulated in dextran-based hydrogels, undifferentiating hESCs, and EBs [10]. In addition, the HIF-2α expression profile in the several experimental groups could not explain the enhanced vasculogenesis in dextran-based scaffolds [10].

HA gels have also been explored for the vascular differentiation of hESCs [70]. HA is one of the glycosaminoglycan components of the natural ECM, which binds specifically to receptors located at the cell surface and within the cellular cytosol [71]. HA gels are formed by covalent cross-linking with hydrazide derivatives or by the photo-cross-linking of acrylated HA [72, 73]. HA gels with pore diameters between 30 and 50 μm, and Young's moduli in a range of 2–100 kPa have been reported [72]. HA gels can be cleaved by a hyaluronidase enzyme [70].

hESC encapsulated in HA gels and cultured in differentiation medium supplemented with VEGF form sprouts and elongate after 48 h of culture [70]. After 1 week of culture, the sprouted cells stained positively for smooth muscle actin, whereas few were positive for CD34 marker [70]. Therefore, HA gels seem to induce the formation of smooth muscle cell progenitor cells.

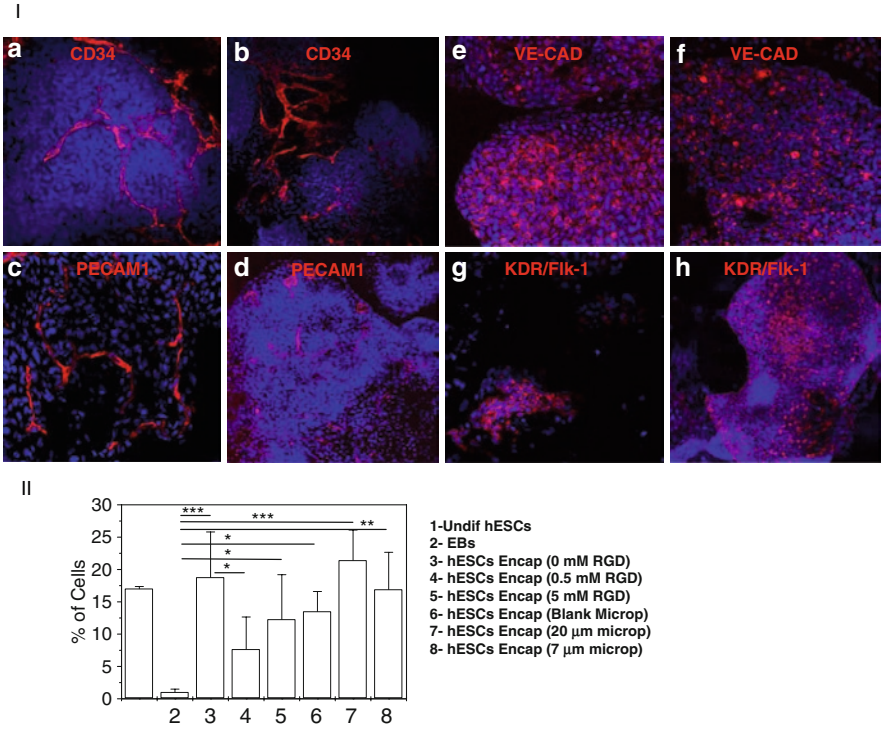

Fig. 3.3 Localization and quantification of endothelial markers on EBs and on hESC aggregates encapsulated in dextran-based hydrogels. (**I**) Confocal images of CD34$^+$ (**a, b**), PECAM1$^+$ (**c, d**), VE-CAD$^+$ (**e, f**), and KDR/Flk-1$^+$ (**g, h**) cells from EBs (**a, c, e, g**) and from hESC aggregates encapsulated in dextran-based hydrogels containing RGD [**b** (×10); **d** (×10); **f** (×25)] or RGD plus microparticles-releasing $VEGF_{165}$ [**h** (×10)]. This figure is reproduced from [10]. (**II**) Summary of FACS analysis of undifferentiating cells (1), EBs at day 10 (2), hESC aggregates encapsulated into dextran-based hydrogels without (3) or containing 0.5 mM (4) or 5 mM chemically immobilized RGD (5), hESC aggregates encapsulated into dextran-based hydrogels containing 0.5 mM chemically immobilized RGD and 5 mg/mL of microparticles loaded with [20 μm (7) and 7 μm (8)] or without [20 μm (6)] $VEGF_{165}$. For all FACS analyses, the values indicate average ± S.D., from at least 3 independent experiments. *, **, and *** denote statistical significance ($P<0.05$, $P<0.01$, and $P<0.001$, respectively). Figure reprinted from [10], with permission from Elsevier

Agarose beads have also been used as a scaffold to drive the differentiation of hESCs into hematopoietic/vascular progenitor cells (CD34$^+$ cells) [37]. Agarose is a purified linear polymer isolated from marine algae, consisting of alternating D-galactose and 3,6-anhydro-L-galactose units. Agarose beads are very often used for cell encapsulation [37, 74]. Elastic modulus of 0.04 MPa has been reported for agarose beads with sizes between 80 and 200 μm [75].

A platform has been established to generate a scalable amount of hESC-derived hematopoietic progenitor cells (CD34$^+$ cells) [37]. hESC cell aggregates (1,000–5,000 ES cells per aggregate) were encapsulated in 200–300 μm diameter agarose-based

Table 3.1 Expression of vascular markers on hESCs differentiated through an EB step or encapsulation in 3D scaffolds

Differentiation methodology	Time	Vascular marker expression			References
		PECAM-1	CD34	Flk-1/KDR	
Embryoid bodies (EBs)	Day 10	<1.5%	~10.5%	<2.5%	[10]
Embryoid bodies	Day 13	2%	N/A	N/A	[15]
Dextran hydrogels	Day 10	<1.5%	~8%	~19%	[10]
Dextran hydrogels with RGD ligands	Day 10	~1.5%	~11%	12.5%	[10]
Dextran hydrogels with RGD ligands and VEGF delivery	Day 10	~6%	~9%	17.5%	[10]
PLGA/PLLA scaffolds coated with Matrigel®	Day 14	~0.5%	1–1.5%	N/A	[9]
PLGA/PLLA scaffolds coated with fibronectin	Day 14	~0.5%	<0.5%	N/A	[9]

capsules for 8 days. The agarose capsules were used to prevent EB agglomeration. It was shown that after 4 days, encapsulated cultures contained 10 times the number of cell aggregates as nonencapsulated cultures [37]. Interestingly, the differentiation of cells into $CD34^+$ cells was similar when encapsulated or cultured in suspension (non-encapsulated) under normoxic conditions for 7 days. Therefore, the agarose beads did not induce the vascular differentiation of stem cells. However, when the encapsulated cells were cultured under hypoxic (low-oxygen, 4%) conditions in a bioreactor, the frequency of hematopoietic progenitor cells was significantly greater than that under normoxia (standard oxygen conditions, 20%) [37]. These results indicate that hypoxia is a key factor during vasculogenesis.

Finally, collagen gels have been also used as a scaffold to drive the differentiation of hESCs into vascular cells [4]. Collagen is a main component in ECM of mammalian tissues. Physically formed collagen gels are thermally reversible and offer a limited range of mechanical properties [76]. A recent study has reported a two-stage vascular differentiation protocol that involved EB formation and culture for 12 days (stage 1), and expansion of endothelial lineage by subculturing EBs in collagen (stage 2) [4]. Remarkably, CD31/CD144 expression was triggered and increased from 1 to 3% (EBs at day 12) to 10–15% after EBs were subcultured in 3D collagen gels for 3 additional days. A highly pure population of endothelial cells ($CD31^+CD144^+$) was then isolated by flow cytometry, after gel digestion [4].

3.4.3 Synthetic Scaffolds for Vascular Differentiation

PGA, PLLA, and the copolymer PLGA have been used as a 3D scaffolding for vasculogenesis [9, 59]. These materials degrade hydrolytically through bulk erosion due to the presence of ester bonds. Polymer molecular weight, copolymerization ratio, and polydispersity can be adjusted to alter stiffness, pore size, and to control degradation rate [53]. Methods used for these alterations are well established and include

salt leaching, sintering, porogen melting, and nanofiber electrospinning [53, 77]. Pore sizes ranging from 2 up to 800 μm and Young's moduli in a range of 65–500 kPa have been described [78]. In some cases, to increase cell adherence and survival, these scaffolds were coated with Matrigel® or fibronectin [9, 59].

PLGA scaffold-supported hESCs were able to differentiate and organize into vessels [9]. Vascular differentiation was assessed by immunohistochemical staining for CD34 and CD31 markers (Table 3.1). Results showed that hESCs seeded on fibronectin-coated scaffolds resulted in higher levels of vascular differentiation (Fig. 3.4). Samples treated with retinoic acid neither formed capillary networks nor expressed CD34 or CD31 genes as shown by RNA analysis [9]. The study also demonstrated that hESCs cultured on fibronectin-coated scaffolds achieved a high level of structure organization than hESCs cultured in fibronectin-coated dish or as EBs [9]. hESCs seeded in PLLA/PLGA scaffolds and cultured in differentiation media supplemented with neurotrophins differentiate at some level into vascular cells [59]. Vascular structures (CD31-positive) were found throughout the 3D constructs surrounding the neuronal rosettes. Interestingly, the addition of retinoic acid inhibited vascular network formation.

Similar to the previously mentioned alginate gels, the porous structure of poly(glycerol-co-sebacate) acrylate (PGSA) (pore sizes between 20 and 200 μm, and Young's moduli between 40 and 60 kPa) was demonstrated to support colony formation within the macropores within 24 h when seeding undifferentiated hESCs [79]. The hESCs were shown to proliferate, and they differentiated in vitro into tissue-like structures containing cells types of all the three germ layers, Brachyuri-positive cells (mesoderm), cytokeratin 18 (ectoderm), and α-Fetoprotein (endoderm) after 7 days [79]. However, no comparison was performed to the differentiation profile of EBs cultured in suspension.

3.5 Future Directions

3D scaffolds are important tools to study embryonic vasculogenesis, since they confer a high level of tissue organization than EBs. In addition, controlling their mechanical, biochemical, (cell adhesion ligands, growth factors, etc.), and morphological (micro- and nanotopography) properties makes it possible to evaluate the effect of these variables in embryonic vasculogenesis. Our proposition is that a better understanding of embryonic vasculogenesis will depend in our ability to control scaffold properties. Future work should focus in the development of scaffolds with (1) variable chemistry, to assess the role of chemistry in the embryonic vasculogenesis, (2) micro- and nanoscale resolution, to elucidate the role of biophysical cues governing 3D embryonic vasculogenesis [80], (3) micro- and nanoparticles, to release vasculogenic factors at desired concentrations and time frames, which will allow unraveling of certain molecular events at early or late vasculogenic stages [81], and (4) the ability to interact with cells (for example, sensitive to cellular enzymes [11, 51]), since this will help in meeting the kinetic change required to drive the cell fate during differentiation, thus likely increase the lineage-specific output.

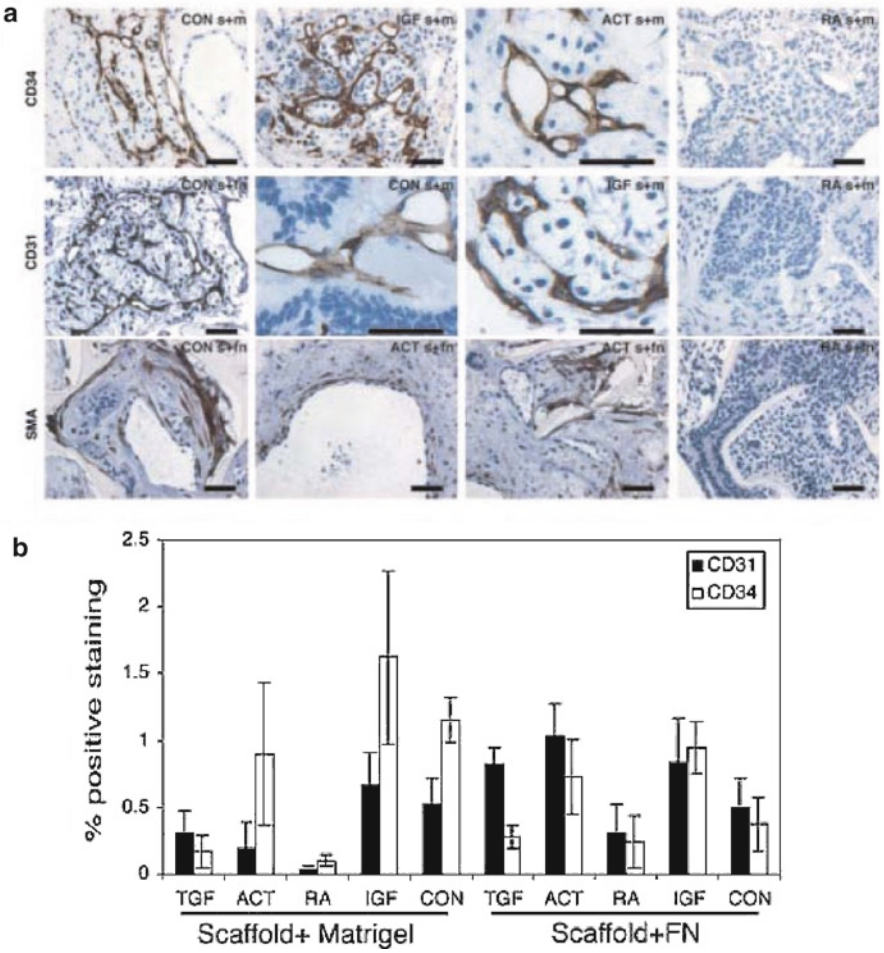

Fig. 3.4 Vasculogenesis in 3D PLLA/PLGA scaffolds (Copyright 2003, National Academy of Sciences, USA, [9]). (**a**) Differentiating hES cells (EB day 8) were seeded on PLLA/PLGA scaffolds by using two methods of cell attachment: seeding the cells onto the scaffold with Matrigel® (scaffold plus Matrigel®, s+m) or coating the scaffold with fibronectin (scaffold plus FN, s+fn). The constructs were incubated in a control medium (CON) or medium supplemented with TGF-β (TGF), activin-A (ACT), RA, or IGF. After 2 weeks of incubation, the samples were fixed, sectioned, and immunostained by using anti-CD31, anti-CD34, or antismooth muscle actin (SMA) antibodies (scale bar = 50 μm). Note the complex network formation in control and IGF-treated samples in contrast to the absence of staining in RA-treated samples. (**b**) Quantitative analysis of antibody staining. Percentage of positive staining corresponds to area of antibody-positive cells within the tissue sections. The results shown are mean values (±SD) of five different sample sections

High-throughput screening methodologies may contribute to discover chemical cues that can be incorporated into 3D scaffolds relevant for vascular differentiation of hESCs. Recently, a high-throughput platform for rapid, nanoliter-scale synthesis

of biomaterials has been developed, which allows to screen arrays of potentially relevant polymers [82]. The most promising polymers can then be used to prepare scaffolds for selective vascular differentiation of hESCs. Alternatively, bioactive small peptides identified by high-throughput approaches can be used for scaffold preparation. Billions of diverse sequences can be assessed by displaying random peptide sequences on the coat proteins of bacteriophages, rendering phage display a powerful means to identify peptides that function as cell-surface ligands. These peptides can be modified chemically to form 3D scaffolds [83].

Scaffolds with micro- and nanoscale resolution can be fabricated by the use of 3D printing, microsyringe deposition, and electrospinning of nanofibers [80]. These methods allow one to control the spatial location of molecules within the scaffold, the scaffold topography at micro and nanoscale, and the assembly of the cells. For example, nanofiber-assembly scaffolds have high porosity and specific surface area, and they present nanometer-scale topographical cues that are potent effectors of cellular behavior. These tools might allow researchers to better control the vascular differentiation program of hESCs. Some of these microtechnologies can be acquired commercially and are inexpensive, and it is expected that they will be implemented in hESC biology laboratories in the next few years.

Many studies indicate that embryonic vasculogenesis is improved on 3D scaffolds relative to EBs. Yet, the mechanism is poorly understood. Factors that might account for this effect are (1) level of tissue organization, (2) hypoxia, (3) cell–matrix interaction, (4) soluble factors released from the scaffold, and (5) mechanical stress. Further research is needed to elucidate the role of each factor in the context of embryonic vasculogenesis. We anticipate some hurdles in this process. For example, the scaffold mechanical properties will likely have an important role during human embryonic vasculogenesis; however, it is difficult to demonstrate such a phenomenon in a 3D model. This is due to the difficulty in isolating this variable from others existing in a 3D model. For example, increasing the stiffness of a hydrogel by increasing the cross-linking density will likely affect the diffusion of oxygen and cellular nutrients, as well as cell migration.

Acknowledgments This work was supported in part by NIH (grant HL060435). TPK was supported by the Swiss National Science Foundation (grant number PBELP3-127902). SA was supported by the FCT (grant number SFRH/BD/42871/2008). LF was supported by a Marie Curie-Reintegration Grant, MIT-Portugal program, Crioestaminal, Associação Viver a Ciência, and FCT (PTDC/SA-BEB/098468/2008; PTDC/CTM/099659/2008).

References

1. Thomson JA, Itskovitz-Eldor J, Shapiro SS, et al. Embryonic stem cell lines derived from human blastocysts. Science. 1998;282:1145–1147.
2. Ferguson JE, 3rd, Kelley RW, Patterson C. Mechanisms of endothelial differentiation in embryonic vasculogenesis. Arterioscler Thromb Vasc Biol. 2005;25:2246–2254.
3. Yang L, Soonpaa MH, Adler ED, et al. Human cardiovascular progenitor cells develop from a KDR+ embryonic-stem-cell-derived population. Nature. 2008;453:524–528.

4. Li Z, Wilson KD, Smith B, et al. Functional and transcriptional characterization of human embryonic stem cell-derived endothelial cells for treatment of myocardial infarction. PLoS One. 2009;4:e8443.
5. Cho SW, Moon SH, Lee SH, et al. Improvement of postnatal neovascularization by human embryonic stem cell derived endothelial-like cell transplantation in a mouse model of hindlimb ischemia. Circulation. 2007;116:2409–2419.
6. Schmidt A, Brixius K, Bloch W. Endothelial precursor cell migration during vasculogenesis. Circ Res. 2007;101:125–136.
7. Astrof S, Hynes RO. Fibronectins in vascular morphogenesis. Angiogenesis. 2009;12:165–175.
8. Hynes RO. Cell-matrix adhesion in vascular development. J Thromb Haemost. 2007;5 Suppl 1:32–40.
9. Levenberg S, Huang NF, Lavik E, et al. Differentiation of human embryonic stem cells on three-dimensional polymer scaffolds. Proc Natl Acad Sci U S A. 2003;100:12741–12746.
10. Ferreira LS, Gerecht S, Fuller J, et al. Bioactive hydrogel scaffolds for controllable vascular differentiation of human embryonic stem cells. Biomaterials. 2007;28:2706–2717.
11. Kraehenbuehl TP, Zammaretti P, Van der Vlies AJ, et al. Three-dimensional extracellular matrix-directed cardioprogenitor differentiation: systematic modulation of a synthetic cell-responsive PEG-hydrogel. Biomaterials. 2008;29:2757–2766.
12. Ribatti D, Nico B, Crivellato E. Morphological and molecular aspects of physiological vascular morphogenesis. Angiogenesis. 2009;12:101–111.
13. Kennedy M, D'Souza SL, Lynch-Kattman M, et al. Development of the hemangioblast defines the onset of hematopoiesis in human ES cell differentiation cultures. Blood. 2007;109:2679–2687.
14. Jakobsson L, Kreuger J, Claesson-Welsh L. Building blood vessels – stem cell models in vascular biology. J Cell Biol. 2007;177:751–755.
15. Levenberg S, Golub JS, Amit M, et al. Endothelial cells derived from human embryonic stem cells. Proc Natl Acad Sci U S A. 2002;99:4391–4396.
16. Wang L, Li L, Shojaei F, et al. Endothelial and hematopoietic cell fate of human embryonic stem cells originates from primitive endothelium with hemangioblastic properties. Immunity. 2004;21:31–41.
17. Gerecht-Nir S, Ziskind A, Cohen S, et al. Human embryonic stem cells as an in vitro model for human vascular development and the induction of vascular differentiation. Lab Invest. 2003;83:1811–1820.
18. Levenberg S, Zoldan J, Basevitch Y, et al. Endothelial potential of human embryonic stem cells. Blood. 2007;110:806–814.
19. Cerdan C, Rouleau A, Bhatia M. VEGF-A165 augments erythropoietic development from human embryonic stem cells. Blood. 2004;103:2504–2512.
20. Ferreira L, Squier T, Park H, et al. Human embryoid bodies containing nano- and microparticulate delivery vehicles. Adv Mater. 2008;20:2285–2291.
21. Ferreira LS, Gerecht S, Shieh HF, et al. Vascular progenitor cells isolated from human embryonic stem cells give rise to endothelial and smooth muscle like cells and form vascular networks in vivo. Circ Res. 2007;101:286–294.
22. Zhang P, Li J, Tan Z, et al. Short-term BMP-4 treatment initiates mesoderm induction in human embryonic stem cells. Blood. 2008;111:1933–1941.
23. Francis SE, Goh KL, Hodivala-Dilke K, et al. Central roles of alpha5beta1 integrin and fibronectin in vascular development in mouse embryos and embryoid bodies. Arterioscler Thromb Vasc Biol. 2002;22:927–933.
24. George EL, Baldwin HS, Hynes RO. Fibronectins are essential for heart and blood vessel morphogenesis but are dispensable for initial specification of precursor cells. Blood. 1997;90:3073–3081.
25. Levenberg S. Engineering blood vessels from stem cells: recent advances and applications. Curr Opin Biotechnol. 2005;16:516–523.
26. Bai H, Wang ZZ. Directing human embryonic stem cells to generate vascular progenitor cells. Gene Ther. 2008;15:89–95.

27. Gerecht-Nir S, Osenberg S, Nevo O, et al. Vascular development in early human embryos and in teratomas derived from human embryonic stem cells. Biol Reprod. 2004;71:2029–2036.
28. Gerecht-Nir S, Dazard JE, Golan-Mashiach M, et al. Vascular gene expression and phenotypic correlation during differentiation of human embryonic stem cells. Dev Dyn. 2005; 232:487–497.
29. Ng ES, Davis RP, Hatzistavrou T, et al. Directed differentiation of human embryonic stem cells as spin embryoid bodies and a description of the hematopoietic blast colony forming assay. Curr Protoc Stem Cell Biol. 2008;Chapter 1:Unit 1D 3.
30. Cerdan C, Hong SH, Bhatia M. Formation and hematopoietic differentiation of human embryoid bodies by suspension and hanging drop cultures. Curr Protoc Stem Cell Biol. 2007;Chapter 1:Unit 1D 2.
31. Khademhosseini A, Ferreira L, Blumling J, 3rd, et al. Co-culture of human embryonic stem cells with murine embryonic fibroblasts on microwell-patterned substrates. Biomaterials. 2006;27:5968–5977.
32. Ungrin MD, Joshi C, Nica A, et al. Reproducible, ultra high-throughput formation of multicellular organization from single cell suspension-derived human embryonic stem cell aggregates. PLoS One. 2008;3:e1565.
33. Ng ES, Davis RP, Azzola L, et al. Forced aggregation of defined numbers of human embryonic stem cells into embryoid bodies fosters robust, reproducible hematopoietic differentiation. Blood. 2005;106:1601–1603.
34. Bauwens CL, Peerani R, Niebruegge S, et al. Control of human embryonic stem cell colony and aggregate size heterogeneity influences differentiation trajectories. Stem Cells. 2008;26:2300–2310.
35. Hwang YS, Chung BG, Ortmann D, et al. Microwell-mediated control of embryoid body size regulates embryonic stem cell fate via differential expression of WNT5a and WNT11. Proc Natl Acad Sci U S A. 2009;106:16978–16983.
36. Gerecht-Nir S, Cohen S, Itskovitz-Eldor J. Bioreactor cultivation enhances the efficiency of human embryoid body (hEB) formation and differentiation. Biotechnol Bioeng. 2004; 86:493–502.
37. Dang SM, Gerecht-Nir S, Chen J, et al. Controlled, scalable embryonic stem cell differentiation culture. Stem Cells. 2004;22:275–282.
38. Fok EY, Zandstra PW. Shear-controlled single-step mouse embryonic stem cell expansion and embryoid body-based differentiation. Stem Cells. 2005;23:1333–1342.
39. Schroeder M, Niebruegge S, Werner A, et al. Differentiation and lineage selection of mouse embryonic stem cells in a stirred bench scale bioreactor with automated process control. Biotechnol Bioeng. 2005;92:920–933.
40. Zandstra PW, Bauwens C, Yin T, et al. Scalable production of embryonic stem cell-derived cardiomyocytes. Tissue Eng. 2003;9:767–778.
41. Sachlos E, Auguste DT. Embryoid body morphology influences diffusive transport of inductive biochemicals: a strategy for stem cell differentiation. Biomaterials. 2008;29:4471–4480.
42. Nguyen TH, Eichmann A, Le Noble F, et al. Dynamics of vascular branching morphogenesis: the effect of blood and tissue flow. Phys Rev E Stat Nonlin Soft Matter Phys. 2006;73:061907.
43. Philp D, Chen SS, Fitzgerald W, et al. Complex extracellular matrices promote tissue-specific stem cell differentiation. Stem Cells. 2005;23:288–296.
44. Metallo CM, Vodyanik MA, de Pablo JJ, et al. The response of human embryonic stem cell-derived endothelial cells to shear stress. Biotechnol Bioeng. 2008;100:830–837.
45. Ofek G, Willard VP, Koay EJ, et al. Mechanical characterization of differentiated human embryonic stem cells. J Biomech Eng. 2009;131:061011.
46. Discher DE, Janmey P, Wang YL. Tissue cells feel and respond to the stiffness of their substrate. Science. 2005;310:1139–1143.
47. Silva GA, Czeisler C, Niece KL, et al. Selective differentiation of neural progenitor cells by high-epitope density nanofibers. Science. 2004;303:1352–1355.
48. Lutolf MP, Hubbell JA. Synthetic biomaterials as instructive extracellular microenvironments for morphogenesis in tissue engineering. Nat Biotechnol. 2005;23:47–55.

49. Drury JL, Mooney DJ. Hydrogels for tissue engineering: scaffold design variables and applications. Biomaterials. 2003;24:4337–4351.
50. Burdick JA, Ward M, Liang E, et al. Stimulation of neurite outgrowth by neurotrophins delivered from degradable hydrogels. Biomaterials. 2006;27:452–459.
51. Kraehenbuehl TP, Ferreira LS, Zammaretti P, et al. Cell-responsive hydrogel for encapsulation of vascular cells. Biomaterials. 2009;30:4318–4324.
52. Griffith LG. Polymeric biomaterials. Acta Mater. 2000;48:263–277.
53. Jain RA. The manufacturing techniques of various drug loaded biodegradable poly(lactide-co-glycolide) (PLGA) devices. Biomaterials. 2000;21:2475–2490.
54. Hirano Y, Mooney DJ. Peptide and protein presenting materials for tissue engineering. Adv Mater. 2004;16:17–25.
55. Hwang NS, Varghese S, Elisseeff J. Derivation of chondrogenically-committed cells from human embryonic cells for cartilage tissue regeneration. PLoS One. 2008;3:e2498.
56. Carlberg B, Axell MZ, Nannmark U, et al. Electrospun polyurethane scaffolds for proliferation and neuronal differentiation of human embryonic stem cells. Biomed Mater. 2009;4:45004.
57. Gauthaman K, Venugopal JR, Yee FC, et al. Nanofibrous substrates support colony formation and maintain stemness of human embryonic stem cells. J Cell Mol Med. 2009; 13:3475–3484.
58. Gerecht S, Bettinger CJ, Zhang Z, et al. The effect of actin disrupting agents on contact guidance of human embryonic stem cells. Biomaterials. 2007;28:4068–4077.
59. Levenberg S, Burdick JA, Kraehenbuehl T, et al. Neurotrophin-induced differentiation of human embryonic stem cells on three-dimensional polymeric scaffolds. Tissue Eng. 2005;11:506–512.
60. Gerecht-Nir S, Cohen S, Ziskind A, et al. Three-dimensional porous alginate scaffolds provide a conducive environment for generation of well-vascularized embryoid bodies from human embryonic stem cells. Biotechnol Bioeng. 2004;88:313–320.
61. Leor J, Gerecht S, Cohen S, et al. Human embryonic stem cell transplantation to repair the infarcted myocardium. Heart. 2007;93:1278–1284.
62. Zmora S, Glicklis R, Cohen S. Tailoring the pore architecture in 3-D alginate scaffolds by controlling the freezing regime during fabrication. Biomaterials. 2002;23:4087–4094.
63. Lindenhayn K, Perka C, Spitzer R, et al. Retention of hyaluronic acid in alginate beads: aspects for in vitro cartilage engineering. J Biomed Mater Res. 1999;44:149–155.
64. Smetana K. Cell biology of hydrogels. Biomaterials. 1993;14:1046–1050.
65. Ferreira L, Gil MH, Cabrita AM, et al. Biocatalytic synthesis of highly ordered degradable dextran-based hydrogels. Biomaterials. 2005;26:4707–4716.
66. Ferreira L, Rafael A, Lamghari M, et al. Biocompatibility of chemoenzymatically derived dextran-acrylate hydrogels. J Biomed Mater Res A. 2004;68:584–596.
67. Mehvar R. Dextrans for targeted and sustained delivery of therapeutic and imaging agents. J Control Release. 2000;69:1–25.
68. Ferreira L, Figueiredo MM, Gil MH, et al. Structural analysis of dextran-based hydrogels obtained chemoenzymatically. J Biomed Mater Res B Appl Biomater. 2006;77B:55–64.
69. Brusselmans K, Bono F, Collen D, et al. A novel role for vascular endothelial growth factor as an autocrine survival factor for embryonic stem cells during hypoxia. J Biol Chem. 2005;280:3493–3499.
70. Gerecht S, Burdick JA, Ferreira LS, et al. Hyaluronic acid hydrogel for controlled self-renewal and differentiation of human embryonic stem cells. Proc Natl Acad Sci U S A. 2007;104:11298–11303.
71. Choudhary M, Zhang X, Stojkovic P, et al. Putative role of hyaluronan and its related genes, HAS2 and RHAMM, in human early preimplantation embryogenesis and embryonic stem cell characterization. Stem Cells. 2007;25:3045–3057.
72. Burdick JA, Chung C, Jia X, et al. Controlled degradation and mechanical behavior of photopolymerized hyaluronic acid networks. Biomacromolecules. 2005;6:386–391.

73. Vercruysse KP, Marecak DM, Marecek JF, et al. Synthesis and in vitro degradation of new polyvalent hydrazide cross-linked hydrogels of hyaluronic acid. Bioconjug Chem. 1997;8:686–694.
74. Sakai S, Kawabata K, Ono T, et al. Preparation of mammalian cell-enclosing subsievesized capsules (<100 microm) in a coflowing stream. Biotechnol Bioeng. 2004;86:168–173.
75. Mu Y, Lyddiatt A, Pacek AW. Manufacture by water/oil emulsification of porous agarose beads: effect of processing conditions on mean particle size, size distribution and mechanical properties. Chem Eng Process. 2005;44:1157–1166.
76. Lee KY, Mooney DJ. Hydrogels for tissue engineering. Chem Rev. 2001;101:1869–1879.
77. Li WJ, Laurencin CT, Caterson EJ, et al. Electrospun nanofibrous structure: a novel scaffold for tissue engineering. J Biomed Mater Res. 2002;60:613–621.
78. Karageorgiou V, Kaplan D. Porosity of 3D biomaterial scaffolds and osteogenesis. Biomaterials. 2005;26:5474–5491.
79. Gerecht S, Townsend SA, Pressler H, et al. A porous photocurable elastomer for cell encapsulation and culture. Biomaterials. 2007;28:4826–4835.
80. Khademhosseini A, Langer R, Borenstein J, et al. Microscale technologies for tissue engineering and biology. Proc Natl Acad Sci U S A. 2006;103:2480–2487.
81. Ferreira L, Karp JM, Nobre L, et al. New opportunities: the use of nanotechnologies to manipulate and track stem cells. Cell Stem Cell. 2008;3:136–146.
82. Anderson DG, Levenberg S, Langer R. Nanoliter-scale synthesis of arrayed biomaterials and application to human embryonic stem cells. Nat Biotechnol. 2004;22:863–866.
83. Derda R, Musah S, Orner BP, et al. High-throughput discovery of synthetic surfaces that support proliferation of pluripotent cells. J Am Chem Soc. 2010;132:1289–1295.
84 Kraehenbuehl TP, Ferreira LS, Hayward AM, et al. Human embryonic stem cell-derived microvascular grafts for cardiac tissue preservation after myocardial infarction. Biomaterials. 2010 (in press).

Chapter 4
Intra- and Extracellular Microrheology of Endothelial Cells in a 3D Matrix

Stephanie I. Fraley, Christopher M. Hale, Ryan J. Bloom, Alfredo Celedon, Jerry S.H. Lee, and Denis Wirtz

4.1 Introduction

Cells that are moved from conventional flat surfaces to a physiologically more relevant 3D matrix undergo dramatic morphological and functional changes. One of the best examples of such a functional switch is endothelial cells, which grow to confluent cobblestone structures on a traditional matrix-coated cell-culture dish, but form distinct tubular structures between thick matrix layers [1]. How cells sense and respond to the dimensionality of their environment – 2D for a flat culture dish vs. 3D for a matrix – remains unclear. Most of what we have learned about cellular functions and signaling pathways, including the molecular mechanisms regulating cell motility and adhesion, stem from studies on 2D surfaces [2]. However, even endothelial cells, which are anchored to the 2D basement membrane in vivo, have to negotiate and respond to a 3D environment during embryonic development, angiogenesis for tumor growth, and invasion into surrounding tissues in metastasis. Accumulating evidence suggests that the molecular and biophysical mechanisms by which cells move in a 3D matrix and adhere to the fibers that constitute the matrix could be fundamentally different from the far better known 2D case. Progress in our understanding of molecular cell functions in 3D has been limited by the lack of quantitative assays that can probe cells in the physiological 3D milieu. In what follows, we describe two quantitative assays based on high-resolution particle-tracking methods, which allow us for the first time to probe the physical properties of the intracellular and extracellular milieu for cells fully embedded inside a 3D matrix. In the first method, the extent of the Brownian movements of nanoparticles embedded in the cytoplasm are analyzed to measure the local micromechanical properties of endothelial cell inside a 3D matrix

D. Wirtz (✉)
Department of Chemical and Biomolecular Engineering, The Johns Hopkins University, Baltimore, MD 21218, USA
and
Johns Hopkins Physical Sciences-Oncology Center, The Johns Hopkins University, Baltimore, MD 21218, USA
e-mail: wirtz@jhu.edu

S. Gerecht (ed.), *Biophysical Regulation of Vascular Differentiation and Assembly*, Biological and Medical Physics, Biomedical Engineering,
DOI 10.1007/978-1-4419-7835-6_4,

and their response to vascular endothelial growth factor (VEGF). In the second method, the 3D movements of large beads tightly lodged in the extracellular matrix report in real time on the local 3D deformation of the matrix mediated by migrating cancer cells. This assay, particle-tracking matrix traction micromechanics, is used to resolve the controversial roles of matrix metalloproteinases and actomyosin contractility in mediating cell motility in a 3D matrix.

4.2 Intracellular Microrheology of Cells Inside a 3D Matrix

4.2.1 Fundamentals of Particle-Tracking Microrheology

Here, we describe the basic principles of the method of particle-tracking microrheology to probe the micromechanical properties of cells embedded inside a 3D matrix (see ref. [3] for more details). Spherical carboxylated fluorescent nanoparticles of submicron diameter are first ballistically injected [4] inside endothelial cells grown in a culture dish (Fig. 4.1). The nanoparticles are injected instead of being passively engulfed by the cells to circumvent the endocytic pathway [5]. Endosomal vesicles containing the engulfed nanoparticles would transport them along cytoskeletal filaments through motor proteins, which would render particle-tracking analysis in terms of cytoplasmic viscoelasticity ambiguous [6]. Instead of coating nanoparticles with nonadhesive polymers such as PEG, the surface of the nanoparticles is carboxylated to allow for limited binding of the nanoparticles to subcellular structures. The absence of direct binding interactions between nanoparticles and cytoplasm, as induced by PEG, would create a zone of depletion in the vicinity of the nanoparticles [7]. Hence PEGylated nanoparticles would probe a milieu, depleted of cytoskeletal filaments, of artificially low viscosity. Finally, carboxylated nanoparticles are preferred over amine-modified nanoparticles, which undergo directed motion in the cell, reminiscent of that observed for nanoparticles passively engulfed in the cell [5].

Nanoparticles are injected inside the cells as following. Helium is accelerated through a gas chamber, which forces a macrocarrier disk coated with the fluorescent nanoparticles to crash into a stopping screen (Fig. 4.1). The momentum of the macrocarrier is transferred to the nanoparticles, which penetrate the target cells. If the pressure drop accelerating helium is too low, nanoparticles may bounce off the cell surface; if too high, nanoparticles may too severely damage the cells. Ballistic injection as opposed to manual microinjection dramatically increases the number of cells amenable to particle-tracking measurements, from ~10 to 1,000 [4]. The number of nanoparticles delivered to individual cells is also more consistent, typically between 10 and 30 per cell. When compared with manual injection, ballistic injection greatly decreases the fraction of damaged cells. Of course, thorough washing post bombardment is critical to prevent nanoparticles that are not lodged inside the cells from entering the cells by endocytosis.

After overnight incubation, the cells are either detached from their substratum and placed inside the 3D matrix or deposited on conventional flat (2D) matrix-coated

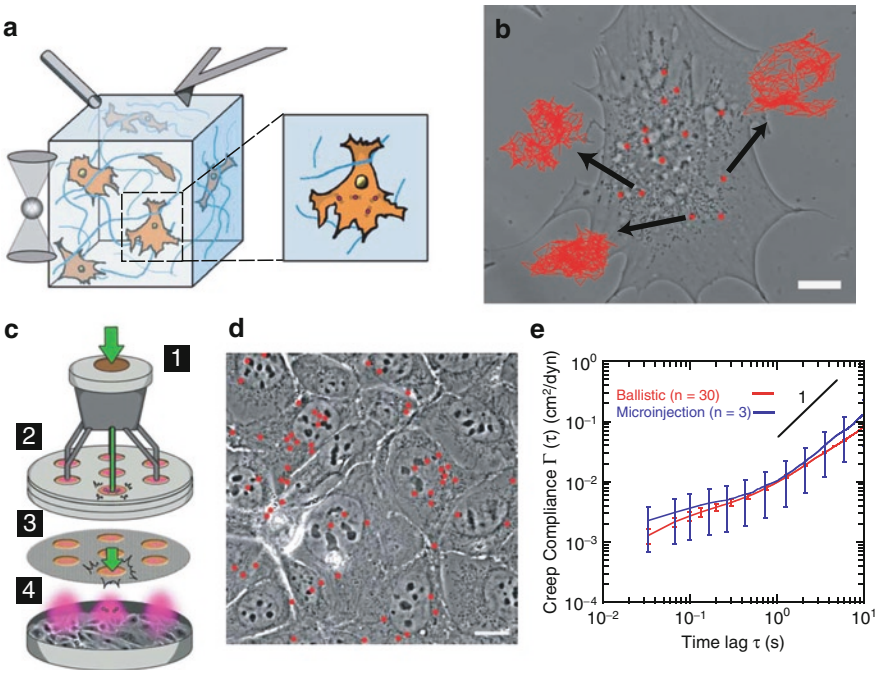

Fig. 4.1 Intracellular particle-tracking microrheology of cells inside a 3D matrix. (**a**) Schematic illustration of endothelial cells fully embedded inside a 3D extracellular matrix. These cells are not amenable to traditional biophysical measurements, including AFM, optical tweezers, and micropipette, because these techniques require a direct physical contact between the cell surface and the probe (i.e., the cantilever of the AFM, the bead of the optical tweezers, and the tip of the micropipette). In contrast, particle-tracking microrheology can probe intracellular mechanics at a distance by tracking the Brownian motion of cytoplasm-embedded beads with high spatial and temporal resolution. (**b**) Trajectories of 100-nm diameter beads inside the cytoplasm of an adherent cell. Nanoparticles are enlarged for ease of visualization. (**c**) Transfer of submicron beads to the cytoplasm of adherent cells using ballistic injection. (1) Helium is accelerated through a gas chamber, (2 and 3) forces a macrocarrier disk coated with the fluorescent nanoparticles to crash into a stopping screen. (4) The momentum of the macrocarrier is transferred to the nanoparticles, which penetrate the target cells. (**d**) Nanoparticles inside adherent cells. Nanoparticles are enlarged for ease of visualization. (**e**) Comparison of the creep compliance of Swiss3T3 fibroblasts using nanoparticles transferred to the cytoplasm using either manual injection (*blue curve*) or ballistic injection (*red curve*). Adapted with permission from Panorchan et al. [14]

substrates to compare the micromechanical properties of cells in 2D vs. 3D microenvironments. After further incubation, nanoparticles disperse throughout the cytoplasm, a reliable test of proper injection since endocytosed nanoparticles are driven toward and accumulate in the perinuclear region of the cell [4]. The movements of the centroids of the diffraction-limited images of the individual fluorescent nanoparticles are subsequently tracked by conventional time-resolved fluorescence microscopy (Fig. 4.1) [8]. Because the displacements, not the actual size, of the nanoparticles is evaluated, one can reach a spatial resolution in the displacements that is significantly smaller than a pixel size, 1–5 nm [8]. The displacements of the

nanoparticles are random in magnitude and direction and, as discussed below, are driven by thermal energy, not by nonthermal forces potentially caused by motor proteins. This distinction is critical to evaluate local viscoelastic properties of the cytoplasm directly from the displacements of the probe nanoparticles.

The mean squared displacement of each nanoparticle in the plane of focus of the microscope,

$$\left\langle \Delta r^2(\tau) \right\rangle = \left\langle \left[x(t+\tau) - x(t) \right]^2 \right\rangle + \left\langle \left[y(t+\tau) - y(t)^2 \right] \right\rangle,$$

is calculated fromthe time-dependent coordinates of the nanoparticles $x(t)$ and $y(t)$ in the x and y directions of the plane of focus; t is the elapsed time, τ is the time lag or duration of observation, and the brackets represent time averaging. The value of the mean squared displacement of a nanoparticle at a given time lag τ indicates how far it has traveled during that time period. To understand how viscosity and elasticity of the cytoplasm can be computed from the mean squared displacements of nanoparticles, we consider the following two extreme cases: a nanoparticle in a viscous liquid (e.g. glycerol or water) and a nanoparticle in a perfectly elastic material (e.g. rubber) [3]. A submicron particle immersed in a quiescent viscous liquid continuously undergoes random Brownian motion. The movements of the nanoparticle can be described by Newton's law in which inertial (gravity) effects are negligible because the nanoparticles are sufficiently small [3]. In a viscous liquid, the nanoparticle is only subjected to two forces of equal magnitude and opposite direction: a random stochastic force and a frictional force that is proportional to the velocity of the nanoparticle and its friction coefficient, which is itself proportional to the size of the nanoparticles and the viscosity of the suspending liquid. Each time the nanoparticle moves in a direction driven by a random force caused by the bombardment of the liquid molecules on the surface of the nanoparticle, that nanoparticle instantaneously loses all memory of where it just came from, i.e. subsequent movements of the nanoparticles are completely uncorrelated in magnitude and direction. One can show [3] that, in these conditions, the mean displacement of the nanoparticles is zero, while the mean squared displacement of the nanoparticles is non-zero and proportional to the duration of observation and the diffusion coefficient of the nanoparticles. Therefore, according to the Stokes–Einstein relationship, the mean squared displacement of the nanoparticle is inversely proportional to the viscosity of the suspending liquid. In addition, one can directly measure the viscosity of a liquid from the measured mean squared displacements of probe beads embedded in that liquid.

The other extreme example illustrating the use of nanoparticles to probe the viscoelastic properties of complex fluids involves a nanoparticle embedded in a perfectly elastic solid material. Each time this nanoparticle attempts to move in an elastic milieu, driven by the thermal energy of the system, it is met by an equal and opposite restoring force that instantaneously pushes it back to its initial position. The mean squared displacement of this nanoparticle is finite, but independent of time. The magnitude of this constant mean squared displacement is inversely proportional to the elasticity of the milieu. The two above examples show that the time dependence of the mean squared displacement of probe nanoparticles in a material will reveal both the viscoelastic nature of that material (whether it is viscous, elastic, or viscoelastic) and determine its viscosity and elasticity [3].

Our work has established that the cytoplasm of adherent cells displays both elastic and viscous characteristics [4, 5, 9–16]. Indeed, at long time scales, the mean squared displacement of nanoparticles embedded inside the cytoplasm is proportional to time, a signature of viscous response, while at intermediate time scales, the mean squared displacement of nanoparticles in the cytoplasm is independent of time, a signature of elastic response. Between these two temporal scales, the cytoplasm behaves as a viscoelastic material, where both elastic and viscous moduli are significant. The method to determine time scale-dependent (or equivalently frequency-dependent) viscoelastic moduli from mean squared displacement is further detailed in ref. [17].

Nanoparticles embedded inside the cytoplasm undergo three-dimensional movements. Even in regions of the lamellipodium in cells placed on a flat substrate, which are very thin (<250 nm) [18], the displacements of the nanoparticles are so small that they are not laterally confined. Moreover, potential long-range interactions, which could be mediated by hydrodynamic interactions, between the plasma membrane and the nanoparticles of the cytoplasm are negligible because the nanoparticles are lodged within the dense meshwork of the cytoskeleton. The diameter of the probe nanoparticles is chosen to be significantly larger than the effective mesh size of the cytoplasm and hydrodynamic interactions are spatially screened with a mesh size of the cytoplasmic network. This mesh size is ~50 nm and was estimated by probing the mobility of fluorescently labeled hydrophilic polymers (e.g. dextran) of increasing radius of gyration through fluorescence recovery after photobleaching [19, 20].

The viscoelastic properties of the cell depend on the probed length scale. Particle-tracking microrheology measures the mesoscale viscoelastic properties of the cytoplasm, at length scales between the cell (~30 μm) and the mesh size of the cytoplasm/cytoskeleton (~50 nm) [10]. For length scales smaller than the cytoskeletal mesh size, the interstitial liquid is only viscous (no elasticity), with a viscosity that is only slightly higher than that of water ($\eta = 1$ cP) [21, 22]. This low viscosity mediates the rapid transport of small globular proteins and ions, whose movements are largely unhindered by cytoskeletal structures in the cytoplasm. For instance, the diffusion of green fluorescence protein (GFP) in control cells is the same as in cells treated by the actin filament depolymerizing drug latrunculin B. For length scales larger than the mesh size but smaller than the size of the cell or nucleus, the length scale probed by particle-tracking microrheology, the cytoplasm displays both viscous and elastic characteristics [3, 10]. For cellular length scales much larger than the cytoskeletal mesh size (greater than several micrometer), the mechanical properties of the cell become dependent on large-subcellular organelles, such as the nucleus which is highly elastic [10], and their interconnections to the cytoskeleton [15, 23, 24]. Coarse, large-scale mechanical properties of single cells can be measured by methods such as micropipette suction [25], which cannot distinguish how different parts of the cells may display different mechanical properties.

Standard fluorescence microscopy and image analysis probe the 3D movements of the nanoparticles in the cytoplasm projected in the 2D plane of focus of the microscope. For such analysis to be rigorous, the milieu surrounding each

nanoparticle has to display physical properties that are locally isotropic. In this case, the displacements in the plane of focus and out-of-plane displacements have to be, on average, statistically similar. We have verified that indeed the time-averaged mean squared displacements of nanoparticles in the cytoplasm projected along the x and y directions of the plane of focus are identical. The cytoplasm is, therefore, mechanically isotropic at the length scales probed by nanoparticles. This may be surprising since regions of the cytoskeleton, including actomyosin stress fibers, are clearly oriented and, therefore, anisotropic. However, due to their finite size, 100–500-nm diameter nanoparticles are excluded from the core region of the stress fibers at the basal surface or the stress fibers in the actin cap of adherent cells [26].

There are several critical advantages of the method of particle-tracking microrheology over classical methods of cell mechanics, including magnetic tweezers, atomic force microscopy (AFM), or micropipette suction [16]. One of them is that particle-tracking microrheology acknowledges the fact that the cytoplasm is highly heterogeneous. Indeed the local elastic modulus on an adherent cell can vary by more than an order of magnitude within the same cell [27]. Another advantage is that particle-tracking microrheology measurements only last between 1 and 30 s, a time that is much smaller than time scales associated with cell motility or cell division. By comparison, high-resolution AFM measurements can last as long as 1 h [28], a time during which the cell can move and organelles such as the nucleus can undergo large excursions [29]. Finally, particle-tracking microrheology is the only quantitative method that has been demonstrated to be useful for cells fully embedded inside a 3D matrix [14].

4.2.2 The Limited Role of Actomyosin Contractility in Intracellular Microrheology

Recent in vitro studies using purified proteins (actin and nonmuscle myosin II) have suggested that the fluctuations of nanoparticles inside cells may stem not only from the thermal energy $k_B T$ (where k_B is Boltzmann's constant and T is the temperature), but also the nonthermal energy generated by the contractile forces of motor proteins [30]. This distinction is important as the interpretation of mean squared displacements of embedded nanoparticles in terms of viscoelastic parameters would become much more complex. Theory and experiments using reconstituted actin filament networks suggest a 100-fold increase in the magnitude of the fluctuations of the nanoparticles mediated by motor proteins compared with nanoparticles in networks containing only F-actin [30]. Moreover, nanoparticles embedded in a reconstituted actin filament network containing myosin II move in a highly correlated fashion, a correlation that disappears when myosin II's motor activity is inhibited [30]. We recently tested the hypothesis that myosin II participates in the movements of nanoparticles in live cells [31]. Nanoparticles are injected in the cytoplasm of live cells and tracked by fluorescence microscopy. Surprisingly, the mean squared displacements of nanoparticles in the cytoplasm of control cells and cells treated with myosin inhibitors ML-7 or blebbistatin are statistically identical [31]. As a positive control,

the mean squared displacements of nanoparticles in the cytoplasm of cells treated with actin depolymerizing drug latrunculin B was significantly larger than those in control cells. Moreover, contrary to the reconstituted actomyosin network, the movements of nanoparticles in untreated (and treated) cells are completely uncorrelated [31]. These important results strongly suggest that, contrary to F-actin, myosin plays no significant role in mediating the microrheology of the cytoplasm of living cells. These results also highlight the danger of extrapolating results obtained with highly simplified in vitro systems to understand complex cell functions.

Nevertheless, cells subjected to myosin inhibitors ML-7 and blebbistatin undergo dramatic cytoskeleton reorganization [31]. Moreover, AFM measurements of cell mechanics suggest that these treated cells become mechanically softer than control cells. How can one reconcile these seemingly contradictory measurements? Particle-tracking microrheology suggests that no effect is caused by ML-7 or blebbistatin treatment, while AFM does. A rather straightforward explanation for this apparent contradiction stems from the subcellular location of myosin II. Myosin II is mainly localized at the cell periphery, bundling actin filaments at the cell cortex and in the actin cap [26], i.e., myosin II is largely excluded from the cytoplasmic regions where nanoparticles are localized. An AFM tip in contact with the surface of a drug-treated cell measures deflections caused by the collapse of cortical and actin-cap structures at the cell periphery, while the body of the cell probed by particle-tracking microrheology remains mechanically intact. Of course, if F-actin is disassembled, then particle-tracking microrheology readily detects mechanical softening of the cytoplasm [31].

4.2.3 Intracellular Microrheology of Endothelial Cells on a 2D Surface vs. Inside a 3D Matrix

Making use of the above method of particle-tracking microrheology, we asked whether human umbilical vein endothelial cells (HUVECs) placed on matrix-coated dish have different micromechanical properties than HUVECs fully embedded in the same matrix [14]. Staining of actin structures suggests that cells in 2D and 3D have drastically different cytoskeletal architectures [14]. HUVECs on flat surfaces typically display a wide lamella (lamellipodium), thin protrusions (filopodia), stress fibers both at the basal surface and on top of the nucleus [26], and focal adhesions that terminate these stress fibers. In contrast, HUVECs inside a matrix show no wide lamella, few thin protrusions, no focal adhesions and display instead thick protrusions (pseudopodia) that colocalize with stress fibers [32]. Using the same particle-tracking microrheology approach, the micromechanical properties of cells in 2D and 3D microenvironment can be compared. The cytoplasm of cells in 3D is significantly softer than the cytoplasm of cells on 2D substrates, showing both a lower viscosity and a lower elastic modulus (Fig. 4.2). Our unpublished results using other types of human cells suggest that placing cells inside a 3D matrix typically decreases the stiffness of the cytoplasm of cells compared with cells placed on the same matrix.

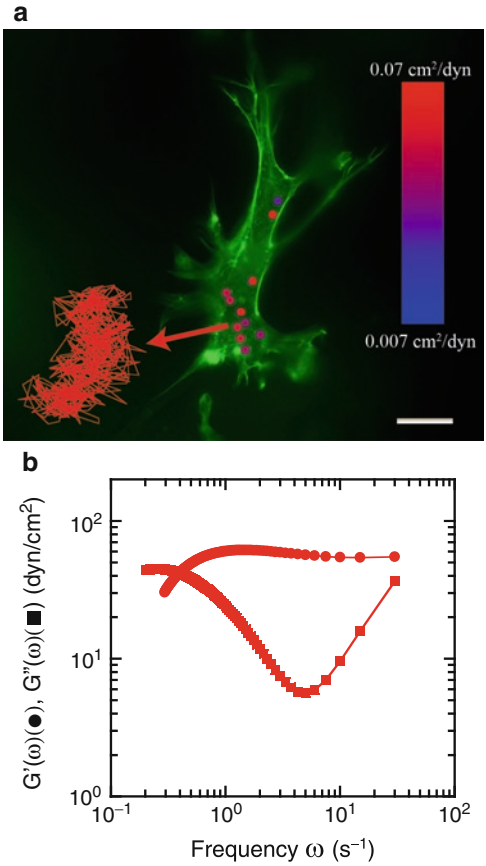

Fig. 4.2 Local micromechanics of the cytoplasm of HUVECs embedded in a matrix. (**a**) Brownian motion of 100-nm diameter nanoparticles embedded in the cytoplasm of an HUVEC inside a 3D peptide (puramatrix) hydrogel. Nanoparticles are color-coded according to the local elasticity of the cytoplasm. *Blue* corresponds to the stiffest regions of the cell; *red* corresponds to the mechanically softest regions of the cell. The size of the nanoparticles is increased to aid visual presentation. Actin filaments are visualized with Alexa 488 phalloidin. Scale bar, 20 μm. (**b**) Mean frequency-dependent viscous and elastic moduli, $G'(\omega)$ (*circles*) and $G''(\omega)$ (*squares*), calculated from the time-dependent mean squared displacements of beads inside cells. Adapted with permission from Panorchan et al. [14]

4.2.4 Intracellular Microrheology of 3D Matrix-Embedded Endothelial Cells Subjected to VEGF

VEGF enhances the angiogenic migration of endothelial cells [33, 34] and activates signaling pathways that regulate actin filament assembly and organization into functional networks [35]. Particle-tracking microrheology demonstrates that VEGF

increases the compliance and decreases the elasticity of the cytoplasm of HUVECs placed inside the 3D matrix [14]. To begin to elucidate the molecular mechanisms by which HUVECs in a 3D matrix mechanically respond to VEGF stimulation, the Rho/ROCK pathway was targeted, a pathway known to regulate actin filament organization in HUVECs following VEGF stimulation [36]. The cells are subjected to VEGF and simultaneously treated with specific ROCK inhibitor Y-27632 [37]. Y-27632 treatment abrogated VEGF-induced softening of HUVECs inside a matrix [14]. Together these results suggest that ROCK plays an essential role in the regulation of the intracellular mechanical response to VEGF of endothelial cells in a 3D matrix.

Angiogenesis refers to the process by which new blood vessels are formed during development or cancer progression. To obtain more nutrient and oxygen during tumor invasion and proliferation, tumor cells release VEGF to promote endothelial migration and angiogenesis. VEGF promotes the formation of highly dynamic protrusions and actin-rich protrusions at the periphery of cells in a 3D matrix and enhances cell motility, as demonstrated by Boyden-chamber and transwell assay [38, 39]. VEGF also enhances in vitro angiogenesis processes where endothelial cells are sandwiched between two matrix layers [36]. These results suggest that VEGF-induced cell motility in a matrix proceeds through the development of highly dynamic pseudopodial protrusions pushing within the cell body against a highly viscous cytoskeleton, while for cells in 2D it proceeds through force propulsion against a more elastic cytoskeleton architecture.

VEGF-induced endothelial migration is completely abrogated and VEGF-induced capillary tube formation is greatly reduced by ROCK inhibition with Y-27632 [36], which also eliminates VEGF-induced intracellular mechanic changes. To eliminate blood supply to tumors, cancer therapies have targeted the inhibition of angiogenesis. Y-27632 is being tested in patients to eliminate angiogenic migration of endothelial cells by inhibiting ROCK.

4.3 Extracellular Matrix Remodeling During Cell Motility in a 3D Matrix

4.3.1 The Role of Matrix Metalloproteinases in 3D Cell Motility

In order to move, endothelial cells embedded inside a 3D matrix need to remodel their surrounding matrix. Matrix remodeling can occur either through cell-mediated physical deformation of the matrix fibers or by degradation of extracellular matrix components by secreted and membrane-bound matrix metalloproteinase (MMPs), including collagenase. Metalloproteinases break peptide bonds in components of the extracellular matrix. The requirement of MMPs for cell migration in 3D matrix has been a highly controversial topic of research [40]. Using collagen I matrix as a model matrix system, Friedl and Wolf initially showed that MMPs were dispensable for the net migration of fibrosarcoma HT-1080 cells and breast cancer MDA-MB-231

cells [41]. Genetic depletion of MMPs in these cells or cell treatment with wide-spectrum MMP inhibitors did not reduce cell migration in dense collagen I matrices [41]. The same noneffect of MMP inhibition occurred when cells were embedded inside matrigel [42], a commercial matrix gel whose molecular composition is similar to that of the basement membrane. Both drug-treated and MT1-MMP-depleted cells underwent a switch from mesenchymal morphology to an amoeboid morphology and moved at about the same speed in the matrix [41]. These observations provided an explanation for the unexpected failed clinical trials of MMP inhibitors [43]. However, Weiss and coworkers suggest that this amoeboid migration displayed by these cells can only be observed for a matrix composed of pepsin-extracted collagen and in matrigel [42, 44, 45], not in native collagen. Pepsin extraction, which was used by Friedl, removes collagen telopeptides that would otherwise crosslink as Schiff-base adducts [46–48]. Similarly, matrigel is formed of uncrosslinked extracellular matrix molecules, including laminin and collagen IV [40]. The resulting gels form uncrosslinked networks with a relatively large pore size, which presumably cannot block cell migration in the absence of MMPs, although a direct comparison of the physical properties of crosslinked and uncrosslinked collagen I matrices remains unavailable.

4.3.2 Particle-Tracking Matrix Traction Micromechanics

How cells fully embedded in crosslinked (native) collagen I gel are able to produce the necessary forces to move in a crosslinked network of mesh size significantly smaller than the sizes of the cell and nucleus is unknown. A cell moving inside a 3D collagen matrix locally deforms the matrix in all three directions. To quantify cell-mediated matrix remodeling, we have introduced a new method, also based on multiple-particle tracking, the particle-tracking matrix traction micromechanics assay [32]. To monitor matrix deformation, large polystyrene beads are incorporated inside a type-I collagen gel matrix prior to matrix impregnation with cells (Fig. 4.3a). The 3D movements of the beads embedded in the matrix are tracked using a new multiple-particle tracking method based on bright-field microscopy (Fig. 4.3b, c) [32, 49]. The carboxylated beads adhere firmly to the collagen matrix, therefore faithfully reporting about the local deformations of the matrix by the cells. Unlike particle-tracking intracellular microrheology described above, the beads are large so that their spontaneous Brownian motion is negligible compared to the magnitude of the movements of the beads induced by cell-mediated deformations of the matrix.

The projections of the 3D displacements of the beads in the plane of focus (in the x and y directions) are obtained by tracking the intensity-weighted center of mass of each bead using time-resolved bright-field microscopy with 20-nm spatial resolution. This lateral resolution is poorer than that obtained by particle-tracking microrheology because bright-field microscopy is intrinsically noisier than fluorescence microscopy. The projection of the 3D displacements of the beads in the

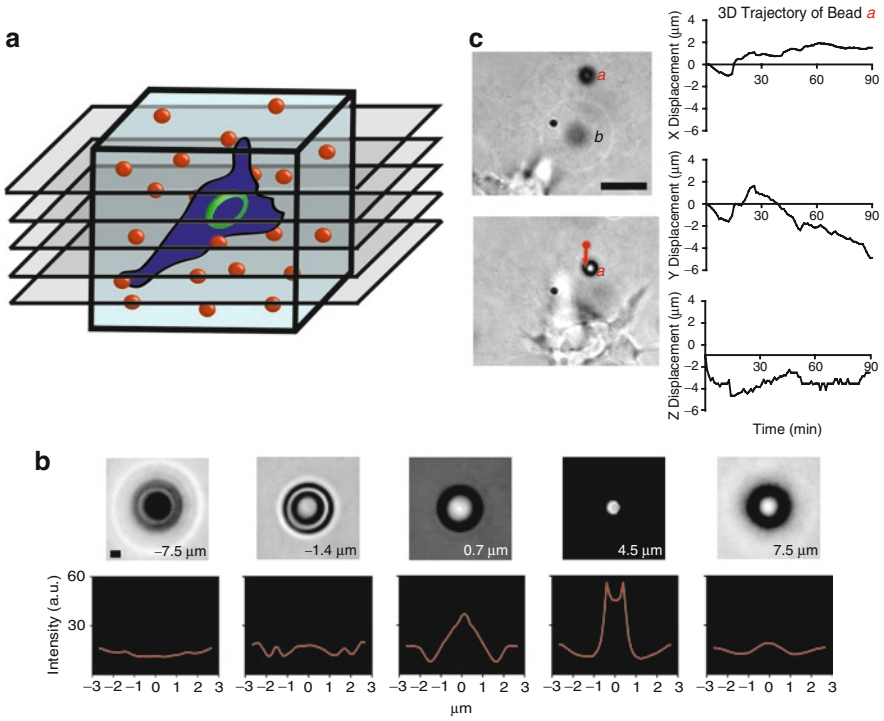

Fig. 4.3 3D particle-tracking matrix micromechanics near cells inside a 3D matrix. (**a**) Schematic illustration of the method of 3D particle-tracking micromechanics used to quantify the local 3D deformation of a matrix induced by a motile cell. Stacks of bright-field micrograph are collected in equally spaced planes of foci to monitor the cell-mediated movements of large (3.6-μm diameter) carboxylated polystyrene beads that are tightly bound to the matrix. (**b**) Prior to each experiment and to calibrate beads movements along the *z* axis, beads in the matrix are moved by the motorized microscope stage to generate a reference image set to which movies collected during experiments are compared. High *z*-movement resolution is achieved by analyzing the diffraction rings of the bead. Scale bar, 3 μm. (**c**) Typical *x*, *y*, and *z* movements of a bead denoted *a*, which is embedded inside a collagen I matrix near a migrating HT-1080 fibrosarcoma cell (*left panel*). In the *right panel*, the initial coordinates of bead *a* are subtracted. Bead *b* illustrates how a bead initially in focus can become out-of-focus, demonstrating the large 3D deformation of the matrix during cell migration. Total time of movie capture was 90 min. Scale bar, 20 μm. Adapted with permission from Bloom et al. [32]

z direction is obtained by analyzing the rings of diffraction of each bead with approximately 120-nm resolution (Fig. 4.3b) [32].

The local displacements of the beads in the collagen matrix in the vicinity of single cells are typically of the order of several microns along each axis for tracking of long durations (>90 min, Fig. 4.3c). Over long periods of time, these large bead displacements are not contained in a single plane of focus. Hence, the positions of the beads in the matrix can be recorded in a stack of equally spaced (8–10-μm) planes spanning the cell in the collagen matrix (Fig. 4.3a). This approach, based on

high-resolution 3D multiple-particle tracking, allows us to detect and quantify local, time-dependent, 3D deformations of the matrix in the vicinity of single motile cells, while simultaneously monitoring changes in cell shape.

4.3.3 Asymmetric Patterns of Local Matrix Deformation During 3D Cell Migration

The direction, magnitude, location near the cell, and timing of local 3D matrix remodeling induced by cells can readily be analyzed using our 3D particle-tracking matrix traction micromechanics assay (Fig. 4.3). Analysis of the trajectories of the matrix-embedded beads in 3D shows that, during single-cell migration, the cell never pushes the matrix and only pulls on it [50]. These local micromechanical measurements are consistent with previous observations that show that collagen matrix-impregnated with fibroblasts display global contraction [51, 52].

Cells typically form major pseudopodial protrusions at the front and back of the cells. These protrusions have a thickness intermediate between that of filopodia and the lamellipodium observed in cells on flat substrates. Multiple-particle tracking revealed spatiotemporal patterns of matrix deformation that are qualitatively and quantitatively different in the regions of the matrix near the front and back of migrating cells (Fig. 4.4a–c). Matrix deformations are typically symmetric at the back and front of the cell, both in magnitude and direction, as they both point toward the cell. Specifically, the maximum matrix displacements toward the cell, l_{max}, measured by beads located in regions of the matrix in the vicinity of the leading and trailing pseudopodial protrusions are statistically similar (Fig. 4.4d). This result leads to the somewhat surprising conclusion that the magnitude of matrix deformation toward the cell is, on average, similar in regions of the matrix at the back and front of the cell.

Particle tracking in the extracellular matrix shows that what explains net cell migration in a 3D matrix is the timing of release of the matrix from the cell by pseudopodial protrusions at the front and back of the cell. After an initial deformation of the matrix fibers toward the cell, the cell releases the fibers connected to the pseudopodia and the matrix relaxes from the cell surface. Matrix relaxation by cellular pseudopodia is timed asymmetrically. Beads in the vicinity of the leading pseudopodium (or what becomes the leading edge of the cell) move first toward the cell and then relax from the cell toward their initial positions. Accordingly, distances between beads and the closest points on the cell surface (normalized by the initial values of these distances) become first <1 and then return to a value close or equal to 1 (Fig. 4.4b). That beads return to their initial position suggest that local cell-mediated matrix deformation is elastic (i.e., no loss) in regions of the matrix near the leading edge of the cell (e.g. Fig. 4.4b).

In contrast, in regions of the matrix near the rear pseudopodium, the matrix is initially pulled toward the cell with a magnitude similar to matrix traction at the front of the cell (Fig. 4.4c, d), but then undergoes relaxation from the cell that is typically much larger than the initial distance between the cell and the beads

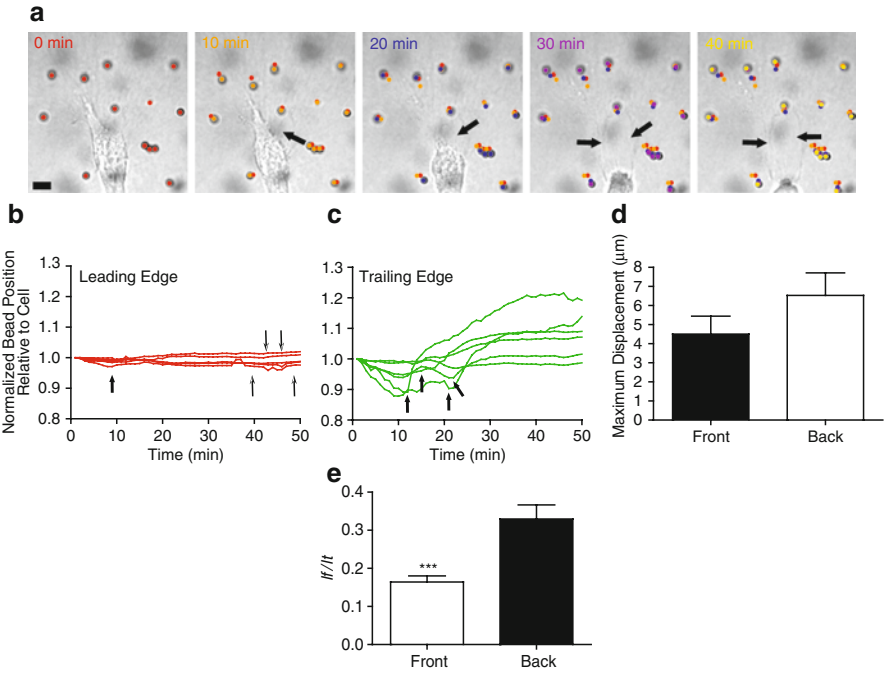

Fig. 4.4 3D matrix deformation at the leading and trailing edges of a migrating cell inside a matrix. (**a**) Initial pulling of the collagen matrix toward the cell is followed by relaxation of the matrix from the cell. *Arrows* indicate the formation of a large defect in the collagen matrix at the back of the cell, a defect that rapidly grows in the wake of the migrating cell. Scale bar, 20 μm. (**b**, **c**) Time-dependent distances between beads and fixed points in the image in the matrix regions near the leading edge (**b**) and near the back (**c**) of a migrating cell [shown in (**a**)]. Distances are normalized by their initial values. *Large arrows* indicate the onset of release of the matrix from the cell surface; *Small arrows* in (**b**) correspond to beads that have not relaxed yet. (**d**) Maximum displacements of the beads toward the cell, l_{max}, in regions of the matrix at the back and front of control cells. (**e**) Ratios of the net distance between initial and final positions of the beads, l_f, and their total displacements, l_t, in regions of the matrix near the front and the back of the cell. A ratio close to 0 indicates an elastic deformation of the matrix; a ratio close to 1 indicates an irreversible deformation of the matrix. $^{***}P<0.001$. Cells studied here are human fibrosarcoma HT-1080 cells. Adapted with permission from Bloom et al. [32]

(e.g. Fig. 4.4c). Accordingly, the normalized distances between the probing beads and the rear of the cell become first <1, then become >1 (Fig. 4.4c). Classical mechanics suggests that this is a signature of material fracture due to a large mechanical stress. Indeed, global relaxation of the matrix at the rear of the cell is rapid and often accompanied by the formation of a large defect in the collagen matrix in the wake of the migrating cell (arrows in Fig. 4.4a). This defect ultimately grows into a 3D path in the matrix along which the cell has traveled.

Using 3D particle-tracking matrix traction micromechanics assay, we can quantify matrix relaxation following the initial deformation of the matrix in the direction of the cell by introducing the ratio of the distance between initial and final positions

of each bead, l_f, to the total displacement of the bead, l_t (Fig. 4.4e). The ratio l_f/l_t is zero for an elastic, reversible recovery after matrix traction toward the cell since in this case $l_f = 0$ μm, which corresponds to an elastic recoil of the matrix after stretching. This ratio is unity when bead movement towards the cell occurs without any matrix relaxation, since in this case $l_f = l_t$. The ratio l_f/l_t is significantly lower in the matrix near the front pseudopodia than in near the back pseudopodia (Fig. 4.4e). Therefore, the deformation of the matrix near the front of the cell is mostly elastic, while that at the back of the cell is more irreversible, an irreversible deformation presumably mediated by MMPs (see more details below).

Taken together, these results indicate that cell migration inside a 3D matrix involves (1) the deformation of the matrix toward the cell without pushing the surrounding matrix, (2) the elastic relaxation of the matrix near the front of the cell, and (3) the irreversible deformation of the matrix near the back of the cell. In general, for each cycle of motility, the cell deforms the matrix with equal magnitude at its front and back, then releases the matrix first at the back, moves forward, and finally releases the matrix at its front.

4.3.4 Protease Inhibitors Block Cell Motility in 3D Matrix

To investigate the role of MMPs in mediating matrix remodeling and cell motility, we measured local 3D matrix deformation when cells are treated with MMP (protease) inhibitors. In protease inhibitors (PI)-treated cells, the magnitude of the deformation of the collagen matrix is greatly reduced. Analysis of the bead trajectories shows that maximum excursions of the beads toward the cell from their initial position (l_{max}) and the mean total displacements of the beads (l_t) are significantly reduced in PI-treated cells compared to untreated cells. Accordingly, the speed of migration of PI-treated cells is drastically reduced compared with control cells. These results using crosslinked collagen I matrices are consistent with Weiss' results, suggesting that MMPs are critical to cell migration in a 3D collagen I matrix.

PI-cocktail treatment also significantly reduces the ratio l_f/l_t, which indicates that the deformation of the matrix becomes elastic, presumably because it does not induce the formation of matrix defects that would prevent a high degree of recovery after cell-induced pulling of the matrix. Moreover, significant difference in the magnitude and type (elastic vs. rupture deformation) of matrix deformation does not occur anymore between the front and the back of PI-treated cells.

4.3.5 Local 3D Matrix Remodeling During 3D Cell Motility is Mediated by Rac1, ROCK, and Myosin II

RhoGTPase inhibitors reduce single-cell migration on planar substrates. The role of RhoGTPases for 3D migration in crosslinked collagen I matrix is less clear. 3D particle-tracking matrix traction micromechanics assay can determine the magnitude

of matrix remodeling following inhibition of myosin II-induced cell contractility and F-actin architecture regulators Rho/ROCK and Rac1 [53]. ROCK and nonmuscle myosin II are two major regulators of membrane protrusion dynamics [54] and Rac1 is a small RhoGTPase that regulates the persistence of migration [42, 55]. Control cells in collagen matrix display mostly cortical actin filament bundles and few cytoplasmic bundles. Cells treated with 5 μM of the specific myosin II inhibitor blebbistatin [56], for which 50% myosin II activity is inhibited [57], display a morphology similar to control cells. Actin filament staining mostly appeared at the cell periphery (cortex) and the number of F-actin bundles in the cell body is reduced. Applying the 3D multiple-particle tacking assay indicated that partial myosin II inhibition greatly reduces the magnitude of local matrix contraction. Accordingly, the speed of migration of blebbistatin-treated cells is reduced compared to control cells.

Cells treated with Y27632 [58, 59], which inactivates ROCKI and ROCKII, display a dendritic morphology with a thin protruding leading edge that is longer than in control cells [60]. Inhibition of ROCK, which is upstream of myosin II and regulates actin filament assembly, reduces significantly the magnitude of matrix contraction and cell speed. Moreover, inhibition of ROCK renders the relaxation of matrix deformation much more elastic-like than in cells treated with 5 μM blebbistatin. Cells treated with specific inhibition of GTPase Rac1 by NSC23766 [61] display a blebbing morphology and membrane protrusions vanish. Rac1 inhibition has an effect on the magnitude of matrix contraction that is intermediate between those produced by ROCK and myosin II inhibitors. Finally, combining MMP inhibition with the inhibition of either ROCK, Rac1, or myosin II synergistically reduce the magnitude of matrix contraction, l_{max}, more than in cells treated with any one of these inhibitors and drastically reduce cell migration [42]. These results suggest that ROCK, Rac1, and myosin II regulate matrix deformation and cell speed and that combining PI treatment with the inhibition of either ROCK, myosin II, or Rac1 synergistically inhibits matrix deformation.

4.3.6 Pseudopodial Protrusions Drive Cell Motility in 3D Through ROCK and Actomyosin Contractility

Exploiting the particle-tracking matrix traction assay, which can simultaneously visualize cell protrusion dynamics and matrix deformation [32], we tested the hypothesis that protrusions locally induce local matrix deformation. Control cells display rapidly growing and retracting protrusions terminated by smaller long finger-like protrusions, which dynamically shift their position along the cell surface. There is a near-perfect correlation between the position of the growing pseudopodial protrusions and the position of local traction of the matrix. Regions along the cell surface where protrusions are absent correlate with regions of the matrix showing no significant traction forces.

Both the number of membrane protrusions and the spatial correlation between the location of a membrane protrusion and local matrix deformation diminish

significantly when myosin II is inhibited and further diminish when ROCK is inhibited. Separately, Rac1 inhibition and PI treatment eliminate membrane protrusions completely and induce cell blebbing. For blebbing cells, matrix contraction is significantly reduced. Together, these results show that the particle-tracking matrix traction assay can probe simultaneously membrane protrusion dynamics and local matrix remodeling. The results suggest that matrix traction and associated cell motility in 3D matrix are driven by growing pseudopodial protrusions mediated by ROCK and myosin II activity.

Acknowledgments Work in Wirtz lab is supported by NIH grants CA143868, CA137686, CA13789, and GM084204, and the Grant-in-aid 0855319E from the American Heart Association. SIF is recipient of a graduate student fellowship from the National Science Foundation and an ARCS Foundation graduate fellowship.

References

1. Folkman, J. and Haudenschild, C. (1980). Angiogenesis in vitro. Nature *288*, 551–556.
2. Ridley, A.J., Schwartz, M.A., Burridge, K., Firtel, R.A., Ginsberg, M.H., Borisy, G., Parsons, J.T., and Horwitz, A.R. (2003). Cell migration: integrating signals from front to back. Science *302*, 1704–1709.
3. Wirtz, D. (2009). Particle-tracking microrheology of living cells: principles and applications. Annu Rev Biophys *38*, 301–326.
4. Lee, J.S., Panorchan, P., Hale, C.M., Khatau, S.B., Kole, T.P., Tseng, Y., and Wirtz, D. (2006). Ballistic intracellular nanorheology reveals ROCK-hard cytoplasmic stiffening response to fluid flow. J Cell Sci *119*, 1760–1768.
5. Tseng, Y., Kole, T.P., and Wirtz, D. (2002). Micromechanical mapping of live cells by multiple-particle-tracking microrheology. Biophys J *83*, 3162–3176.
6. Suh, J., Wirtz, D., and Hanes, J. (2003). Efficient active transport of gene nanocarriers to the cell nucleus. Proc Natl Acad Sci USA *100*, 3878–3882.
7. McGrath, J.L., Hartwig, J.H., and Kuo, S.C. (2000). The mechanics of F-actin microenvironments depend on the chemistry of probing surfaces. Biophys J *79*, 3258–3266.
8. Apgar, J., Tseng, Y., Federov, E., Herwig, M.B., Almo, S.C., and Wirtz, D. (2000). Multiple-particle tracking measurements of heterogeneities in solutions of actin filaments and actin bundles. Biophys J *79*, 1095–1106.
9. Kole, T.P., Tseng, Y., and Wirtz, D. (2004). Intracellular microrheology as a tool for the measurement of the local mechanical properties of live cells. Methods Cell Biol. *78*, 45–64.
10. Tseng, Y., Lee, J.S., Kole, T.P., Jiang, I., and Wirtz, D. (2004). Micro-organization and viscoelasticity of the interphase nucleus revealed by particle nanotracking. J Cell Sci *117*, 2159–2167.
11. Gupton, S.L., Anderson, K.L., Kole, T.P., Fischer, R.S., Ponti, A., Hitchcock-DeGregori, S.E., Danuser, G., Fowler, V.M., Wirtz, D., Hanein, D., and Waterman-Storer, C.M. (2005). Cell migration without a lamellipodium: translation of actin dynamics into cell movement mediated by tropomyosin. J Cell Biol *168*, 619–631.
12. Kole, T.P., Tseng, Y., Jiang, I., Katz, J.L., and Wirtz, D. (2005). Intracellular mechanics of migrating fibroblasts. Mol Biol Cell *16*, 328–338.
13. Daniels, B.R., Masi, B.C., and Wirtz, D. (2006). Probing single-cell micromechanics in vivo: the microrheology of *C. elegans* developing embryos. Biophys J *90*, 4712–4719.
14. Panorchan, P., Lee, J.S., Kole, T.P., Tseng, Y., and Wirtz, D. (2006). Microrheology and ROCK signaling of human endothelial cells embedded in a 3D matrix. Biophys J *91*, 3499–3507.

15. Lee, J.S., Hale, C.M., Panorchan, P., Khatau, S.B., George, J.P., Tseng, Y., Stewart, C.L., Hodzic, D., and Wirtz, D. (2007). Nuclear lamin A/C deficiency induces defects in cell mechanics, polarization, and migration. Biophys J *93*, 2542–2552.
16. Panorchan, P., Lee, J.S., Daniels, B.R., Kole, T.P., Tseng, Y., and Wirtz, D. (2007). Probing cellular mechanical responses to stimuli using ballistic intracellular nanorheology. Methods Cell Biol *83*, 115–140.
17. Mason, T.G., Ganesan, K., van Zanten, J.V., Wirtz, D., and Kuo, S.C. (1997). Particletracking microrheology of complex fluids. Phys Rev Lett *79*, 3282–3285.
18. Atilgan, E., Wirtz, D., and Sun, S.X. (2005). Morphology of the lamellipodium and organization of actin filaments at the leading edge of crawling cells. Biophys J *89*, 3589–3602.
19. Luby-Phelps, K., Castle, P.E., Taylor, D.L., and Lanni, F. (1987). Hindered diffusion of inert tracer particles in the cytoplasm of mouse 3T3 cells. Proc Natl Acad Sci USA *84*, 4910–4913.
20. Luby-Phelps, K. (1993). Physical properties of cytoplasm. Curr Opin Cell Biol *6*, 3–9.
21. Lukacs, G.L., Haggie, P., Seksek, O., Lechardeur, D., Freedman, N., and Verkman, A.S. (2000). Size-dependent DNA mobility in cytoplasm and nucleus. J Biol Chem *275*, 1625–1629.
22. Seksek, O., Biwersi, J., and Verkman, A.S. (1997). Translational diffusion of macromolecule-sized solutes in cytoplasm and nucleus. J Cell Biol *138*, 131–142.
23. Stewart-Hutchinson, P.J., Hale, C.M., Wirtz, D., and Hodzic, D. (2008). Structural requirements for the assembly of LINC complexes and their function in cellular mechanical stiffness. Exp Cell Res *314*, 1892–1905.
24. Hale, C.M., Shrestha, A.L., Khatau, S.B., Stewart-Hutchinson, P.J., Hernandez, L., Stewart, C.L., Hodzic, D., and Wirtz, D. (2008). Dysfunctional connections between the nucleus and the actin and microtubule networks in laminopathic models. Biophys J *95*, 5462–5475.
25. Pajerowski, J.D., Dahl, K.N., Zhong, F.L., Sammak, P.J., and Discher, D.E. (2007). Physical plasticity of the nucleus in stem cell differentiation. Proc Natl Acad Sci USA *104*, 15619–15624.
26. Khatau, S.B., Hale, C.M., Stewart-Hutchinson, P.J., Patel, M.S., Stewart, C.L., Searson, P.C., Hodzic, D., and Wirtz, D. (2009). A perinuclear actin cap regulates nuclear shape. Proc Natl Acad Sci USA *106*, 19017–19022.
27. Heidemann, S.R. and Wirtz, D. (2004). Towards a regional approach to cell mechanics. Trends Cell Biol *14*, 160–166.
28. Hoh, J.H. and Schoenenberger, C.A. (1994). Surface morphology and mechanical properties of MDCK monolayers by atomic force microscopy. J Cell Sci *107*, 1105–1114.
29. Lee, J.S., Chang, M.I., Tseng, Y., and Wirtz, D. (2005). Cdc42 mediates nucleus movement and MTOC polarization in Swiss 3T3 fibroblasts under mechanical shear stress. Mol Biol Cell *16*, 871–880.
30. Mizuno, D., Tardin, C., Schmidt, C.F., and Mackintosh, F.C. (2007). Nonequilibrium mechanics of active cytoskeletal networks. Science *315*, 370–373.
31. Hale, C.M., Sun, S.X., and Wirtz, D. (2009). Resolving the role of actoymyosin contractility in cell microrheology. PLoS One *4*, e7054.
32. Bloom, R.J., George, J.P., Celedon, A., Sun, S.X., and Wirtz, D. (2008). Mapping local matrix remodeling induced by a migrating tumor cell using three-dimensional multiple-particle tracking. Biophys J *95*, 4077–4088.
33. Ghosh, P.K., Vasanji, A., Murugesan, G., Eppell, S.J., Graham, L.M., and Fox, P.L. (2002). Membrane microviscosity regulates endothelial cell motility. Nat Cell Biol *4*, 894–900.
34. Byzova, T.V., Goldman, C.K., Pampori, N., Thomas, K.A., Bett, A., Shattil, S.J., and Plow, E.F. (2000). A mechanism for modulation of cellular responses to VEGF: activation of the integrins. Mol Cell *6*, 851–860.
35. Gong, C., Stoletov, K.V., and Terman, B.I. (2004). VEGF treatment induces signaling pathways that regulate both actin polymerization and depolymerization. Angiogenesis *7*, 313–322.
36. van Nieuw Amerongen, G.P., Koolwijk, P., Versteilen, A., and van Hinsbergh, V.W. (2003). Involvement of RhoA/Rho kinase signaling in VEGF-induced endothelial cell migration and angiogenesis in vitro. Arterioscler Thromb Vasc Biol *23*, 211–217.

37. Kimura, K., Ito, M., Amano, M., Chihara, K., Fukata, Y., Nakafuku, M., Yamamori, B., Feng, J., Nakano, T., Okawa, K., Iwamatsu, A., and Kaibuchi, K. (1996). Regulation of myosin phosphatase by Rho and Rho-associated kinase (Rho-kinase). Science *273*, 245–248.
38. Rousseau, S., Houle, F., Kotanides, H., Witte, L., Waltenberger, J., Landry, J., and Huot, J. (2000). Vascular endothelial growth factor (VEGF)-driven actin-based motility is mediated by VEGFR2 and requires concerted activation of stress-activated protein kinase 2 (SAPK2/p38) and geldanamycin-sensitive phosphorylation of focal adhesion kinase. J Biol Chem *275*, 10661–10672.
39. Somlyo, A.V., Phelps, C., Dipierro, C., Eto, M., Read, P., Barrett, M., Gibson, J.J., Burnitz, M.C., Myers, C., and Somlyo, A.P. (2003). Rho kinase and matrix metalloproteinase inhibitors cooperate to inhibit angiogenesis and growth of human prostate cancer xenotransplants. FASEB J *17*, 223–234.
40. Sabeh, F., Shimizu-Hirota, R., and Weiss, S.J. (2009). Protease-dependent versus – independent cancer cell invasion programs: three-dimensional amoeboid movement revisited. J Cell Biol *185*, 11–19.
41. Friedl, P. and Wolf, K. (2003). Proteolytic and non-proteolytic migration of tumour cells and leucocytes. Biochem Soc Symp *70*, 277–285.
42. Sahai, E. and Marshall, C.J. (2003). Differing modes of tumour cell invasion have distinct requirements for Rho/ROCK signalling and extracellular proteolysis. Nat Cell Biol *5*, 711–719.
43. Corbitt, C.A., Lin, J., and Lindsey, M.L. (2007). Mechanisms to inhibit matrix metalloproteinase activity: where are we in the development of clinically relevant inhibitors? Recent Pat Anticancer Drug Discov *2*, 135–142.
44. Zaman, M.H., Trapani, L.M., Sieminski, A.L., MacKellar, D., Gong, H., Kamm, R.D., Wells, A., Lauffenburger, D.A., and Matsudaira, P. (2006). Migration of tumor cells in 3D matrices is governed by matrix stiffness along with cell-matrix adhesion and proteolysis. Proc Natl Acad Sci USA *103*, 10889–10894.
45. Wolf, K., Mazo, I., Leung, H., Engelke, K., von Andrian, U.H., Deryugina, E.I., Strongin, A.Y., Brocker, E.B., and Friedl, P. (2003). Compensation mechanism in tumor cell migration: mesenchymal-amoeboid transition after blocking of pericellular proteolysis. J Cell Biol *160*, 267–277.
46. Hotary, K., Li, X.Y., Allen, E., Stevens, S.L., and Weiss, S.J. (2006). A cancer cell metalloprotease triad regulates the basement membrane transmigration program. Genes Dev *20*, 2673–2686.
47. Demou, Z.N., Awad, M., McKee, T., Perentes, J.Y., Wang, X., Munn, L.L., Jain, R.K., and Boucher, Y. (2005). Lack of telopeptides in fibrillar collagen I promotes the invasion of a metastatic breast tumor cell line. Cancer Res *65*, 5674–5682.
48. Woodley, D.T., Yamauchi, M., Wynn, K.C., Mechanic, G., and Briggaman, R.A. (1991). Collagen telopeptides (cross-linking sites) play a role in collagen gel lattice contraction. J Invest Dermatol *97*, 580–585.
49. Celedon, A., Nodelman, I.M., Wildt, B., Dewan, R., Searson, P., Wirtz, D., Bowman, G.D., and Sun, S.X. (2009). Magnetic tweezers measurement of single molecule torque. Nano Lett *9*, 1720–1725.
50. Meshel, A.S., Wei, Q., Adelstein, R.S., and Sheetz, M.P. (2005). Basic mechanism of three-dimensional collagen fibre transport by fibroblasts. Nat Cell Biol *7*, 157–164.
51. Chang, M.I., Panorchan, P., Dobrowsky, T.M., Tseng, Y., and Wirtz, D. (2005). Single-molecule analysis of human immunodeficiency virus type 1 gp120-receptor interactions in living cells. J Virol *79*, 14748–14755.
52. Grinnell, F. (2000). Fibroblast-collagen-matrix contraction: growth-factor signalling and mechanical loading. Trends Cell Biol *10*, 362–365.
53. Ridley, A.J. (2001). Rho GTPases and cell migration. J Cell Sci *114*, 2713–2722.
54. Delanoe-Ayari, H., Al Kurdi, R., Vallade, M., Gulino-Debrac, D., and Riveline, D. (2004). Membrane and acto-myosin tension promote clustering of adhesion proteins. Proc Natl Acad Sci USA *101*, 2229–2234.

55. Pankov, R., Endo, Y., Even-Ram, S., Araki, M., Clark, K., Cukierman, E., Matsumoto, K., and Yamada, K.M. (2005). A Rac switch regulates random versus directionally persistent cell migration. J Cell Biol *170*, 793–802.
56. Ramamurthy, B., Yengo, C.M., Straight, A.F., Mitchison, T.J., and Sweeney, H.L. (2004). Kinetic mechanism of blebbistatin inhibition of nonmuscle myosin IIB. Biochemistry *43*, 14832–14839.
57. Shu, S., Liu, X., and Korn, E.D. (2005). Blebbistatin and blebbistatin-inactivated myosin II inhibit myosin II-independent processes in Dictyostelium. Proc Natl Acad Sci USA *102*, 1472–1477.
58. Uehata, M., Ishizaki, T., Satoh, H., Ono, T., Kawahara, T., Morishita, T., Tamakawa, H., Yamagami, K., Inui, J., Maekawa, M., and Narumiya, S. (1999). Calcium sensitization of smooth muscle mediated by a Rho-associated protein kinase in hypertension. Nature *389*, 990–994.
59. Kole, T.P., Tseng, Y., Huang, L., Katz, J.L., and Wirtz, D. (2004). Rho kinase regulates the intracellular micromechanical response of adherent cells to rho activation. Mol Biol Cell *15*, 3475–3484.
60. Carragher, N.O., Walker, S.M., Scott Carragher, L.A., Harris, F., Sawyer, T.K., Brunton, V.G., Ozanne, B.W., and Frame, M.C. (2006). Calpain 2 and Src dependence distinguishes mesenchymal and amoeboid modes of tumour cell invasion: a link to integrin function. Oncogene *25*, 5726–5740.
61. Gao, Y., Dickerson, J.B., Guo, F., Zheng, J., and Zheng, Y. (2004). Rational design and characterization of a Rac GTPase-specific small molecule inhibitor. Proc Natl Acad Sci USA *101*, 7618–7623.

Chapter 5
Biophysical Properties of Scaffolds Modulate Human Blood Vessel Formation from Circulating Endothelial Colony-Forming Cells

Paul J. Critser and Mervin C. Yoder

5.1 Introduction

Early in development, the rapidly growing embryo exceeds a size that permits appropriate diffusion of nutrients or oxygen sufficiently deep into the organism, requiring the development of a primitive vascular plexus. This process of de novo blood vessel formation known as vasculogenesis [1] allows for the development of tissues beyond the diffusion limit of 100–200 μm [2, 3]. The primitive vascular plexus and other vessels are continuously remodeled to accommodate growing or damaged tissues via sprouting and intussusceptive angiogenesis providing a system for transport of not only oxygen and nutrients, but also cytokines and cells throughout the organism. This vascular system is lined by endothelial cells with a subjacent basement membrane. Small caliber vessels are lined by a single layer of perivascular cells, while larger more complex vessels have a wall composed of a complex extracellular matrix (ECM), nerves, and even smaller vessels. The endothelium is crucial in maintaining normal vessel function. When the ability of the endothelium to repair or generate new vasculature is altered, the result is tissue damage and disease due to either ischemia or inappropriate angiogenesis which can contribute to tumor growth and metastasis. Hence, an ability to understand the molecular mechanisms that govern vessel formation and remodeling is of great interest for the treatment of these disease states [3, 4].

M.C. Yoder (✉)
Department of Pediatrics, Indiana University School of Medicine, 1044 West Walnut Street, R4-W125A, Indianapolis, IN 46202, USA
and
Herman B Wells Center for Pediatric Research, Indiana University School of Medicine, Indianapolis, IN, USA
and
Department of Biochemistry and Molecular Biology, Indiana University School of Medicine, Indianapolis, IN, USA
e-mail: myoder@iupui.edu

S. Gerecht (ed.), *Biophysical Regulation of Vascular Differentiation and Assembly*, Biological and Medical Physics, Biomedical Engineering,
DOI 10.1007/978-1-4419-7835-6_5,

The remodeling of the vascular system to repair or generate new vessels involves alterations to the surrounding matrix, cellular migration, and proliferation, as well as tightly controlled signaling cascades. This chapter focuses on the role of the ECM in regulating the formation and remodeling of blood vessels. Specifically, it explores how matrix scaffolds can modulate the in vivo vessel formation by human endothelial progenitor cells (EPCs) by altering the biophysical environment including mechanical and chemical properties. Additionally, potential applications to tissue engineering are discussed.

5.2 Concepts in Matrix Regulation of Vessel Formation

5.2.1 Cell Sources

Investigation into vasculogenesis and angiogenesis in matrix scaffolds in vitro and in vivo [5–12] has often utilized mature endothelial cell populations such as human umbilical vein endothelial cells (HUVECs) and EPCs from umbilical cord and peripheral blood as well as from human embryonic stem cells (hESCs). The formation of vascular networks for therapeutic applications requires a population of endothelial cells that can be easily isolated, displays a high proliferative potential, and an ability to form vascular networks in vivo. While mature endothelial cell populations such as HUVECs have displayed the potential to form functional vessels in vivo [9, 13, 14], they possess limited proliferative capacity, which prohibit their use in large-scale tissue constructs.

EPCs, known to circulate in the bloodstream and home to sites in need of vessel formation in both physiological and pathological settings, have been examined over the past decade by numerous investigators for their therapeutic potential [15–18]. While studies have demonstrated positive results in animal models, human trials have resulted in mixed success [4, 16]. This is due, in part, to several factors including: the rarity of the cells [19], controversy in isolation and expansion of EPCs [15, 17, 18, 20–22], and the use of systemic, rather than local delivery [4]. A major limitation has been the lack of a specific marker to identify an EPC and thus, great heterogeneity in the types of cells that have been tested under the guise of an EPC.

During the formation of the primitive vascular plexus, angioblasts, which are precursors to endothelial cells [23], surround emerging hematopoietic elements in close approximation [1]. Isolation of putative EPC populations was originally based on cell surface antigens known to be expressed on hematopoietic stem cells and endothelial cells resulting in the isolation of cells of both hematopoietic and endothelial lineages (reviewed in [24]). This method, first described by Asahara et al. [15], was later modified [17, 25] to deplete mature endothelial cells from culture to potentially enrich for EPCs. Low-density mononuclear cells (MNCs) form adherent colonies, referred to as colony forming unit-HILL (CFU-HILL) after 5–9 days, when plated on fibronectin-coated tissue culture surfaces. CFU-HILL cells have been shown to express cell surface antigens consistent with an

endothelial cell phenotype and ingest acetylated low-density lipoprotein (AcLDL), a behavior common to both endothelial cells and monocytes (Table 5.1). CFU-HILL cells also express several monocyte/macrophage cell surface antigens such as CD14, CD45, and CD115, ingest bacteria, display nonspecific esterase activity, and display limited proliferative potential [6, 15, 26, 27]. Thus, the CFU-HILL assay does not identify EPCs but rather permits enumeration of colonies of hematopoietic cells. While the hematopoietic cells do not directly contribute to the formation of new blood vessels (are not endothelium), these cells do contribute to neoangiogenesis via paracrine signaling pathways and function as circulating proangiogenic cells [28].

Recently another method of EPC isolation has identified a cell population termed endothelial colony forming cells (ECFCs), [21] which are also known as blood outgrowth endothelial cells (BOECs) [20, 29]. Human umbilical cord or adult peripheral blood-derived low-density MNCs plated on type I collagen-coated tissue culture surfaces form adherent colonies with a cobblestone morphology. These colonies first appear in culture between day 7 and 21, with cord blood-derived colonies emerging earlier and at a higher frequency than adult blood-derived colonies [21]. Ingram et al. developed a single-cell assay to investigate the proliferative capacity of putative EPC populations. ECFCs demonstrated an ability to produce progeny in a clonal fashion, display a hierarchy of proliferative potential, and an ability to give rise to secondary colonies when isolated from both umbilical cord and adult peripheral blood. Consistent with high-proliferative behavior, ECFC colonies exhibit relatively high levels of telomerase [21]. While ECFCs express cell surface antigens consistent with an endothelial cell phenotype [6, 21], they do not express hematopoietic or monocyte/macrophage cell surface markers such as CD14, CD45, or CD115 [6] (Table 5.1).

The original defining concept of an EPC was that of a circulating cell that possessed postnatal vasculogenic activity; the ability to form a vascular system from a suspension of angioblast-like cells. ECFCs have displayed the potential to form blood vessels de novo in vivo when implanted in a type I collagen matrix [6, 7] or a matrigel-based scaffold [8]. No other cell type that has been referred to as an EPC can spontaneously form a vasculature in vivo, though many of the hematopoietic-derived cells are capable of extravasating from the blood stream, migrating into a tissue, and attaching to any remnants of an endothelial basement membrane that may have persisted following endothelial dropout following cessation of blood flow at a site of ischemia. Thus, the hematopoietic cells that attach to the basement membrane remnant may appear to be forming a vascular structure, but the cells are not synthesizing the matrix to which they are attaching, a necessary step in stabilizing remodeled vasculature [30], and are therefore not endothelial cells. While ECFCs could be isolated from peripheral blood to provide a patient-specific cell source, adult blood-derived ECFCs have a decreased proliferative potential [21] and decreased ability to form functional vessels when implanted in a type I collagen ECM [7] compared with umbilical cord blood-derived ECFCs (Fig. 5.1). Thus, ECFCs display all of the properties of a cell that one would envision as an EPC. Unfortunately, circulating ECFCs are extremely rare, being present at a frequency of $1/10^6$ cord blood and $1/10^8$ adult peripheral

Table 5.1 Phenotypic and functional characterization of CFU-HILL and ECFCs [6]

Assay	CFU-HILL	ECFC
Endothelial surface antigens		
CD31	92.31 ± 5.47	92.29 ± 1.32
CD105	74.36 ± 6.32	96.73 ± 1.79
CD144	34.80 ± 8.74	99.15 ± 0.85
CD146	56.52 ± 10.00	94.21 ± 3.71
KDR	99.19 ± 0.81	68.61 ± 11.26
VWF	67.21 ± 12.78	97.09 ± 2.05
UEA-1	41.80 ± 11.67	100
AcLDL	73.68 ± 9.05	99.75 ± 0.25
Hematopoietic surface antigens		
CD45	98.15 ± 1.85	0.37 ± 0.37
CD14	98.53 ± 1.04	1.20 ± 0.74
CD115	94.42 ± 2.52	0.28 ± 0.21
Macrophage properties		
Phagocytosis of bacteria	Yes	No
Nonspecific esterase activity	Yes	No
Vasculogenic properties		
Proliferative potential	Some	Robust
Secondary colony-forming capacity	Some CFU-GM	EC colonies
In vivo vessel formation	No	Yes

VWF Von Willebrand factor, *UEA-1* Ulex europaeus agglutinin 1, *AcLDL* lectin, acetylated low-density lipoprotein, vascular endothelial growth factor II receptor (KDR).

blood MNCs plated. Furthermore, there is no specific antigen that currently permits prospective isolation of the rare ECFC in the blood stream and discriminates this cell from the occasional viable sloughed endothelial cells derived from the intima of systemic blood vessels.

Another opportunity exists to differentiate EPCs from hESCs. Endothelial cells derived from hESCs have shown the potential to form luminal structures in vitro in both matrigel and type I collagen scaffolds [31], and functional vessels when implanted in type I collagen scaffolds in vivo with murine 10T1/2 cells [32]. Additionally, vascular progenitor cells derived from hESCs were shown to form blood vessels when implanted with and without hESC-derived smooth muscle-like cells in a Matrigel scaffold [33]. Additionally, hESC seeded on to poly-(lactic-*co*-glycolic acid) scaffolds and transplanted between liver lobules of immunodeficient mice were extensively vascularized by both host and human vessels, suggesting the in vivo differentiation of hESC into EPC [34].

Additionally, the recent ability to reprogram adult differentiated somatic cells using a defined set of transcription factors to form induced pluripotent stem cells (iPSCs) could provide a source of patient-derived cells for vascularized tissue constructs [35–38]. Recent reports have demonstrated endothelial cells can be differentiated from fibroblast-derived human iPSCs [39, 40], which could be a source of autologous cells for angiogenic therapies. However, the proliferative potential of both hESC- and iPSC-derived endothelial cells has not been fully

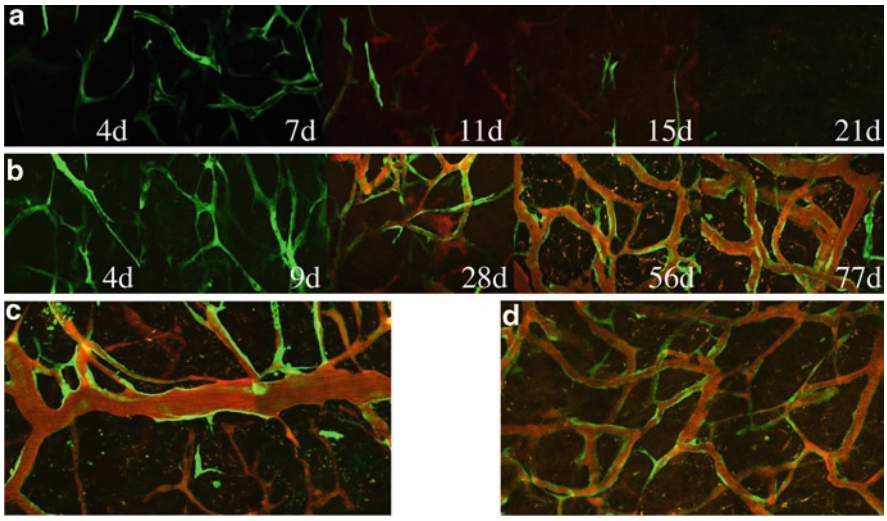

Fig. 5.1 ECFCs derived from adult and umbilical cord blood demonstrate varied vasculogenic capabilities. Adult blood-derived ECFCs formed vascular structures that were not functional and quickly regressed in the absence of perivascular cells (**a**) and were present at a low density when co-implanted with perivascular cells (**c**). While implantation of cord blood-derived ECFCs alone resulted in the regression of vascular structures, co-implantation with perivascular cells resulted in robust and long-lasting functional vessel formation (**b**, **d**). Scale bars (**a**, **c**) 50 μm and (**c**, **d**) 100 μm. Reprinted from ref. [7] with permission from the American Society of Hematology

characterized. Further the ability of iPSC-derived endothelial cells to form functional vessels in vivo has not yet been tested and further investigation is needed.

5.2.2 Signaling Matrix–Integrin–Cytoskeleton

5.2.2.1 Scaffolds Used for Vasculogenesis

The native ECM is a complex network of structural proteins such as collagen, elastin, fibronectin, and proteoglycans [41]. The engineering of such a complex matrix is very challenging and most approaches have used a simplified matrix as a model of the ECM [41] consisting of either synthetic or biological components. Synthetic matrices used to study angiogenesis and vasculogenesis have been derived from several polymers including polyglycolic acid (PGA), polylactic acid (PLA), polyethylene glycol (PEG), and others. Additionally, combinations of polymers have been used to take advantage of specific properties of each component, such as poly-(lactide-*co*-glycolide) (PLGA). Further, scaffolds from self-assembling ionic peptides have been used to study endothelial capillary network formation [42]. One advantage of these synthetic-based scaffolds is the ability to fine tune microstructure and degradation profiles by altering the processing and components of the scaffolds [12, 42].

Biological-based matrices are typically composed of type I collagen or fibrin as the main component [41]. Other materials used to generate biological scaffolds to study angiogenesis and vasculogenesis include Matrigel [8], elastin, hyaluronic acid [43], dextran, and alginate [44]. These biological-based matrices have the advantage of being biocompatible, enzymatically degradable, and interacting with host cells to promote vascularization. Scaffolds have additionally been modified to include growth factors [43, 44] and peptide sequences such as arginine–glycine–aspartic acid (RGD) [44] to increase endothelial cell survival and adhesion.

While the ability to tune specific parameters in these scaffolds has been more challenging than for synthetic-based scaffolds, methods such as altering source of matrix proteins, combining different biological proteins in scaffolds and cross-linking matrix proteins provide potential tools to modulate the biophysical properties. Several studies have demonstrated these effects on biophysical properties of collagen-based scaffolds. Collagen source and extraction method have been shown to affect collagen fiber diameter and mechanical properties [45]. Additionally, a recent report has demonstrated that the addition of hyaluronic acid (HA) to the collagen-based scaffolds alters the biophysical properties [46]. Further, chemical fixations such as aldehydes, epoxides, and quinines as well as physical methods such as UV light and dye-mediated photo oxidation can be used to cross-link collagen fibrils in vitro [47]. Although these cross-linking methods may alter the biocompatibility of the scaffolds, further investigation is needed to examine the role of cross-linking of matrix components and the addition of various proteins into biological scaffolds on the biophysical properties of these matrices.

5.2.2.2 Matrix Regulation of Cell Behavior

Cells embedded in a 3D scaffold bind to and interact with the matrix components. Cells embedded into a collagen-based scaffold are able to reorganize the matrix [48, 49]. This interaction occurs because the collagen fibrils bind to integrin receptors that are anchored to the actin cytoskeleton [50]. Peptides such as RGD also facilitate scaffold adhesion to integrin receptors on embedded cells. Once bound the integrin receptors cluster and begin to form aggregates of proteins such as talin, vinculin, and α-actinin known as focal adhesions [50, 51]. Focal adhesions serve as the entry point of mechanical cues from the ECM into the cell and these cues influence cell shape, cell migration, cell survival, and cell differentiation [52–54].

The impact of the ECM on cell behavior has been well demonstrated for mesenchymal stem cells (MSCs). McBeath et al. provided evidence that mechanical parameters of the microenvironment dictate MSC shape and lineage commitment [55]. MSCs were plated on a PDMS (polydimethylsiloxane) micropatterned substrate, which dictated the extent of cell spreading and shape. While MSCs that exhibited a spread morphology underwent osteogenic differentiation, MSCs that exhibited a rounded morphology underwent adipogenic differentiation. However, when the cytoskeletal tension was inhibited, MSCs underwent adipogenic differentiation independent of cell shape or morphology [55].

Ruiz and colleagues also demonstrated that force gradients can regulate MSC lineage commitment [51]. MSC plated on a sinusoidal band where cells cultured on the convex regions experienced high force, while cells grown on the concave regions were exposed to reduced forces. Cells cultured in regions of high force preferentially differentiated down an osteogenic lineage, while cells in the regions of low force underwent adiopogenic differentiation. Further osteogenic differentiation could be abrogated by inhibitors of cytoskeletal force generation [56].

Engler et al. further demonstrated the impact of the microenvironment on MSC behavior by showing that modulating matrix stiffness can direct MSC lineage commitment [57]. Engler et al. modulated matrix stiffness by altering the concentration of bis-acrylamide cross-linking. Three matrix regimes were investigated: a low stiffness matrix that approximated the stiffness of brain, a medium stiffness matrix that was similar to the stiffness of muscle, and a high stiffness matrix that was close to the stiffness of osteoid. MSCs exhibited characteristics of neurons, muscle cells, and osteocytes on the low, medium, and high stiffness matrix, respectively. Further, morphology and lineage-specific protein expression of MSCs was dictated by the matrix stiffness supporting the importance of matrix stiffness on cell behavior [57].

5.2.2.3 Matrix Role on In Vitro Vasculogenesis/Angiogenesis

The study of angiogenesis and vasculogenesis has evolved over several decades and includes both 2D and 3D assays. While the mechanism of tube formation varies in different assays, all assays have demonstrated that endothelial cell–matrix and cell–cell interactions are crucial for in vitro endothelial cell network formation. One of the first in vitro assays was developed by Folkman and Haudenschild [58], in which endothelial cells formed tubular networks on top of an endothelial cell monolayer. The endothelial cell monolayer secreted its own matrix consisting mainly of type I collagen that was required for tube formation [59].

In 2D in vitro endothelial cell vessel formation assays, the density of matrix proteins and endothelial cells influences the potential for tube formation. Endothelial cells stimulated by fibroblast growth factor (FGF), known to induce endothelial spreading [60] and endothelial cell tube formation in vitro [61], were plated on nonadhesive plates with different density coatings of fibronectin, gelatin, or type IV collagen [62]. A high density of matrix proteins promoted cell spreading and growth, whereas a low density of matrix proteins resulted in cell rounding and death, but intermediate density resulted in tube formation. Tube formation could be induced at a high-matrix protein density by plating endothelial cells at a higher cell density [62].

In 3D assays of in vitro capillary morphogenesis, endothelial cells are seeded into a collagen solution so that the cells are evenly distributed in the scaffold [63]. Many studies have investigated the cellular mechanisms of EC lumen formation in 3D type I collagen scaffolds in vitro [9, 11, 63–73]. These studies have identified a matrix–integrin–cytoskeleton signaling axis that is critical in EC tube formation [63, 66, 70, 72]. Matrix signals enter through integrin receptors and activate Rho

GTPase family members Rac1 and Cdc42 to initiate vacuole formation by embedded endothelial cells [72]. Vacuoles then merge and coalesce to form multicellular structures. As these complex structures are forming, the cells are also remodeling the surrounding matrix. Membrane type I-matrix metalloproteinase (MT1-MMP)-dependent proteolysis allows the resident endothelial cells to create vascular guidance tunnels within the scaffold [74]. These channels, once created, allow endothelial cell migration throughout the network of guidance pathways. Interestingly, the integrin ligands that are engaged by the endothelial cells to interact with the scaffold switch during this process. Initially, endothelial cells utilize $\alpha 2\beta 1$ for vacuole and lumen formation in 3D collagen scaffolds [63]. As new matrix components are deposited, including fibronectin, laminins, nidogens, and type IV collagen, the endothelial cells upregulate expression of integrins typically associated with these new matrix components and then use the receptors for migration throughout the network of tunnels [74].

Endothelial cell behavior in 3D scaffolds is altered by the presence of pericytes and other perivascular cells. In vivo vessel formation of ECFCs has been shown to be stabilized by mesenchymal progenitor cells derived from either adult peripheral or umbilical cord blood leading to a longer time of persistence of ECFC-derived vessels when implanted in matrigel [75]. This effect has also been demonstrated in type I collagen scaffolds. HUVEC-derived in vivo vessels were stabilized by MSCs allowing the functional vessels to persist for greater than 130 days. Additionally, these HUVEC–MSC composite vessels demonstrated a vasoconstrictive response to endothelin-1 [76]. In vitro investigations have suggested that this stabilization effect could be due to pericyte interaction with endothelial cells within a scaffold inducing endothelial cell basement membrane deposition. Endothelial cells form vascular guidance channels, which serve to recruit pericytes to the newly formed vascular networks in vitro. Pericytes induce endothelial cells to deposit basement membrane proteins including fibronectin, laminin, nidogen-1, and perlecan. The deposition of basement membrane components serves to stabilize the vascular structures and diminishes remodeling in vitro [30]. Understanding the role of accessory cells including pericytes, CACs, and others will be crucial to the development of functional vascular networks.

5.3 Review of Work

5.3.1 Matrix Regulation of In Vitro Endothelial Cell Network Formation

While the above studies have focused on the importance of the matrix–integrin–cytoskeleton signaling axis on capillary morphogenesis, only a few studies have investigated the effects of the mechanical properties of scaffolds on endothelial cell tube formation in vitro [67, 71]. Korff et al. [67] seeded type I collagen matrices with endothelial cell spheroids. When two spheroids were placed within 500–700 μm

of each other, collagen fibrils were induced to align along the axis between the spheroids. Further, endothelial spheroid sprouts would change direction toward other spheroids, suggesting a role for the matrix of transmitting mechanical signals and aiding in the formation of multicellular structures before cell–cell contacts are formed. Additionally, soluble RGD peptides, which inhibit collagen fibril–integrin binding, abrogated spheroid sprouting [67].

Sieminski et al. [71] seeded HUVECs or ECFCs into type I collagen scaffolds with different collagen concentrations. The matrices were either left adhered to the well (adhered) or released (free floating) to further modify the mechanical properties of the scaffolds. Sieminski noted that changing the collagen concentration altered the matrix stiffness, ligand density, and had other biochemical effects [71].

The average lumen size and tube length of structures were dependent on collagen concentration, endothelial cell type, and whether the matrix was adherent or free floating. ECFCs seeded in 1.5 mg/ml collagen scaffolds that were adherent or free floating caused extreme contraction and cell death. ECFCs in 3 mg/ml collagen matrices formed tube-like structures. These structures were shorter and had wider lumens in 3 mg/ml scaffolds that were adherent compared with those that were free floating. HUVECs in 1.5 mg/ml matrices formed structures that were similar to those formed by ECFCs in free floating 3 mg/ml scaffolds, while structures formed by HUVECs in 3 mg/ml scaffolds had an appearance similar to ECFC structures in adherent 3 mg/ml scaffolds. The authors suggest that the ratio of matrix stiffness and cell generated tension are critical in regulation capillary morphogenesis [71].

Decreasing stiffness of an ionic self-assembling peptide scaffold increases capillary network formation in vitro. HUVECs were seeded into scaffold of stiffness ranging from 46 to 753 Pa. As stiffness decreased, elongation of capillary structures and the extent of single endothelial cells decreased. At the lowest stiffness tested, multicellular capillary structures were seen. Further decrease of scaffold stiffness below 46 Pa led to compaction of the scaffold and did not permit endothelial cell network formation. These results are similar to the results seen in type I collagen matrices where compaction of gels at low concentration did not permit endothelial network formation [42]. These data provide evidence that the matrix microenvironment impacts EC tube formation in vitro.

Scaffold contraction is dependent on cell type in type I collagen matrices. ECFCs were able to contract the matrices to a greater extent when compared with HUVECs, suggesting ECFCs can generate a greater amount of traction [71]. Sieminski speculated that the increased cell traction generated by ECFCs could be due to increased expression of integrins, increased affinity for integrin ligands, increased sensitivity to FGF, or increased sensitivity to phorbol esters [71].

5.3.2 Matrix Modulation of In Vivo Vessel Formation

ECFCs seeded in type I collagen/fibronectin scaffolds have been shown to form functional vessels when implanted into the flank of an immunocompromised mouse [6, 7]. The formation and persistence of the ECFC-derived vessels in vivo has been

shown to depend upon cell passage number [8], source [7], and presence of perivascular cells [75, 76]. While in vitro evidence suggests that physical properties of type I collagen matrices including fibril density and stiffness influence endothelial cell capillary morphogenesis [67, 71, 77], the effect of matrix physical properties has only recently begun to be studied on ECFC in vivo vessel formation.

Collagen fibril density and stiffness impact the extent of scaffold remodeling, ECFC vessel density, and extent of host vascularization. Scaffolds with distinct biophysical environments were created with different shear storage moduli (stiffness) and fibril densities by altering the collagen concentration. The stiffness was varied from 3.5 to 46.67 Pa and the fibril density (fibril volume fraction) was increased from 8.65 to 16.42%. Contraction and remodeling of scaffolds with decreased collagen concentration was increased compared with matrices with higher collagen concentration. While ECFCs were able to form functional matrices in all scaffold formulations, the extent of vascularization was altered. Human and total vascular density was greater in scaffolds with lower collagen concentrations and shear storage moduli. Also, host vessel invasion was increased in scaffolds with low collagen concentration. This is possibly due to decreased stiffness and fibril density resulting in less resistance to host vessel ingrowth. It is also possible that the increased ECFC vessel density served to actively recruit host vessels into the scaffold [78].

The vessel morphology was also altered in scaffolds with varying biophysical properties (Fig. 5.2). Analysis of vessel morphology demonstrated that average vessel size was increased in scaffolds with increasing collagen concentration and shear storage modulus. Vessels of varying size existed in all scaffolds, but the distribution of vessel sizes was shifted toward larger vessel structures in scaffolds with increased collagen concentration. Further, vascular area, which was dependent upon both vessel size and density, increased with increasing collagen concentration and shear storage modulus. As a result, the increase in average vessel area was large enough to compensate for decreased vessel density. This increase in vascular area is a potentially more descriptive indicator of the extent of vascularization of the scaffold than either vessel density or vessel size alone [78]. The changes observed in ECFC vascularization of type I collagen matrices induced by varying matrix properties could be due to alteration in matrix–integrin–cytoskeletal signaling as well as by alterations in cytokine, nutrients, and host cells ability to infiltrate the matrix. Indeed, it is likely that complex processes such as angiogenesis and vasculogenesis are regulated by a combination of the above factors.

Ingber and colleagues recently reported that a signaling pathway influenced endothelial cell tube and vessel formation for which there was cross talk between matrix mechanical properties and cytokine expression [75]. In this signaling pathway, a Rho inhibitor, P190RhoGAP, regulates the expression of antagonistic transcription factors TFII-I and GATA binding protein 2 (GATA2), which alters vascular endothelial growth factor (VEGF) receptor 2 (VEGFR2) expression levels in endothelial cells. P190RhoGAP knockdown increased the expression level of nuclear TFII-I and nuclear GATA2. This regulation occurs via P190RhoGAP sequestration of both transcription factors. Additionally, TFII-I knockdown

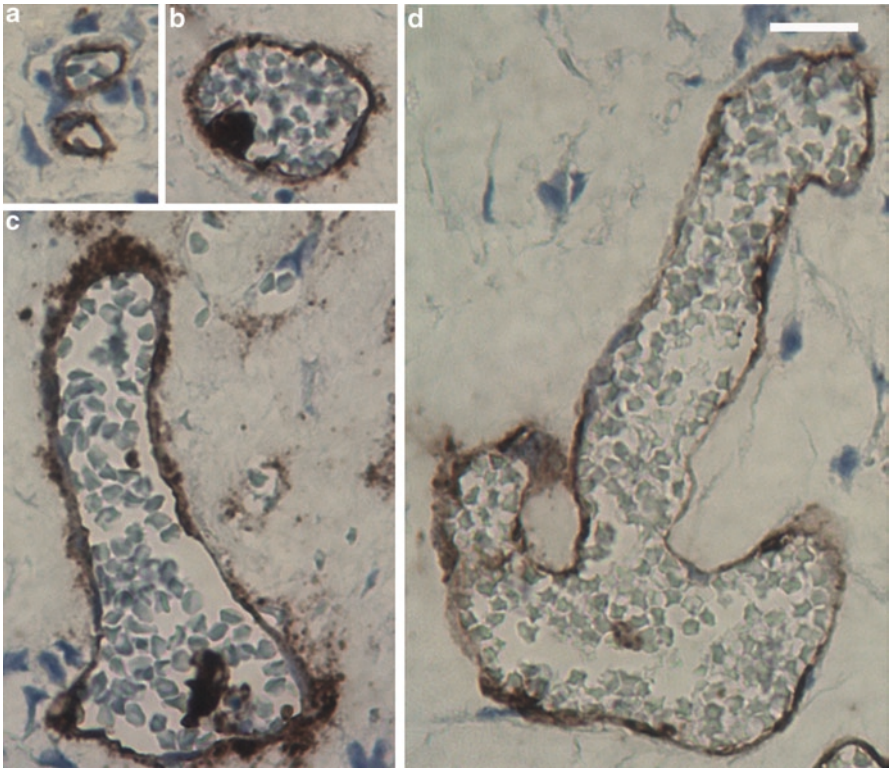

Fig. 5.2 Matrix biophysical properties modulate vessel morphology. The distribution of vessel areas was altered by changing in matrix stiffness and fibril density. Shown are representative images of vessels of varying sizes of between 51 and 100 μm^2 (**a**), between 501 and 1,000 μm^2 (**b**), between 1,001 and 2,000 μm^2 (**c**), and greater than 4,000 μm^2 (**d**, scale bar **a**–**d** 100 μm) [78]

increased VEGFR2 promoter activity and expression levels, while GATA2 knockdown decreased VEGFR2 promoter activity, mRNA, and protein levels. This regulation of VEGFR2 expression is mediated by competition for occupancy of a common region of the VEGFR2 promoter [79]. Matrix stiffness altered cell morphology, nuclear GATA-2 expression, VEGFR2 expression, but not TFII-I expression. Human microvascular endothelial cells (HMVECs) were cultured on fibronectin-coated polyacrylamide gels with varying elasticity with Young's moduli ranging from 150 to 4,000 Pa. Cell morphology was altered by matrix stiffness, with cells assuming a round morphology on compliant matrices and a flat or elongated morphology on relatively stiff matrices. Nuclear GATA2 and VEGFR2 mRNA and protein levels were increased on matrices of increased stiffness, while TFII-I expression levels were high at all stiffness levels. The effect of stiffness on VEGFR2 expression could be overcome by knockdown of either transcription factor. Knockdown of p190RhoGAP or TFII-I resulted in increased VEGFR2

expression on soft matrices, while knockdown of GATA2 resulted in decreased VEGFR2 expression levels on stiffer matrices [79].

Alterations in transcription factors impact endothelial tube formation in vitro and vessel formation in vivo. TFII-I and GATA2 regulate VEGF-stimulated endothelial tube formation on Matrigel in vitro [75]. TFII-I knockdown increased, and GATA2 knockdown decreased the impact of VEGF on endothelial cell tube formation. Further, Matrigel was implanted subcutaneously in mice with varied matrix stiffness (700–900 Pa), with 800 Pa scaffolds resulting in increased level of host capillary in growth. TFII-I and P190RhoGAP knockdown increased vessel in growth in soft matrices, while GATA2 knockdown decreased vessel in growth in stiff matrices. It is interesting to note that the optimal matrix stiffness was reduced for in vivo vessel in growth (800 Pa) compared with the stiffness found optimally responsive to the transcriptional regulation of VEGFR2 expression in vitro (4,000 Pa). The authors suggest that this discrepancy is likely due to differences in endothelial cell behavior in 2D versus 3D [79]. Other factors such as host cell invasion and diffusion of nutrients and growth factors into the scaffolds could also contribute to the differences. These results suggest that increasing matrix stiffness results in increased vascularization in vivo, which is consistent with results found in type I collagen for ECFC vessel formation [78].

The effect of matrix stiffness was also tested on ECFC tube formation on hyaluronic acid (HA)-based scaffolds. Cord blood-derived ECFCs were seeded onto HA–gelatin scaffolds. The percent of PEG diacrylate was varied to modulate scaffold stiffness. Matrices were formed with Young's moduli of 15 Pa (yielding), 85 Pa (firm), and 780 Pa (rigid), which were used to interrogate ECFC network formation in vitro in a 2D angiogenesis assay [43].

Matrix metalloproteinase (MMP) expression was altered by VEGF concentration and matrix stiffness. ECFC expression levels of MMP-1, MMP-2, and MT1-MMP increased for all matrices with increasing VEGF concentration. Additionally, MMP-1, MMP-2, and MT1-MMP expression increased with increasing scaffold stiffness [43]. MT1-MMP has previously been demonstrated to be necessary for endothelial cell capillary morphogenesis in a 3D vasculogenesis assay in vitro [74].

Stiffness of HA-based scaffolds modulated the extent of ECFC capillary network formation in vitro. ECFC tube length, thickness, and area increased with decreasing scaffold stiffness. Further, the extent of vacuole and lumen formation was increased with decreasing scaffold stiffness [43]. This is interesting to note, since the concentration of MT1-MMP, an enzyme shown to be necessary for endothelial cell capillary morphogenesis [74], was shown to be lower in scaffolds that exhibited increased ECFC tube formation. Further knockdown of MT1-MMP with siRNA abrogated ECFC tube formation on all scaffolds, suggesting that the process of tube formation is dependent on MMP expression in this assay [43]. This suggests that while MT1-MMP is required for endothelial cell-mediated scaffold remodeling and capillary morphogenesis, there is not a direct relationship between enzyme concentration and the extent of endothelial network formation.

The dependence of endothelial cell network formation on matrix stiffness is shown to vary in different studies dependent upon scaffold source, assay, and context (in vitro or in vivo) [42, 43, 78]. 3D capillary morphogenesis in ionic self-assembling peptide scaffolds increased with decreasing stiffness (46 Pa optimal) in vitro. The range of stiffness investigated in this study included 46–753 Pa. Softer scaffolds resulted in excessive contraction and so were unable to direct capillary morphogenesis [42]. In another in vitro study, 2D tube formation on HA-based scaffolds increased with decreasing stiffness (15 Pa optimal). For these studies, stiffness was varied from 15 to 780 Pa [43]. Considering the differences in scaffold composition and assay (2D versus 3D), the trend observed in both studies is in reasonable agreement. In vivo capillary in growth into Matrigel-based scaffolds increased at an intermediate scaffold stiffness (800 Pa optimal). Matrix stiffness ranged from 700 to 900 Pa in these studies [79]. While the matrix stiffness that resulted in maximal vascularization is different from those reported by Sieminski [42] and Hanjaya-Putra [43], it is important to note that host capillary in growth was assayed and not vasculogenesis of resident endothelial cells. It is reasonable that the optimal microenvironment for capillary invasion, sprouting angiogenesis, could be different than what is supportive of vasculogenesis. In another study of in vivo vasculogenesis, ECFC vascular density decreased, but vascular area increased in type I collagen matrices over the range of matrix stiffness tested (3.5–46.67 Pa) [78]. While the relationship between scaffold stiffness and capillary morphogenesis appears to be in disagreement with the results of Sieminski [42] and Hanjaya-Putra [43], the range of matrix stiffness examined in these studies represents the lower stiffness range in the previous experiments. Type I collagen scaffolds with stiffness greater than 46.67 Pa were not investigated, and so conclusions about the impact of matrix stiffness of ECFC in vivo vasculogenesis at higher values of matrix stiffness remains to be determined. While differences in matrix composition between all studies limit the ability to make direct comparisons based on stiffness values, these studies [42, 43, 78] suggest the possibility that a specific regime of matrix stiffness could be a supportive microenvironment for vasculogenesis, which will need to be investigated with future studies in various scaffold types.

Despite the differences in matrix composition (collagen, HA, matrigel, and ionic peptides), culture conditions (in vitro versus in vivo), and assay type (2D versus 3D), these studies demonstrate a role for the modulation of endothelial-derived vessel formation by the mechanical properties of the surrounding matrix. It is important to note that alterations in other biophysical properties such as fibril diameter, fibril volume fraction, and diffusion of nutrients and growth factors are also modified when the matrix mechanical properties are modulated. These additional factors likely contribute to alterations in angiogenesis and vasculogenesis.

One example of the effect of growth factors and accessory cells on neoangiogenesis in matrices was demonstrated by Silva et al. [44] in a hindlimb ischemia model in immunocompromised mice. ECFCs and colony forming unit-HILL cells (CFU-HILLs), a putative EPC population consisting of monocytes and T lymphocytes (reviewed in [24]), were isolated from human umbilical cord blood. The role of these

two cell population in sprouting angiogenesis was investigated in fibrin matrices in vitro. While CFU-HILLs were unable to form sprouts, they did stimulate ECFC and differentiated endothelial cell sprouting, suggesting a proangiogenic role for these cells. Additionally, it was demonstrated that VEGF isoforms with decreasing molecular weight result in increased migration of ECFCs out of alginate-based matrices. Macroporous alginate scaffolds were modified to include RGD ligands and various VEGF isoforms. While $VEGF_{165}$ resulted in increased ECFC migration, $VEGF_{121}$ further increased ECFC emigration from the scaffold [44].

Delivery of ECFCs in alginate-based scaffolds improved tissue perfusion and regeneration. ECFCs delivered in alginate scaffolds led to functional chimeric vessels and increased capillary density, decreased levels of tissue necrosis and autoamputation in immunocompromised mice who had undergone femoral artery and vein ligation. Scaffolds devoid of ECFCs had little impact on tissue recovery. Additionally, injection of ECFCs and VEGF resulted in modest increase in capillary density. However, capillaries formed from injected ECFCs were large and disorganized. Further, injection of ECFCs and VEGF had minimal impact on tissue recover. Delivery of ECFCs in scaffolds without VEGF yielded a modest increase in capillary density. However, as with the injection of ECFCs and VEGF, this treatment did not lead to significant tissue repair and regeneration. In contrast, ECFCs delivered in fibrin scaffolds with VEGF resulted in an increase in capillary density, the formation of functional chimeric vessels, and led to tissue repair as measured by a reduction in tissue necrosis and autoamputation [44].

The accessory cells, CFU-HILLs, also contribute to neoangiogenesis and tissue recover in the hindlimb ischemia mouse model. The delivery of both ECFCs and CFU-HILLs led to an increased rate of tissue recovery suggesting a synergistic effect of the two cell populations. Delivery of CFU-HILLs in scaffolds with VEGF resulted in tissue recovery. However, histological examination revealed a substantial amount of adipose tissue in these animals. Delivery of both ECFCs and CFU-HILLs delivered in alginate scaffolds with VEGF led to a further improvement in recovery and normal tissue formation [44].

5.4 Future Directions

Control of vascular system homeostasis is a complex process that is critical to maintaining normal tissue function. When the ability to repair and regenerate the vasculature is altered, disease states often ensues necessitating intervention to restore tissue function. Recent evidence suggests that localized cellular delivery could improve the efficacy of therapeutic angiogenesis strategies [4] and that EPCs represent an excellent cell source for vascular engineering strategies [7]. Understanding the biophysical properties of scaffolds used for cell delivery is crucial for improvements in these therapies. It is clear from the current literature that matrix stiffness influences endothelial cell behavior and capillary morphogenesis. Further investigation is needed to better understand how these mechanical

properties and biophysical properties can be tailored to modulate vessel formation. Additionally, it will be necessary to understand how the biophysical properties of the microenvironment impact other cell populations, which are critical to neoangiogenesis and the formation of specific tissues of interest.

One recent area of investigation involves creating vascularized tissue constructs using a method of cell sheet stacking (Fig. 5.3). Poly-(*N*-isopropylacrylamide), a polymer which is thermoresponsive, was used as a substrate for endothelial cell culture. As the temperature is lowered below 32°C, the confluent cell layer is released from the substrate as a cell sheet. Additionally, the cell layer maintains the basement membrane proteins the cells have secreted during culture. Individual cell sheets are manipulated by using a plunger-like device that is coated with ECM proteins such as fibrin or gelatin. Incubation of the coated plunger with the cell sheet results in the adhesion of the cell sheet to the plunger and allows for transfer of the cell sheet onto another tissue culture dish or cell layer. Repeated manipulations allow for the formation of a tissue construct composed of stacked cell layers [80].

Using this technique, Okano and colleagues [80] have recently demonstrated that tissue engineering constructs consisting of alternating layers of HUVECs and myoblasts were able to form a capillary network in vitro and able to support neovascularization when implanted in the subcutaneous space of nude rats.

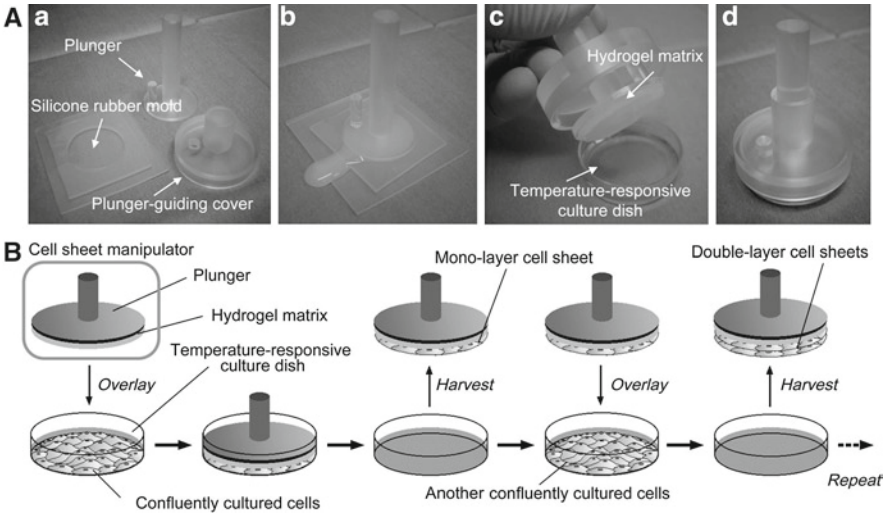

Fig. 5.3 Cell sheet stacking is a novel method with potential to create vascularized tissue constructs. (**A**) The components used to manipulate cell sheets are depicted including plunger, plunger guiding cover (**a**), and hydrogel matrix (**c**). The silicone rubber mold is used to apply a matrix coating to the surface of the plunger (**b**). The matrix-coated plunger can then be used to manipulate cell sheets released from the temperature responsive culture system (**d**). (**B**) Schematic diagram demonstrating the process of manipulating cell sheets to create tissue constructs. Reprinted from ref. [80] with permission from Elsevier

HUVECs stacked between two layers of myoblasts were able to initiate capillary morphogenesis after 3 days in culture. In contrasts, HUVECs seeded onto a single-myoblast layer proliferated to form a monolayer, suggesting the cell stacking configuration was differentially able to direct network formation. Additionally, a tissue construct consisting of two layers of HUVECs alternating between three layers of myoblasts was shown to form an interconnecting network of endothelial cell throughout multiple cell layers. Finally, five-layered constructs consisting of either myoblasts alone or myoblasts and HUVECs were implanted into nude mice. After 1 week, in vivo coculture constructs contained functional vessels, which were absent in constructs composed of only myoblast [80]. While these results are quite promising, the ease of manipulation and the ability to stack many cell layers to generate complex tissue constructs is uncertain. However, if this technique can be extended to generate tissue constructs of substantial thickness, it could offer a promising new therapeutic angiogenesis strategy.

The generation of these complex tissue constructs will require the understanding of how multiple cell type work together not only to vascularize the tissue, but also for the organization and growth of the functional parenchyma. Levenberg and colleagues have recently demonstrated this type of cellular interactions necessary for complex tissue formation in the form of vascularized cardiac muscle constructs from cardiomyocytes, endothelial cells, and embryonic fibroblasts [14, 81]. For these studies, a poly-L-lactic acid (PLLA)/PLGA scaffold was used to culture hESC-derived cardiomyoctyes, HUVECS, and embryonic fibroblasts. Cells were seeded into the scaffold with Matrigel to increase cell adhesion and then cultured in vitro.

The addition of other cell types impacted capillary network formation, as well as cell proliferation and survival in vitro. Addition of embryonic fibroblast was necessary to initiate endothelial cell capillary network formation. Further, the triculture tissue constructs demonstrated alpha-smooth muscle actin $(\alpha SMA)^+$ cells adjacent to capillary networks, suggesting the embryonic fibroblast served a stabilizing perivascular cell role. Embryonic fibroblasts also increased endothelial cell viability and proliferation in the tissue constructs. Endothelial cells also served to modulate cell behavior by increasing cardiomyocyte proliferation in the triculture system [81].

In vitro culture of the tissue constructs leads to the development of tissue with characteristics of cardiac muscle. Synchronous beating of the tissue constructs was observed within 6 days of in vitro culture. Further, the tissue engineering constructs displayed some characteristics of cardiac muscle including the expression of markers of mature cardiomyocytes such as a troponin I and myosin light chain-2V as well as ultrastructural characteristics such as sarcomeric organization, the beginnings of T tubules and a sarcoplasmic reticulum. Additionally, intracellular Ca^{2+} flux was shown to be synchronous with construct contraction, and frequency of tissue contraction could be appropriately modified by pharmacologic agents such as isoproterenol and carbamylcholine [81].

These studies were then extended to an in vivo model to test the ability of the tissue construct to integrate with host cardiac tissue and to inosculate with the host

vasculature. Triculture cardiac tissue engineering constructs were cultured in vitro for 2 weeks, and then engrafted onto the anterior wall of the left ventricle of immunosuppressed rats. After 2 weeks in vivo, hESC-derived cardiomyocytes underwent varied extent of maturation.

Tissue constructs supported neoangiogenesis and anastomosis to host vasculature which was influence by the presence of both endothelial and fibroblast cell types. The scaffold exhibited vascularization that was greater than the surrounding host cardiac tissue. Histological analysis revealed that triculture constructs had increased lumens per graft area, lumen area density, an increase in human vessel contribution to tissue vessel formation and an increase in vessels with an area >200 μm^2 compared with scaffolds seeded with only hESC-derived cardiomyocytes. Further, mouse embryonic fibroblasts stained positive for αSMA and were found adjacent to the vascular wall, suggesting that they had assumed a perivascular cell phenotype. Red blood cells were identified in lumens of human $CD31^+$-labeled vessels and additionally, fluorescently labeled microspheres that had been injected into the left ventricle were found in human $CD31^+$ vessels, indicating that the HUVECs had formed functional vessels [14]. These studies demonstrate the potential for vascularized tissue constructs to aid in repair and regeneration of tissue and improve current treatment.

Another potential clinical use of vascularized tissue constructs is in the treatment of patients with defective wound healing due to impaired neoangiogenesis. Shepherd et al. [10] seeded tissue engineered human skin substitutes with keratinocytes and ECFCs or HUVECs, and then transplanted them onto immunodeficient mice. Skin substitutes were vascularized by functional human endothelial cell vessels, but the extent of vascularization was dependent upon endothelial cell type. Umbilical cord blood-derived ECFCs yielded an increase in human-derived vessels in the skin substitutes when compared with both HUVECs and adult blood-derived ECFCs. Host vessels were also shown to have invaded the skin substitute. This host vessel invasion could be diminished by the use of rapamycin, but the use of rapamycin did not inhibit the formation of human-derived blood vessels. The differential response of host and implanted endothelial cell populations to vascularize the transplanted skin substitute is promising for treating patients with impaired vascular function and nonhealing wounds [10].

The cellular microenvironment plays a crucial role in regulating the formation and remodeling of vascular beds. Understanding how the biophysical cues of the microenvironment in concert with cytokine and cellular signaling modulate vessel formation will be necessary to make these tissue engineering strategies therapeutically beneficial. Currently, there are no tissue-engineered constructs available that have an inherent vascular network ready to be connected to the host vascular system [82]. However, the recent advancements using vascularized scaffolds in preclinical rodent models demonstrate the potential impact of these therapies on the treatment of patients suffering from vascular dysfunction.

Acknowledgments This work was supported by the Riley Children's Foundation, Indianapolis, Indiana and the National Institutes of Health Grant F30-HL096350-01.

References

1. Conway EM, Collen D, Carmeliet P. Molecular mechanisms of blood vessel growth. Cardiovasc Res. 2001;49:507–521.
2. Carmeliet P, Jain RK. Angiogenesis in cancer and other diseases. Nature. 2000;407: 249–257.
3. Jain RK, Au P, Tam J, Duda DG, Fukumura D. Engineering vascularized tissue. Nat Biotechnol. 2005;23:821–823.
4. Kawamoto A, Asahara T. Role of progenitor endothelial cells in cardiovascular disease and upcoming therapies. Catheter Cardiovasc Interv. 2007;70:477–484.
5. Levenberg S. Engineering blood vessels from stem cells: recent advances and applications. Curr Opin Biotechnol. 2005;16:516–523.
6. Yoder MC, Mead LE, Prater D, et al. Redefining endothelial progenitor cells via clonal analysis and hematopoietic stem/progenitor cell principals. Blood. 2007;109:1801–1809.
7. Au P, Daheron LM, Duda DG, et al. Differential in vivo potential of endothelial progenitor cells from human umbilical cord blood and adult peripheral blood to form functional long-lasting vessels. Blood. 2008;111:1302–1305.
8. Melero-Martin JM, Khan ZA, Picard A, Wu X, Paruchuri S, Bischoff J. In vivo vasculogenic potential of human blood-derived endothelial progenitor cells. Blood. 2007;109:4761–4768.
9. Schechner JS, Nath AK, Zheng L, et al. In vivo formation of complex microvessels lined by human endothelial cells in an immunodeficient mouse. Proc Natl Acad Sci USA. 2000;97:9191–9196.
10. Shepherd BR, Enis DR, Wang F, Suarez Y, Pober JS, Schechner JS. Vascularization and engraftment of a human skin substitute using circulating progenitor cell-derived endothelial cells. FASEB J. 2006;20:1739–1741.
11. Ng CP, Helm CL, Swartz MA. Interstitial flow differentially stimulates blood and lymphatic endothelial cell morphogenesis in vitro. Microvasc Res. 2004;68:258–264.
12. Luong E, Gerecht S. Stem cells and scaffolds for vascularizing engineered tissue constructs. Adv Biochem Eng Biotechnol. 2009;114:129–172.
13. Koike N, Fukumura D, Gralla O, Au P, Schechner JS, Jain RK. Tissue engineering: creation of long-lasting blood vessels. Nature. 2004;428:138–139.
14. Lesman A, Habib M, Caspi O, et al. Transplantation of a tissue-engineered human vascularized cardiac muscle. Tissue Eng Part A. 2010;16:115–125.
15. Asahara T, Murohara T, Sullivan A, et al. Isolation of putative progenitor endothelial cells for angiogenesis. Science. 1997;275:964–967.
16. Vasa M, Fichtlscherer S, Aicher A, et al. Number and migratory activity of circulating endothelial progenitor cells inversely correlate with risk factors for coronary artery disease. Circ Res. 2001;89:e1–e7.
17. Hill JM, Zalos G, Halcox JPJ, et al. Circulating endothelial progenitor cells, vascular function, and cardiovascular risk. N Engl J Med. 2003;348:593–600.
18. Schatteman GC, Dunnwald M, Jiao C. Biology of bone marrow-derived endothelial cell precursors. Am J Physiol Heart Circ Physiol. 2007;292:H1–H18.
19. Prater DN, Case J, Ingram DA, Yoder MC. Working hypothesis to redefine endothelial progenitor cells. Leukemia. 2007;21:1141–1149.
20. Lin Y, Weisdorf DJ, Solovey A, Hebbel RP. Origins of circulating endothelial cells and endothelial outgrowth from blood. J Clin Invest. 2000;105:71–77.
21. Ingram DA, Mead LE, Tanaka H, et al. Identification of a novel hierarchy of endothelial progenitor cells using human peripheral and umbilical cord blood. Blood. 2004;104:2752–2760.
22. Peichev M, Naiyer AJ, Pereira D, et al. Expression of VEGFR-2 and AC133 by circulating human CD34+ cells identifies a population of functional endothelial precursors. Blood. 2000;95:952–958.
23. Risau W, Flamme I. Vasculogenesis. Annu Rev Cell Dev Biol. 1995;11:73–91.

24. Hirschi KK, Ingram DA, Yoder MC. Assessing identity, phenotype, and fate of endothelial progenitor cells. Arterioscler Thromb Vasc Biol. 2008;28:1584–1595.
25. Vasa M, Fichtlscherer S, Adler K, et al. Increase in circulating endothelial progenitor cells by statin therapy in patients with stable coronary artery disease. Circulation. 2001;103:2885–2890.
26. Rehman J, Li J, Orschell CM, March KL. Peripheral blood "endothelial progenitor cells" are derived from monocyte/macrophages and secrete angiogenic growth factors. Circulation. 2003;107:1164–1169.
27. Kalka C, Masuda H, Takahashi T, et al. Transplantation of ex vivo expanded endothelial progenitor cells for therapeutic neovascularization. Proc Natl Acad Sci USA. 2000; 97:3422–3427.
28. Asosingh K, Aldred MA, Vasanji A, et al. Circulating angiogenic precursors in idiopathic pulmonary arterial hypertension. Am J Pathol. 2008;172:615–627.
29. Hur J, Yoon C-H, Kim H-S, et al. Characterization of two types of endothelial progenitor cells and their different contributions to neovasculogenesis. Arterioscler Thromb Vasc Biol. 2004;24:288–293.
30. Stratman AN, Malotte KM, Mahan RD, Davis MJ, Davis GE. Pericyte recruitment during vasculogenic tube assembly stimulates endothelial basement membrane matrix formation. Blood. 2009;114:5091–5101.
31. Gerecht-Nir S, Ziskind A, Cohen S, Itskovitz-Eldor J. Human embryonic stem cells as an in vitro model for human vascular development and the induction of vascular differentiation. Lab Invest. 2003;83:1811–1820.
32. Wang ZZ, Au P, Chen T, et al. Endothelial cells derived from human embryonic stem cells form durable blood vessels in vivo. Nat Biotechnol. 2007;25:317–318.
33. Ferreira LS, Gerecht S, Shieh HF, et al. Vascular progenitor cells isolated from human embryonic stem cells give rise to endothelial and smooth muscle like cells and form vascular networks in vivo. Circ Res. 2007;101:286–294.
34. Lees JG, Lim SA, Croll T, et al. Transplantation of 3D scaffolds seeded with human embryonic stem cells: biological features of surrogate tissue and teratoma-forming potential. Regen Med. 2007;2:289–300.
35. Park IH, Arora N, Huo H, et al. Disease-specific induced pluripotent stem cells. Cell. 2008;134:877–886.
36. Ebert AD, Yu J, Rose FF, Jr, et al. Induced pluripotent stem cells from a spinal muscular atrophy patient. Nature. 2009;457:277–280.
37. Tateishi K, He J, Taranova O, Liang G, D'Alessio AC, Zhang Y. Generation of insulin-secreting islet-like clusters from human skin fibroblasts. J Biol Chem. 2008;283:31601–31607.
38. Maehr R, Chen S, Snitow M, et al. Generation of pluripotent stem cells from patients with type 1 diabetes. Proc Natl Acad Sci USA. 2009;106:15768–15773.
39. Choi KD, Yu J, Smuga-Otto K, et al. Hematopoietic and endothelial differentiation of human induced pluripotent stem cells. Stem Cells. 2009;27:559–567.
40. Taura D, Sone M, Homma K, et al. Induction and isolation of vascular cells from human induced pluripotent stem cells – brief report. Arterioscler Thromb Vasc Biol. 2009;29:1100–1103.
41. Pedersen JA, Swartz MA. Mechanobiology in the third dimension. Ann Biomed Eng. 2005;33:1469–1490.
42. Sieminski AL, Was AS, Kim G, Gong H, Kamm RD. The stiffness of three-dimensional ionic self-assembling peptide gels affects the extent of capillary-like network formation. Cell Biochem Biophys. 2007;49:73–83.
43. Hanjaya-Putra D, Yee J, Ceci D, Truitt R, Yee D, Gerecht S. Vascular endothelial growth factor and substrate mechanics regulate in vitro tubulogenesis of endothelial progenitor cells. J Cell Mol Med. 2010;14:2436–2447.
44. Silva EA, Kim E-S, Kong HJ, Mooney DJ. Material-based deployment enhances efficacy of endothelial progenitor cells. Proc Natl Acad Sci USA. 2008;105:14347–14352.

45. Zeugolis DI, Paul RG, Attenburrow G. Factors influencing the properties of reconstituted collagen fibers prior to self-assembly: animal species and collagen extraction method. J Biomed Mater Res A. 2008;86A:892–904.
46. Kreger ST, Voytik-Harbin SL. Hyaluronan concentration within a 3D collagen matrix modulates matrix viscoelasticity, but not fibroblast response. Matrix Biol. 2009;28:336–346.
47. Zeugolis DI, Paul GR, Attenburrow G. Cross-linking of extruded collagen fibers – A biomimetic three-dimensional scaffold for tissue engineering applications. J Biomed Mater Res A. 2009;89:895–908.
48. Guidry C, Grinnell F. Studies on the mechanism of hydrated collagen gel reorganization by human skin fibroblasts. J Cell Sci. 1985;79:67–81.
49. Guidry C. Contraction of hydrated collagen gels by fibroblasts: evidence for two mechanisms by which collagen fibrils are stabilized. Collagen Rel Res. 1986;6:515–529.
50. Wang N, Butler JP, Ingber DE. Mechanotransduction across the cell surface and through the cytoskeleton. Science. 1993;260:1124–1127.
51. Rupp PA, Little CD. Integrins in vascular development. Circ Res. 2001;89:566–572.
52. Galbraith CG, Sheetz MP. Forces on adhesive contacts affect cell function. Curr Opin Cell Biol. 1998;10:566–571.
53. Ingber D. In search of cellular control: signal transduction in context. J Cell Biochem. 1998;72:232–237.
54. Chen CS, Mrksich M, Huang S, Whitesides GM, Ingber DE. Geometric control of cell life and death. Science. 1997;276:1425–1428.
55. McBeath R, Pirone DM, Nelson CM, Bhadriraju K, Chen CS. Cell shape, cytoskeletal tension, and RhoA regulate stem cell lineage commitment. Dev Cell. 2004;6:483–495.
56. Ruiz SA, Chen CS. Emergence of patterned stem cell differentiation within multicellular structures. Stem Cells. 2008;26:2921–2927.
57. Engler AJ, Sen S, Sweeney HL, Discher DE. Matrix elasticity directs stem cell lineage specification. Cell. 2006;126:677–689.
58. Folkman J, Haudenschild C. Angiogenesis in vitro. Nature. 1980;288:551–556.
59. Vernon RB, Sage EH. Between molecules and morphology. Extracellular matrix and creation of vascular form. Am J Pathol. 1995;147:873–883.
60. Ingber DE, Madri JA, Folkman J. Endothelial growth factors and extracellular matrix regulate DNA synthesis through modulation of cell and nuclear expansion. In Vitro Cell Dev Biol. 1987;23:387–394.
61. Montesano R, Vassalli JD, Baird A, Guillemin R, Orci L. Basic fibroblast growth factor induces angiogenesis in vitro. Proc Natl Acad Sci USA. 1986;83:7297–7301.
62. Ingber DE, Folkman J. Mechanochemical switching between growth and differentiation during fibroblast growth factor-stimulated angiogenesis in vitro: role of extracellular matrix. J Cell Biol. 1989;109:317–330.
63. Davis GE, Camarillo CW. An [alpha]2[beta]1 integrin-dependent pinocytic mechanism involving intracellular vacuole formation and coalescence regulates capillary lumen and tube formation in three-dimensional collagen matrix. Exp Cell Res. 1996;224:39–51.
64. Kanzawa S, Endo H, Shioya N. Improved in vitro angiogenesis model by collagen density reduction and the use of type III collagen. Ann Plast Surg. 1993;30:244–251.
65. Ment L, Stewart W, Scaramuzzino D, Madri J. An in vitro three-dimensional coculture model of cerebral microvascular angiogenesis and differentiation. In Vitro Cell Dev Biol Anim. 1997;33:684–691.
66. Ilan N, Mahooti S, Madri JA. Distinct signal transduction pathways are utilized during the tube formation and survival phases of in vitro angiogenesis. J Cell Sci. 1998;111:3621–3631.
67. Korff T, Augustin HG. Tensional forces in fibrillar extracellular matrices control directional capillary sprouting. J Cell Sci. 1999;112(Pt 19):3249–3258.
68. Salazar R, Bell SE, Davis GE. Coordinate Induction of the actin cytoskeletal regulatory proteins gelsolin, vasodilator-stimulated phosphoprotein, and profilin during capillary morphogenesis in vitro. Exp Cell Res. 1999;249:22–32.

69. Vernon RB, Sage EH. A novel, quantitative model for study of endothelial cell migration and sprout formation within three-dimensional collagen matrices. Microvasc Res. 1999; 57:118–133.
70. Yang S, Graham J, Kahn JW, Schwartz EA, Gerritsen ME. Functional roles for PECAM-1 (CD31) and VE-Cadherin (CD144) in tube assembly and lumen formation in three-dimensional collagen gels. Am J Pathol. 1999;155:887–895.
71. Sieminski AL, Hebbel RP, Gooch KJ. The relative magnitudes of endothelial force generation and matrix stiffness modulate capillary morphogenesis in vitro. Exp Cell Res. 2004;297:574–584.
72. Koh W, Mahan RD, Davis GE. Cdc42- and Rac1-mediated endothelial lumen formation requires Pak2, Pak4 and Par3, and PKC-dependent signaling. J Cell Sci. 2008;121:989–1001.
73. Matsumura T, Wolff K, Petzelbauer P. Endothelial cell tube formation depends on cadherin 5 and CD31 interactions with filamentous actin. J Immunol. 1997;158:3408–3416.
74. Stratman AN, Saunders WB, Sacharidou A, et al. Endothelial cell lumen and vascular guidance tunnel formation requires MT1-MMP-dependent proteolysis in 3-dimensional collagen matrices. Blood. 2009;114:237–247.
75. Melero-Martin JM, De Obaldia ME, Kang SY, et al. Engineering robust and functional vascular networks in vivo with human adult and cord blood-derived progenitor cells. Circ Res. 2008;103:194–202.
76. Au P, Tam J, Fukumura D, Jain RK. Bone marrow-derived mesenchymal stem cells facilitate engineering of long-lasting functional vasculature. Blood. 2008;111:4551–4558.
77. Yamamura N, Sudo R, Ikeda M, Tanishita K. Effects of the mechanical properties of collagen gel on the in vitro formation of microvessel networks by endothelial cells. Tissue Eng. 2007;13:1443–1453.
78. Critser PJ, Kreger ST, Voytik-Harbin SL, Yoder MC. Collagen matrix physical properties modulate endothelial colony forming cell derived vessels in vivo. Microvasc Res. 2010;80:23–30.
79. Mammoto A, Connor KM, Mammoto T, et al. A mechanosensitive transcriptional mechanism that controls angiogenesis. Nature. 2009;457:1103–1108.
80. Sasagawa T, Shimizu T, Sekiya S, et al. Design of prevascularized three-dimensional cell-dense tissues using a cell sheet stacking manipulation technology. Biomaterials. 2010;31:1646–1654.
81. Caspi O, Lesman A, Basevitch Y, et al. Tissue engineering of vascularized cardiac muscle from human embryonic stem cells. Circ Res. 2007;100:263–272.
82. Kannan RY, Salacinski HJ, Sales K, Butler P, Seifalian AM. The roles of tissue engineering and vascularisation in the development of micro-vascular networks: a review. Biomaterials. 2005;26:1857–1875.

Chapter 6
Physiological and Therapeutic Vascular Remodeling Mediated by Hypoxia-Inducible Factor 1

Kakali Sarkar and Gregg L. Semenza

6.1 Introduction

Hypoxia is defined as a reduction in the amount of oxygen available to a cell, tissue, or organism. Normal tissue function depends on adequate delivery of oxygen and nutrients and removal of toxic metabolic by-products through blood vessels. The transcription factor, hypoxia-inducible factor 1 (HIF-1), is a master regulator of tissue oxygen homeostasis in metazoan organisms. HIF-1 modulates the transcription of hundreds of target genes in response to reduced oxygen availability [1]. HIF-1 is composed of a constitutively expressed HIF-1β subunit, and an O_2-regulated HIF-1α subunit. In the presence of normal O_2 concentrations, HIF-1α is hydroxylated at two conserved proline residues, ubiquitinated, and then degraded by the proteasome. The degradation of HIF-1α is controlled by binding of the von Hippel–Lindau (VHL) protein, which is the recognition component of an E3 ubiquitin-protein ligase that targets HIF-1α for proteasomal degradation. When the O_2 concentration is low, hydroxylation is inhibited, allowing HIF-1α protein levels to rise. The HIF-1α/HIF-1β heterodimer then binds to the consensus sequence 5′-(A/G)CGTG-3′ contained within hypoxia response elements (HREs) in target genes and activates their transcription [2].

G.L. Semenza (✉)
Vascular Program, Institute for Cell Engineering, The Johns Hopkins University School of Medicine, 733 North Broadway, Baltimore, MD 21205, USA
and
Department of Medicine, The Johns Hopkins University School of Medicine, 733 North Broadway, Baltimore, MD 21205, USA
and
McKusick-Nathans Institute of Genetic Medicine, The Johns Hopkins University School of Medicine, 733 North Broadway, Baltimore, MD 21205, USA
and
Departments of Pediatrics, Oncology, Radiation Oncology, and Biological Chemistry, The Johns Hopkins University School of Medicine, 733 North Broadway, Baltimore, MD 21205, USA
e-mail: gsemenza@jhmi.edu

S. Gerecht (ed.), *Biophysical Regulation of Vascular Differentiation and Assembly*, Biological and Medical Physics, Biomedical Engineering,
DOI 10.1007/978-1-4419-7835-6_6,

For many years, it was believed that vasculogenesis, which is the formation of new blood vessels by endothelial progenitor cells (EPCs), occurs only in the embryo, whereas sprouting of new vessels from a preexisting vasculature (angiogenesis) occurs in the adult. However, recent studies indicate that EPCs contribute to postnatal physiological and pathological neovascularization [3, 4]. Though embryonic and adult vasculogenesis are similar processes, the embryonic environment is very different than that in the adult. Tissue hypoxia resulting from deficient blood flow is a potent stimulator of angiogenesis and vasculogenesis in the adult. Vascularization fails in *Hif1a*$^{-/-}$ mouse embryos, which are homozygous for a knockout allele at the locus that encodes HIF-1α [5, 6], whereas *Hif1a*$^{+/-}$ adult mice, which are heterozygous for the knockout allele, have impaired vascularization following arterial occlusion [7], demonstrating a key role for HIF-1 in the regulation of vascularization.

Dysregulated vessel growth has a major impact on health and contributes to the pathogenesis of many disorders [8]. Insufficient vessel growth and abnormal vessel regression not only cause brain, heart, and limb ischemia but also contribute to the pathogenesis of hypertension, neurodegeneration, and preeclampsia. On the other hand, excessive angiogenesis contributes to the pathogenesis of cancer, rheumatoid arthritis, and ischemic retinopathies.

Peripheral arterial disease (PAD) is a common vascular disorder with significant morbidity and mortality and is characterized by various degrees of stenosis and obstruction in arteries of the leg resulting in tissue hypoxia/ischemia due to reduced perfusion. PAD has high socio-economic and medical impacts as a result of its high incidence, which ranges from 3 to 10% in the general population, increasing to 15–20% in individuals over the age of 70 [9]. Other risk factors include diabetes or impaired glucose tolerance, smoking, and hypertension [9, 10]. One of the major clinical manifestations of PAD is critical limb ischemia (CLI). CLI is estimated to develop in 500–1,000 individuals per million per year [11]. Limb perfusion is decreased in CLI patients resulting in ischemic rest pain, ulcers, and gangrene. CLI is the leading cause of nontraumatic amputation in western countries. A surgical approach such as distal bypass is still the "gold standard" for the treatment of CLI. In addition, due to recent advances in endovascular technologies, catheter-based intervention has become a viable option, and percutaneous treatment is becoming more widely used. Unfortunately, many patients cannot be helped with currently available surgical or endovascular revascularization procedures because of the complex anatomy of the vascular occlusion and/or the presence of other risk factors. The relative risk of amputation is 40 times greater in people with diabetes [12]. Limb salvage rates in diabetic patients with CLI have been reported to be lower than nondiabetic patients, and diabetes is an independent risk factor for postoperative below-knee amputation and other complications [13]. Prostanoids [iloprost and prostaglandin (PGE1)] have been used as the pharmacological treatment of choice for no-option CLI patients. A recent meta-analysis of randomized controlled trials (RCTs) of prostanoids for CLI have shown that despite some positive results regarding rest-pain relief, ulcer healing, and amputations, there is no conclusive evidence of the long-term effectiveness and safety of different prostanoids in patients with CLI [14].

Spinal cord stimulation (SCS) has been used as an alternative for the management of ischemic pain and the prevention of amputations in CLI patients. However,

a recent meta-analysis including data from all randomized trials shows insufficient evidence for higher efficacy of SCS treatment compared with best medical treatment alone [15]. Thus, a critical need for new therapies to treat CLI exists.

The identification of molecular and cellular mechanisms [16] underlying vascular responses to ischemia has provided potential opportunities for the treatment of such patients by therapeutic angiogenesis. Currently, gene and cell therapies, aimed at stimulating angiogenesis, are being evaluated through clinical trials in CLI patients. This review will focus on the adaptive responses to hypoxia and ischemia, the molecular mechanisms by which ischemia-induced angiogenesis is impaired in chronic limb ischemia associated with aging and diabetes and how impaired responses can be corrected by HIF-1 gene and cell therapy.

6.2 Vascular Responses to Hypoxia and Ischemia

Decreased oxygen availability leads to increased HIF-1 transcription activity in hypoxic cells. Each cell responds to hypoxia by modulating the transcription of a subset of HIF-1 target genes in a cell-type specific manner [17]. Most cells respond to hypoxia by increasing transcription of vascular endothelial growth factor (VEGF) in a HIF-1-dependent manner [17, 18]. Other HIF-1-regulated angiogenic growth factors include angiopoietin-2 (ANGPT2), placental growth factor (PLGF), stromal-derived factor-1 (SDF-1), stem cell factor (SCF), and platelet-derived growth factor B (PDGF-B) [7, 17, 19, 20]. HREs have been identified within the promoters of the genes encoding VEGF [18], SDF-1 [19], and SCF [7]. The exact molecular mechanisms by which HIF-1 regulates the expression of PLGF and PDGF-B are not known. There is evidence that ANGPT2 expression is both directly and indirectly regulated by HIF-1 [20, 21].

Angiogenesis not only requires angiogenic growth factor production by hypoxic cells but also involves responding cells including vascular endothelial cells (ECs), arterial smooth muscle cells, and vascular pericytes, which bear cognate receptors for the angiogenic factors described above. HIF-1 mediates both cell-autonomous and non-cell-autonomous EC responses to hypoxia. For example, HIF-1 accumulation in nonendothelial cells drives the production and secretion of angiogenic growth factors, which then bind to their cognate receptors on ECs to initiate angiogenesis. Similarly, HIF-1 also directly activates hypoxic ECs. Hypoxia or transduction of cells with AdCA5, an adenovirus encoding a constitutively active form of HIF-1α, stimulated the ability of primary arterial EC cultures to form tube-like networks on Matrigel, which is an ex vivo assay of EC activation, thereby indicating that HIF-1 mediates cell-autonomous activation of ECs [22]. The signaling systems comprised of PDGF-B and its receptor PDGFRβ, as well as ANGPT1/ANGPT2 and their receptor Tie2, are involved in recruiting pericytes and smooth muscle cells to vascular ECs [23, 24].

Angiogenic factors not only stimulate vascular ECs, smooth muscle cells, and pericytes that express their cognate receptors but also mobilize a variety of cells from bone marrow or other tissues into the peripheral blood. These circulating angiogenic cells (CACs) home to the ischemic tissue and promote vascularization. CACs are a

heterogeneous population of cells, including EPCs, mesenchymal stem cells (MSCs), hematopoietic stem cells (HSCs), and other proangiogenic myeloid cells. Whereas EPCs or their progeny are incorporated into growing neovessels, the other cell types may act primarily through the production of paracrine factors that stimulate vascularization. These cells are recruited based on their surface expression of receptors for the same growth factors that are produced at the ischemic sites and act locally to stimulate angiogenesis and arteriogenesis. Mouse bone marrow-derived MSCs express VEGFR1 and migrate in response to VEGF or PLGF [25]. HIF-1α expression is necessary for the expression of VEGFR1 in these cells and for their ability to migrate toward gradients of VEGF or PLGF. Hypoxia-induced SDF-1 expression is crucially important in the selective homing and migration of $CXCR4^+$ CACs to ischemic tissues [19].

Other than expressing receptors for angiogenic growth factors, CACs also express progenitor cell markers such as CD34 and Sca-1. Ischemia-induced mobilization of $CD34^+/VEGFR2^+$ and $CXCR4^+/Sca\text{-}1^+$ CACs is impaired in *Hif1a*$^{+/-}$ mice compared to their wild-type (WT) littermates, which parallels the impaired induction of VEGF and SDF-1 in ischemic *Hif1a*$^{+/-}$ mice [7], indicating an important role for HIF-1 in mobilization and recruitment of CACs to ischemic tissue to promote neovascularization. Thus, HIF-1 plays a key role both in the production of angiogenic signals by muscle cells in the ischemic limb and in the response to those signals by ECs and other vascular and proangiogenic cell types (e.g., vascular smooth muscle cells and pericytes as well as EPCs and other CACs).

In a burn wound healing model, increased mobilization of $CXCR4^+/Sca\text{-}1^+$ CACs on day 2 that parallels increased serum levels of SDF-1 has been found in *HIF1a*$^{+/+}$ mice but not in *Hif1a*$^{+/-}$ mice [26]. Impaired wound healing in *Hif1a*$^{+/-}$ mice is associated with reduced blood flow in burn wounds and reduced number of $CD31^+$ vessels at the healing margin of burn wounds. These data delineate a signaling pathway by which HIF-1 promotes angiogenesis during burn wound healing.

In coronary artery disease (CAD), coronary collateral vessels supply blood to ischemic regions and thus promote tissue survival. Higher levels of HIF-1α mRNA and protein expression were found in blood leukocytes from patients with coronary collaterals compared to controls without collaterals [27]. Furthermore, there is a positive correlation between HIF-1α protein and scores of coronary collaterals, suggesting that the level of HIF-1α induced by myocardial ischemia is a major factor in determining the extent of collateral circulation. The frequency of a single nucleotide (C–T) polymorphism in the gene encoding HIF-1α, which changes residue 582 of HIF-1 from proline to serine is significantly higher among patients without collaterals compared to patients with collaterals [28]. Similarly, another study has shown that three polymorphisms in the *HIF1A* gene (Pro582Ser, rs11549465; rs1087314; and Thr418Ile, rs41508050) are found at a significantly higher frequency in patients who presented with stable exertional angina rather than acute myocardial infarction as the initial manifestation of CAD [29]. The ability to develop collaterals in an individual is likely to provide an important response to vascular occlusive disease and to determine in part the severity of ischemic tissue damage.

Despite the importance of reestablishing blood flow to ischemic tissue, it is recognized that reperfusion itself can trigger cell death [30–32], which is

well-known as ischemia-reperfusion injury (I/R). The duration of ischemia determines the severity of ischemic tissue damage. Short episodes of ischemia are well tolerated but prolonged episodes lead to significant cell death. Ischemic preconditioning (IPC) is an innate mechanism to protect against I/R-induced cell death. IPC consists of several brief episodes of ischemia followed by reperfusion that generates profound protection against a subsequent prolonged and otherwise lethal I/R injury [33]. Two phases of protection occurs in IPC: an acute or early phase is observed immediately following the IPC stimulus and is known as "classic" preconditioning, which lasts 2–3 h, and the other is delayed or late-phase preconditioning, which occurs 12–24 h after the IPC stimulus [34]. It has been recently demonstrated that HIF-1α is necessary for acute (early)-phase IPC, as a partial deficiency of HIF-1α in *Hif1a*$^{+/-}$ mice results a complete loss of cardioprotection against I/R injury [35]. Loss of cardiac protection is associated with impaired mitochondrial reactive oxygen species production, PTEN (phosphatase and tensin homolog) oxidation, AKT (protein kinase B) phosphorylation, and cell survival. A more recent study has demonstrated significantly increased expression of HIF-1α mRNA and protein levels in IPC group compared with I/R group in a rat model of myocardial I/R injury [36]. Delayed preconditioning requires gene transcription and translation of new proteins. Several HIF-1-dependent genes have been reported to mediate the delayed phase of preconditioning, including the inducible isoform of nitric oxide synthase (iNOS), cyclooxygenase-2 (COX-2), and heme oxygenase-1 (HO-1) [37, 38]. Genetic reprogramming of the heart in the delayed phase of preconditioning allows the heart to cope with the ischemic stress.

6.3 Review of Work

Tissue regeneration is accompanied by angiogenesis, arteriogenesis, and vasculogenesis, which are adaptive responses to limited oxygen availability in ischemic tissue. These adaptive responses are impaired by aging and chronic diseases. Therapeutic angiogenesis aims to improve neovascularization in ischemic tissues by delivering angiogenic growth factors or progenitor cells or both in the form of gene therapy and/or cell therapy, respectively. As HIF-1 is a crucial mediator of vascular responses, there is great interest in developing therapeutic strategies to activate HIF-1 as a means to overcome impaired adaptive responses to tissue hypoxia and ischemia.

In preclinical limb ischemia models, early gene therapy approaches to promote angiogenesis utilized the gene encoding VEGF. Alternative splicing of VEGF mRNA results in the synthesis of several different isoforms [39], which play important roles in EC proliferation, differentiation, and survival. VEGF exerts its effects through interaction with its receptors (VEGFR1, VEGFR2) expressed on the surface of ECs and CACs [40, 41]. VEGF has been shown to induce a significant increase in perfusion and vessel density [42–45]. However, it has also been shown that intraocular administration of VEGF is not sufficient to induce angiogenesis in the superficial capillary bed of the retina [46] whereas adenoviral expression of a

constitutively active form of HIF-1α (AdCA5) induces a marked angiogenic response [17], which may reflect the combined expression of both VEGF and PLGF, because both of these factors are required for ischemia-induced retinal vascularization [47]. The combination of VEGF and ANGPT1 gene therapy has been found to be more effective than either single gene therapy in a rabbit model of hindlimb ischemia [48]. Intramuscular administration of an adeno-associated virus vector, encoding the both 165-amino acid isoform of human VEGF and ANGPT1 was superior in restoring blood flow in the ischemic limb compared to administration of VEGF or ANGPT1 alone. Capillary density of the combined treatment group was similar to the VEGF treatment group. However, blood vessels in the VEGF-injected areas were leaky. When VEGF was coexpressed with ANGPT1, the permeability of vessels was remarkably reduced. Whereas VEGF is a strong inducer of vascular permeability [49], ANGPT1 has been shown to be essential for the maturation of blood vessels during embryonic angiogenesis [50]. A recent study demonstrated that sustained VEGF expression induced the formation of leaky and poorly functional vessels, whereas regulated induction of VEGF-promoted functional angiogenesis, which is consistent with the concept that adult angiogenesis is a multistep process requiring highly regulated action of multiple angiogenic factors and cell types. Other angiogenic growth factors that have been exploited for single growth factor-mediated gene therapy to promote neovascularization in ischemic limb models include fibroblast growth factors and ANGPT1 [51–53].

Recent studies have demonstrated that stabilization of HIF-1α expression either by inhibiting HIF-1α degradation or by using a chemical inducer, rescued impaired HIF-1 signaling and promoted angiogenesis in diabetic mouse wound and myocardial ischemia models [54, 55]. HIF-1 regulates the expression of multiple critical angiogenic growth factors, cytokines, and their receptors [56], which may explain why stabilized HIF-1 produces a more physiological vascular response than the use of any single growth factor for therapeutic angiogenesis [57]. All these results indicate the necessity of multiple angiogenic factors to induce functional angiogenesis and the importance of HIF-1 as a master regulator of angiogenesis. In rabbits, injection of AdCA5 at the time of intravascular occlusion of the femoral artery leads to accelerated remodeling of existing collateral blood vessels, in which the luminal diameter increases to allow increased blood flow, resulting in recovery of normal blood pressure within 2 weeks after complete femoral artery occlusion [58].

Diabetes is one of the major risk factors associated with CLI. Several preclinical studies have demonstrated that neovascularization, facilitated via administration of angiogenic growth factors including VEGF [59], PLGF [60], or hepatocyte growth factor (HGF) [61], either as recombinant protein therapy or gene therapy, may be augmented following limb ischemia in diabetic animals. Intramuscular injection of AdCA5 into the ischemic limb of *Lepr*$^{db/db}$ mice, a model for type 2 diabetes, significantly improved tissue perfusion, viability, and motor function relative to mice treated with AdLacZ (a control adenovirus encoding β-galactosidase). AdCA5-treated ischemic limbs showed significantly increased smooth muscle α-actin-expressing (SMA$^+$) vessels relative to contralateral nonischemic or AdLacZ-treated ischemic limbs. SMA is expressed in both pericytes and smooth muscle cells of mature blood vessels. Vessel luminal area also increased in the

ischemic limbs of AdCA5-treated, as compared to AdLacZ-treated, *Lepr*$^{db/db}$ mice [62]. CACs are significantly reduced in diabetic patients, which is thought to contribute to impaired angiogenesis [63]. The number of CD117$^+$/VEGFR2$^+$ and CXCR4$^+$ cells circulating in peripheral blood are decreased in patients with type 2 diabetes and the number of CXCR4$^+$ cells is further decreased in diabetic patients with vascular complications [64]. Diabetic patients with ischemic foot lesions due to end-stage peripheral vascular disease have a greater reduction of CD34$^+$ and CD34$^+$/VEGFR2$^+$ cells as compared with diabetic patients with peripheral vascular disease but without foot lesions [65]. AdCA5 administration can correct the impaired mobilization of CD34$^+$/VEGFR2$^+$ and CXCR4-expressing CACs in *Lepr*$^{db/db}$ diabetic mice [62].

The activity of endothelial nitric oxide synthase (eNOS) is essential for mobilization of CACs from bone marrow to peripheral blood and for effective ischemia-induced vascularization [66, 67]. Nitric oxide (NO) generated by eNOS has been identified as promoting the mobilization of EPCs and other CACs from the bone marrow through nitrosylation and elevated VEGF expression [49]. Chronic incubation with high glucose decreases eNOS, FoxO1, and Akt phosphorylation and bioavailable nitric oxide (NO) in putative human EPCs [68]. Activation of eNOS, as determined by its phosphorylation at serine residue 1177, is impaired in diabetic bone marrow, resulting in depressed CAC mobilization [69] in a diabetic wound model. Hyperoxia reverses the defect in CAC mobilization by increasing bone marrow NO, whereas treatment of wounds with SDF-1, the chemokine responsible for recruiting CACs, reverses diabetic homing defects. Hyperglycemia contributes to accelerated arterial stiffening by increasing formation of advanced glycation end-products (AGE), which alter vessel wall structure and function. AGE inhibit EPC function and increase EPC apoptosis via upregulated expression of receptor for AGE (RAGE) and activation of p38 and ERK mitogen-activated protein kinase (MAPK) pathways [70]. AGE-induced MAPK activation is associated with reduced eNOS expression and NO release in EPCs, supporting an important role of eNOS in EPC function and apoptosis in diabetes [71]. eNOS uncoupling in diabetic bone marrow is associated with impaired mobilization of CACs and increased O_2^- production in bone marrow [72]. AdCA5 gene therapy can correct the impaired mobilization of CD34$^+$/VEGFR2$^+$ and CXCR4$^+$ CACs in *Lepr*$^{db/db}$ diabetic mice [62], indicating another mechanism by which HIF-1 gene therapy overcomes the impairment of ischemia-induced vascularization that is observed in diabetes.

The prevalence of PAD increases with age. Similarly, aging has been found to be associated with a progressive impairment in the recovery of limb perfusion after femoral artery ligation in mice [7]. With increasing age, *Hif1a*$^{+/-}$ mice recovered progressively less well than their WT littermates. Whereas young WT mice recovered without any permanent tissue damage, aging was associated with an increasing frequency and severity of tissue damage, ranging from soft tissue necrosis to the spontaneous amputation of one or more toes, due to a failure to recover sufficient blood flow to maintain tissue viability. At each age, the frequency and severity of tissue damage was greater in *Hif1a*$^{+/-}$ than in WT mice. Intramuscular injection of AdCA5 following femoral artery ligation resulted in improved recovery of perfusion both in young and old mice.

Differences in recovery of perfusion have been found to be associated with differences in mobilization of CACs. CAC mobilization in response to limb ischemia is impaired in older mice. Similarly, in a murine ischemic flap model, mobilization of putative EPCs was markedly reduced with aging, which correlated with reduced tissue perfusion and vasculogenesis [73]. Impaired neovascularization may be the result of an aging-associated decrease in HIF-1α stabilization due to an increase in prolyl hydroxylase-mediated hydroxylation and proteasomal degradation of HIF-1α. Intraperitoneal injection of desferioxamine, a known HIF-1α stabilizer [74], promotes ischemic flap survival in aged mice compared with their untreated counterparts, which is associated with increased mobilization of putative EPCs [73].

Aging is also associated with impairment of ischemia-induced HIF-1α protein levels and of HIF-1α, SDF-1, PLGF, ANGPT1, ANGPT2, VEGF, and SCF mRNA levels in HIF-1α mice [7]. These results indicate that aging-associated deficiency of HIF-1α is responsible for diminished production of angiogenic growth factors, which in turn affects CAC mobilization. Thus, HIF-1α is necessary for ischemia-induced mobilization of CACs and the aging-associated deficiency of HIF-1α can be corrected by HIF-1α gene therapy.

It is thought that bone marrow-derived angiogenic cells (BMDACs) play a significant role in the reendothelization of injured endothelium through their incorporation into new or remodeling vessels or through paracrine effects [4]. Recruitment and incorporation of these cells requires a coordinated sequence of multistep signaling events including adhesion and migration (e.g., by integrins), chemoattraction (e.g., by SDF-1/CXCR4), and finally the differentiation to endothelial cells [75]. Intramuscular injection of AdCA5 not only improved perfusion, production of angiogenic cytokines, and mobilization of CACs [7, 62] but also improved the homing of BMDACs to the ischemic limb [76]. Dimethyloxalylglycine (DMOG), a prolyl-4-hydroxylase inhibitor, blocks the oxygen dependent degradation of HIF-1α and has been shown to improve recovery in mouse models of intestinal and cerebral ischemia [77–79]. DMOG treatment of BMDACs increases cell surface expression of β_2 integrins, which mediate increased adherence of these cells to vascular endothelial cells, thereby increasing the retention of these cells in the ischemic tissue after homing.

Shear forces and flow dynamics in the microvascular environment have a crucial impact on the adhesion of newly recruited angiogenic cells to the endothelium. As a result, it is important that the molecular mechanisms underlying the retention of bone marrow-derived angiogenic cells be studied under conditions that simulate this environment. Thus, adhesion of BMDACs to ECs was tested using a dynamic microfluidic adhesion assay that takes place in the presence of shear flow, a factor not accounted for in conventional static plate assays. In addition, hypoxic human umbilical vein ECs (HUVECs), which mimic effects of the ischemic tissue environment on the vasculature, were utilized [76]. Increasing the perfusion pressure from 0.1 Pa (physiological sheer stress) to 2.5 Pa was sufficient to remove angiogenic cells bound to HUVECs cultured under nonhypoxic conditions but did not remove BMDACs bound to HUVECs that were cultured under hypoxic conditions, which is consistent with the known activation of vascular endothelium in ischemic tissue.

The effect of DMOG was abolished by cotreatment with the HIF-1 inhibitor digoxin or by addition of β_2 integrin-blocking antibody. Hypoxic exposure of HUVECs increases expression of ICAM-1 and E-selectin, the β_2 integrin ligands, indicating HIF-1 as a regulatory molecule in the multistep neovascularization process. Combined AdCA5 gene therapy and DMOG-treated angiogenic cell therapy is effective in improving functional recovery and limb salvage (i.e., recovery without permanent tissue damage) in aging mice following femoral artery ligation. In contrast, AdCA5 gene therapy or BMDACs alone is not sufficient to improve limb salvage in old mice. Other studies have also shown the beneficial effect of HIF-1α-modified BMDACs for improving neovascularization in animal models of ischemia [80, 81]. However, these studies involved transduction of BMDACs with viral or plasmid vectors, whereas DMOG treatment induces HIF-1 without exposure of cells to a recombinant vector that might cause neoplastic cell transformation. Additionally, compared to prior studies, a tenfold lower number of DMOG-treated BMDACs was sufficient to induce therapeutic effects in young as well as in old mice in combination with AdCA5. Thus, combined HIF-1α gene therapy and DMOG-treated cell therapy is capable of reducing the number of cells as well as improving their retention in ischemic sites.

Despite promising results obtained in animal models, clinical studies of angiogenic therapies for vascular disease using single growth factors have yielded disappointing results [82–85]. In a small group of diabetic patients with CLI, gene therapy using VEGF gene-carrying plasmid failed to meet the primary end point of a significantly reduced incidence of amputation [83]. One potential explanation based on the animal studies is that the use of a single angiogenic growth factor may be insufficient to generate adequate and durable neovascularization. A phase I clinical study in no-option patients with CLI demonstrating safety of intramuscular administration of adenoviral vector encoding a HIF-1α/VP16 fusion protein was reported [86]. However, administration of this fusion protein, which is likely to have properties that differ from those of HIF-1α, did not result in significant clinical benefit in a phase II/III trial.

Limited success with gene therapy in clinical settings calls for more careful design of preclinical models. Thus, many of the clinical trials were based on data generated used young healthy animals, whereas the subjects in the clinical trials represent an aged population with other risk factors including diabetes. Incorporating the effects of aging and diabetes into the preclinical model is an important advance. However, current models still have major limitations. Most importantly, in most of the animal models, ischemia is induced by acute arterial occlusion, whereas CLI in patients is the result of a chronic and progressive process that develops over decades. It is not clear whether this aspect of the disease can be modeled in animals that only live 2–3 years.

Following the unsuccessful gene therapy clinical trials, trials involving the administration of various cell types for therapeutic angiogenesis have been reported. The clinical trials were based on success in preclinical models that again mostly involved young, healthy animals as both donors and recipients. The cell types that have been utilized include bone marrow mononuclear cells, either unsorted cell or

those selected for expression of CD34 or aldehyde dehydrogenase, and peripheral blood mononuclear cells from either untreated or granulocyte colony-stimulating factor (G-CSF)-treated individuals [87–92]. These trials have been conducted with a relatively small number of patients and with a short follow-up period. Only a few trials with 1 year or longer follow-up periods have been reported so far [93, 94]. Large randomized, controlled trials with longer follow-up are needed to evaluate the safety and long-term efficacy of cell therapy.

6.4 Future Directions

Therapeutic angiogenesis in no-option CLI patients is still a very new field in which impressive effects in preclinical studies have not been translated to the clinic. Several factors including optimal dose, route of delivery, choice of gene, and/or choice of functional cell population need to be considered when designing clinical trials. Future therapies for correcting vascular complications should focus on correcting multiple deficits to achieve an optimal angiogenic response. HIF-1 plays critical roles in mediating vascular responses to hypoxia and ischemia. Impairment of HIF-1α generation and subsequent impaired production of angiogenic growth factors and mobilization of CACs represents a major pathogenic mechanism underlying impaired responses to ischemia associated with aging and diabetes. Stimulation of angiogenesis, arteriogenesis, and vasculogenesis remains an important potential therapeutic option in patients with severe tissue ischemia. Results from the preclinical studies discussed above indicate that combined HIF-1α gene therapy and HIF-1-activated BMDAC therapy is a promising approach to induce therapeutic angiogenesis in ischemic tissue and clinical trials in patients with CLI are needed to test this hypothesis.

Acknowledgments Relevant work from the authors' laboratory was supported by American Diabetes Association grant 1-06-RA-121, NIH grant R01-HL55338, and the Johns Hopkins Institute for Cell Engineering. G.L.S. is the C. Michael Armstrong Professor at The Johns Hopkins University.

References

1. Semenza GL (2010) Oxygen homeostasis. Wiley Interdiscip Rev Syst Biol Med 2(3):336–361 doi:10.1002/wsbm.69
2. Semenza GL, Jiang BH, Leung SW et al. (1996) Hypoxia response elements in the aldolase A, enolase 1, and lactate dehydrogenase A gene promoters contain essential binding sites for hypoxia-inducible factor 1. J Biol Chem 271:32529–32537
3. Asahara T, Murohara T, Sullivan A et al. (1997) Isolation of putative progenitor endothelial cells for angiogenesis. Science 275:964–967
4. Asahara T, Masuda H, Takahashi T et al. (1999) Bone marrow origin of endothelial progenitor cells responsible for postnatal vasculogenesis in physiological and pathological neovascularization. Circ Res 85:221–228

5. Iyer NV, Kotch LE, Agani F et al. (1998) Cellular and developmental control of O_2 homeostasis by hypoxia-inducible factor 1a. Genes Dev 12:149–162
6. Ryan HE, Lo J, & Johnson RS (1998) HIF-1a is required for solid tumor formation and embryonic vascularization. EMBO J 17:3005–3015
7. Bosch-Marce M, Okuyama H, Wesley JB et al. (2007) Effects of aging and hypoxia-inducible factor 1 activity on angiogenic cell mobilization and recovery of perfusion after limb ischemia. Circ Res 101:1310–1318
8. Carmeliet P (2003) Angiogenesis in health and disease. Nat Med 9:653–660
9. Norgren L, Hiatt WR, Dormandy JA et al. (2007) Inter-Society Consensus for the Management of Peripheral Arterial Disease (TASC II). J Vasc Surg 45(Suppl S):S5–S67
10. Hirsch AT, Haskal ZJ, & Hertzer NR (2006) ACC/AHA 2005 Practice guidelines for the management of patients with peripheral arterial disease (lower extremity, renal, mesenteric, and abdominal aortic): a collaborative report from the American Association for Vascular Surgery/Society for Vascular Surgery, Society for Cardiovascular Angiography and Interventions, Society for Vascular Medicine and Biology, Society of Interventional Radiology, and the ACC/AHA Task Force on Practice Guidelines (Writing Committee to Develop Guidelines for the Management of Patients With Peripheral Arterial Disease): endorsed by the American Association of Cardiovascular and Pulmonary Rehabilitation; National Heart, Lung, and Blood Institute; Society for Vascular Nursing; TransAtlantic Inter-Society Consensus; and Vascular Disease Foundation. Circulation 113:e463–e654
11. Novo S, Coppola G, & Milio G (2004) Critical limb ischemia: definition and natural history. Curr Drug Targets Cardiovasc Haematol Disord 4:219–225
12. Nathan DM (1993) Long-term complications of diabetes mellitus. N Engl J Med 328:1676–1685
13. Virkkunen J, Heikkinen M, Lepantalo M et al. (2004) Diabetes as an independent risk factor for early postoperative complications in critical limb ischemia. J Vasc Surg 40:761–767
14. Ruffolo AJ, Romano M, & Ciapponi A (2010) Prostanoids for critical limb ischaemia. Cochrane Database Syst Rev CD006544
15. Klomp HM, Steyerberg EW, Habbema JD et al. (2009) What is the evidence on efficacy of spinal cord stimulation in (subgroups of) patients with critical limb ischemia? Ann Vasc Surg 23:355–363
16. Carmeliet P (2000) Mechanisms of angiogenesis and arteriogenesis. Nat Med 6:389–395
17. Kelly BD, Hackett SF, Hirota K et al. (2003) Cell type-specific regulation of angiogenic growth factor gene expression and induction of angiogenesis in nonischemic tissue by a constitutively active form of hypoxia-inducible factor 1. Circ Res 93:1074–1081
18. Forsythe JA, Jiang BH, Iyer NV et al. (1996). Activation of vascular endothelial growth factor gene transcription by hypoxia-inducible factor 1. Mol Cell Biol 16:4604–4613
19. Ceradini DJ, Kulkarni AR, Callaghan MJ et al. (2004) Progenitor cell trafficking is regulated by hypoxic gradients through HIF-1 induction of SDF-1. Nat Med 10:858–864
20. Simon MP, Tournaire R, & Pouyssegur J (2008) The angiopoietin-2 gene of endothelial cells is up-regulated in hypoxia by a HIF binding site located in its first intron and by the central factors GATA-2 and Ets-1. J Cell Physiol 217:809–818
21. Oikawa M, Abe M, Kurosawa H et al. (2001) Hypoxia induces transcription factor ETS-1 via the activity of hypoxia-inducible factor 1. Biochem Biophys Res Commun 289:39–43
22. Manalo DJ, Rowan A, Lavoie T et al. (2005) Transcriptional regulation of vascular endothelial cell responses to hypoxia by HIF-1. Blood 105:659–669
23. Karamysheva AF (2008) Mechanisms of angiogenesis. Biochemistry (Mosc) 73:751–762
24. Lindahl P, Johansson BR, Leveen P et al. (1997) Pericyte loss and microaneurysm formation in PDGF-B-deficient mice. Science 277:242–245
25. Okuyama H, Krishnamachary B, Zhou YF et al. (2006) Expression of vascular endothelial growth factor receptor 1 in bone marrow-derived mesenchymal cells is dependent on hypoxia-inducible factor 1. J Biol Chem 281:15554–15563
26. Zhang X, Liu L, Wei X et al. (2010) Impaired angiogenesis and mobilization of circulating angiogenic cells in HIF-1alpha heterozygous-null mice after burn wounding. Wound Repair Regen 18:193–201

27. Chen SM, Li YG, Zhang HX et al. (2008) Hypoxia-inducible factor-1alpha induces the coronary collaterals for coronary artery disease. Coron Artery Dis 19:173–179
28. Resar JR, Roguin A, Voner J et al. (2005) Hypoxia-inducible factor 1alpha polymorphism and coronary collaterals in patients with ischemic heart disease. Chest 128:787–791
29. Hlatky MA, Quertermous T, Boothroyd DB et al. (2007) Polymorphisms in hypoxia inducible factor 1 and the initial clinical presentation of coronary disease. Am Heart J 154:1035–1042
30. Dirksen MT, Laarman GJ, Simoons ML et al. (2007) Reperfusion injury in humans: a review of clinical trials on reperfusion injury inhibitory strategies. Cardiovasc Res 74:343–345
31. Fliss H & Gattinger D (1996) Apoptosis in ischemic and reperfused rat myocardium. Circ Res 79:949–956
32. Logue SE, Gustafsson AB, Samali A et al. (2005) Ischemia/reperfusion injury at the intersection with cell death. J Mol Cell Cardiol 38:21–33
33. Murry CE, Jennings RB, & Reimer KA (1986) Preconditioning with ischemia: a delay of lethal cell injury in ischemic myocardium. Circulation 74:1124–1136
34. Stein AB, Tang XL, Guo Y et al. (2004) Delayed adaptation of the heart to stress: late preconditioning. Stroke 35:2676–2679
35. Cai Z, Zhong H, Bosch-Marce M et al. (2008) Complete loss of ischaemic preconditioning-induced cardioprotection in mice with partial deficiency of HIF-1 alpha. Cardiovasc Res 77:463–470
36. Niu TS, Qi GX, Fu P et al. (2010) Protective effects of hypoxia-inducible factor-1alpha on myocardial ischemia/reperfusion injury in rat and the role of protein kinase C in signal pathway. Zhongguo Wei Zhong Bing Ji Jiu Yi Xue 22:101–104
37. Bolli R (2007) Preconditioning: a paradigm shift in the biology of myocardial ischemia. Am J Physiol Heart Circ Physiol 292:H19–H27
38. Loor G & Schumacker PT (2008) Role of hypoxia-inducible factor in cell survival during myocardial ischemia-reperfusion. Cell Death Differ 15:686–690
39. Tischer E, Mitchell R, Hartman T et al. (1991) The human gene for vascular endothelial growth factor. Multiple protein forms are encoded through alternative exon splicing. J Biol Chem 266:11947–11954
40. Coultas L, Chawengsaksophak K, & Rossant J (2005) Endothelial cells and VEGF in vascular development. Nature 438:937–945
41. Ferrara N, Gerber HP, & LeCouter J (2003) The biology of VEGF and its receptors. Nat Med 9:669–676
42. Bauters C, Asahara T, Zheng LP et al. (1995) Site-specific therapeutic angiogenesis after systemic administration of vascular endothelial growth factor. J Vasc Surg 21:314–324
43. Becit N, Ceviz M, Kocak H et al. (2001) The effect of vascular endothelial growth factor on angiogenesis: an experimental study. Eur J Vasc Endovasc Surg 22:310–316
44. Takeshita S, Weir L, Chen D et al. (1996) Therapeutic angiogenesis following arterial gene transfer of vascular endothelial growth factor in a rabbit model of hindlimb ischemia. Biochem Biophys Res Commun 227:628–635
45. Tsurumi Y, Takeshita S, Chen D et al. (1996) Direct intramuscular gene transfer of naked DNA encoding vascular endothelial growth factor augments collateral development and tissue perfusion. Circulation 94:3281–3290
46. Ozaki H, Hayashi H, Vinores SA et al. (1997) Intravitreal sustained release of VEGF causes retinal neovascularization in rabbits and breakdown of the blood-retinal barrier in rabbits and primates. Exp Eye Res 64:505–517
47. Carmeliet P, Moons L, Luttun A et al. (2001) Synergism between vascular endothelial growth factor and placental growth factor contributes to angiogenesis and plasma extravasation in pathological conditions. Nat Med 7:575–583
48. Chen F, Tan Z, Dong CY et al. (2007) Adeno-associated virus vectors simultaneously encoding VEGF and angiopoietin-1 enhances neovascularization in ischemic rabbit hind-limbs. Acta Pharmacol Sin 28:493–502
49. Dvorak HF, Nagy JA, Feng D et al. (1999) Vascular permeability factor/vascular endothelial growth factor and the significance of microvascular hyperpermeability in angiogenesis. Curr Top Microbiol Immunol 237:97–132

50. Suri C, Jones PF, Patan S et al. (1996) Requisite role of angiopoietin-1, a ligand for the TIE2 receptor, during embryonic angiogenesis. Cell 87:1171–1180
51. Huang J, Inoue M, Hasegawa M et al. (2009) Sendai viral vector mediated angiopoietin-1 gene transfer for experimental ischemic limb disease. Angiogenesis 12:243–249
52. Ohara N, Koyama H, Miyata T et al. (2001) Adenovirus-mediated ex vivo gene transfer of basic fibroblast growth factor promotes collateral development in a rabbit model of hind limb ischemia. Gene Ther 8:837–845
53. Rissanen TT, Markkanen JE, Arve K et al. (2003) Fibroblast growth factor 4 induces vascular permeability, angiogenesis and arteriogenesis in a rabbit hindlimb ischemia model. FASEB J 17:100–102
54. Chen JX & Stinnett A (2008) Ang-1 gene therapy inhibits hypoxia-inducible factor-1a (HIF-1alpha)-prolyl-4-hydroxylase-2, stabilizes HIF-1a expression, and normalizes immature vasculature in db/db mice. Diabetes 57:3335–3343
55. Mace KA, Yu DH, Paydar KZ et al. (2007) Sustained expression of HIF-1a in the diabetic environment promotes angiogenesis and cutaneous wound repair. Wound Repair Regen 15:636–645
56. Semenza GL (2009) Regulation of oxygen homeostasis by hypoxia-inducible factor 1. Physiology (Bethesda) 24:97–106
57. Pajusola K, Kunnapuu J, Vuorikoski S et al. (2005) Stabilized HIF-1a is superior to VEGF for angiogenesis in skeletal muscle via adeno-associated virus gene transfer. FASEB J 19:1365–1367
58. Patel TH, Kimura H, Weiss CR et al. (2005) Constitutively active HIF-1a improves perfusion and arterial remodeling in an endovascular model of limb ischemia. Cardiovasc Res 68:144–154
59. Rivard A, Silver M, Chen D et al. (1999) Rescue of diabetes-related impairment of angiogenesis by intramuscular gene therapy with adeno-VEGF. Am J Pathol 154:355–363
60. Tamarat R, Silvestre JS, Le Ricousse-Roussanne S et al. (2004) Impairment in ischemia-induced neovascularization in diabetes: bone marrow mononuclear cell dysfunction and therapeutic potential of placenta growth factor treatment. Am J Pathol 164:457–466
61. Taniyama Y, Morishita R, Hiraoka K et al. (2001) Therapeutic angiogenesis induced by human hepatocyte growth factor gene in rat diabetic hind limb ischemia model: molecular mechanisms of delayed angiogenesis in diabetes. Circulation 104:2344–2350
62. Sarkar K, Fox-Talbot K, Steenbergen C et al. (2009) Adenoviral transfer of HIF-1a enhances vascular responses to critical limb ischemia in diabetic mice. Proc Natl Acad Sci USA 106:18769–18774
63. Fadini GP, Agostini C, & Avogaro A (2005) Endothelial progenitor cells and vascular biology in diabetes mellitus: current knowledge and future perspectives. Curr Diabetes Rev 1:41–58
64. Egan CG, Lavery R, Caporali F et al. (2008) Generalized reduction of putative endothelial progenitors and CXCR4-positive peripheral blood cells in type 2 diabetes. Diabetologia 51:1296–1305
65. Fadini GP, Miorin M, Facco M et al. (2005) Circulating endothelial progenitor cells are reduced in peripheral vascular complications of type 2 diabetes mellitus. J Am Coll Cardiol 45:1449–1457
66. Aicher A, Heeschen C, Mildner-Rihm C et al. (2003) Essential role of endothelial nitric oxide synthase for mobilization of stem and progenitor cells. Nat Med 9:1370–1376
67. Murohara T, Asahara T, Silver M et al. (1998) Nitric oxide synthase modulates angiogenesis in response to tissue ischemia. J Clin Invest 101:2567–2578
68. Chen YH, Lin SJ, Lin FY et al. (2007) High glucose impairs early and late endothelial progenitor cells by modifying nitric oxide-related but not oxidative stress-mediated mechanisms. Diabetes 56:1559–1568
69. Gallagher KA, Liu ZJ, Xiao M et al. (2007) Diabetic impairments in NO-mediated endothelial progenitor cell mobilization and homing are reversed by hyperoxia and SDF-1 alpha. J Clin Invest 117:1249–1259
70. Sun C, Liang C, Ren Y et al. (2009) Advanced glycation end products depress function of endothelial progenitor cells via p38 and ERK 1/2 mitogen-activated protein kinase pathways. Basic Res Cardiol 104:42–49

71. Shen C, Li Q, Zhang YC et al. (2010) Advanced glycation endproducts increase EPC apoptosis and decrease nitric oxide release via MAPK pathways. Biomed Pharmacother 64:35–43
72. Thum T, Fraccarollo D, Schultheiss M et al. (2007) Endothelial nitric oxide synthase uncoupling impairs endothelial progenitor cell mobilization and function in diabetes. Diabetes 56:666–674
73. Chang EI, Loh SA, Ceradini DJ et al. (2007) Age decreases endothelial progenitor cell recruitment through decreases in hypoxia-inducible factor 1a stabilization during ischemia. Circulation 116:2818–2829
74. Wang GL & Semenza GL (1993) Desferrioxamine induces erythropoietin gene expression and hypoxia-inducible factor 1 DNA-binding activity: implications for models of hypoxia signal transduction. Blood 82:3610–3615
75. Urbich C & Dimmeler S (2004) Endothelial progenitor cells: characterization and role in vascular biology. Circ Res 95:343–353
76. Rey S, Lee K, & Wang CJ (2009) Synergistic effect of HIF-1a gene therapy and HIF-1-activated bone marrow-derived angiogenic cells in a mouse model of limb ischemia. Proc Natl Acad Sci USA 106:20399–20404
77. Cummins EP, Seeballuck F, Keely SJ et al. (2008) The hydroxylase inhibitor dimethyloxalylglycine is protective in a murine model of colitis. Gastroenterology 134:156–165
78. Elvidge GP, Glenny L, Appelhoff RJ et al. (2006) Concordant regulation of gene expression by hypoxia and 2-oxoglutarate-dependent dioxygenase inhibition: the role of HIF-1a, HIF-2a, and other pathways. J Biol Chem 281:15215–15226
79. Siddiq A, Ayoub IA, Chavez JC et al. (2005) Hypoxia-inducible factor prolyl 4-hydroxylase inhibition. A target for neuroprotection in the central nervous system. J Biol Chem 280:41732–41743
80. Jiang M, Wang B, Wang C et al. (2008) Angiogenesis by transplantation of HIF-1a modified EPCs into ischemic limbs. J Cell Biochem 103:321–334
81. Jiang M, Wang B, Wang C et al. (2008) In vivo enhancement of angiogenesis by adenoviral transfer of HIF-1a-modified endothelial progenitor cells (Ad-HIF-1a-modified EPC for angiogenesis). Int J Biochem Cell Biol 40:2284–2295
82. Henry TD, Annex BH, McKendall GR et al. (2003) The VIVA trial: vascular endothelial growth factor in Ischemia for vascular angiogenesis. Circulation 107:1359–1365
83. Kusumanto YH, van Weel V, Mulder NH et al. (2006) Treatment with intramuscular vascular endothelial growth factor gene compared with placebo for patients with diabetes mellitus and critical limb ischemia: a double-blind randomized trial. Hum Gene Ther 17:683–691
84. Rajagopalan S, Mohler ER, III, Lederman RJ et al. (2003) Regional angiogenesis with vascular endothelial growth factor in peripheral arterial disease: a phase II randomized, double-blind, controlled study of adenoviral delivery of vascular endothelial growth factor 121 in patients with disabling intermittent claudication. Circulation 108:1933–1938
85. Simons M, Annex BH, Laham RJ et al. (2002) Pharmacological treatment of coronary artery disease with recombinant fibroblast growth factor-2: double-blind, randomized, controlled clinical trial. Circulation 105:788–793
86. Rajagopalan S, Olin J, Deitcher S et al. (2007) Use of a constitutively active hypoxia-inducible factor-1alpha transgene as a therapeutic strategy in no-option critical limb ischemia patients: phase I dose-escalation experience. Circulation 115:1234–1243
87. Huang P, Li S, Han M et al. (2005) Autologous transplantation of granulocyte colony-stimulating factor-mobilized peripheral blood mononuclear cells improves critical limb ischemia in diabetes. Diabetes Care 28:2155–2160
88. Kajiguchi M, Kondo T, Izawa H et al. (2007) Safety and efficacy of autologous progenitor cell transplantation for therapeutic angiogenesis in patients with critical limb ischemia. Circ J 71:196–201
89. Kawamoto A, Katayama M, Handa N et al. (2009) Intramuscular transplantation of G-CSF-mobilized CD34(+) cells in patients with critical limb ischemia: a phase I/IIa, multicenter, single-blinded, dose-escalation clinical trial. Stem Cells 27:2857–2864

90. Keller LH (2009) Bone marrow-derived aldehyde dehydrogenase-bright stem and progenitor cells for ischemic repair. Congest Heart Fail 15:202–206
91. Prochazka V, Gumulec J, Chmelova J et al. (2009) Autologous bone marrow stem cell transplantation in patients with end-stage chronical critical limb ischemia and diabetic foot. Vnitr Lek 55:173–178
92. Wester T, Jorgensen JJ, Stranden E et al. (2008) Treatment with autologous bone marrow mononuclear cells in patients with critical lower limb ischaemia. A pilot study. Scand J Surg 97:56–62
93. Matoba S, Tatsumi T, Murohara T et al. (2008) Long-term clinical outcome after intramuscular implantation of bone marrow mononuclear cells (Therapeutic Angiogenesis by Cell Transplantation [TACT] trial) in patients with chronic limb ischemia. Am Heart J 156:1010–1018
94. Van Tongeren RB, Hamming JF, Fibbe WE et al. (2008) Intramuscular or combined intramuscular/intra-arterial administration of bone marrow mononuclear cells: a clinical trial in patients with advanced limb ischemia. J Cardiovasc Surg (Torino) 49:51–58

Chapter 7
Hypoxia and Matrix Manipulation for Vascular Engineering

Hasan E. Abaci, Donny Hanjaya-Putra, and Sharon Gerecht

7.1 Introduction

It is not surprising that characteristics of many cell types are regulated by both oxygen (O_2) availability and extracellular matrix (ECM) context, which play crucial roles in the permanency of multicellular organisms on Earth.

According to the most recent findings, O_2 reached sufficient levels (estimated to be 0.2–2% O_2) for aerobic organisms to be able to survive between 2.2 and 2.45 billion years ago in the oceans [15] and between 540 and 600 million years ago in Earth's atmosphere [58, 159]. Ever since, O_2 has been a highly available potential source of energy for multicellular organisms to commence, survive, and multiply on Earth. Multicellular organisms require specialized systems to enable sufficient amounts of O_2 to reach their cells. For instance, insects regulate the transport of O_2 into their tissues with a special respiratory system consisting of spiracles and trachea. Around their tissues, they retain the relatively low oxygen levels (1.4 mmHg) thought to be equivalent to the atmospheric O_2 concentrations at the time of their evolution [131, 132]. In vertebrates, O_2 is carried by proteins in the blood, particularly by hemoglobin, and is transported to tissues through endothelial cells (ECs). The cells throughout the body are highly dependent on the dynamics of O_2. In humans, O_2 concentrations vary between 1 and 5% in tissues and between 5 and 7% in blood vessels [125]. Therefore, O_2 has always been a signaling molecule for cells, regulating their metabolism, survival, cell–cell interactions, migration, and differentiation.

The transition from unicellular to multicellular organisms required, besides O_2 availability, that the cells be connected together in a way that allowed them to interact with each other as parts of the same system. This interconnectedness could happen

S. Gerecht (✉)
Department of Chemical and Biomolecular Engineering, Johns Hopkins Physical Sciences-Oncology Center, Institute for NanoBioTechnology, Johns Hopkins University, Baltimore, MD 21218, USA
e-mail: gerecht@jhu.edu

S. Gerecht (ed.), *Biophysical Regulation of Vascular Differentiation and Assembly*, Biological and Medical Physics, Biomedical Engineering,
DOI 10.1007/978-1-4419-7835-6_7,

either by having junctions at the cell peripheries or by having connecting cement between the cells. Many multicellular organisms connect their cells in both ways: they use cellular junctions to allow direct signaling between cells, and they use the ECM to regulate the transport of molecules (e.g., O_2, glucose, and signaling proteins) between the cells by remodeling the components of the ECM. Thus, both cell–cell and cell–ECM interactions are significant for determining the fate of cells in tissues. Surface proteins known as integrins are responsible for signaling from the ECM to the cell. Therefore, cells have different responses in respect to the composition and structure of the surrounding ECM. In particular, vascular morphogenesis is regulated by endothelial cell (EC) interactions with the ECM through integrins and is highly dependent on the ECM context [39].

In the field of vascular engineering, the effects of both O_2 tension and the ECM on blood vessel formation should be extensively investigated. Blood vessel formation essentially occurs by angiogenesis or vasculogenesis. Angiogenesis is the formation of blood vessels from preexisting vasculature, orchestrated with the proliferation, migration, and assembly of ECs, as well as the remodeling of the ECM [105, 176]. Normally, most of the ECs comprising the blood vessel walls are in a state of quiescence in physiological conditions. A stimulus is required for ECs to switch from their resting state to their navigating state, in which they are activated to produce angiogenesis-promoting proteins [56]. Angiogenesis occurs in several situations, such as wound healing, arthritis, cardiovascular ischemia, and solid tumor growth [34, 164]. In all of these situations, the tissue or vasculature is deprived of oxygen, leading to hypoxic conditions that promote angiogenesis. For vessel sprouting, the ECM surrounding the vasculature needs to be degraded so that ECs can easily navigate into the tissue and proliferate. Hypoxia was shown to promote the production of ECM-degrading enzymes and the secretion of ECs [17, 47, 51]. Thus, EC sprouting more likely continues toward the hypoxic regions in the ECM through which the secretion of enzymes is upregulated by hypoxia, whereas the invasion of vessels into the ECM is not favored in the direction of sufficiently oxygenated regions.

The oxygen gradient also occurs to a great extent in early development [115]. While the O_2 uptake of early embryonic cells relies on the simple diffusion of oxygen, hypoxia starts being observed in different regions as the embryo expands [2, 115]. The initial vascularization, vasculogenesis, starts with the differentiation of angioblasts (embryonic progenitors of ECs) and is followed by tubulogenesis and vascular network formation throughout the yolk sac [126, 190]. This process of vasculogenesis has been suggested to occur in hypoxic conditions [115, 126]. Hypoxia also stimulates microvascularization and the capillary network around the developing organs. Vasculogenesis in adult organs has been demonstrated to originate from endothelial progenitor cells (EPCs) circulating in the blood [187]. The migration of EPCs and their recruitment to the appropriate sites to induce the formation of new blood vessels depend on complex cell signaling. Investigations of tumor growth and wound healing have revealed that hypoxia occurs in both situations, inducing EPCs to migrate from the circulating blood through the ECM. Hypoxia also plays a role in the recruitment of EPCs by promoting the receptor

expression on the tissue that recognizes EPCs, which is followed by their differentiation into ECs [27]. Moreover, vascular endothelial growth factor (VEGF), a key regulatory protein known to induce vasculogenesis and angiogenesis, was found to be upregulated in hypoxia [129]. These processes take place in the milieu of the ECM, which is mostly composed of fibronectin during early development [39, 119]. In adult tissue, on the other hand, collagen becomes abundant and controls the cellular fate.

Overall, the formation of new blood vessels through angiogenesis or vasculogenesis depends on dynamic effects and interplay between the ECM and oxygen tensions. A thorough understanding of the mechanisms involving the ECM and O_2 during angiogenesis and vasculogenesis is essential for the fundamental understanding that could be extrapolated for vascular engineering applications. Indeed, the effects of these two factors on vascular cells are being investigated extensively. The in vitro vascularization of primary vascular cells has been studied using many different biomaterials [6, 20, 71] as three-dimensional (3D) matrix components, and they were shown to have various effects on angiogenesis/vasculogenesis. Similarly, a considerable amount of work has focused on the effects of hypoxia-inducible factors (HIF1α, HIF2α, HIF3α) on the regulation of several genes that induce vasculature formation [54, 129, 199]. In addition, some researchers have also investigated the effects of hypoxia and the ECM context together [139, 145]. Success in engineering blood vessels from primary vascular cells or stem cells relies on understanding the influence of all critical parameters and controlling them in targeted directions.

The main focus of this chapter is a review and discussion of how the cells in the body respond to the variations in oxygen tension and ECM components leading to new vasculature formation.

7.2 Concepts in the Regulation of the Vasculature by Oxygen and the ECM

7.2.1 The Influence of Oxygen Tension on Vascularization

Variations in oxygen concentrations at every stage of embryogenesis and in different regions of adult tissues lead to diverse vascular responses, depending on the cell type and microenvironment. Many cell types respond differently, but also collectively, to the changes in O_2 equilibrium through specialized sensing mechanisms and effectors in order to maintain homeostasis. This section will first discuss the formation and location of poorly oxygenated regions in the body, as well as the mechanisms that cells utilize to sense changes in oxygen levels. It will then focus on several responses of pluripotent and vascular cells to low O_2 tensions in terms of gene regulation, differentiation, oxygen consumption, and cell survival.

7.2.1.1 The In Vivo Consequences of Oxygen Gradients

Oxygen Availability in the Body

In vertebrates, O_2 transport to the tissues relies on three main processes: the oxygenation of the blood in the alveoli in the lungs, the convectional transport of oxygen in blood along the arteries, and the diffusion of oxygen across the vessel walls followed by penetration of O_2 to the deeper tissues. It encounters three distinct resistances to the mass transfer of the O_2 molecule, which result in O_2 gradients throughout the body.

O_2 deprivations have been observed early in the development of mouse embryos [115]. Also, polarographic oxygen measurements in the human placenta have shown that O_2 levels are 1.3–3.5% in the first 8–10 weeks and reach between 7.2 and 9.5% in weeks 12–13 of pregnancy [154, 167]. Oxygen levels measured in the gestational sac revealed even lower O_2 levels in earlier stages of embryogenesis, where O_2 is only transported by simple diffusion [95]. Diffusion, as opposed to convection, transports nutrients between cells very slowly. Before vasculogenesis begins, the maximum diameter that a spherical embryo can reach without having any cells under anoxia was calculated as 2 mm [24]. This value varies with the embryo's geometry and, most importantly, with the O_2 consumption of the animal cells. The results of in vivo imaging of various animal embryos show that the maximum diameter remains below 1 mm, which agrees with the theoretically estimated value [24, 190].

Vasculogenesis is crucial for cells to proliferate and for the embryo to grow larger. In mouse embryos, vasculogenesis starts taking place after day 7, with the differentiation of the mesoderm into angioblasts, which then assemble to form a simple circulatory system consisting of a heart, dorsal aorta, and yolk sac by day 8 [43, 86]. Afterwards, spatial increases are observed in O_2 levels in the course of embryo development [115]. These profound spatiotemporal O_2 level changes in the embryo can be accepted as the supporting evidence for vascular formation during embryogenesis. The large existing vasculature then sprouts and proliferates to supply O_2 and nutrients to cells located in poorly oxygenated regions. Hypoxia, considered the most critical factor controlling the angiogenesis process, works via numerous protein-signaling pathways. The mechanism determining the directions of angiogenesis and the complex networking of endothelial capillaries around the tissues is manipulated by several other parameters, including hemodynamic forces and cytokines; this mechanism will be discussed later in the chapter [121].

Once embryonic development is accomplished and a sufficient amount of O_2 and nutrients is supplied to the tissues, the oxygen gradient still persists in some tissues, providing several benefits to specific cell types. O_2 distribution in adults ranges from 0.5 to 14%. Although the formation of blood vessels and capillary networking is completed, some tissues still lack of a vasculature, such as the bone marrow niche [73, 111, 143]. Thus, diffusion is the controlling mechanism for nutrient transport to internal parts of the tissue and is responsible for the wide range of O_2 distributions.

The discovery of circulating EPCs in blood vessels revealed that neovascularization in adults is directed not only by angiogenesis but also by the vasculogenesis process, which depends on the renewal, mobility, recruitment, and differentiation of EPCs [8, 9, 78, 182]. Bone marrow (BM) provides a host microenvironment for a variety of cells, including hematopoietic stem cells (HSCs), mesenchymal stem cells (MSCs), and EPCs. The development of EPCs occurs in the BM, which has a unique structure and vasculature that allow severe hypoxic regions to exist. Although the BM is inaccessible for noninvasive oxygen measurements, both simulation studies and qualitative measurements have demonstrated the existence of hypoxic regions.

Several theoretical models have been developed in order to simulate the distribution of oxygen throughout the BM [32, 109, 111]. Chow et al. used homogeneous Kroghian models to estimate oxygen levels in the BM [32]. Their simulations suggested that both HSCs and EPCs are exposed to low O_2 tensions in the BM. There are various possible BM architectural organizations depending on the parameters, such as the spatial arrangement of vasculature and the distribution of many different cell types populating the BM. Therefore, in the absence of supporting evidence from in vivo quantitative measurements, only model predictions can be used to assess the effects of different parameters on the O_2 tension distribution in the BM. The model by Kumar et al. considered three possible vessel arrangements to simulate oxygen level variations under various conditions [111]. They suggested that hypoxic, and even anoxic, regions could be found in the BM, assuming that the cells' oxygen consumption is constant and that the density of arterioles in the BM is low.

On the other hand, qualitative observations in the study by Parmar et al. have also demonstrated that HSCs are distributed according to oxygen availability in the BM [143]. Staining with pimonidazole and sectioning revealed the oxygen gradient throughout the BM, showing that HSCs more likely reside at the lower end of the gradient. These results are in good agreement with the in vitro studies suggesting that hypoxia supports the maintenance of stemness [35, 50, 55]. Moreover, BM transplantation studies have shown that BM-derived EPCs enhance neovascularization and the formation of arteries [191, 194]. The renewal of EPCs in the BM depends on the differentiation dynamics of HSCs, which is regulated by the microenvironments (i.e., the niches) they reside in. Osteoblasts, bone cell progenitors, bind to each other and to HSCs via adhesion molecules to form the osteoblastic niche that is located far from the sinusoidal arteries. Researchers have discovered the existence of another type of niche within the BM, the vascular niche, which is located closer to the sinusoidal arteries than the osteoblastic niche. The differences in physicochemical factors within the various niches play fundamental roles in controlling the dynamics of HSC migration and differentiation. Since the vascular niche's close proximity to arteries means that it is richer in O_2 than the osteoblastic niche. Heissnig's group hypothesized that HSCs are in a quiescent state in the osteoblastic niche's severe hypoxic conditions [74]. When vasculogenesis is necessary in neighboring tissues, specific cell signaling stimulates the migration of HSCs from the osteoblastic niche to the more oxygenated vascular niche, where

HSCs can switch from their quiescent state to a proliferative state. The proliferation and differentiation of HSCs reconstitute the EPC pool in the vascular niche before they enter the circulation.

Wound healing, another situation where hypoxia occurs, consists of a series of events that include new vasculature formation, which is regulated by varying O_2 levels. Platelets interfere with microcirculation in the wounded tissue, followed by the release of coagulation factors to reinforce the clotting process. Histamine and bradykinin, secreted by mast cells, also influence the microcirculation by enhancing vascular permeability and arteriolar vasodilation, thereby increasing the blood flow rate [7, 84]. Recruitment of leukocytes and macrophages into the damaged tissue is followed by their activation in response to several growth factors (GFs) and integrins. High rates of O_2 consumption in activated macrophages, along with perturbation of the microcirculation, leads to a further decrease in O_2 levels and results in hypoxia [87], which results in the accumulation of HIF1α at the wound site [203]. Albina et al. [5] showed that the HIF1α mRNA of inflammatory cells peaks about 6 h after injury. On the other hand, HIF1α protein levels could be detected between 1 and 5 days after wounding. More recently, Zhang et al. [203] demonstrated that, during the burn wound-healing process, the accumulation of HIF1α increases the number of circulating angiogenic cells, as well as smooth muscle actin-positive cells, in the wounded tissue. These hypoxic conditions – either directly or, through the accumulation of HIF, indirectly – stimulate angiogenesis during wound healing. Moreover, O_2 is required for ECM production, which is necessary for maturing blood vessels [84]. Therefore, the wound-healing process is finely tuned by O_2 levels, which is required not only for neovascularization to occur, but also for the fibroblasts to produce more ECM to support the newly formed vessels.

Oxygen-Sensing Mechanisms of Vascular Cells

Most cell types in the body respond to variations in O_2 tensions [192]. Gene expression, viability, metabolism, and the oxygen uptake rate of the cells change, with alterations in O_2 levels, in order to maintain homeostasis. When cells experience a difference in extracellular O_2 levels, they accord with the new conditions, which may occur immediately. Hence, O_2 sensing in cells is expected to be controlled by well-organized mechanisms.

Several mechanisms have been proposed in the literature to account for O_2 sensing in cells. Although their sensitivities may differ from one another, more than one such mechanism can coexist in a cell, resulting in various cellular responses. In the cell, the O_2 molecule mainly takes part in two distinct processes: it is involved directly in biosynthesis reactions, or it participates in metabolic processes, such as the electron transport chain occurring in mitochondria. Any change in the concentration of O_2 extensively perturbs these processes and, following a sequence of events, has a number of different effects on the cell. Therefore, O_2 sensors in cells can be mainly categorized as mitochondria-related sensors (bio-energetic) and

biosynthesis-related sensors (biosynthetic) – although they can be linked to each other in some cases, making the distinction less than completely clear [192].

Among the several effectors of O_2-sensing mechanisms, HIFs are the most essential ones in terms of the diversity of their influences. The family of HIFα subunits (HIF1α, HIF2α, and HIF3α) has been shown to be responsible for regulating a large number of gene expressions, including key regulatory proteins of angiogenesis and vasculogenesis. Although HIFα is expressed at every oxygen tension, it is rapidly ubiquitinated in normoxic conditions, resulting in its degradation. Thus, the amount of intracellular HIFα protein depends on the balance between its expression and degradation. In conditions of low O_2 availability, all HIFα proteins heterodimerize with HIFβ (ARNT) and form a transcriptional complex which regulates the transcriptions of numerous genes [129]. Stabilization of HIFα in the cell is controlled by two main O_2 sensing proteins, prolyl hydroxylase domain (PHD) and factor-inhibiting HIFα (FIH), which belong to the previously mentioned biosynthetic sensors category. Three isoforms of PHDs are present in all mammals [23]. Specific proline residues on the oxygen-dependent domain of HIFα are hydroxylated by PHDs at separate hydroxylization sites. The activity of PHDs in cytoplasm is controlled by various O_2-dependent molecular events and, directly, by the concentration of the O_2 molecule [54]. All three PHDs remain partially active in normoxia. PHD activity is expected to be very sensitive to small changes in cytoplasmic O_2 levels, since K_m, the Michaelis–Menten parameter for the activation of PHDs, is approximately 230–250 μM, which is much higher than physiological oxygen concentration (approximately 60 μM) [80]. Besides, mitochondrion is also involved in the PHD activation process through their consumption of O_2, regulation of reactive oxygen species (ROS), and production of nitric oxide (NO). While the stabilization of HIFα depends on PHD activity, the expression of HIFα is controlled by FIHs. Therefore, when O_2 levels are lowered, both the stabilization and transactivation of HIFα increase, resulting in several angiogenic responses that will be discussed in the following section.

NO and ROS not only contribute to the HIFα stabilization process, but they also have several direct effects on vascular cells and blood vessels. A number of studies have shown that NO induces angiogenesis, hyperpermeability, and vasodilation [59]. Moreover, NO also perturbs EC respiration through the inhibition of cytochrome c oxidase, which causes lower mitochondrial O_2 consumption [98]. Mitochondrial ROS are also increased as a consequence of electron transport chain inhibition, which then contributes to the deactivation of PHDs via oxidizing cofactor Fe (II) and helps to stabilize HIFα. ROS production, in respect to hypoxia, is proportional to the concentrations of intracellular O_2 and electron donors. Under hypoxia, the amount of O_2 required to form superoxides is decreased, whereas the concentration of the electron donors increases as a consequence of the reduction in the proximal electron transport chain. Therefore, ROS production can change in both manners, depending on the variations in these molecules' concentrations [192]. Ushio-Fukai and Nakamura [188] have shown that ROS influence the expression of surface adhesion molecules of

ECs and stimulate EC proliferation and vessel permeability. Moreover, the hypoxia-induced decrease in ROS production leads to the inhibition of K^+ channels of pulmonary artery smooth muscle cells (SMCs), whereas an increase in ROS production leads to intracellular Ca^+ release from ryanodine-sensitive stores [192]. Another molecular path found between mitochondrial energy generation and K^+ channel inhibition occurs through AMP kinases. The energy of the cell is generated by the conversion of ADP to one molecule of ATP and AMP. Hence, AMP kinase becomes highly dependent on the ADP/ATP ratio, which is very sensitive to changes in cytoplasmic O_2 concentrations. AMP kinases were shown to inhibit K^+ channels through the regulation of Ca^+ release in pulmonary arterial SMCs and also to induce cellular survival in tumor cells when exposed to severe hypoxia [49, 140].

Moreover, heme oxygenases (HOs) and NADPH oxidases (NOXs) play important roles in the biosynthetic oxygen sensing of cells. NOX-2, one of the three isoforms of NOX, is used for superoxide production from molecular O_2. Hypoxic conditions can cause a decrease in NOX-2-derived ROS concentrations, due to the low K_m values (18 μM) of NOX-2; this helps Ca^+ release in pulmonary artery SMCs [197]. However, some studies also suggest that hypoxia increases NOX-2 activity, therefore causing the generation of a greater amount of ROS [192]. On the other hand, Ca^+-activated K^+ channels in glomus cells were shown to be related to the activity of HO-2, an isoform of HO which can convert heme to CO, biliverdin, and Fe (II) using O_2 and NADPH [196].

The effectiveness of an oxygen sensor can be determined by evaluating (a) its sensitivity to small changes in intracellular O_2 levels and (b) the subsequent diversity of triggered cellular responses. Comparing the activities of O_2 sensors, FIHs and PHDs have much lower affinity to O_2 than the others, which causes dramatic decreases in their activities in respect to lowered O_2 concentrations [76]. Deactivation of these two sensors leads to HIFα stabilization, initiating the regulation of hundreds of different genes. Using O_2 as a controlling parameter to engineer vascular tissues demands a clear understanding of the biochemical events that follow changes in O_2 tension, as well as the net response of the cells and how O_2 affects their collective behaviors.

7.2.1.2 Cellular Responses to Different Oxygen Concentrations

Metabolism and Oxygen Uptake Rate

Several studies have observed that the O_2 consumption of cells depends on O_2 availability [1, 21, 140, 173]. We have recently shown that the O_2 uptake rates (OURs) of EPCs and human umbilical vein endothelial cells (HUVECs) are similar, but not identical, to each other and that both decrease when O_2 availability is lowered (Fig. 7.1a) [1]. Many mechanisms have been proposed to explain the relation between mitochondrial O_2 consumption and variations in O_2 levels. HIF1α was

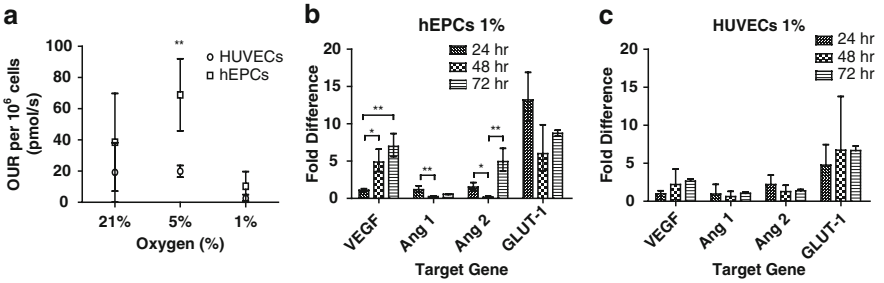

Fig. 7.1 O_2 tension regulates vascular cell responses. Comparison of EPCs and HUVECs at three different O_2 tensions in terms of (**a**) oxygen uptake rate (OUR) and (**b**, **c**) gene regulation [1]

found to be responsible for inducing the enzymes required for glycolysis [140]. It also plays a role in activating pyruvate dehydrogenase kinase-1, which reduces the amount of pyruvate that flows into the TCA cycle and therefore decreases aerobic respiration in mitochondria [140]. In addition, the increases in both the transcription and expression of glucose transporter protein 1 (GLUT-1) were shown to be HIF1α-dependent in hypoxic conditions [3]. In other words, deactivation of PHDs and FIHs at low O_2 levels leads to the stabilization of HIFα, which then reduces O_2 aerobic respiration by inducing pyruvate degradation but, at the same time, promotes glycolysis by increasing the expression of glucose transporter proteins. Another proposed mechanism involves the inhibition of cytochrome oxidase by NO, which is known to be regulated by shear stress and O_2 tension. NO influences mitochondrial respiration by the competitive inhibition of cytochrome oxidase with O_2 and by inhibiting electron transfer between cytochrome b and c, therefore increasing ROS production [21].

The effects of blood flow and O_2 tension are crucially important for the ECs comprising the vessel walls, since these conditions can be perturbed in many situations in the body. Some studies have shown mitochondrial respiration of ECs to be lower than other cell types, and most of the O_2 consumption is nonmitochondrial [63, 186]. Helmlinger et al. demonstrated that ECs consume O_2 during capillary formation, whereas they also preserve and expand the capillary structures even under severe hypoxia (about 0.6% O_2) by upregulating VEGF expression [75]. It is not surprising that ECs possess a special type of metabolism – aerobic glycolysis in their resting state (physiological conditions) and anaerobic glycolysis in their navigating state (hypoxic conditions) – since O_2 is transported through ECs to other tissues and they should survive and commence angiogenesis under hypoxic conditions [56].

Moreover, when ECs are exposed to excess glucose, their ATP generation shifts to glycolysis, and lactate levels, increased as a by-product of glycolysis, contribute to the inactivation of PHDs and, therefore, the stabilization of HIFα [198]. Where blood flow is perturbed, such as in ischemia and wound healing, both NO and O_2 levels are changed in blood vessels, and all of the metabolic variations discussed above gain more importance.

Transcription of Angiogenic Genes

Manalo et al. have shown in their study of ECs that 245 genes are upregulated and 325 genes are downregulated at least 1.5-fold in response to hypoxia and HIF1α [129]. These genes are responsible for the expression of collagens, GFs, receptors, and transcription factors, all of which are very significant for angiogenesis/vasculogenesis processes. This wide range of hypoxia-related transcription factors also indirectly affects HIF1α. The genes directly regulated by HIF1α include VEGF-A, VEGFR-1, Flt1-1, and erythropoietin (EPO). Examples of indirectly regulated genes include fibroblast growth factor (FGF); placental growth factor (PLGF); platelet-derived growth factor (PDGF); angiopoietins (ANG-1 and 2); and Tie-2, the receptor of ANGs [54]. Although VEGF is the major GF that stimulates blood vessel formation, when it alone was transgenically overexpressed in mice, defective blood vessels formed, which then led to tissue edema and inflammation [152]. On the other hand, overexpressing both VEGF and ANG-1, which is important for maintaining vascular integrity, has been shown to induce hypervascularity without imperfections in mice [181]. ANG-2 is responsible for EC apoptosis and vascular regression in the absence of VEGF, whereas, when combined with VEGF expression, it enhances angiogenic responses by destabilizing the blood vessels [82, 83]. More recently, ANG-4 was shown to function similarly to ANG-1 and to induce angiogenesis by binding the ANG receptor TIE-2, which is also upregulated by HIF1α [199]. We have recently shown that VEGF and ANG-2 genes are upregulated in hypoxic (1% O_2) cultures of EPCs and HUVECs [1], and the fold differences in upregulation levels of VEGF and ANG-2 in EPCs were shown to vary during the 3-day exposure period (Fig. 7.1b), where no significant change was observed for HUVECs (Fig. 7.1c). How hypoxia affects the regulation of these angiogenic genes depends on the cell type; for instance, VEGF is upregulated in ECs, SMCs, cardiac fibroblasts, and myocardiocytes, whereas ANG-2 is induced only in ECs [129]. Therefore, from a tissue engineering perspective, coculturing of different cell types under controlled hypoxic conditions should be considered, since a combination of hypoxia-induced angiogenic proteins is required to obtain vascular formation without excessive permeability.

Cell Death and Survival

Hypoxia influences the proliferation and viability of many cell types [1, 55, 141, 202]. The wide spectrum of HIF1α-dependent genes also includes proapoptotic and prosurvival genes. BH3-only proapoptotic genes, a subfamily of BCL-2 that includes BNIP3, BNIP3L, NOXA, RTP801, HGTP-P, are directly activated by HIF1α [193]. Although these genes play important roles in cellular apoptosis, a growing body of evidence suggests that hypoxia mediates cellular survival in many cell types [130, 141, 202]. Programmed cell death is, of course, a very critical step for cells and is most likely taken only after all possible survival mechanisms have been exhausted. One of these mechanisms, autophagy, is a cellular catabolic process

where cytoplasmic organelles are degraded to provide ATP generation in nutrient deprivation. Hypoxia was found to induce mitochondrial autophagy via both HIF1α-dependent and HIF1α-independent pathways [141, 202]. Small-interfering RNA silencing of BNIP3 and BNIP3L together suppresses autophagy to a greater extent than silencing only one of them at a time [16]. Zhang et al. have shown that mitochondrial autophagy is induced by HIF1α-dependent upregulation of BNIP3 incorporated into the constitutive expression of BECLIN-1 and ATG-5 [202]. On the other hand, the neuron-derived orphan receptor (NOR-1), which is overexpressed in ECs exposed to hypoxia, mediates cellular survival as a downstream effector of HIF1α signaling [130]. CD105, one of the EC markers, also shown to play a role in cellular survival, is significantly upregulated under hypoxia [118]. In vivo studies of rats subjected to hypoxia also found the induction of mitochondrial autophagy by overexpression of BNIP3 [13]. In addition, Papandreou et al. have proposed that hypoxia induces autophagy in tumor cells through AMP kinase, which is activated by hypoxia independently of HIF1α, as discussed previously in the O_2 sensing section [141].

Cell Pluripotency and Differentiation

Vasculogenesis takes place in low O_2 environments, such as the early development of embryo, EPC regeneration in the BM, or EPC attachment and differentiation into mature ECs at neovascularization sites. All of these processes rely on pluripotent/unipotent cells differentiating into the endothelium, where O_2 tension is a crucial parameter regulating their differentiation characteristics. More particularly, as already discussed, EPC regeneration in the BM depends on cellular dynamics between the osteoblastic niche (low O_2) and vascular niche (high O_2); HSCs are quiescent in the osteoblastic niche and differentiate into EPCs in the vascular niche before joining the circulation [91]. Therefore, it is important to understand the effect of O_2 tension on the differentiation of cells into EPCs/ECs as a primary step of vasculogenesis. Hypoxia enhances human embryonic stem cell (hESC) pluripotency via the upregulation of Oct-4, NANOG, and SOX-2, which are pluripotent markers [35, 50, 55, 96]. HIF2α was shown to be responsible for the overexpression of Oct-4, SOX-2, and NANOG, while HIF3α also plays a role in the process by inducing HIF2α transcription [35, 55]. Prasad et al. demonstrated that hypoxic conditions (5% O_2) prevent the spontaneous differentiation of hESCs, whereas the inhibition of Notch activation revoked this effect, suggesting that hypoxia-induced pluripotency occurs via Notch signaling [150]. On the other hand, the efficiency of the process of reprogramming mouse and human somatic cells into induced pluripotent stem cells (iPSC) was shown to be improved in 5% O_2 cultures compared to atmospheric O_2 cultures [200]. In contrast, other studies have demonstrated that hypoxia induces the expression of early cardiac genes in spontaneously differentiating embryoid bodies (EBs) [104, 138]. In a more recent study, Prado-Lopez et al. showed that EPCs/ECs can be obtained from hESCs more efficiently when cultured in 5% O_2 compared to previous methods that induce EB formation

in atmospheric O_2 [149]. On the other hand, HIF1α induces the differentiation of peripheral blood mononuclear cells into EPCs, and hypoxia stimulates the further differentiation of EPCs into mature ECs [4, 97].

All of these findings have highlighted the significance of O_2 tension as a critical parameter to control vascular differentiation of pluripotent cells. Although some of these studies suggest contrary hypotheses, they all agree on the induction of pluripotent markers by HIF2α and the upregulation of angiogenic factors by HIF1α. Therefore, O_2 tension can be manipulated to prevent spontaneous differentiation of pluripotent cells and to enhance the efficiency of the differentiation into EPCs and mature ECs.

7.2.2 Vascular Responses to ECM

In the human body, vascular cells are surrounded by diverse components of the ECM, the unique spatial and temporal distribution of which affects GF availability and matrix properties which, in turn, regulate vasculogenesis and angiogenesis. Just like oxygen tension, which varies throughout vascular development, ECM components are also uniquely distributed; for example, hyaluronic acid (HA; also known as hyaluronan) levels were found to be highest during embryogenesis and to be replaced by fibronectin and then collagen, which remains abundant throughout adulthood. The first part of this section will discuss ECM distribution and its effects on vascular development and maintenance. Then, the second part will discuss various ECM components that affect vascular morphogenesis. Lastly, we will describe strategies for manipulating the ECM using synthetic biomaterials and emerging technology.

7.2.2.1 Types of ECM Found Participating in Vascularization

The ECM surrounding blood vessels contributes significantly to their diverse functions and complexity. This ECM diversity encompasses different vascular development periods (i.e., embryonic vs. adult) and specialized vessels at various location of the body (i.e., capillary, arteriole, and venule). During early vascular development, the ECM provides informational cues to the vascular cells, thus regulating their differentiation, proliferation, and migration. Fibronectin and HA, which are major components of the embryonic ECM, have been shown to be vital regulators for vascularization during embryogenesis [185]. Fibronectin, a unique glycoprotein, contains cell adhesion and heparin-binding sites that synergically modulate the activity of VEGF to enhance angiogenesis [195]. Various lineage studies have found developmental abnormalities in embryonic hearts and vessels in fibronectin-null mice, suggesting its crucial role in mediating EC interactions [10, 57]. The levels of hyaluronan, a nonsulfated linear polysaccharide, are greatest during embryogenesis and then decreases at the onset of differentiation [184], where it

plays a crucial role in regulating vascular development [14]. Hyaluronan and its receptor, CD44, have been shown to be essential in the formation and remodeling of blood vessels [14, 25, 48]. We have previously reported that a completely synthetic HA hydrogel can maintain the self-renewal and pluripotency of hESCs [65, 70]. Interestingly, when VEGF is introduced into the culture media, this unique HA microenvironment can direct the differentiation of hESCs into vascular cells, as indicated by positive staining for α-smooth-muscle-actin and an early stage of the endothelial cell marker CD34 (Fig. 7.2a).

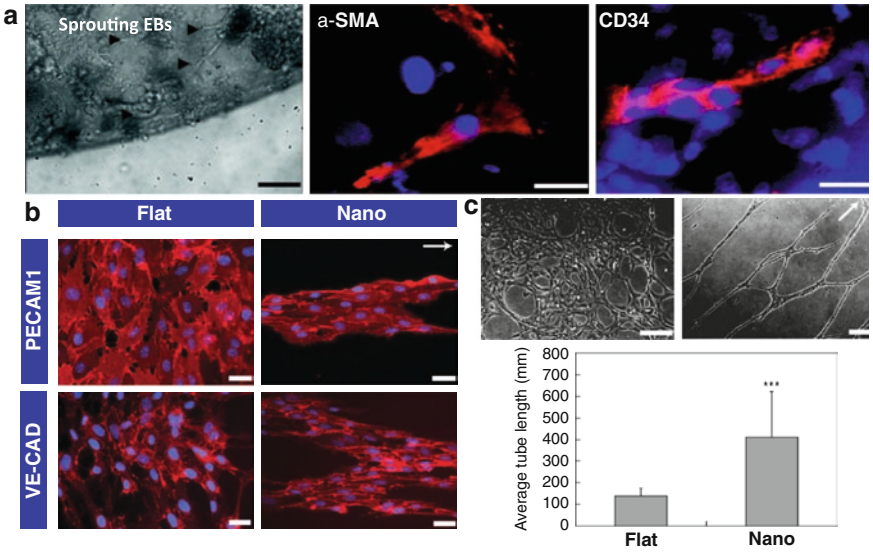

Fig. 7.2 Matrix composition and orientation affect vasculogenesis. (**a**) Hyaluronic acid microenvironment for vasculogenesis. Human ESC colonies were cultured in conditioned medium for 1 week, followed by the replacement of medium containing 50 ng/ml $VEGF_{165}$. *Left*: Cell sprouting was observed after 48 h of culture in medium containing VEGF (indicated by *arrowheads*). *Middle and right*: After 1 week of differentiation, sprouting elongating cells were mainly positive for v-SMC actin (*middle*), while some were positive for the early-stage endothelial marker CD34 (*right*). Scale bars – *left*: 100 μm; *middle* and *right*: 25 μm. Printed with permission [65]. (**b**) Nanotopography induces the formation of supercellular band structures in long-term EPC culture. EPCs cultured on flat substrates began forming confluent layers of cells after 6 days of culture. In contrast, EPCs cultured on nanotopography began to form supercellular band structures aligned in the direction of the features (as indicated by the *arrow*) after 6 days of culture. These morphological differences are evident through staining of PECAM-1 and VE-CAD. Scale bars are 50 μm. Printed with permission [19]. (**c**) Organized capillary tube formation in vitro. Capillary-like structures (CLSs) were induced by the addition of Matrigel after 6 days. EPCs cultured on flat substrates (*upper left*) formed low-density unorganized structures, while EPCs cultured on nanotopographic substrates (*upper right*) formed extensive networks of organized structures with (*lower panel*) longer average tube lengths than EPCs cultured on flat substrates (***$p < 0.001$). The direction of the linear nanotopographic features is indicated by the *arrow*. Scale bars are 200 μm. Printed with permission [19]

In contrast, the adult ECM consists mostly of laminin-rich basement membrane, which maintains the integrity of the mature endothelium, and interstitial collagen I, which promotes capillary morphogenesis [40]. Although collagen I is present during development, its role becomes increasingly important in postnatal angiogenesis after its reactive groups have been cross-linked to further stabilize the interstitial matrix [153]. EC integrins, which interact with collagens and fibrin, are key receptors in EC activation, proliferation, and tubular morphogenesis. The collagen-I-mediated activation of Src and Rho and the suppression of PKA promote the formation of prominent actin stress fibers, which mediate EC retraction and capillary morphogenesis. Moreover, the activation of Src also disrupts VE-cadherin from cell junction and cell–cell contact which, in turn, facilitates multicellular reorganization. On the contrary, basement membrane laminin-1 responsible in maintaining mature endothelium. During the proliferative stage of morphogenesis, the laminin-rich basal lamina is degraded, exposing the tips of sprouting ECs to the underlying interstitial collagens and activating signaling pathways that drive cytoskeletal reorganization and vascular morphogenesis. This sharp difference in how ECM components affect capillary morphogenesis is responsible for controlling the delicate balance between vascular sprouting and maturation.

Once nascent vessels are formed, ECM components regulate their maturation and specialization into capillaries, arteries, and veins. Capillaries, the most abundant vessels in our body, consist of ECs surrounded by pericytes and basement membrane. Exchanges of nutrients and oxygen occur through diffusion between blood and tissue in these regions, due to the capillary's thin wall structure and large surface-area-to-volume ratio. Maturation of the vessel wall involves the recruitment of mural cells, development of the surrounding matrix, and organ-specific specialization [93]. ECM distribution in various tissues dictates the specialization of these capillaries to support the functions of specific organs. The capillary endothelial layer is continuous in most tissues (e.g., muscle), while it is fenestrated in exocrine and endocrine glands (e.g., kidney and pancreas). Moreover, the enlarged sinusoidal capillaries of the liver, spleen, and BM are discontinuous, allowing increased exchanges of hormones and metabolites between the blood and the surrounding tissues. In contrast, where the excess exchange of molecules is not desirable, such as at the blood–brain barrier and the blood–retina barrier, the interendothelial connection is further reinforced with tight junctions.

Compared with capillaries, arterioles and venules have an increased coverage of mural cells and ECM components. Arterioles are completely surrounded with vascular SMCs that form a closely packed basement membrane. The walls of larger vessels are composed of three layers: the tunica intima, the tunica media, and the tunica adventitia. The EC layer of blood vessels is anchored on a basement membrane, which is the major component of the tunica intima [44]. The basement membrane contains network-organizing proteins, such as collagen IV, collagen XVIII, laminin, nidogen, entactin, and the proteoglycan perlecan. The tunica media contains vascular SMCs (v-SMCs) and elastic tissue composed of elastin, fibrillins, fibulins, emilins, and microfibril-associated proteins. The tunica adventitia contains fibroblasts and elastic laminae and has its own blood supply, known as the vasa

vasorum [44]. SMCs and elastic laminae contribute to the vessel tone and regulate vessel diameter and blood flow. This generic blood vessel architecture is modified with various ECM components to fulfill their individual tasks. Arteries, which function to deliver oxygenated blood, usually have a thick tunica media with numerous concentric layers of v-SMCs, whereas veins have a thick tunica adventitia layer enriched in ECM components with elastic properties, such as elastin and fibrillin.

7.2.2.2 Properties of the ECM that Affect Vascular Morphogenesis

Recent decades have vastly expanded our understanding of how ECM properties affect vascular assembly, primarily due to newly available, well-defined in vitro models. The most common models are cultures of ECs in gels made of different ECM components, such as collagen, fibrin, fibronectin, and Matrigel. These ECM components contain instructive physical and chemical cues that direct vascular morphogenesis, which involves several steps (1) proteolytic degradation of basement membrane proteins by both soluble and membrane-bound matrix metalloproteinases (MMPs); (2) cell activation, proliferation, and migration; (3) vacuole and lumen assembly into a tube with tight junctions at cell–cell contacts; (4) branching and sprouting; (5) synthesis of basement membrane proteins to support the formation of capillary tube networks; and (6) tube maturation and stabilization by pericytes. Apparently, these complex processes require a delicate balance between various immobilized factors and soluble GFs, as well as endothelial and prevascular cell interactions. Gels made from ECM components, engineered to have properties resembling those of native tissues, have been widely explored as a tool to study the molecular regulation underlying vascular development [39] and as a scaffold to transplant vascular progenitor cells [12, 36, 134]. However, their manipulation for vascular tissue engineering has been narrowly limited by their inherent chemical and physical properties. Therefore, a great need exists to chemically modify these ECM components [31, 108] or to utilize biomaterials to form scaffolds from hydrogels, which are xeno-free and instructive for vascular tissue engineering [123]. Hydrogels are cross-linked polymer networks which can store a large amount of fluid and which have biophysical properties similar to many soft tissues [113]. Hydrogels can be engineered from natural biomaterials (excluding ECM components), artificial protein polymers, self-assembling peptides, and synthetic polymers to form scaffolds which mimic the native ECM. For example, dextran and chitosan, natural biomaterials with similar structures, do not possess any inherent cross-linking ability [177, 178]. However, a simple chemical modification, like introducing double bonds into the repeating unit, allows the cross-linking of these polysaccharides to form hydrogels. Alginate is another natural material which can be physically cross-linked by adding cations (e.g., Ca^{2+} or Mg^{2+}) [64]. Another approach utilizes a purely synthetic polymer, like polyethylene glycol (PEG) or poly-[lactic-co-glycolic acid] (PLGA), whose physical and chemical properties can be easily manipulated. A simple modification can turn PEG, a cell-resistant material, into instructive scaffolds that promote

vascularization [45, 46, 136, 144]. Furthermore, the synthetic material of choice must be biodegradable and biocompatible, and such physical properties as pore size, degradation kinetics, and elasticity must be easily tunable to favor vascular morphogenesis. Bioactive molecules – like GFs, arginine–glycine–aspartic acid (RGD), and MMP-sensitive peptides – must be presented with correct spatial and temporal distributions within the synthetic biomaterials. Such physical properties of the scaffolds as matrix elasticity, pore size, and orientation must be tuned to favor vascular morphogenesis. Next, we will discuss several strategies for manipulating the chemical and physical properties of synthetic biomaterials.

Cell Adhesion Regulates Neovascularization

In order to support vascular cells and instruct them to undergo vascular morphogenesis, synthetic biomaterials must first be able to provide cell adhesion. Instead of incorporating ECM components to make such materials bioactive, certain synthetic peptides important for vascular morphogenesis can be incorporated into these inert synthetic materials. The most common template is the integrin-binding domain of fibronectin, RGD [146], and the laminin-derived peptide IKVAV [168]. The first crucial step in vascular morphogenesis occurs when vascular cells utilize integrin receptors to sense their surrounding microenvironments. Integrin is a transmembrane receptor which not only maintains cell adhesion to ECM but also controls cell proliferation, migration, differentiation, and cytoskeletal organization. Since blood vessels must be able to assemble in diverse tissue environments (e.g., adult vs. embryo and muscle vs. kidney) which have different distributions of ECM components (as discussed in the previous section), it is evident that both β and α integrins can support vascular morphogenesis. For example, $\alpha_1\beta_1$ and $\alpha_2\beta_1$ integrins associate with vascular morphogenesis in collagen-rich ECM, like adult tissue, while $\alpha_5\beta_1$ and $\alpha_v\beta_3$ integrins involve fibronectin- and fibrin-rich ECM, like in embryonic tissue and healing wounds [40]. Regardless of the types of integrin involved, the binding of integrins onto RGD triggers several downstream signaling events mediated by Rho GTPase, particularly Rac1 and Cdc42 [39]. Extensive work by Davis and his colleagues has revealed the molecular mechanism that regulates this EC morphogenesis in fibrin and collagen gels (an excellent review of their work can be found in Chapter 2 of this book).

The number of RGD adhesion sites and the method of their presentation to the vascular cells are also crucial in affecting cell migration [67] and vascular morphogenesis [90]. Using an in vitro angiogenesis model, Folkman and Ingber were able to show that, when cultured on a moderate coating density that only partially resisted cell traction forces, ECs could retract and differentiate into branching capillary networks [53, 90]. High ECM density was saturated with RGD adhesion peptide, which allowed the ECs to spread and proliferate, while low ECM density resulted in rounded and apoptotic cells. Interestingly, in medium ECM density, with the appropriate RGD adhesion peptide, ECs collectively retracted and differentiated into branching capillary networks with hollow tubular structures. It is evident that

ECs exerted mechanical forces on the surrounding ECM to create a pathway for migration and branching in forming vascular structures [38]. Hence, both the quantity of RGD peptide and the method of presentation within the engineered synthetic biomaterials determine the initial morphogenetic events in angiogenesis.

Scaffold Degradation Regulates Vascular Morphogenesis

Scaffolds made from ECM components, like collagen and fibrin gels, contain proteolytic degradable sequences, which can be degraded by the MMPs secreted by vascular cells. This cell-mediated degradation controls both structural integrity and temporal properties, which dictate the presentation of chemical and mechanical cues at various stages of angiogenesis. However, the degradation kinetics of these ECM-based scaffolds is determined by their inherent cross-linking density which, in turn, limits their manipulation for vascular tissue engineering. In contrast, the synthetic biomaterials can be engineered to have degradation profiles ranging from days to months in order to suit the specific needs of the engineered vascularized tissue constructs [178]. The polymer backbone can be cross-linked using a nondegradable cross-linker that provides structural integrity and/or a degradable cross-linker that allows directed cell migration and vascular morphogenesis. Hydrolytic degradation by the body fluid can break down the ester bonds within the polymer backbone, allowing tissue infiltration over time [177, 178]. MMP-sensitive peptides can also be used to cross-link hydrogels, allowing cell-mediated degradation, leading to a rapid response of vascular growth. Overall, by adjusting the percentages of nondegradable and degradable cross-linkers, scaffold degradation can be tuned to allow cellular infiltration, lumen formation, and ECM synthesis and distribution.

In order for the intracellular vacuoles to coalesce into a lumen, ECs require adhesive ligands for traction [123] and utilize membrane-type-1-MMPs (MT1-MMPs) to create physical spaces which facilitate the directed migration of cells to align with neighboring cells [38, 157, 175]. Therefore, ECs can only invade this synthetic scaffold if the minimal pore size is larger than the cell diameter (e.g., a soft self-assembling peptide) [166] or if the scaffold bears an MMP-degradable sequence [124]. The Hubbell research group has pioneered this approach by incorporating an MMP-degradable sequence as a cross-linker into PEG scaffolds to promote vascular healing and therapeutic angiogenesis [161, 205]. When grafted in vivo, ECs were able to invade, remodel, and vascularize this MMP-sensitive scaffold [205, 206]. Hence, incorporating MMP-degradable peptides is essential for directing vascular morphogenesis in 3D synthetic biomaterials.

Physical Orientation of the ECM

The native ECM provides an instructive template for ECs and perivascular cells to orient, interact, and organize into tubular structures. Studies have demonstrated that a stable vasculature could be achieved by cotransplantation of ECs and perivascular

cells, such as MSCs or SMCs [11, 12, 106, 116, 134]. Recent studies further showed that engineering a stable vascularized tissue construct required the triculture of ECs, fibroblasts, and tissue-specific cells, such as cardiac or skeletal muscle cells [26, 72, 116]. Perivascular cells, such as fibroblasts, stabilize the developing vascular tube through both physical support, by differentiating into v-SMCs and wrapping around the nascent tube [94] [189], and chemical support, by secreting Ang-1, PDGF-BB, and tissue inhibitor of metalloproteinase-3 (TIMP-3) [77, 79]. These perivascular cells are also responsible for laying down ECM components in early embryogenesis and continue to do so throughout adulthood. Many studies using fibroblast-derived matrices have further revealed the 3D complexity of these ECM networks [169–171]. A recent study by Soucy and Romer showed that fibroblast-derived matrix alone is sufficient to induce HUVECs to undergo vascular morphogenesis independent of any angiogenic factors. Further analysis of protein colocalization suggested that fibronectin with a distinct structure and organization was uniquely distributed among other secreted matrix components, such as collagen, tenascin-C, versican, and decorin. Cell matrix adhesions and MT1-MMP activities were reported to orient and localize within this fibrous fibronectin, which is indicative of integrin-mediated vascular morphogenesis [156]. In fact, ECs initiate neovascularization by unfolding soluble fibronectin and depositing a pericellular network of fibrils that serve as a structural scaffolding on a mechanically ideal substratum for vessel development [204].

The unique orientation, organization, and nanotopography of fibrous fibronectin represent features that can be integrated into synthetic scaffolds. Synthetic polymers, like PLGA and polycaprolactone (PCL), can be electrospun to produce various fiber sizes with micro- to nanoscale features that resemble fibrous fibronectin. We have previously shown that surface nanotopography enhanced the formation of capillary-like structures (CLSs) in vitro [19]. Growing EPCs on grooves that were 600 nm wide reduced their proliferation and enhanced their migration without changing the expression of EC markers. Moreover, after 6 days of culture, the EPCs organized into superstructures along the nanogrooves, in significant contrast to the EPCs grown on planar surfaces (Fig. 7.2b). The addition of Matrigel further induced the formation of CLSs, with enhanced alignment, organization, and tube length compared to a flat surface (Fig. 7.2c). This underscores the increasingly important role of nanotopography in guiding and orienting vascular assembly. When integrated into the tissue-engineered construct – for instance, using filamentous scaffold geometry [60] and micropatterning [88, 135] [42] – the orientation and structure of the engineered vasculature can be controlled.

Regulating Matrix Mechanics

It has become increasingly evident that the biomechanical properties of the ECM, such as matrix orientation and mechanics, profoundly influence the control of vascular morphogenesis. Due to its versatility and mechanical properties (e.g., cross-linking density, pore sizes, and topography), synthetic biomaterials

have powerful features that can be exploited to further direct vascularization. Changes in ECM mechanics can lead to focal changes in GF availability [31, 90], drive capillary morphogenesis [89], and stimulate angiogenesis in vivo [101]. By altering matrix adhesivity and mechanics, Ingber and Folkman illustrated how bFGF-stimulated ECs can be switched between growth and differentiation during angiogenesis [90]. Recently, biomechanical cues from the ECM and signals from GF receptors have been implicated as regulating the balance of activity between TFII-I and GATA2 transcription factors, which govern the expression of VEGFR2 to instigate angiogenesis [128]. Matrix stiffness not only regulates the cell's response to soluble GFs, but also cell morphogenesis during angiogenic sprouting. Primarily due to MMP activity, the tip of a new capillary sprout has been found to become thinner, locally degrading the basement membrane proteins. This region, with its high rate of ECM turnover and thin basement membrane, becomes more compliant and stretches more than the neighboring tissue. Consequently, the decrease in matrix stiffness changes the balance of forces across the cell integrin receptors, increases cell tension, and results in cytoskeletal arrangement to form branching patterns that are characteristic of all growing vascular networks [89].

The pioneering work by Deroanne et al. showed that a decrease of matrix stiffness increased capillary branching and the elongation of tubes. A reduced tension between ECs and ECM, accompanied by a profound remodeling of the actin–FAP complex, is sufficient to trigger an intracellular signaling cascade leading to tubulogenesis [41]. This observation has been further confirmed in collagen gels [41, 165], fibrin gels [174], self-assembling peptides [166], and HA-gelatin hydrogels [71].

Although ECM-based gels, such as collagen, fibrin, and Matrigel, have been widely used in angiogenesis assays, their inherent physical properties have limited their usage to study the effects of matrix mechanics on angiogenesis. The stiffness of ECM-based gels can be increased either by increasing their concentration, which also alters their ligand and fibril density [155], or by altering the cross-linking of ECM proteins in a narrow range using a microbial transglutaminase [201]. Therefore, examining the effects of matrix stiffness alone on angiogenesis requires the use of synthetic hydrogels, the stiffness of which can be easily adjusted over a wide range of moduli without altering other chemical properties. Unlike naturally available ECM-based gels, the elasticity of which is limited to their inherent cross-linking density, synthetic HA-hydrogels can be used to study a physiological relevant range of matrix elasticity [71]. When the cross-linking density of the HA-gelatin hydrogels was further reduced, the matrix elasticity became relatively compliant, resulting in an increase of capillary branching, elongated tubes, and enlarged lumen structures [71]. On a relatively compliant matrix, EPCs can produce fewer MMPs than a stiffer matrix would require and still degrade, exert mechanical tension on, and contract the matrix to enable vascular morphogenesis. On the other hand, on a stiffer matrix, EPCs must produce more MMPs to overcome the extra mechanical barriers; even then, this local decrease in substrate stiffness cannot support vascular morphogenesis (Fig. 7.3) [71]. This model also explains the rapid appearance of large functional vessels in granulation tissue as a response to the wound-healing mechanism [101].

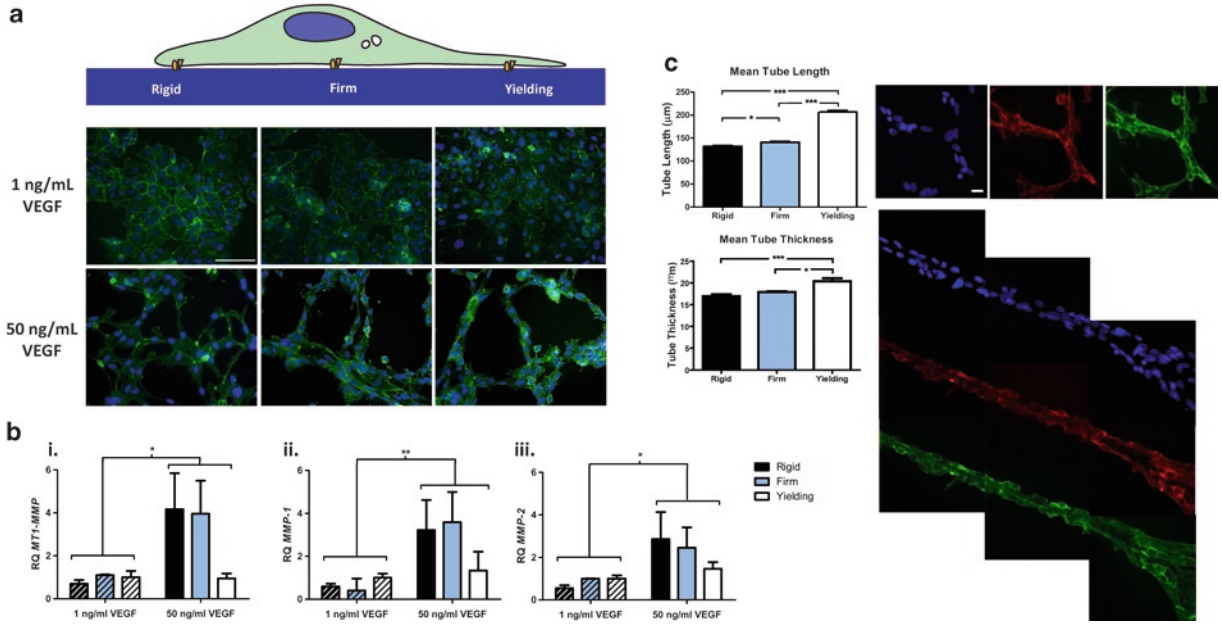

Fig. 7.3 Mechanoregulation of vascularization. (**a**) EPCs were seeded on rigid, firm, and yielding substrates for 12 h, supplemented with 1 ng/ml (low) VEGF (*upper panel*) and formed CLSs when supplemented with 50 ng/ml (high) VEGF (*lower panel*), as demonstrated by fluorescence microscopy of F-actin (*green*) and nuclei (*blue*). (**b**) Real-time RT-PCR revealed a significantly increased expression of (**i**) MT1-MMP, (**ii**) MMP-1, and (**iii**) MMP-2 in response to 50 ng/ml VEGF (high) concentration for EPCs cultured on the rigid, firm, and yielding substrates, respectively. As the matrix substrate was reduced, EPCs cultured in medium supplemented with 50 ng/ml (high) VEGF showed a decrease in expression of these MMPs. (**c**) Metamorph analysis of CLSs revealed a significant increase of mean tube length and mean tube area as substrate stiffness decreased. Confocal analysis of nuclei (*blue*), VE-CAD (*red*), and lectin (*green*) further revealed that branching and hollow tubular structures formed on the yielding substrate. Significance levels were set at $*p<0.05$, $**p<0.01$, and $***p<0.001$. Scale bars (**a**) 100 μm and (**c**) 20 μm. Printed with permission [71]

These studies underline the importance of engineering a tissue construct with the correct matrix stiffness to promote in vivo vascularization. However, investigating how matrix stiffness may affect in vivo vascularization remains challenging due to the complexity of the system, which involves matrix remodeling, host capillary ingrowth, as well as anastomosis of the vascular construct. In vivo vascular ingrowth into Matrigel scaffolds was found to be optimal at intermediate matrix stiffness, in sharp contrast to the observed in vitro ingrowth [128]. Recent elegant work by Yoder's research group also found that increasing the collagen concentration yielded stiffer scaffolds, which, in turn, promoted host capillary ingrowth in vivo. Compared to stiffer scaffolds, the softest scaffolds might have experienced excessive in vivo remodeling and failed to retain the vascular constructs. Moreover, in vitro angiogenesis studies have found that ECM-based gels produced a much narrower range of stiffness [36, 128] than synthetic hydrogels [71, 128, 166]. Future investigations are needed to evaluate vascularization by both the host capillary and the engineered vascular construct over a wider range of physiologically relevant matrix elasticities. Despite the differences in scaffold composition (ECM-based gels vs. synthetic hydrogels), culture conditions (in vitro vs. in vivo), assay type (2D vs. 3D), and ranges of matrix stiffness, all of these studies highlighted the relevance of engineering scaffolds with mechanical elasticity suited to the specific needs of tissue vascularization.

7.2.3 The Effects of Oxygen Availability and the ECM

This section will consider O_2 tension and the ECM as two interdependent factors determining the efficiency of vasculature formation. First, it will review currently available O_2 measurement techniques and challenges, along with the mathematical modeling approaches used to overcome some of these challenges in describing O_2 gradients in 3D environments. Then, the second part will discuss cellular adaptations and responses to O_2 availability in 3D ECM constructs and the possible outcomes of variations in O_2 distribution in 3D cultures of vascular cells.

7.2.3.1 Varying Oxygen Tensions in the ECM of Tissue and Matrix Scaffolds: Measuring and Modeling

Oxygen Measurement Techniques and Challenges

Manipulation of oxygen in order to direct pluripotent or vascular cells to form blood vessels requires knowing the precise O_2 tension that the cells are exposed to under varying conditions. Many different O_2 measurement techniques have been used in vitro and in vivo. The accuracy of these measurements is fundamental to describe the cellular responses under various O_2 availabilities, as well as to controlling the O_2 tension in order to direct angiogenesis/vasculogenesis. An O_2 measurement

method needs several properties to be considered superior, including accuracy, sensitivity, repeatability, rapidity, and noninvasiveness. Although some methods are used more commonly in a broader range of applications, no "gold standard" exists for all applications, since the method chosen usually depends on the purpose of the measurement. In vivo O_2 measurements can be divided into two main categories (1) direct measurements, where the concentration or the partial pressure of O_2 is directly measured and (2) indirect measurements, where levels of O_2-indicative molecules (e.g., hemoglobin, cytochrome) are detected and correlated to relative O_2 concentrations.

The most common direct measurements are electrodes, phosphorescent probes, electron paramagnetic resonance (EPR) oximetry, and nuclear magnetic resonance (NMR). Some of the indirect measurement methods involve monitoring of hemoglobin/myoglobin, mitochondrial cytochromes, and NADH/FADH [172]. Springett's paper thoroughly reviews the benefits and limitations of the most recent methods [172].

In addition, in vitro studies have applied these currently available methods to monitor O_2 levels quantitatively, such as by measuring O_2 tensions at the cellular level in 2D monolayer cell cultures or O_2 gradients in 3D gels or scaffolds. Two major methods used to measure O_2 levels during in vitro cultures are polarographic and fluorescence quenching techniques. The latter has been shown to surpass the polarographic technique, which consumes O_2 during the measurements [162]. When the implemented measurement technique, like the polarographic technique, consumes O_2, it more likely generates even greater inaccuracies and leads to incorrect conclusions in low O_2 environments, as occurred in the studies investigating the effect of hypoxia in 3D scaffolds [28, 99, 117]. Fluorescence quenching technology is available both for invasive applications, using a electrode probe with a very thin (approximately 5 μm) tip, and for noninvasive applications, using a sensor patch composed of a ruthenium-based metal complex that can be excited by an external fluorescent light source.

Modeling Oxygen Transport in Tissues

The limitations of the measurement techniques, caused mostly by the difficulties in measuring spatial O_2 concentrations in tissues or scaffolds, raise a need for predictive mathematical models. Transport of O_2 in vivo is controlled by several parameters; such as the blood flow rate; the degree of vascularization in the tissue; the physiological distance of the cells from the microvasculature; and, depending on cell type, the cells' rate of O_2 consumption. These factors affect O_2 distribution in the tissue, and some can also have an impact on O_2 transport in 3D in vitro cultures of pluripotent or vascular cells. Additional factors that in vitro studies should consider are the geometry of the scaffold, the available surface area for O_2 transport from the environment to the system, and controlled dissolved O_2 levels in the culture media.

In general, fundamental mathematical models estimating O_2 distribution in 3D constructs can be classified into (1) static models, where O_2 is only transported via

diffusion and (2) dynamic models, where convective transport of O_2 is also incorporated using such perfusion systems as microfluidic devices or microcirculation in the tissues.

Static Models

In tissues cultivated under static conditions within scaffolds using different types of biomaterials, spatial O_2 concentration can be described with a one-dimensional (1D), unsteady-state species continuity equation:

$$\frac{\partial C_{O2}}{\partial t} = D_{O2}\frac{\partial C_{O2}^2}{\partial z^2} - R \tag{7.1}$$

where C_{O2} is the spatial O_2 concentration in the scaffold changing with time (t) and axial position (z), D_{O2} is the diffusion coefficient of O_2 in the scaffold material, and R is the oxygen consumption rate of cells. This form of the transport equation has been used in many studies attempting to predict the O_2 gradients in 3D scaffolds [22, 62, 112]. The equation implies that O_2 changes both with time and depth while being consumed by the cells as it diffuses from the environment into the scaffold. Boundary conditions, which are critical for O_2 distribution, depend on the O_2 equilibrium between the environment (media/air) and the boundaries of the scaffold. Therefore, for a 3D scaffold with a depth of L and open boundaries from both sides, the boundary conditions can be given as follows:

$$\text{At } z = 0 \text{ and } z = L,\ C_{O2} = SP_{O2} \tag{7.2}$$

Thus, the solubility (S) of O_2 in the scaffold material is one of the determining parameters of O_2 distribution. Although the diffusion coefficient can also be considered a critical factor in relatively stiff scaffolds of the sort usually used for cartilage and cardiomyocyte tissues [22], it has been shown to be less significant for the natural hydrogel scaffolds commonly used for vascular tissues, such as collagen and HA. For instance, the diffusion coefficient of O_2 in collagen gels was found to be 99% of that in water [68]. Therefore, modeling studies usually assumed that it has the same O_2 diffusion coefficient as water or cell media (3.3×10^{-5} cm^2/s at 37°C) [127]. The consumption rate of O_2 (R) given in (7.1) is a function of both C_{O2} and ρ_{cell} and is governed by the Michaelis–Menten equation, which states that the O_2 uptake rate of each cell increases with O_2 availability, reaching a maximum V_{max}:

$$R = \rho_{cell}\frac{V_{max}C_{O2}}{K_m + C_{O2}} \tag{7.3}$$

where K_m is the O_2 concentration at which the O_2 uptake rate is half of its maximum value and ρ_{cell} is the cell density as a function of time and position. Different groups have reported V_{max} and K_m parameters of many vascular cell types at various cell seeding densities [63, 133]. For example, the V_{max} and K_m of HUVECs, at a density of 1×10^6 cells/ml, are found to be 22.05 ± 1.92 (pmol s^{-1} 10^{-6} cells) and 0.55 ± 0.02

(μM), respectively [63]. It should be noted that these parameters are estimated as to mitochondrial consumption of O_2. However, as already discussed, ECs also consume O_2 for ROS production, and the theoretical models should also take this additional O_2 consumption into account by, for example, including a linear correlation in the O_2 consumption rate equation (7.3). Besides, all estimations of the V_{max} and K_m parameters for the O_2 consumption of different cell types are carried out in 2D cultures. The literature currently lacks studies investigating whether or not, depending on the composition of the extracellular matrix, encapsulating cells in 3D gels changes their consumption of O_2.

Vascular cells proliferate/die, migrate, and assemble during 3D cultivation, which affects their spatial and temporal density and, therefore, O_2 distribution. Models developed for 3D cultures of cardiomyocytes take into account the cellular proliferation and changes in the dimensions of the cells during nutrient transport in scaffolds [61, 62]. However, we need more detailed models that consider how capillary formation affects O_2 transport to achieve more reliable estimations of spatial O_2 concentration. Tube formation and the networking of ECs in 3D gels have been simulated by more complicated numerical models [37, 114], although the effects of O_2 concentrations on tube formation dynamics still need to be incorporated.

Dynamic and In Vivo Models

The models used for static cultures in 3D scaffolds can also be used to describe O_2 distributions in vivo when combined with a fluid perfusion model that considers the convective O_2 transport to the tissues. The velocity profile of a fluid in capillaries or in an engineered microchannel system can be calculated using the simplified Navier–Stokes equation with cylindrical coordinates given for a laminar, one-dimensional, steady-state, and fully developed flow of an incompressible fluid:

$$\frac{dP}{dz} = \mu\left[\frac{1}{r}\frac{d}{dr}\left(r\frac{dV_z}{dr}\right)\right] \tag{7.4}$$

where P is the total pressure in the fluid changing in an axial direction, μ is the viscosity of the fluid, and V_z is the axial velocity of the fluid changing in a radial direction. After estimating the blood velocity profile, the species continuity equation, which involves both diffusive and convective transport of O_2, can be used to obtain the O_2 distribution inside the capillary or microchannel:

$$V_z\frac{\partial C_{O2}}{\partial z} = D_{O2}^{Blood}\left[\frac{1}{r}\frac{\partial}{\partial r}\left(r\frac{\partial C_{O2}}{\partial r}\right)+\frac{\partial^2 C_{O2}}{\partial z^2}\right] \tag{7.5}$$

The technical difficulties of making quantitative O_2 measurements in BM have led many researchers to develop mathematical models to describe BM O_2 distribution [32, 109, 110]. Additional parameters that need to be considered in vivo are the vascularization of the tissue and the transport of O_2 via hemoglobin proteins, making the concentration of hemoglobin another essential factor for determining the

oxygenation of the tissue. Studies take these additional factors into account using the following equation:

$$D_{O2}^{j}\left[\nabla^2 C_{O2}^{j}\right] = V_z \frac{\partial}{\partial z}\left[C_{O2}^{j} + N\varphi_{O2}\right] \tag{7.6}$$

The superscript j denotes each sinusoid/arteriole around the BM. N is the O_2 carrying capacity of the blood and φ_{O2} is the concentration of O_2 bound to hemoglobin, which depends on the plasma O_2 concentrations [148]. Finally, spatial and temporal C_{O2} in tissue can be estimated in a similar manner to the in vitro models, using (7.1) incorporated with the continuity of fluxes assumption at the ECM-vessel interface as a boundary condition.

7.2.3.2 Targeted Cellular Responses to O_2 Availability in Matrix Hydrogel

Engineering vascular tissues in 3D ECM is orchestrated with the proliferation, apoptosis, migration, activation, and assembly of vascular cells or precursor cells inside the construct. As discussed in the previous section, the composition of the biomaterial used to encapsulate the cells is critical for cellular fate and vessel formation. In addition to the effects of chemical and physical properties of the ECM material on blood vessel formation, temporal and spatial levels of O_2 and other nutrients are also crucial for various targeted cellular responses. A number of studies have investigated the effects of matrix content and stiffness on angiogenesis/vasculogenesis [89], and many others have proposed using different types of biosynthetic materials to develop more precise blood vessels [6, 123]. However, only a few studies have highlighted how O_2 gradients occurring in the matrix contribute to the angiogenic process [75, 139, 145]. The availability of O_2 and other nutrients decreases at the center of the gel compared to the peripheries, especially due to the requirements of high cell seeding density for vascular tissue generation or repair. Hence, cells that reside along different layers of the matrix respond differently to the nonuniform distribution of O_2 and nutrients. For primary vascular cells to form blood vessels, they require survival, activation, and the induction of angiogenesis by GFs, cell signaling, and regression. All of these responses, necessary for blood vessel formation, are controlled by ECM properties, as well as by O_2 availability. Therefore, the influences of both the ECM and dissolved O_2 distribution should be considered simultaneously.

Cell assembly and tube formation in the ECM require a sufficient cell density. Deprived of O_2 and nutrients, vascular cells can undergo apoptosis or necrosis [17]. These two cellular death mechanisms should be distinguished, since apoptosis has been shown to contribute to the process of angiogenesis at any O_2 tension, whereas necrosis usually results in the collapsing and deformation of tubes [160]. In order to prevent cellular necrosis during 3D vascular cell cultures, the critical issues to consider are the permeability of the ECM material to O_2 and glucose, the cell seeding density, and the thickness of the gel. Thus, cell seeding density is constrained by an

upper limit, above which the cells undergo necrosis due to nutrient deprivation, and a lower limit, below which the cells cannot assemble sufficiently to form tube-like structures. Both limits depend on the equilibrium O_2 levels in the environment.

The cells may also die as a result of apoptosis after their encapsulation in the gel. Interestingly, some groups have demonstrated that programmed cellular death is necessary for angiogenesis/vasculogenesis [160]. Segura et al. having studied tube formation of ECs in both 2D Matrigel and 3D collagen, concluded that a considerable number of cells undergoes apoptosis at the initial stages of cultivation and that, once angiogenesis is induced and tube formation has started, no further apoptosis occurs throughout the process. Inhibition of proapoptotic proteins has been shown to correlate with defective tube formations, suggesting that apoptosis is important for avoiding imperfections during blood vessel growth. Hypoxia, as already discussed, induces angiogenic responses and also regulates proapoptotic gene expressions. Thus, spatial variations in O_2 levels may alter the apoptotic responses in the gel and therefore regulate vascular tube morphogenesis.

MMPs are promoted by integrin–ligand interactions between cells and the ECM, leading to the degradation of the ECM and facilitating the migration of the cells [66]. It is hypothesized that ECM fragmentation orchestrated by the secretion of MMPs can mediate caspase activity through the rebinding of ECM protein fragments to unligated integrins, namely death receptors [29]. Therefore, the survival of ECs depends on the balance between cell survival promoters, such as FAK, Src, and Raf, and cellular apoptosis promoters, such as caspase 8 and caspase 3. Hypoxia may again play a critical role here, affecting both sides of the equilibrium by upregulating MMPs and VEGF at the same time [17, 75]. Hypoxia, accompanied by nonuniform distribution of O_2 throughout the gel, can result in spatial differences of cellular viability, which may subsequently disrupt vascular networking.

Overall, blood vessel growth requires remodeling of the ECM, which is based on two distinct mechanisms (1) degradation of the ECM by secreted proteases and (2) production of new ECM to support the invading vasculature. Many studies have shown that hypoxia can regulate the degradation, maintenance, and synthesis of the ECM [47, 147]. ECM degradation is important for cellular migration and blood vessel invasion of tissue. MMPs, as mentioned above, are a major family of proteinases that participate in the process of degrading the ECM during angiogenesis. In particular, MMP-2 and MMP-9, both members of the gelatinase subgroup of MMPs, have been shown to contribute to the process of angiogenesis [69]. MMP-2 secreted by the cells is activated through membrane MT1-MMPs where the activation can be avoided in the presence of tissue inhibitor of MMP-2 (TIMP-2) at high levels [81]. Furthermore, hypoxia was shown to influence the expression of MMP-2, as well as of MT1-MMP and TIMP-2, in ECs [17]. Lahat's group has demonstrated the upregulation of MMP-2 expression in hypoxic (0.3% O_2) cultures of HUVECs, whereas MT1-MMP and TIMP-2 are downregulated, enhancing migration and tube formation [17].

ECM degradation is accompanied by ECM production and the secretion of cells. Once the quiescent state of the ECs composing the blood vessel walls is perturbed and angiogenesis is induced, ECs start to proliferate and invade the neighboring ECM by using proteinases. At the same time, they start to remodel the existing ECM by synthesizing new ECM. In healing wounds, ECs produce transitional

ECM proteins, including fibrinogen and fibronectin, and temporarily deposit them in the ECM in order to provide available ligands during vessel growth [29]. Moreover, ECs also produce such matricellular proteins as tenascin C and SPARC in the ECM to mediate angiogenesis [29]. Clearly, the new ECM synthesis of cells is crucial for angiogenesis, and hypoxia, through HIF1α, has been shown to regulate the expressions of many different types of ECM proteins [137]. For example, many in vivo and in vitro studies have shown that hypoxia enhanced the synthesis of collagen, the most abundant protein in mammalian tissues [18, 85, 180].

Moreover, proliferation of the cells during angiogenesis/vasculogenesis in 3D scaffolds is regulated by beta fibroblast growth factor (bFGF) and VEGF, which are known to be hypoxia-dependent proteins [145]. In most studies focusing on the vascularization of 3D scaffolds, both GFs are broadly used as soluble factors that supplement cell growth medium to induce proliferation and migration [105, 158]. In addition, Shen et al. have demonstrated that immobilization of VEGF into a 3D collagen scaffold promotes EC viability, proliferation, and vascularization [163]. VEGF has been shown to promote blood vessel formation not only by inducing cellular proliferation and migration but also by directly regulating elongation and capillary networking in 3D ECM constructs deprived of O_2 and nutrients [75]. Helmlinger et al. used a sandwich system to seed HUVECs inside a collagen gel [75]. The transfer of O_2 and nutrients was accomplished with only simple diffusion through the edges of the collagen, so that O_2 and nutrient levels decreased toward the center. They found that, in a short time period (about 9 h), VEGF intensity increased in the interior regions deprived of O_2, which correlates well with cell elongation and branching. VEGF promoted capillary networking independently of proliferation, highlighting the role of autocrine VEGF in the reorganization of vascular networks in hypoxic regions of solid tumors. Another study focusing on quantitative measurements of O_2 gradients in 3D collagen has also shown that increased VEGF concentrations correlated well to decreasing O_2 levels throughout the 3D constructs during a 10-day period of cultivation [28].

A few studies, considering the induction of angiogenesis by hypoxia in 3D scaffolds, have emphasized that lowering the O_2 tension in 3D gels improved the cellular branching and tube formation of ECs [139, 145]. A growing body of publications have both investigated the influence of the ECM composition on angiogenesis/vasculogenesis and suggested the crucial roles of hypoxia in blood vessel formation. In addition, the evidence discussed above is sufficient to suggest that the ECM composition and O_2 tension are two coupled factors that need to be taken into account concurrently when developing and repairing vascular tissues in 3D microenvironments.

7.3 Future Directions

Understanding the simultaneous effects of the ECM and O_2 tension on the processes of angiogenesis/vasculogenesis will enable researchers to control these two factors and thereby to manipulate cellular responses in desired directions. Recent developments in many different fields of research, such as smart biomaterials

and microfluidics, could make possible the design and construction of novel in vitro microenvironments for cells. Smart biomaterials have been developed that can dynamically respond to external stimuli, such as light [65], pH [142], temperature [179], and cytokines [103]; these materials can truly mimic the complexity of a native ECM environment. The ability to control the physical and chemical properties of the gels at different spaces and times will provide better control over different stages of angiogenesis. Light-sensitive hydrogels can be used to create biomaterials with distinct cross-linking densities to promote and inhibit cell spreading and migration [100], which, in turn, can be used to pattern complex vascular networks. Since vascular morphogenesis is sensitive to tissue stiffness [41, 71], orientation [19], and polarity [33, 120], researchers could also induce vascular assembly into a tube by creating elasticity, GFs, and an oxygen gradient along the 3D scaffold [122]. The recent invention of photodegradable hydrogels, whose mechanical and chemical properties are controllable during the timescale of cellular development [102], could, in turn, be useful to promote various stages of vascular assembly. On the other hand, creating smart biomaterials that can shrink, swell, or degrade in response to oxygen tension would also be desirable to prevent the formation of anoxic regions inside the gels. Controlled regulation of O_2 gradients inside the constructs could also be beneficial to explain various phenomena that take place in the body, such as EPC regeneration in the BM, where the O_2 gradient plays a critical role in differentiation and migration dynamics.

Figure 7.4 illustrates two proposed approaches for controlling oxygen distribution and ECM properties. One possible solution to the problem of regulating O_2 gradients inside the gel would incorporate microfluidic technology [52, 107, 133, 183]. Although this approach provides better O_2 control over 3D microenvironments, we must still address the problem of the spatial variations in O_2 levels throughout the gel due to the cells' O_2 consumption. Advancements in microfluidic

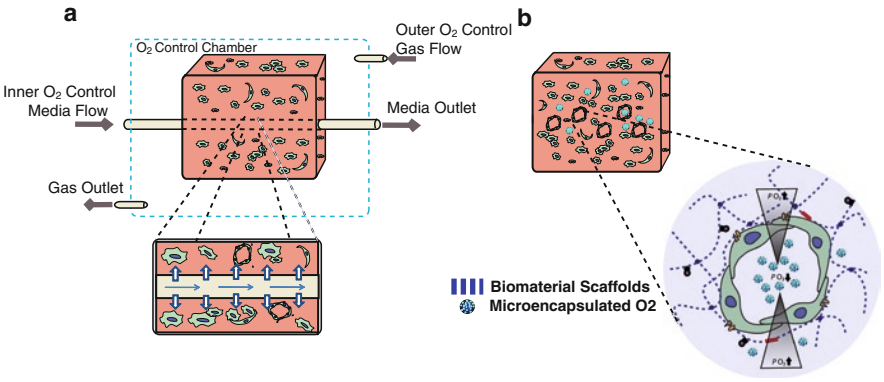

Fig. 7.4 Controlling ECM and O_2 in vitro by (**a**) 3D gel prepared around a microtube supplying O_2 (*insert*: *white arrows* indicate oxygen transport; *blue arrows* indicate the direction of airflow); (**b**) microencapsulated O_2 carriers, such as PFCs, embedded within 3D gel. Drawing not to scale

technology could also enable spatial O_2 control over 3D microenvironments; for instance, the gel could be prepared around a microtube, which would then be used to supply O_2 by flushing growth media containing a desired amount of O_2 (Fig. 7.4a). Hence, different O_2 gradients could be generated via the manipulation of O_2 concentrations in the outside environment and inside the microtube.

Another method for controlling and improving O_2 transport in the gel would microencapsulate O_2 carrier liquids, such as perfluorocarbons (PFCs). Due to their high capacity to dissolve O_2, PFCs have been used as a blood replacement to improve O_2 delivery to tissues [92, 151]. Based on the high oxygen-carrying capacity of PFCs, Radisic et al. [151] have developed a PFC-perfused system to supply sufficient levels of oxygen to 3D cardiomyocyte cultures. A study by Chin et al. [30] made a similar attempt, developing hydrogel–PFC composite scaffolds to improve oxygenation throughout the gel. In a similar manner, taking advantage of the high O_2 solubility of PFCs, controlled release of O_2 in 3D microenvironments could be improved via microencapsulation of PFCs (Fig. 7.4b).

Acknowledgments We would like to acknowledge funding from the AHA-Scientist Development grant, March of Dimes Basil O'Conner Starter Scholar award (both to S.G), and the National Institute of Health grant U54CA143868.

References

1. Abaci HE, Truitt R, Luong E, Drazer G, and Gerecht S. Adaptation to oxygen deprivation in cultures of human pluripotent stem cells, endothelial progenitor cells, and umbilical vein endothelial cells. *Am J Physiol Cell Physiol* 298: C1527–C1537, 2010.
2. Adelman DM, Maltepe E, and Simon MC. Multilineage embryonic hematopoiesis requires hypoxic ARNT activity. *Genes Dev* 13: 2478–2483, 1999.
3. Airley R, Loncaster J, Davidson S, Bromley M, Roberts S, Patterson A, Hunter R, Stratford I, and West C. Glucose transporter glut-1 expression correlates with tumor hypoxia and predicts metastasis-free survival in advanced carcinoma of the cervix. *Clin Cancer Res* 7: 928–934, 2001.
4. Akita T, Murohara T, Ikeda H, Sasaki K, Shimada T, Egami K, and Imaizumi T. Hypoxic preconditioning augments efficacy of human endothelial progenitor cells for therapeutic neovascularization. *Lab Invest* 83: 65–73, 2003.
5. Albina JE, Mastrofrancesco B, Vessella JA, Louis CA, Henry WL, Jr., and Reichner JS. HIF-1 expression in healing wounds: HIF-1alpha induction in primary inflammatory cells by TNF-alpha. *Am J Physiol Cell Physiol* 281: C1971–C1977, 2001.
6. Almany L and Seliktar D. Biosynthetic hydrogel scaffolds made from fibrinogen and polyethylene glycol for 3D cell cultures. *Biomaterials* 26: 2467–2477, 2005.
7. Artuc M, Hermes B, Steckelings UM, Grutzkau A, and Henz BM. Mast cells and their mediators in cutaneous wound healing – active participants or innocent bystanders? *Exp Dermatol* 8: 1–16, 1999.
8. Asahara T and Kawamoto A. Endothelial progenitor cells for postnatal vasculogenesis. *Am J Physiol Cell Physiol* 287: C572–C579, 2004.
9. Asahara T, Masuda H, Takahashi T, Kalka C, Pastore C, Silver M, Kearne M, Magner M, and Isner JM. Bone marrow origin of endothelial progenitor cells responsible for postnatal vasculogenesis in physiological and pathological neovascularization. *Circ Res* 85: 221–228, 1999.

10. Astrof S, Crowley D, and Hynes RO. Multiple cardiovascular defects caused by the absence of alternatively spliced segments of fibronectin. *Dev Biol* 311: 11–24, 2007.
11. Au P, Daheron LM, Duda DG, Cohen KS, Tyrrell JA, Lanning RM, Fukumura D, Scadden DT, and Jain RK. Differential in vivo potential of endothelial progenitor cells from human umbilical cord blood and adult peripheral blood to form functional long-lasting vessels. *Blood* 111: 1302–1305, 2008.
12. Au P, Tam J, Fukumura D, and Jain RK. Bone marrow derived mesenchymal stem cells facilitate engineering of long-lasting functional vasculature. *Blood* 111: 4551–4558, 2008.
13. Band M, Joel A, Hernandez A, and Avivi A. Hypoxia-induced BNIP3 expression and mitophagy: in vivo comparison of the rat and the hypoxia-tolerant mole rat, *Spalax ehrenbergi*. *FASEB J* 23: 2327–2335, 2009.
14. Banerjee SD and Toole BP. Hyaluronan-binding protein in endothelial cell morphogenesis. *J Cell Biol* 119: 643–652, 1992.
15. Bekker A, Holland HD, Wang PL, Rumble D, III, Stein HJ, Hannah JL, Coetzee LL, and Beukes NJ. Dating the rise of atmospheric oxygen. *Nature* 427: 117–120, 2004.
16. Bellot G, Garcia-Medina R, Gounon P, Chiche J, Roux D, Pouyssegur J, and Mazure NM. Hypoxia-induced autophagy is mediated through hypoxia-inducible factor induction of BNIP3 and BNIP3L via their BH3 domains. *Mol Cell Biol* 29: 2570–2581, 2009.
17. Ben-Yosef Y, Miller A, Shapiro S, and Lahat N. Hypoxia of endothelial cells leads to MMP-2-dependent survival and death. *Am J Physiol Cell Physiol* 289: C1321–C1331, 2005.
18. Berg JT, Breen EC, Fu Z, Mathieu-Costello O, and West JB. Alveolar hypoxia increases gene expression of extracellular matrix proteins and platelet-derived growth factor-B in lung parenchyma. *Am J Respir Crit Care Med* 158: 1920–1928, 1998.
19. Bettinger CJ, Zhang Z, Gerecht S, Borenstein J, and Langer R. Enhancement of in vitro capillary tube formation by substrate nanotopography. *Adv Mater* 20: 99–103, 2008.
20. Bianchi F, Rosi M, Vozzi G, Emanueli C, Madeddu P, and Ahluwalia A. Microfabrication of fractal polymeric structures for capillary morphogenesis: applications in therapeutic angiogenesis and in the engineering of vascularized tissue. *J Biomed Mater Res B Appl Biomater* 81: 462–468, 2007.
21. Boveris A, Costa LE, Poderoso JJ, Carreras MC, and Cadenas E. Regulation of mitochondrial respiration by oxygen and nitric oxide. *Ann NY Acad Sci* 899: 121–135, 2000.
22. Brown DA, MacLellan WR, Laks H, Dunn JC, Wu BM, and Beygui RE. Analysis of oxygen transport in a diffusion-limited model of engineered heart tissue. *Biotechnol Bioeng* 97: 962–975, 2007.
23. Bruick RK and McKnight SL. A conserved family of prolyl-4-hydroxylases that modify HIF. *Science* 294: 1337–1340, 2001.
24. Burggren WW. What is the purpose of the embryonic heart beat? Or how facts can ultimately prevail over physiological dogma. *Physiol Biochem Zool* 77: 333–345, 2004.
25. Camenisch TD, Spicer AP, Brehm-Gibson T, Biesterfeldt J, Augustine ML, Calabro Jr A, Kubalak S, Klewer SE, and McDonald JA. Disruption of hyaluronan synthase-2 abrogates normal cardiac morphogenesis and hyaluronan-mediated transformation of epithelium to mesenchyme. *J Clin Invest* 106: 349–360, 2000.
26. Caspi O, Lesman A, Basevitch Y, Gepstein A, Arbel G, Habib IH, Gepstein L, and Levenberg S. Tissue engineering of vascularized cardiac muscle from human embryonic stem cells. *Circ Res* 100: 263–272, 2007.
27. Ceradini DJ and Gurtner GC. Homing to hypoxia: HIF-1 as a mediator of progenitor cell recruitment to injured tissue. Trends Cardiovasc Med 15: 57–63, 2005.
28. Cheema U, Brown RA, Alp B, and MacRobert AJ. Spatially defined oxygen gradients and vascular endothelial growth factor expression in an engineered 3D cell model. *Cell Mol Life Sci* 65: 177–186, 2008.
29. Cheresh DA and Stupack DG. Regulation of angiogenesis: apoptotic cues from the ECM. *Oncogene* 27: 6285–6298, 2008.
30. Chin K, Khattak SF, Bhatia SR, and Roberts SC. Hydrogel-perfluorocarbon composite scaffold promotes oxygen transport to immobilized cells. *Biotechnol Prog* 24: 358–366, 2008.

31. Chiu LLY and Radisic M. Scaffolds with covalently immobilized VEGF and Angiopoietin-1 for vascularization of engineered tissues. *Biomaterials* 31: 226–241, 2010.
32. Chow DC, Wenning LA, Miller WM, and Papoutsakis ET. Modeling pO(2) distributions in the bone marrow hematopoietic compartment. I. Krogh's model. *Biophys J* 81: 675–684, 2001.
33. Chung S and Andrew DJ. The formation of epithelial tubes. *J Cell Sci* 121: 3501–3504, 2008.
34. Colville-Nash PR and Scott DL. Angiogenesis and rheumatoid arthritis: pathogenic and therapeutic implications. *Ann Rheum Dis* 51: 919–925, 1992.
35. Covello KL, Kehler J, Yu H, Gordan JD, Arsham AM, Hu CJ, Labosky PA, Simon MC, and Keith B. HIF-2alpha regulates Oct-4: effects of hypoxia on stem cell function, embryonic development, and tumor growth. *Genes Dev* 20: 557–570, 2006.
36. Critser PJ, Kreger ST, Voytik-Harbin SL, and Yoder MC. Collagen matrix physical properties modulate endothelial colony forming cell-derived vessels in vivo. *Microvasc Res* 80: 23–30, 2010.
37. Daphne M. A mechanochemical model of angiogenesis and vasculogenesis. *Esaim Math Model Numer Anal* 37: 581–599, 2003.
38. Davis GE and Camarillo CW. Regulation of endothelial cell morphogenesis by integrins, mechanical forces, and matrix guidance pathways. *Exp Cell Res* 216: 113–123, 1995.
39. Davis GE, Koh W, and Stratman AN. Mechanisms controlling human endothelial lumen formation and tube assembly in three-dimensional extracellular matrices. *Birth Defects Res C Embryo Today* 81: 270–285, 2007.
40. Davis GE and Senger DR. Extracellular matrix mediates a molecular balance between vascular morphogenesis and regression. *Curr Opin Hematol* 15: 197–203, 2008.
41. Deroanne CF, Lapiere CM, and Nusgens BV. In vitro tubulogenesis of endothelial cells by relaxation of the coupling extracellular matrix-cytoskeleton. *Cardiovasc Res* 49: 647–658, 2001.
42. Dickinson LE, Ho CC, Wang GM, Stebe KJ, and Gerecht S. Functional surfaces for high-resolution analysis of cancer cell interactions on exogenous hyaluronic acid. *Biomaterials* 31: 5472–5478, 2010.
43. Drake CJ and Fleming PA. Vasculogenesis in the day 6.5 to 9.5 mouse embryo. *Blood* 95: 1671–1679, 2000.
44. Eble JA and Niland S. The extracellular matrix of blood vessels. *Curr Pharm Des* 15: 1385–1400, 2009.
45. Ehrbar M, Djonov VG, Schnell C, Tschanz SA, Martiny-Baron G, Schenk U, Wood J, Burri PH, Hubbell JA, and Zisch AH. Cell-demanded liberation of VEGF121 from fibrin implants induces local and controlled blood vessel growth. *Circ Res* 94: 1124–1132, 2004.
46. Ehrbar M, Metters A, Zammaretti P, Hubbell JA, and Zisch AH. Endothelial cell proliferation and progenitor maturation by fibrin-bound VEGF variants with differential susceptibilities to local cellular activity. *J Control Release* 101: 93–109, 2005.
47. Erler JT, Bennewith KL, Cox TR, Lang G, Bird D, Koong A, Le QT, and Giaccia AJ. Hypoxia-induced lysyl oxidase is a critical mediator of bone marrow cell recruitment to form the premetastatic niche. *Cancer Cell* 15: 35–44, 2009.
48. Evanko SP, Parks WT, and Wight TN. Intracellular hyaluronan in arterial smooth muscle cells: association with microtubules, RHAMM, and the mitotic spindle. *J Histochem Cytochem* 52: 1525–1535, 2004.
49. Evans AM, Mustard KJ, Wyatt CN, Peers C, Dipp M, Kumar P, Kinnear NP, and Hardie DG. Does AMP-activated protein kinase couple inhibition of mitochondrial oxidative phosphorylation by hypoxia to calcium signaling in O2-sensing cells? *J Biol Chem* 280: 41504–41511, 2005.
50. Ezashi T, Das P, and Roberts RM. Low O2 tensions and the prevention of differentiation of hES cells. *Proc Natl Acad Sci USA* 102: 4783–4788, 2005.
51. Fahling M, Perlewitz A, Doller A, and Thiele BJ. Regulation of collagen prolyl 4-hydroxylase and matrix metalloproteinases in fibrosarcoma cells by hypoxia. *Comp Biochem Physiol C Toxicol Pharmacol* 139: 119–126, 2004.

52. Figallo E, Cannizzaro C, Gerecht S, Burdick JA, Langer R, Elvassore N, and Vunjak-Novakovic G. Micro-bioreactor array for controlling cellular microenvironments. *Lab Chip* 7: 710–719, 2007.
53. Folkman J, Haudenschild CC, and Zetter BR. Long-term culture of capillary endothelial cells. *Proc Natl Acad Sci USA* 76: 5217–5221, 1979.
54. Fong GH. Regulation of angiogenesis by oxygen sensing mechanisms. *J Mol Med* 87: 549–560, 2009.
55. Forristal CE, Wright KL, Hanley NA, Oreffo RO, and Houghton FD. Hypoxia inducible factors regulate pluripotency and proliferation in human embryonic stem cells cultured at reduced oxygen tensions. *Reproduction* 139: 85–97, 2010.
56. Fraisl P, Mazzone M, Schmidt T, and Carmeliet P. Regulation of angiogenesis by oxygen and metabolism. *Dev Cell* 16: 167–179, 2009.
57. Francis SE, Goh KL, Hodivala-Dilke K, Bader BL, Stark M, Davidson D, and Hynes RO. Central roles of alpha5beta1 integrin and fibronectin in vascular development in mouse embryos and embryoid bodies. *Arterioscler Thromb Vasc Biol* 22: 927–933, 2002.
58. Frei R, Gaucher C, Poulton SW, and Canfield DE. Fluctuations in Precambrian atmospheric oxygenation recorded by chromium isotopes. *Nature* 461: 250–253, 2009.
59. Fukumura D, Kashiwagi S, and Jain RK. The role of nitric oxide in tumour progression. *Nat Rev Cancer* 6: 521–534, 2006.
60. Gafni Y, Zilberman Y, Ophir Z, Abramovitch R, Jaffe M, Gazit Z, Domb A, and Gazit D. Design of a filamentous polymeric scaffold for in vivo guided angiogenesis. *Tissue Eng* 12: 3021–3034, 2006.
61. Galban CJ and Locke BR. Analysis of cell growth kinetics and substrate diffusion in a polymer scaffold. *Biotechnol Bioeng* 65: 121–132, 1999.
62. Galban CJ and Locke BR. Effects of spatial variation of cells and nutrient and product concentrations coupled with product inhibition on cell growth in a polymer scaffold. *Biotechnol Bioeng* 64: 633–643, 1999.
63. Garedew A, Kammerer U, and Singer D. Respiratory response of malignant and placental cells to changes in oxygen concentration. *Respir Physiol Neurobiol* 165: 154–160, 2009.
64. Gerecht-Nir S, Cohen S, Ziskind A, and Itskovitz-Eldor J. Three-dimensional porous alginate scaffolds provide a conducive environment for generation of well-vascularized embryoid bodies from human embryonic stem cells. *Biotechnol Bioeng* 88: 313–320, 2004.
65. Gerecht S, Burdick JA, Ferreira LS, Townsend SA, Langer R, and Vunjak-Novakovic G. Hyaluronic acid hydrogel for controlled self-renewal and differentiation of human embryonic stem cells. *Proc Natl Acad Sci USA* 104: 11298–11303, 2007.
66. Giannelli G, Falk-Marzillier J, Schiraldi O, Stetler-Stevenson WG, and Quaranta V. Induction of cell migration by matrix metalloprotease-2 cleavage of laminin-5. *Science* 277: 225–228, 1997.
67. Gobin AS and West JL. Cell migration through defined, synthetic extracellular matrix analogues. *FASEB J* 16(7): 751–753, 2002.
68. Guaccio A, Borselli C, Oliviero O, and Netti PA. Oxygen consumption of chondrocytes in agarose and collagen gels: a comparative analysis. *Biomaterials* 29: 1484–1493, 2008.
69. Hagemann T, Robinson SC, Schulz M, Trumper L, Balkwill FR, and Binder C. Enhanced invasiveness of breast cancer cell lines upon co-cultivation with macrophages is due to TNF-alpha dependent up-regulation of matrix metalloproteases. *Carcinogenesis* 25: 1543–1549, 2004.
70. Hanjaya-Putra D and Gerecht S. Vascular engineering using human embryonic stem cells. *Biotechnol Prog* 25: 2–9, 2009.
71. Hanjaya-Putra D, Yee J, Ceci D, Truitt R, Yee D, and Gerecht S. Vascular endothelial growth factor and substrate mechanics regulate in vitro tubulogenesis of endothelial progenitor cells. *J Cell Mol Med* 14: 2436–2447, 2010. doi: 10.1111/j.1582-4934.2009.00981.x.
72. Hanjaya-Putra D and Gerecht S. Mending the failing heart with a vascularized cardiac patch. *Cell Stem Cell* 5(6): 575–576, 2009.

73. Harrison JS, Rameshwar P, Chang V, and Bandari P. Oxygen saturation in the bone marrow of healthy volunteers. *Blood* 99: 394, 2002.
74. Heissig B, Hattori K, Dias S, Friedrich M, Ferris B, Hackett NR, Crystal RG, Besmer P, Lyden D, Moore MA, Werb Z, and Rafii S. Recruitment of stem and progenitor cells from the bone marrow niche requires MMP-9 mediated release of kit-ligand. *Cell* 109: 625–637, 2002.
75. Helmlinger G, Endo M, Ferrara N, Hlatky L, and Jain RK. Formation of endothelial cell networks. *Nature* 405: 139–141, 2000.
76. Hirota K and Semenza GL. Regulation of hypoxia-inducible factor 1 by prolyl and asparaginyl hydroxylases. *Biochem Biophys Res Commun* 338: 610–616, 2005.
77. Hirschi KK and D'Amore PA. Pericytes in the microvasculature. *Cardiovasc Res* 32: 687–698, 1996.
78. Hirschi KK, Ingram DA, and Yoder MC. Assessing identity, phenotype, and fate of endothelial progenitor cells. *Arterioscler Thromb Vasc Biol* 28: 1584–1595, 2008.
79. Hirschi KK, Rohovsky SA, and D'Amore PA. PDGF, TGF-Î², and heterotypic cell–cell interactions mediate endothelial cell-induced recruitment of 10T1/2 cells and their differentiation to a smooth muscle fate. *J Cell Biol* 141: 805–814, 1998.
80. Hirsila M, Koivunen P, Gunzler V, Kivirikko KI, and Myllyharju J. Characterization of the human prolyl 4-hydroxylases that modify the hypoxia-inducible factor. *J Biol Chem* 278: 30772–30780, 2003.
81. Hofmann UB, Westphal JR, Van Kraats AA, Ruiter DJ, and Van Muijen GN. Expression of integrin alpha(v)beta(3) correlates with activation of membrane-type matrix metalloproteinase-1 (MT1-MMP) and matrix metalloproteinase-2 (MMP-2) in human melanoma cells in vitro and in vivo. *Int J Cancer* 87: 12–19, 2000.
82. Holash J, Maisonpierre PC, Compton D, Boland P, Alexander CR, Zagzag D, Yancopoulos GD, and Wiegand SJ. Vessel cooption, regression, and growth in tumors mediated by angiopoietins and VEGF. *Science* 284: 1994–1998, 1999.
83. Holash J, Wiegand SJ, and Yancopoulos GD. New model of tumor angiogenesis: dynamic balance between vessel regression and growth mediated by angiopoietins and VEGF. *Oncogene* 18: 5356–5362, 1999.
84. Hopf HW and Rollins MD. Wounds: an overview of the role of oxygen. *Antioxid Redox Signal* 9: 1183–1192, 2007.
85. Horino Y, Takahashi S, Miura T, and Takahashi Y. Prolonged hypoxia accelerates the posttranscriptional process of collagen synthesis in cultured fibroblasts. *Life Sci* 71: 3031–3045, 2002.
86. Huber TL, Kouskoff V, Fehling HJ, Palis J, and Keller G. Haemangioblast commitment is initiated in the primitive streak of the mouse embryo. *Nature* 432: 625–630, 2004.
87. Silver IA. Cellular microenvironment in healing and non-healing wounds. In: *Soft and hard tissue repair*, edited by Hunt TK. New York: Praeger, 1984, pp. 50–66.
88. Igarashi S, Tanaka J, and Kobayashi H. Micro-patterned nanofibrous biomaterials. *J Nanosci Nanotechnol* 7: 814–817, 2007.
89. Ingber DE. Mechanical signaling and the cellular response to extracellular matrix in angiogenesis and cardiovascular physiology. *Circ Res* 91: 877–887, 2002.
90. Ingber DE and Folkman J. Mechanochemical switching between growth and differentiation during fibroblast growth factor-stimulated angiogenesis in vitro: role of extracellular matrix. *J Cell Biol* 109: 317–330, 1989.
91. Rajasekhar VK, Vemuri MC, Iwasaki H, and Suda T. The niche regulation of hematopoietic stem cells. In: *Regulatory networks in stem cells*. Humana Press, 2009. pp. 165–173.
92. Iyer RK, Radisic M, Cannizzaro C, and Vunjak-Novakovic G. Synthetic oxygen carriers in cardiac tissue engineering. *Artif Cells Blood Substit Immobil Biotechnol* 35: 135–148, 2007.
93. Jain RK. Molecular regulation of vessel maturation. Nat Med 9: 685–693, 2003.
94. Jain RK, Au P, Tam J, Duda DG, and Fukumura D. Engineering vascularized tissue. *Nat Biotechnol* 23: 821–823, 2005.

95. Jauniaux E, Gulbis B, and Burton GJ. The human first trimester gestational sac limits rather than facilitates oxygen transfer to the foetus – a review. *Placenta* 24 Suppl A: S86–S93, 2003.
96. Ji L, Liu YX, Yang C, Yue W, Shi SS, Bai CX, Xi JF, Nan X, and Pei XT. Self-renewal and pluripotency is maintained in human embryonic stem cells by co-culture with human fetal liver stromal cells expressing hypoxia inducible factor 1alpha. *J Cell Physiol* 221: 54–66, 2009.
97. Jiang M, Wang B, Wang C, He B, Fan H, Guo TB, Shao Q, Gao L, and Liu Y. Angiogenesis by transplantation of HIF-1 alpha modified EPCs into ischemic limbs. *J Cell Biochem* 103: 321–334, 2008.
98. Jones CI, III, Han Z, Presley T, Varadharaj S, Zweier JL, Ilangovan G, and Alevriadou BR. Endothelial cell respiration is affected by the oxygen tension during shear exposure: role of mitochondrial peroxynitrite. *Am J Physiol Cell Physiol* 295: C180–C191, 2008.
99. Kellner K, Liebsch G, Klimant I, Wolfbeis OS, Blunk T, Schulz MB, and Gopferich A. Determination of oxygen gradients in engineered tissue using a fluorescent sensor. *Biotechnol Bioeng* 80: 73–83, 2002.
100. Khetan S, Chung C, and Burdick JA. Tuning hydrogel properties for applications in tissue engineering. *Conf Proc IEEE Eng Med Biol Soc* 1: 2094–2096, 2009.
101. Kilarski WW, Samolov B, Petersson L, Kvanta A, and Gerwins P. Biomechanical regulation of blood vessel growth during tissue vascularization. *Nat Med* 15: 657–664, 2009.
102. Kloxin AM, Kasko AM, Salinas CN, and Anseth KS. Photodegradable hydrogels for dynamic tuning of physical and chemical properties. *Science* 324: 59–63, 2009.
103. Klumb LA and Horbett TA. Design of insulin delivery devices based on glucose sensitive membranes. *J Control Release* 18: 59–80, 1992.
104. Koay EJ and Athanasiou KA. Hypoxic chondrogenic differentiation of human embryonic stem cells enhances cartilage protein synthesis and biomechanical functionality. *Osteoarthritis Cartilage* 16: 1450–1456, 2008.
105. Koh W, Stratman AN, Sacharidou A, and Davis GE. In vitro three dimensional collagen matrix models of endothelial lumen formation during vasculogenesis and angiogenesis. *Methods Enzymol* 443: 83–101, 2008.
106. Koike N, Fukumura D, Gralla O, Au P, Schechner JS, and Jain RK. Tissue engineering: creation of long-lasting blood vessels. *Nature* 428: 138, 2004.
107. Korin N, Bransky A, Dinnar U, and Levenberg S. Periodic "flow-stop" perfusion microchannel bioreactors for mammalian and human embryonic stem cell long-term culture. *Biomed Microdevices* 11: 87–94, 2009.
108. Kreger ST and Voytik-Harbin SL. Hyaluronan concentration within a 3D collagen matrix modulates matrix viscoelasticity, but not fibroblast response. *Matrix Biol* 28: 336–346, 2009.
109. Kumar R, Panoskaltsis N, Stepanek F, and Mantalaris A. Coupled oxygen-carbon dioxide transport model for the human bone marrow. *Food Bioprod Process* 86: 211–219, 2008.
110. Kumar R, Stepanek F, and Mantalaris A. A conceptual model for oxygen transport in the human marrow. *Ifac Symp Series* 365–370 538, 2003.
111. Kumar R, Stepanek F, and Mantalaris A. An oxygen transport model for human bone marrow microcirculation. *Food and Bioproducts* 82(C2): 105–116, 2004.
112. Landman KA and Cai AQ. Cell proliferation and oxygen diffusion in a vascularising scaffold. *Bull Math Biol* 69: 2405–2428, 2007.
113. Langer R and Tirrell DA. Designing materials for biology and medicine. *Nature* 428: 487–492, 2004.
114. Lanza V, Ambrosi D, and Preziosi, L. Exogenous control of vascular network formation in vitro: a mathematical model. *Networks Heterogen Media* 1: 621–638, 2006.
115. Lee YM, Jeong CH, Koo SY, Son MJ, Song HS, Bae SK, Raleigh JA, Chung HY, Yoo MA, and Kim KW. Determination of hypoxic region by hypoxia marker in developing mouse embryos in vivo: a possible signal for vessel development. *Dev Dyn* 220: 175–186, 2001.
116. Levenberg S, Rouwkema J, Macdonald M, Garfein ES, Kohane DS, Darland DC, Marini R, van Blitterswijk CA, Mulligan RC, D'Amore PA, and Langer R. Engineering vascularized skeletal muscle tissue. *Nat Biotechnol* 23: 879–884, 2005.

117. Lewis MC, Macarthur BD, Malda J, Pettet G, and Please CP. Heterogeneous proliferation within engineered cartilaginous tissue: the role of oxygen tension. *Biotechnol Bioeng* 91: 607–615, 2005.
118. Li C, Issa R, Kumar P, Hampson IN, Lopez-Novoa JM, Bernabeu C, and Kumar S. CD105 prevents apoptosis in hypoxic endothelial cells. *J Cell Sci* 116: 2677–2685, 2003.
119. Limper AH and Roman J. Fibronectin. A versatile matrix protein with roles in thoracic development, repair and infection. *Chest* 101: 1663–1673, 1992.
120. Lubarsky B and Krasnow MA. Tube morphogenesis: making and shaping biological tubes. *Cell* 112: 19–28, 2003.
121. Lucitti JL, Jones EA, Huang C, Chen J, Fraser SE, and Dickinson ME. Vascular remodeling of the mouse yolk sac requires hemodynamic force. *Development* 134: 3317–3326, 2007.
122. Lutolf MP. Biomaterials: spotlight onF hydrogels. *Nat Mater* 8: 451–453, 2009.
123. Lutolf MP and Hubbell JA. Synthetic biomaterials as instructive extracellular microenvironments for morphogenesis in tissue engineering. *Nat Biotechnol* 23: 47–55, 2005.
124. Lutolf MP, Lauer-Fields JL, Schmoekel HG, Metters AT, Weber FE, Fields GB, and Hubbell JA. Synthetic matrix metalloproteinase-sensitive hydrogels for the conduction of tissue regeneration: engineering cell-invasion characteristics. *Proc Natl Acad Sci USA* 100: 5413–5418, 2003.
125. Ma T, Grayson WL, Frohlich M, and Vunjak-Novakovic G. Hypoxia and stem cell-based engineering of mesenchymal tissues. *Biotechnol Prog* 25: 32–42, 2009.
126. Maltepe E and Simon MC. Oxygen, genes, and development: an analysis of the role of hypoxic gene regulation during murine vascular development. *J Mol Med* 76: 391–401, 1998.
127. Mamchaoui K and Saumon G. A method for measuring the oxygen consumption of intact cell monolayers. *Am J Physiol Lung Cell Mol Physiol* 278: L858–L863, 2000.
128. Mammoto A, Connor KM, Mammoto T, Yung CW, Huh D, Aderman CM, Mostoslavsky G, Smith LEH, and Ingber DE. A mechanosensitive transcriptional mechanism that controls angiogenesis. *Nature* 457: 1103–1108, 2009.
129. Manalo DJ, Rowan A, Lavoie T, Natarajan L, Kelly BD, Ye SQ, Garcia JG, and Semenza GL. Transcriptional regulation of vascular endothelial cell responses to hypoxia by HIF-1. *Blood* 105: 659–669, 2005.
130. Martorell L, Gentile M, Rius J, Rodriguez C, Crespo J, Badimon L, and Martinez-Gonzalez J. The hypoxia-inducible factor 1/NOR-1 axis regulates the survival response of endothelial cells to hypoxia. *Mol Cell Biol* 29: 5828–5842, 2009.
131. Massabuau JC. From low arterial- to low tissue-oxygenation strategy. An evolutionary theory. *Respir Physiol* 128: 249–261, 2001.
132. Massabuau JC. Primitive, and protective, our cellular oxygenation status? *Mech Ageing Dev* 124: 857–863, 2003.
133. Mehta G, Mehta K, Sud D, Song JW, Bersano-Begey T, Futai N, Heo YS, Mycek MA, Linderman JJ, and Takayama S. Quantitative measurement and control of oxygen levels in microfluidic poly(dimethylsiloxane) bioreactors during cell culture. *Biomed Microdevices* 9: 123–134, 2007.
134. Melero-Martin JM, De Obaldia ME, Kang SY, Khan ZA, Yuan L, Oettgen P, and Bischoff J. Engineering robust and functional vascular networks in vivo with human adult and cord blood-derived progenitor cells. *Circ Res* 103: 194–202, 2008.
135. Moon JJ, Hahn MS, Kim I, Nsiah BA, and West JL. Micropatterning of poly(ethylene glycol) diacrylate hydrogels with biomolecules to regulate and guide endothelial morphogenesis. *Tissue Eng Part A* 15: 579–585, 2009.
136. Moon JJ, Saik JE, Poché RA, Leslie-Barbick JE, Lee S-H, Smith AA, Dickinson ME, and West JL. Biomimetic hydrogels with pro-angiogenic properties. *Biomaterials* 31: 3840–3847, 2010.
137. Myllyharju J and Schipani E. Extracellular matrix genes as hypoxia-inducible targets. *Cell Tissue Res* 339: 19–29, 2010.

138. Niebruegge S, Bauwens CL, Peerani R, Thavandiran N, Masse S, Sevaptisidis E, Nanthakumar K, Woodhouse K, Husain M, Kumacheva E, and Zandstra PW. Generation of human embryonic stem cell-derived mesoderm and cardiac cells using size-specified aggregates in an oxygen-controlled bioreactor. *Biotechnol Bioeng* 102: 493–507, 2009.
139. Ottino P, Finley J, Rojo E, Ottlecz A, Lambrou GN, Bazan HE, and Bazan NG. Hypoxia activates matrix metalloproteinase expression and the VEGF system in monkey choroid-retinal endothelial cells: involvement of cytosolic phospholipase A2 activity. *Mol Vis* 10: 341–350, 2004.
140. Papandreou I, Cairns RA, Fontana L, Lim AL, and Denko NC. HIF-1 mediates adaptation to hypoxia by actively downregulating mitochondrial oxygen consumption. *Cell Metab* 3: 187–197, 2006.
141. Papandreou I, Lim AL, Laderoute K, and Denko NC. Hypoxia signals autophagy in tumor cells via AMPK activity, independent of HIF-1, BNIP3, and BNIP3L. *Cell Death Differ* 15: 1572–1581, 2008.
142. Park TG and Hoffman AS. Synthesis and characterization of PH- and or temperature-sensitive hydrogels. *J Appl Polym Sci* 46: 659–671, 1992.
143. Parmar K, Mauch P, Vergilio JA, Sackstein R, and Down JD. Distribution of hematopoietic stem cells in the bone marrow according to regional hypoxia. *Proc Natl Acad Sci USA* 104: 5431–5436, 2007.
144. Phelps EA, Landázuri N, Thulé PM, Taylor WR, García AJ. Bioartificial matrices for therapeutic vascularization. *Proc Natl Acad Sci USA* 107: 3323–3328, 2010.
145. Phillips PG, Birnby LM, and Narendran A. Hypoxia induces capillary network formation in cultured bovine pulmonary microvessel endothelial cells. *Am J Physiol* 268: L789–L800, 1995.
146. Pierschbacher MD and Ruoslahti E. Cell attachment activity of fibronectin can be duplicated by small synthetic fragments of the molecule. *Nature* 309: 30–33, 1984.
147. Pollard PJ, Loenarz C, Mole DR, McDonough MA, Gleadle JM, Schofield CJ, and Ratcliffe PJ. Regulation of Jumonji-domain-containing histone demethylases by hypoxia-inducible factor (HIF)-1alpha. *Biochem J* 416: 387–394, 2008.
148. Popel AS. Theory of oxygen transport to tissue. *Crit Rev Biomed Eng* 17: 257–321, 1989.
149. Prado-Lopez S, Conesa A, Arminan A, Martinez-Losa M, Escobedo-Lucea C, Gandia C, Tarazona S, Melguizo D, Blesa D, Montaner D, Sanz-Gonzalez S, Sepulveda P, Gotz S, O'Connor JE, Moreno R, Dopazo J, Burks DJ, and Stojkovic M. Hypoxia promotes efficient differentiation of human embryonic stem cells to functional endothelium. *Stem Cells* 28: 407–418, 2010.
150. Prasad SM, Czepiel M, Cetinkaya C, Smigielska K, Weli SC, Lysdahl H, Gabrielsen A, Petersen K, Ehlers N, Fink T, Minger SL, and Zachar V. Continuous hypoxic culturing maintains activation of Notch and allows long-term propagation of human embryonic stem cells without spontaneous differentiation. *Cell Prolif* 42: 63–74, 2009.
151. Radisic M, Deen W, Langer R, and Vunjak-Novakovic G. Mathematical model of oxygen distribution in engineered cardiac tissue with parallel channel array perfused with culture medium containing oxygen carriers. *Am J Physiol Heart Circ Physiol* 288: H1278–H1289, 2005.
152. Risau W. Mechanisms of angiogenesis. *Nature* 386: 671–674, 1997.
153. Robins SP. Biochemistry and functional significance of collagen cross-linking. *Biochem Soc Trans* 35: 849–852, 2007.
154. Rodesch F, Simon P, Donner C, and Jauniaux E. Oxygen measurements in endometrial and trophoblastic tissues during early pregnancy. *Obstet Gynecol* 80: 283–285, 1992.
155. Roeder BA, Kokini K, Sturgis JE, Robinson JP, and Voytik-Harbin SL. Tensile mechanical properties of three-dimensional type I collagen extracellular matrices with varied microstructure. *J Biomech Eng* 124: 214–222, 2002.
156. Romer LH, Birukov KG, and Garcia JG. Focal adhesions: paradigm for a signaling nexus. *Circ Res* 98: 606–616, 2006.
157. Sage EH and Vernon RB. Regulation of angiogenesis by extracellular matrix: the growth and the glue. *J Hypertens Suppl* 12: S145–S152, 1994.

158. Saunders WB, Bayless KJ, and Davis GE. MMP-1 activation by serine proteases and MMP-10 induces human capillary tubular network collapse and regression in 3D collagen matrices. *J Cell Sci* 118: 2325–2340, 2005.
159. Scott C, Lyons TW, Bekker A, Shen Y, Poulton SW, Chu X, and Anbar AD. Tracing the stepwise oxygenation of the Proterozoic ocean. *Nature* 452: 456–459, 2008.
160. Segura I, Serrano A, De Buitrago GG, Gonzalez MA, Abad JL, Claveria C, Gomez L, Bernad A, Martinez AC, and Riese HH. Inhibition of programmed cell death impairs in vitro vascular-like structure formation and reduces in vivo angiogenesis. *FASEB J* 16: 833–841, 2002.
161. Seliktar D, Zisch AH, Lutolf MP, Wrana JL, and Hubbel JA. MMP-2 sensitive, VEGF-bearing bioactive hydrogels for promotion of vascular healing. *J Biomed Mater Res A* 68: 704–716, 2004.
162. Shaw AD, Li Z, Thomas Z, and Stevens CW. Assessment of tissue oxygen tension: comparison of dynamic fluorescence quenching and polarographic electrode technique. *Crit Care* 6: 76–80, 2002.
163. Shen YH, Shoichet MS, and Radisic M. Vascular endothelial growth factor immobilized in collagen scaffold promotes penetration and proliferation of endothelial cells. *Acta Biomater* 4: 477–489, 2008.
164. Shweiki D, Neeman M, Itin A, and Keshet E. Induction of vascular endothelial growth factor expression by hypoxia and by glucose deficiency in multicell spheroids: implications for tumor angiogenesis. *Proc Natl Acad Sci USA* 92: 768–772, 1995.
165. Sieminski AL, Hebbel RP, and Gooch KJ. The relative magnitudes of endothelial force generation and matrix stiffness modulate capillary morphogenesis in vitro. *Exp Cell Res* 297: 574–584, 2004.
166. Sieminski AL, Was AS, Kim G, Gong H, and Kamm RD. The stiffness of three-dimensional ionic self-assembling peptide gels affects the extent of capillary-like network formation. *Cell Biochem Biophys* 49: 73–83, 2007.
167. Siggaard-Andersen O and Huch R. The oxygen status of fetal blood. *Acta Anaesthesiol Scand Suppl* 107: 129–135, 1995.
168. Silva GA, Czeisler C, Niece KL, Beniash E, Harrington DA, Kessler JA, and Stupp SI. Selective differentiation of neural progenitor cells by high-epitope density nanofibers. *Science* 303: 1352–1355, 2004.
169. Sorrell JM, Baber MA, and Caplan AI. A self-assembled fibroblast-endothelial cell co-culture system that supports in vitro vasculogenesis by both human umbilical vein endothelial cells and human dermal microvascular endothelial cells. *Cells Tissues Organs* 186: 157–168, 2007.
170. Sottile J and Hocking DC. Fibronectin polymerization regulates the composition and stability of extracellular matrix fibrils and cell-matrix adhesions. *Mol Biol Cell* 13: 3546–3559, 2002.
171. Soucy PA and Romer LH. Endothelial cell adhesion, signaling, and morphogenesis in fibroblast-derived matrix. *Matrix Biol* 28: 273–283, 2009.
172. Springett R and Swartz HM. Measurements of oxygen in vivo: overview and perspectives on methods to measure oxygen within cells and tissues. *Antioxid Redox Signal* 9: 1295–1301, 2007.
173. Steinlechner-Maran R, Eberl T, Kunc M, Margreiter R, and Gnaiger E. Oxygen dependence of respiration in coupled and uncoupled endothelial cells. *Am J Physiol* 271: C2053–C2061, 1996.
174. Stephanou A, Meskaoui G, Vailhe B, and Tracqui P. The rigidity in fibrin gels as a contributing factor to the dynamics of in vitro vascular cord formation. *Microvasc Res* 73: 182–190, 2007.
175. Stratman AN, Saunders WB, Sacharidou A, Koh W, Fisher KE, Zawieja DC, Davis MJ, and Davis GE. Endothelial cell lumen and vascular guidance tunnel formation requires MT1-MMP-dependent proteolysis in 3-dimensional collagen matrices. *Blood* 114: 237–247, 2009.
176. Stupack DG and Cheresh DA. ECM remodeling regulates angiogenesis: endothelial integrins look for new ligands. *Sci STKE* 2002: pe7, 2002.

177. Sun G and Chu C-C. Synthesis, characterization of biodegradable dextran-allyl isocyanate-ethylamine/polyethylene glycol-diacrylate hydrogels and their in vitro release of albumin. *Carbohydr Polym* 65: 273–287, 2006.
178. Sun G, Shen Y-I, Ho CC, Kusuma S, and Gerecht S. Functional groups affect physical and biological properties of dextran-based hydrogels. *J Biomed Mater Res A* 93: 1080–1090, 2010.
179. Sun GM, Zhang XZ, and Chu CC. Formulation and characterization of chitosan-based hydrogel films having both temperature and pH sensitivity. *J Mater Sci Mater Med* 18: 1563–1577, 2007.
180. Tajima R, Kawaguchi N, Horino Y, Takahashi Y, Toriyama K, Inou K, Torii S, and Kitagawa Y. Hypoxic enhancement of type IV collagen secretion accelerates adipose conversion of 3T3-L1 fibroblasts. *Biochim Biophys Acta* 1540: 179–187, 2001.
181. Thurston G, Suri C, Smith K, McClain J, Sato TN, Yancopoulos GD, and McDonald DM. Leakage-resistant blood vessels in mice transgenically overexpressing angiopoietin-1. *Science* 286: 2511–2514, 1999.
182. Timmermans F, Plum J, Yöder MC, Ingram DA, Vandekerckhove B, and Case J. Endothelial progenitor cells: identity defined? *J Cell Mol Med* 13: 87–102, 2009.
183. Toh YC, Zhang C, Zhang J, Khong YM, Chang S, Samper VD, van Noort D, Hutmacher DW, and Yu H. A novel 3D mammalian cell perfusion-culture system in microfluidic channels. *Lab Chip* 7: 302–309, 2007.
184. Toole BP. Hyaluronan in morphogenesis. *Semin Cell Dev Biol* 12: 79–87, 2001.
185. Toole BP. Hyaluronan: from extracellular glue to pericellular cue. *Nat Rev Cancer* 4: 528–539, 2004.
186. Tsai AG, Johnson PC, and Intaglietta M. Oxygen gradients in the microcirculation. *Physiol Rev* 83: 933–963, 2003.
187. Urbich C and Dimmeler S. Endothelial progenitor cells: characterization and role in vascular biology. *Circ Res* 95: 343–353, 2004.
188. Ushio-Fukai M and Nakamura Y. Reactive oxygen species and angiogenesis: NADPH oxidase as target for cancer therapy. *Cancer Lett* 266: 37–52, 2008.
189. Vo E, Hanjaya-Putra D, Zha Y, Kusuma S, and Gerecht S. Smooth-muscle-like cells derived from human embryonic stem cells support and augment cord-like structures in vitro. *Stem Cell Rev* 6: 237–247, 2010.
190. Walls JR, Coultas L, Rossant J, and Henkelman RM. Three-dimensional analysis of vascular development in the mouse embryo. *PLoS One* 3: e2853, 2008.
191. Walter DH, Rittig K, Bahlmann FH, Kirchmair R, Silver M, Murayama T, Nishimura H, Losordo DW, Asahara T, and Isner JM. Statin therapy accelerates reendothelialization: a novel effect involving mobilization and incorporation of bone marrow-derived endothelial progenitor cells. *Circulation* 105: 3017–3024, 2002.
192. Ward JP. Oxygen sensors in context. *Biochim Biophys Acta* 1777: 1–14, 2008.
193. Webster KA. Puma joins the battery of BH3-only proteins that promote death and infarction during myocardial ischemia. *Am J Physiol Heart Circ Physiol* 291: H20–H22, 2006.
194. Werner N, Junk S, Laufs U, Link A, Walenta K, Bohm M, and Nickenig G. Intravenous transfusion of endothelial progenitor cells reduces neointima formation after vascular injury. *Circ Res* 93: e17–e24, 2003.
195. Wijelath ES, Rahman S, Namekata M, Murray J, Nishimura T, Mostafavi-Pour Z, Patel Y, Suda Y, Humphries MJ, and Sobel M. Heparin-II domain of fibronectin is a vascular endothelial growth factor-binding domain: enhancement of VEGF biological activity by a singular growth factor/matrix protein synergism. *Circ Res* 99: 853–860, 2006.
196. Williams SE, Wootton P, Mason HS, Bould J, Iles DE, Riccardi D, Peers C, and Kemp PJ. Hemoxygenase-2 is an oxygen sensor for a calcium-sensitive potassium channel. *Science* 306: 2093–2097, 2004.
197. Wolin MS, Ahmad M, and Gupte SA. Oxidant and redox signaling in vascular oxygen sensing mechanisms: basic concepts, current controversies, and potential importance of cytosolic NADPH. *Am J Physiol Lung Cell Mol Physiol* 289: L159–L173, 2005.

198. Xu W, Koeck T, Lara AR, Neumann D, DiFilippo FP, Koo M, Janocha AJ, Masri FA, Arroliga AC, Jennings C, Dweik RA, Tuder RM, Stuehr DJ, and Erzurum SC. Alterations of cellular bioenergetics in pulmonary artery endothelial cells. *Proc Natl Acad Sci USA* 104: 1342–1347, 2007.
199. Yamakawa M, Liu LX, Date T, Belanger AJ, Vincent KA, Akita GY, Kuriyama T, Cheng SH, Gregory RJ, and Jiang C. Hypoxia-inducible factor-1 mediates activation of cultured vascular endothelial cells by inducing multiple angiogenic factors. *Circ Res* 93: 664–673, 2003.
200. Yoshida Y, Takahashi K, Okita K, Ichisaka T, and Yamanaka S. Hypoxia enhances the generation of induced pluripotent stem cells. *Cell Stem Cell* 5: 237–241, 2009.
201. Yung CW, Wu LQ, Tullman JA, Payne GF, Bentley WE, and Barbari TA. Transglutaminase crosslinked gelatin as a tissue engineering scaffold. *J Biomed Mater Res A* 83A: 1039–1046, 2007.
202. Zhang H, Bosch-Marce M, Shimoda LA, Tan YS, Baek JH, Wesley JB, Gonzalez FJ, and Semenza GL. Mitochondrial autophagy is an HIF-1-dependent adaptive metabolic response to hypoxia. *J Biol Chem* 283: 10892–10903, 2008.
203. Zhang X, Liu L, Wei X, Tan YS, Tong L, Chang R, Ghanamah MS, Reinblatt M, Marti GP, Harmon JW, and Semenza GL. Impaired angiogenesis and mobilization of circulating angiogenic cells in HIF-1alpha heterozygous-null mice after burn wounding. *Wound Repair Regen* 18: 198–201, 2010.
204. Zhou X, Rowe RG, Hiraoka N, George JP, Wirtz D, Mosher DF, Virtanen I, Chernousov MA, and Weiss SJ. Fibronectin fibrillogenesis regulates three-dimensional neovessel formation. *Genes Dev* 22: 1231–1243, 2008.
205. Zisch AH, Lutolf MP, Ehrbar M, Raeber GP, Rizzi SC, Davies N, Schmokel H, Bezuidenhout D, Djonov V, Zilla P, and Hubbell JA. Cell-demanded release of VEGF from synthetic, biointeractive cell ingrowth matrices for vascularized tissue growth. *FASEB J* 17: 2260–2262, 2003.
206. Zisch AH, Lutolf MP, and Hubbell JA. Biopolymeric delivery matrices for angiogenic growth factors. *Cardiovasc Pathol* 12: 295–310, 2003.

Chapter 8
Microenvironmental Regulation of Tumor Angiogenesis: Biological and Engineering Considerations

David W. Infanger, Siddharth P. Pathi, and Claudia Fischbach

8.1 Introduction

The formation of new blood vessels through angiogenesis is a universally recognized hallmark of cancer that promotes tumor aggressiveness in various ways [1]. Historically, it was believed that tumors recruit blood vessels to meet their increasing nutrient and oxygen (O_2) demands and to remove the resulting metabolic waste products [2]. However, more recently, it has become clear that the newly formed vascular channels also serve as conduits for host cells (e.g., bone-marrow-derived endothelial and hematopoietic progenitor cells), soluble signaling factors, and cancer cells, which collectively promote further tumor growth and metastasis [1]. Additionally, the tumor vasculature also plays a critical role in the success of anticancer therapies. While perfusion processes are necessary for uniform distribution of therapeutic agents throughout the tumor mass, the aberrant and leaky nature of tumor vessels frequently precludes efficacious drug delivery [3]. As such, the field of cancer biology is heavily invested in resolving the biological and physical contributions that culminate in tumor angiogenesis.

The observation that tumor microenvironments are characterized by newly infiltrated blood vessels was first established over a century ago [4], and the concept to inhibit this process by antiangiogenic strategies has been explored for nearly four decades now [5]. The most widely investigated avenue of antiangiogenic therapy targets vascular endothelial growth factor (VEGF), a secreted protein factor that is upregulated in most cancers in response to decreased tissue O_2-tension (i.e., hypoxia) [6]. Following secretion, VEGF is sequestered within the extracellular matrix (ECM) and drives tumor angiogenesis by regulating the behavior of endothelial cells (i.e., the cells lining blood vessels) in a spatially and temporally controlled manner [7]. In hopes of thwarting angiogenesis, and hence tumor

C. Fischbach (✉)
Department of Biomedical Engineering, Cornell University, 157 Weill Hall, Ithaca, NY 14853, USA
e-mail: cf99@cornell.edu

S. Gerecht (ed.), *Biophysical Regulation of Vascular Differentiation and Assembly*, Biological and Medical Physics, Biomedical Engineering,
DOI 10.1007/978-1-4419-7835-6_8,

growth, a variety of therapeutic agents have been developed that directly (e.g., VEGF-blocking antibodies) or indirectly (e.g., inhibitors of matrix-degrading enzymes that block the cell-demanded liberation of VEGF from its ECM depots) inhibit VEGF signaling [8–11]. However, despite their therapeutic promise, clinical trials involving these agents have revealed varied efficacy [2] – and in some instances have even promoted tumor growth and metastasis [12, 13]. Furthermore, antiangiogenic therapies are typically associated with considerable side effects, ranging from musculoskeletal pain and inflammation to direct drug toxicity [8, 14–16]. Gaining an improved understanding of the mechanisms and effects of tumor angiogenesis will be critical to advance current antiangiogenic therapies and enhance their overall clinical benefit for patients.

Three-dimensional (3D) microenvironmental conditions are critical to human tumor growth in general and angiogenesis in particular; however, conventional in vitro and in vivo approaches are limited in their ability to accurately recapitulate these environmental scenarios. The unique tumor microenvironment, including cell–cell and cell–ECM interactions, as well as spatiotemporal fluctuations in mechanical forces, nutrient gradients, and O_2, is considered to be an essential component of tumor survival and progression [1, 17]. These variables are difficult to control and measure in animals, and furthermore, mouse models of cancer fail to faithfully represent the phenotype or progression of human disease [18]. While two-dimensional (2D) culture approaches allow for the systematic dissection of cellular and molecular signaling pathways, these approaches are unsuccessful in recapitulating the complexity of the environment that influences tumor angiogenesis. For example, tumor cells grown in conventional 2D monolayer culture exhibit a vastly different proangiogenic profile as compared to the same cells maintained in vivo or cultured within a 3D tumor model [19]. The ability to precisely control cell–microenvironment interactions in a pathologically relevant context makes 3D culture models particularly attractive for studying tumor angiogenesis. Original 3D designs, including gel-based systems as well as spheroid cultures, have significantly improved our understanding of cell–microenvironment interactions [20, 21], but new 3D engineering-based models offer new inroads to specifically address limitations of these early prototypes.

This chapter discusses the role of cell–microenvironment interactions in tumor angiogenesis and highlights specific engineering approaches that will likely advance our knowledge of underlying signaling mechanisms and their effects. As a model, we review the impact of VEGF and chemokine signaling (in particular, interleukin-8 [IL-8]) on tumor vascularization and discuss a subset of microenvironmental conditions that modulate the signaling transduced by these proangiogenic factors. Specifically, we address the impact of cell–cell and cell–ECM interactions, as well as mechanical stimuli and environmental stress (i.e., hypoxia and acidosis). A short overview of the underlying biology precedes the description of engineering approaches for these individual design parameters (Fig. 8.1). Lastly, we provide an outlook for future studies of angiogenesis that may further our understanding of the events involved in this process, with the hope of broadening the therapeutic spectrum of antiangiogenic therapies.

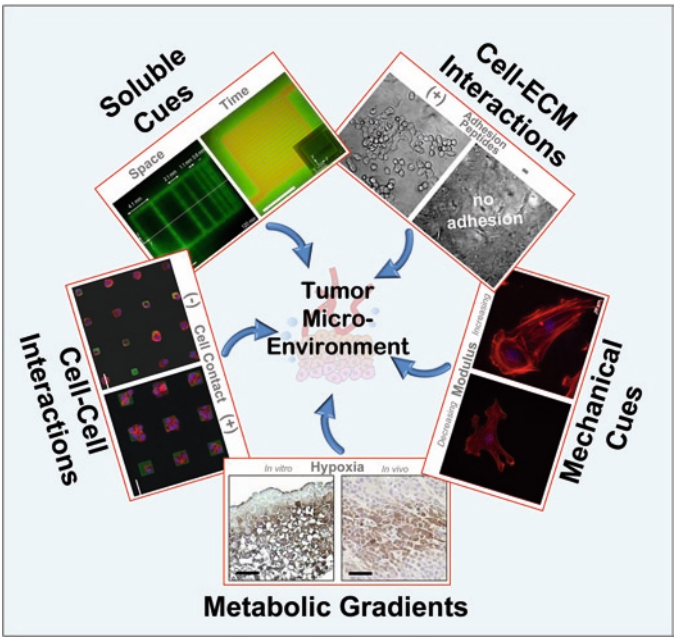

Fig. 8.1 Recreation of tumor microenvironmental conditions by engineered model systems. (**a**) Microfluidic channels embedded in hydrogel scaffolds can be used to mimic spatiotemporal gradients of soluble factors contributing to tumor angiogenesis (Modified from [19]). (**b**) Modification of nonadhesive polymers (e.g., alginate) with adhesion peptides (e.g., RGD) enables studies of the angiogenic capacity of tumor-residing cells in response to cell–ECM interactions. (**c**) Modulation of hydrogel stiffness (e.g., RGD-alginate) via adjusting the cross-linking density allows to evaluate the role of matrix-derived mechanical cues that, for example, regulate cell morphological changes during tumor angiogenesis (Modified from [34]). (**d**) 3D culture of tumor cells within porous PLGA scaffolds recreates hypoxic niches as typical of tumors in vivo (Modified from [47]). (**e**) Micropatterning of differently sized fibronectin features with Parylene templates makes it possible to study the angiogenic phenotype of cells cultured individually or in the presence of direct cell-to-cell contact (Modified from [88])

8.2 Concepts in Tissue Engineering and Tumor Angiogenesis

8.2.1 Biomaterial Systems for Engineering-Based Investigations of Angiogenesis

Biomaterials describe artificial ECMs that can serve as readily adaptable platforms to develop engineering models of tumor angiogenesis. These platforms can be fabricated into drug delivery and cell culture matrices that simulate specific biological and physicochemical interactions present in the tumor microenvironment in vivo. The biomaterials that are typically employed for this purpose are polymeric in nature and can be processed into 2D and 3D substrates. While the microarchitecture

of 3D polymeric scaffolds offers a more realistic context for in vivo-like growth conditions, 2D systems are sometimes preferable as they permit defined studies at the single cell level, which can be readily imaged.

Biomaterials used for engineering-based study of tumor angiogenesis can be of synthetic and natural origin [22, 23]. Synthetic polymers offer the advantages of simple customization and manipulation of material properties and are easily fabricated and readily available. On the other hand, natural polymers are typically more cytocompatible and often contain cell-adhesion peptides necessary for cell–material interactions [22, 24]. However, natural biomaterials are subject to batch-to-batch variability and limited by the extent to which physicochemical properties can be modulated [22, 23]. Commonly used natural polymers include collagen [24–27], fibrin [28], chitosan [24], alginate [29], and Matrigel™ [19, 30], while poly(glycolic acid) (PGA), poly(lactic acid) (PLA), and their copolymers (PLGA) are the most widely used synthetic polymers (Fig. 8.2). These polyesters are FDA-approved and are considered biocompatible [31, 32]. When placed in an aqueous environment, the otherwise water-insoluble materials degrade through hydrolysis, yielding naturally occurring metabolic by-products (lactic and glycolic acids). Both natural and synthetic polymers can be processed into different substrates for scaffold engineering.

Hydrogel-based systems exhibit structural similarity to the macromolecule-based ECM of many tissues and can be incorporated into in vivo studies using minimally invasive approaches (e.g., injection with syringe). They are amenable to encapsulation of cells and other bioactive molecules such as growth factors or chemokines [29, 33, 34], and their mechanical characteristics can be easily controlled by varying cross-linking density. Synthetic materials used to form hydrogels most often include derivatives of poly(ethylene glycol) (PEG). Despite offering suitable physical and chemical properties, PEG-based materials may be limited

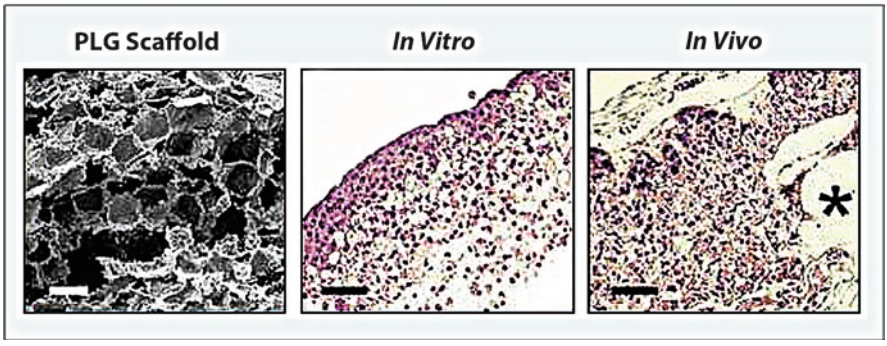

Fig. 8.2 3D culture of cancer cells within porous PLGA scaffolds. Oral squamous cell carcinoma cells seeded into porous PLGA scaffolds (*left*, scanning electron micrograph, scale bar 250 μm) develop into 3D tumor tissues with histological characteristics (*middle*, hematoxylin and eosin [H&E] staining, scale bar 100 μm) that closely resemble tumors formed by the same cells in vivo (*right*, H&E staining, scale bar 100 μm). *Asterisk* denotes fragments of PLG scaffold (Modified from [19])

with regard to their biocompatibility and biodegradability. Instead, hydrogels formed from naturally derived polymers may provide highly biocompatible vehicles and can be fabricated from collagen, hyaluronic acid, and fibrin [20]. Alginates represent another class of naturally derived materials, which are widely used given their biocompatibility, low toxicity, relatively low cost, and gentle gelling properties [20]. Alginates are linear polysaccharide copolymers extracted from seaweeds and consist of (1–4)-linked beta-D-mannuronic acid (M) and alpha-L-guluronic acid (G). Gelation occurs in the presence of divalent cations (e.g., Ca^{2+}), which ionically cross-links the carboxylate groups in the poly-G blocks.

Alternatively, porous scaffolds made from solid polymers often serve as cell carriers to study angiogenesis. These systems provide structural support for 3D cell proliferation and tissue formation and are easy to handle due to their inherent durability. In order to facilitate functional tissue formation, the porosity of these scaffolds can be adjusted by using different scaffold fabrication techniques. For example, processing synthetic materials such as PLGA via particulate leaching [19, 29, 35], phase separation [36], or rapid-prototyping [37] approaches results in highly porous structures that ensure adequate nutrient and O_2 transfer (Fig. 8.2). Alternatively, electrospinning [38–40], which uses high voltages to draw polymers into fibers, can be applied to yield solid polymer scaffolds from materials ranging from synthetic PLGA to natural collagen. While electrospinning recreates the 3D fibrillar characteristics of the ECM, it typically prevents cellular invasion into deeper scaffold layers due to small pore size resulting from the electrospinning process.

8.2.2 Working Model of Tumor Angiogenesis

Angiogenesis is a complex process that is initiated by activation of an angiogenic switch and subsequently regulated by the multifaceted interplay between numerous cell types and protein factors (Fig. 8.3). In healthy patients, pro- and antiangiogenic factors are well balanced to maintain blood vessel homeostasis, but during tumorigenesis, an imbalance of proangiogenic factors leads to the activation of vessel-promoting signaling cascades [1, 2]. As a result, endothelial cells are recruited from neighboring blood vessels to the tumor, where they degrade the former vessel basement membrane (BM) to allow for subsequent rearrangement, proliferation, and migration into the adjacent ECM [41]. In normal tissues, the resulting new blood vessels are stabilized through recruitment of and association with mural cells (e.g., smooth muscle cells and pericytes), which halt the angiogenic process and stabilize the vasculature. However, this process is compromised during tumor angiogenesis due to the relative lack of vessel-stabilizing factors (e.g., angiopoietin-1 [Ang-1], platelet-derived growth factor [PDGF]) [42, 43], ultimately contributing to perpetual angiogenesis and dysfunctional vessel morphology.

While angiogenesis specifically refers to the formation of new blood vessels from local depots of preexisting endothelial cells, vasculogenesis also plays an

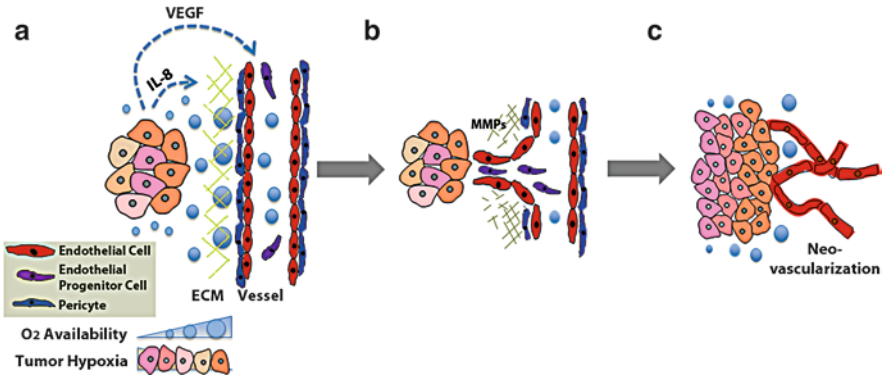

Fig. 8.3 A working model of tumor-mediated angiogenesis. (**a**) The increased metabolic demand of proliferating cancer cells exceeds the oxygen supply (*blue circles*) mediated by neighboring host vessels. This creates gradients of hypoxia in the tumor microenvironment and leads to the upregulation of proangiogenic factors, including vascular endothelial growth factor (VEGF) and interleukin 8 (IL-8). (**b**) These factors stimulate neovascularization by destabilizing adjacent vessels, activating endothelial cells (EC), and recruiting circulating endothelial progenitor cells (EPC). Simultaneous secretion of proteolytic enzymes from the tumor stroma including matrix metalloproteases (MMPs) stimulates the rearrangement of the ECM to allow for tube formation by ECs and EPCs. (**c**) Neovascularization of the tumor environment improves oxygen and nutrient delivery to the existing tumor cells, allowing tumor growth and metastasis

important role in tumor neoperfusion. Vasculogenesis is characterized by de novo formation of blood vessels via the recruitment of circulating cells that originate from the bone marrow (Fig. 8.3). These cells are activated and released into the circulation in response to tumor-secreted soluble factors. In particular, bone-marrow-derived endothelial progenitor cells (EPCs) have the capability to differentiate into endothelial cells and to assemble into blood vessels. In addition, myeloid cells are attracted to perivascular regions of the tumor, and this engagement contributes to increased tumor growth and perfusion. However, the rate at which EPCs associate with tumor vessels is relatively rare, and it has been suggested that the role of these cells in tumor vascularization is related to their secretion of proangiogenic molecules rather than their contribution to de novo neovascularization [44]. Therefore, EPCs assume a critical role in the formation of new tumor vasculature; however, their participation may be biased toward soluble signaling cues that promote angiogenesis.

To gain a more comprehensive and mechanistic understanding of tumor vascularization, it is paramount to elucidate the molecular underpinnings that shift homeostasis to favor angiogenesis. To this end, qualitative and quantitative analysis of the dynamic and functional relationship between cellular interactions (e.g., cell–ECM interactions, cell–cell contact), physical alterations (e.g., local differences in tumor O_2 tension, mechanical effects, transport phenomena), and chemical profiles (e.g., spatiotemporal changes in growth factors, cytokines) will be essential.

8.3 Review of Work: Biological and Engineering Considerations of Tumor Angiogenesis

Cell–microenvironment interactions typically support large-scale tissue homeostasis under normal conditions; however, during tumorigenesis, these interactions become perturbed and contribute to dysfunction. It has become increasingly clear that multiscale perturbation of the tissue, cellular, and molecular interactions not only influences tumor and endothelial cells but also affects the behavior of secondary host cell types (e.g., stromal cells and EPCs). Hence, the integrated effects of these variations and their role in instigating the angiogenic switch and subsequent formation of vessels need to be considered to improve the clinical efficacy of current antiangiogenic treatments, as well as to develop new therapeutic strategies.

8.3.1 Soluble Cues

8.3.1.1 Biological Perspective

The imbalance of environmental cues driving angiogenesis occurs when tumors upregulate multiple proangiogenic factors that ultimately promote tumor growth, progression, and metastasis. These secreted molecules include growth factors, chemokines, or small peptides (e.g., VEGF, IL-8), which act both locally and systemically to drive angiogenesis. Specifically, proangiogenic factors mediate local effects by altering tumor and host cell responses via autocrine and/or paracrine signaling, while endocrine effects aid in the recruitment of additional cell types (e.g., bone-marrow-derived EPCs) that can participate in neovascularization either by directly integrating in the vasculature or by secreting a chemical environment that further stimulates the formation of the tumor vasculature [44]. Of the myriad factors that contribute to angiogenesis, both physiologically as well as in the context of tumor growth, VEGF is the best characterized and most widely investigated. However, more recently, the chemokine IL-8 has received increasing attention because of its direct and indirect roles in tumor angiogenesis and its upregulation in response to VEGF-inhibiting therapies [45].

Vascular Endothelial Growth Factor

The VEGF family consists of multiple isoforms; however, the 45 kDa homolog VEGF-A (subsequently referred to as VEGF) is commonly considered the most important for tumor angiogenesis and is therefore the focus of this chapter. VEGF expression is drastically upregulated in tumors in response to a multitude of microenvironmental conditions that are characteristic of cancerous – but absent in

normal – tissues. For example, decreased O_2 levels and increased acidosis, as well as altered cell–cell contact, can all lead to enhanced VEGF concentrations in the tumor interstitium (discussed in more detail later in this chapter) [6, 41, 46, 47]. In order to initiate its downstream effects, VEGF binds to two primary receptors: VEGF-R1 (Flt-1) and VEGF-R2 (KDR/Flk-1) [48]. Historically, VEGF receptor-2 (VEGF-R2) has been considered the main receptor responsible for proangiogenic signaling, whereas VEGF-R1 is thought to function as a decoy receptor that prevents VEGF binding to VEGF-R2 [6]. However, recent experimental evidence indicates that VEGF-R1 may play a more important role in tumor neovascularization than originally thought, since it promotes vasculogenesis by enhancing the recruitment and incorporation of EPCs [49].

Tumors regulate VEGF signaling not only through modified gene expression and receptor pathways but also by sequestration of the secreted protein within the surrounding ECM, which thereby functions as a biological delivery system. Specifically, tumors secrete VEGF in four different isoforms ($VEGF_{121}$, $VEGF_{165}$, $VEGF_{189}$, and $VEGF_{206}$) that all originate from the same gene but vary in the molecular size of their ECM-binding regions [22]. $VEGF_{121}$ is freely diffusible and immediately bioavailable upon cellular secretion as it lacks a heparin-binding domain, and this may affect endothelial cell responses (Fig. 8.4). $VEGF_{165}$, the predominant isoform in tumors [50], exists in both free and bound forms, whereas $VEGF_{189}$ and $VEGF_{209}$ are almost entirely confined to the ECM and are liberated only upon cellular demand. Cells trigger the release of VEGF from these ECM depots by secreting proteolytic, ECM-degrading enzymes (e.g., heparanase or matrix metalloproteinases [MMPs]), which stratify VEGF diffusion that is believed to be critical for guided blood-vessel recruitment [7]. ECM-bound VEGF influences not only the bioavailability of VEGF but also VEGF receptor signaling. In particular, VEGF signaling via VEGF-R2 occurs in cooperation with neuropilin-1 (NRP-1), and ECM-binding enhances the effectiveness of this process by improving the interactions between VEGF, VEGF-R2, and NRP-1. Finally, the importance of ECM components in VEGF-R2 signal transduction is further underlined by the finding that $VEGF_{121}$ elicits reduced biologic potency relative to the ECM-binding isoforms [7].

Historically, VEGF has been presumed to exert its action exclusively on the vascular endothelium. This notion was based on the assumption that tumor cells are largely responsible for the production of VEGF but not its cognate receptor and that endothelial cells (as well as EPCs) express VEGF receptors but not the cognate ligand [6]. However, it is now increasingly clear that VEGF also modulates the behavior of many other cell types present within the tumor microenvironment. For example, recent evidence indicates that cancer cells express VEGF receptors and that autocrine, nonangiogenic VEGF signaling is critical for the ability of these cells to evade apoptosis and progress toward invasive and metastatic disease [51–53]. Additionally, inflammatory cells enhance migration in response to tumor-derived VEGF [54]. Consequently, nonvascular VEGF signal transduction may promote tumor vascularization through secondary, indirect mechanisms that need to be considered to fully elucidate the role of VEGF in the tumor microenvironment.

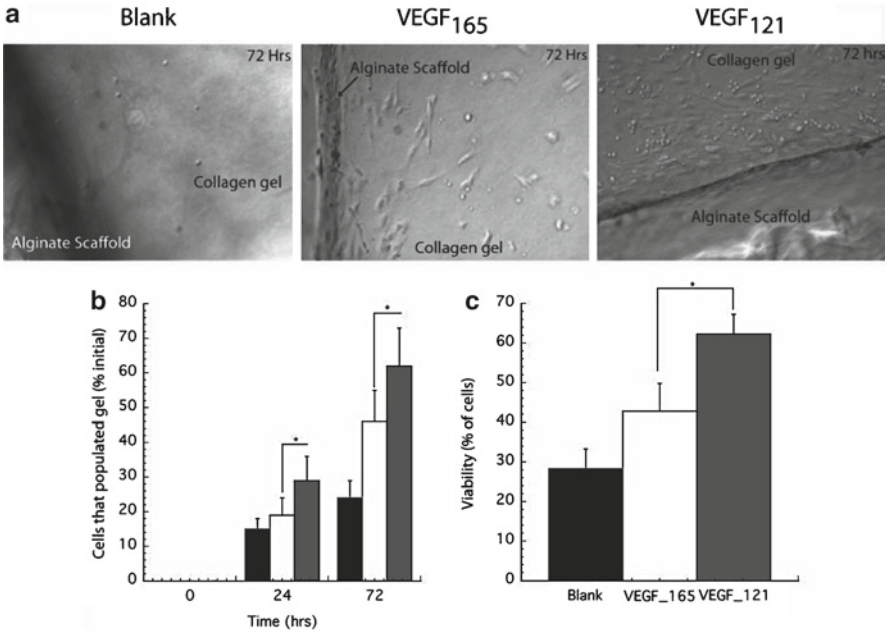

Fig. 8.4 Diffusion characteristics of matrix-binding proangiogenic factors influence endothelial cell behavior. (**a**) Phase-contrast micrographs and (**b**) quantification of endothelial cell migration out of alginate scaffolds into collagen tissue mimics in the absence (Blank, *black bar*) or presence of matrix-bound ($VEGF_{165}$, *open bar*) or freely diffusable ($VEGF_{121}$, *gray bar*) morphogen. (**c**) Viability of the cells that migrated out from scaffolds incorporating no VEGF (blank), $VEGF_{165}$, or $VEGF_{121}$. These results indicate that release of diffusible VEGF from its ECM depots is necessary for angiogenesis. Magnification ×200 for all photomicrographs (Modified from [90])

Chemokines (IL-8)

Chemokines are small (8–10 kDa), heparin-binding proteins that modulate tumor angiogenesis via both indirect and direct mechanisms. While chemokines have originally been identified for their role in leukocyte recruitment during inflammation [55], they can also directly modulate tumor angiogenesis by affecting endothelial and EPC cell behavior [56–59]. In particular, members of the CXC (cysteine–amino acid–cysteine) chemokine family either stimulate or inhibit angiogenesis depending on their specific molecular structure. Specifically, chemokines that contain a glutamic acid–leucine–arginine (i.e., ELR) motif immediately proximal to the CXC motif promote tumor angiogenesis [59–61], whereas CXC chemokines lacking this ELR sequence are thought to be angiostatic [56, 59].

Of the proangiogenic ELR^+ CXC chemokines, most attention has focused on CXCL8 (IL-8) [62]. IL-8 is upregulated in various experimental cancer models including ovarian cancer [63], non-small cell lung cancer [64], and renal cell tumors [65], and blockade of IL-8 signaling reduces angiogenesis-dependent tumor growth and metastasis [66]. Although IL-8 binds and activates both CXCR1 and

CXCR2 G-protein-coupled receptors [67, 68], CXCR2 seems to be the main receptor mediating IL-8-dependent changes in endothelial cell behavior and consequential tumor growth [66, 69, 70]. In addition to directly promoting angiogenesis by enhancing endothelial cell migration, proliferation, and capillary tube formation [71], IL-8 can also indirectly stimulate tumor neovascularization. For example, IL-8 signaling leads to upregulation of MMP-2 and MMP-9 in both endothelial and tumor cells [72–74], and increases the recruitment of neutrophils to the tumor microenvironment [75]. These effects collectively promote angiogenesis by enabling endothelial cells to more readily invade their surrounding and by enhancing the total concentration of proangiogenic factors, respectively.

Multiple microenvironmental conditions contribute to IL-8 upregulation and signaling in tumors. For example, cell–ECM interactions, cell–cell contact, and culture dimensionality all affect IL-8 secretion [19, 34, 47]. Similarly, spatiotemporal variations in tumor O_2 levels play a critical role in establishing the proangiogenic effects mediated by IL-8 [76] as hypoxia stimulates activator protein (AP-1) and nuclear factor-κB (NF-κB) transcription factors, both of which stimulate IL-8 expression [77]. Finally, simultaneous and/or sequential interactions with other soluble factors induce IL-8 transcription. In particular, increased VEGF levels can elevate IL-8 concentrations in the tumor microenvironment by activating IL-8 expression in endothelial cells [78]. Increased IL-8, in turn, maintains the angiogenic phenotype of endothelial cells via a positive feedback mechanism as the initiation of CXCR2 signaling pathways culminates in many of the same signaling events that are activated by VEGF receptors (e.g., cell proliferation, migration, and inhibition of apoptosis) [61]. Since VEGF and IL-8 exhibit distinct diffusion kinetics due to their different molecular weights (and possibly extent of ECM-binding) [34], a complex spatiotemporal pattern of VEGF and IL-8 expression may exist in tumors. Gaining a thorough qualitative and quantitative understanding of these patterns may enhance the efficacy of current antiangiogenic therapies, which globally inhibit VEGF signaling, but do not consider its interactions with IL-8.

8.3.1.2 Engineering Perspective

Pathologically relevant culture models of tumor angiogenesis need to recreate the characteristics of the biological growth factor delivery system. Proangiogenic factors and other morphogens promote the formation of new blood vessels by regulating endothelial cell behavior in a well-concerted, spatiotemporal manner. Hence, global application of individual factors such as VEGF or IL-8 to 2-D monolayer cultures is unlikely to recapitulate in vivo-like cell responses. Similarly, bolus injection of these molecules (or their inhibitors) into tumor-implanted animals may not lead to a thorough quantitative understanding of tumor angiogenesis, as this method typically results in unlocalized supply, short tissue-exposure times (due to rapid elimination and degradation of these molecules), and encourages experimental artifacts in tissues outside of the tumor [20, 79]. Polymeric scaffolds can overcome these limitations by simultaneously enabling biologically inspired drug delivery and cell culture.

Temporal Control of Factor Release

The release rate of polymeric scaffolds can be adjusted via the choice and molecular composition of the respective polymer. Natural polymers (e.g., prepared from fibrin or heparinized collagen) frequently result in rapid (i.e., "burst") release of proteins, thus prohibiting the sustained and localized presentation of factors to cells [80]. However, the physicochemical characteristics of polymeric matrices can be readily adjusted to result in prolonged delivery by exploiting diffusion and/or polymer degradation mechanisms, i.e., the main mechanisms by which proteins are released from drug delivery vehicles [20]. For example, physical or covalent cross-linking of hydrated polymer chains allows for fine tuning of pore size and, hence, diffusion-mediated release from hydrogels. The resulting delivery can be further modulated by varying the concentration, charge, and degree of hydration of the respective polymer [81, 82]. As the release from solid, degrading polymeric systems (e.g., PLGA) is determined by the rate of degradation and subsequent dissolution, it is possible to adjust protein release kinetics by varying the molecular weight as well as the molar ratio of lactic and glycolic acids [83, 84].

Choosing an appropriate scaffold fabrication strategy provides another avenue to modulate the physicochemical characteristics, and hence release kinetics, of the delivery vehicle. PLGA scaffolds are frequently used as scaffold systems for 3D tumor models and can be fabricated by a gas-foaming particulate leaching technique [85] (Fig. 8.2). This organic solventless process allows for incorporation of bioactive molecules by simply mixing them with polymer particles prior to further processing of the protein–polymer mixture [29]. The release kinetics of these systems (typically on the order of days to weeks) can be further delayed by preencapsulating the proteins into PLGA microspheres that are subsequently used to fabricate the scaffolds. Typically, proteins are processed with this approach, but an even more sustained release can be achieved by incorporating DNA instead. This strategy additionally relies on the cellular production and secretion of the encoded proangiogenic molecule and, therefore, results in a delay in factor availability, relative to direct protein delivery [86].

Spatial Control of Factor Release

Polymer processing techniques not only allow for control of the temporal presentation of angiogenic molecules but can also be exploited to generate spatial gradients of soluble factors that play a role in directing blood-vessel recruitment. For example, PLGA scaffolds with spatially compartmentalized VEGF can be designed based on mathematical models of VEGF release required to generate appropriate tissue concentrations and gradients. These systems can be fabricated by assembling multiple individual scaffolds into layers and subsequently forming a single scaffold using the gas-foaming particulate leaching technique described above [87]. Alternatively, microfabrication strategies may be exploited to control the chemical environment of a tumor on a micrometer scale. In particular, the inclusion of

microchannels into macroscopic hydrogel scaffolds (e.g., alginate) maintains the benefits inherent to 3D culture (viz., reconstitution of 3D cell–microenvironment interactions), while enabling well-controlled spatial and temporal distribution gradients of soluble factors in these biomimetic model systems (Fig. 8.1a) [88].

Spatial control of soluble factor concentrations can also be achieved with artificial ECMs that exploit the heparin-binding characteristics of proangiogenic molecules and their subsequent cell-demanded release. In particular, the presence of ECM-binding sites in $VEGF_{165}$ and their absence in $VEGF_{121}$ affect the diffusion characteristics of these molecules in the ECM, which may be critical for directing cell behavior during angiogenesis [89]. This concept has been supported by a recent study in which EPCs were incorporated into alginate in combination with either $VEGF_{121}$ or $VEGF_{165}$. Outward migration of EPCs into the surrounding tissue was rapid with $VEGF_{121}$ yet stunted with $VEGF_{165}$ (Fig. 8.4) [90]. To mimic enzymatically driven angiogenic factor release from ECM stores, polymeric vehicles have been developed that respond to the local activity of proteolytic enzymes (e.g., MMPs, plasmin, heparanase) provided by invading cells. For example, fibrin or peptide cross-linked PEG gels can incorporate VEGF via covalent linkages, or by covalently linking heparin-binding peptides, which then provide affinity binding sites for VEGF [91–93].

Systems to Mimic Signaling by Multiple Factors

Biomimicry of multiple soluble-factor signaling using a single 3D matrix allows for the study of reciprocal growth-factor interactions on tumor angiogenesis. Specifically, delivery approaches that allow for simultaneous and sequential supply of factors have been developed. Simultaneous interactions between multiple growth factors may be recreated by simply incorporating the different proteins into the same polymer delivery system. The utility of this general concept has earlier been demonstrated in the context of bone regeneration in which simultaneous delivery of bone morphogenetic protein-2 (BMP-2) and transforming growth factor-beta (TGF-beta) improved bone formation relative to the individual delivery of either growth factor [94]. Composite systems that are composed of multiple polymer phases with distinct release kinetics may be used to achieve sequential delivery of angiogenic factors. The molecule(s) acting initially during regeneration are typically incorporated into a rapidly releasing phase, whereas the factor(s) involved in later signaling are loaded in a phase with more sustained release characteristics. This approach has been applied in the context of therapeutic angiogenesis for sequential delivery of VEGF and PDGF from poly (lactic-*co*-glycolic acid) (PLGA) scaffolds [29]. In this study, scaffolds were designed to release the two growth factors with differential kinetics by mixing polymer microspheres containing preencapsulated PDGF with lyophilized VEGF before processing by gas-foaming particulate leaching. A similar scaffold system may be appropriate to model the sequential expression profiles of VEGF and IL-8 in tumors in vivo [19].

8.3.2 Cell–ECM Interactions

8.3.2.1 Biological Perspective

The ECM regulates tumor vascularization not only by functioning as a biological delivery system for proangiogenic factors but also by directly modulating the proangiogenic capacity of cells participating in tumor vascularization. Specifically, soluble and insoluble cues presented by the ECM collectively act to promote or inhibit angiogenesis by influencing the physicochemical characteristics of the ECM itself and by altering the adhesion-dependent behavior of the cells residing within the matrix.

ECM Structure and Composition

The ECM comprises a cell-secreted, amorphous environment, which provides structural support and regulates cell behavior. In normal epithelial tissues, the origin of most cancers, as well as the endothelium, the ECM is organized into a specialized structure that is organized as a 50–100 nm-sheet, primarily composed of type IV collagen, laminin, and proteoglycans, termed the basement membrane (BM) [95–97]. The organization of the BM is largely dependent on assembly processes that depend on interactions with cell surface receptors and typically ensures blood vessel homeostasis by promoting cellular growth arrest. However, during physiological angiogenesis, the BM becomes remodeled, and its physicochemical characteristics are similarly altered. The resulting provisional matrix varies in composition (e.g., fibronectin, collagen I, and cryptic collagen domains that are otherwise sequestered within the BM) and exposes endothelial cells to proliferative cues, which ultimately enable vascular sprouting [95, 97, 98]. The ECM in tumors features typical characteristics of this provisional matrix and therefore exposes endothelial cells constantly to enhanced concentrations of ECM-derived proliferative cues [99, 100]. Additionally, the ECM in tumors is less cross-linked – and hence proteolytically less stable – which is conducive to abnormal sprouting and the leaky vasculature typical of tumors [101].

Integrins

Cells respond to tumor-inherent changes in ECM structure and composition via altered integrin signaling [102], and the resulting changes in cell behavior play an important role in tumor angiogenesis. Integrins are heterodimeric cell-surface receptors that confer ECM-binding specificity via their pairing of α- and β-subunits. For example, β1-containing integrins can mediate binding to fibronectin (e.g., $\alpha_4\beta_1$, $\alpha_5\beta_1$), collagen (e.g., $\alpha_1\beta_1$, $\alpha_2\beta_1$), or laminin (e.g., $\alpha_3\beta_1$, $\alpha_6\beta_1$) depending on the α-subunits with which they heterodimerize. Endothelial cells exhibit a subset

of these receptors in homeostatic blood vessels, but adjust their integrin expression profile to enable vascular sprouting. In particular, quiescent endothelial cells minimally express the fibronectin receptors $\alpha_5\beta_1$ and $\alpha_v\beta_3$; however, these integrins are significantly upregulated during tumor angiogenesis [103]. These changes are of particular relevance as fibronectin concentrations in tumors are concomitantly increased, which collectively promotes vascular endothelial cell survival [104, 105], proliferation, and motility [106, 107].

While integrin downstream signaling experts direct effects on endothelial cell behavior, cell–ECM interactions may also modulate these processes via secondary mechanisms. Specifically, integrin-binding can activate growth factor signaling pathways [108], and experimental evidence indicates that receptor cross talk between β_3-integrins and VEGF-R2 is necessary for the activation of VEGF-mediated downstream signaling [109]. Consequently, increased levels of $\alpha_v\beta_3$ as present in tumor-residing endothelial cells may further enhance VEGF signaling. Finally, integrin-dependent tumor cell interactions with ECM proteins that contain RGD-adhesion peptides (e.g., fibronectin) increase the angiogenic capacity of the tumor cells themselves [34]. Collectively, antiangiogenic therapies that target integrin signaling may decrease tumor vascularization via multiple mechanisms, i.e., by inhibiting the proangiogenic phenotype of not only endothelial cells but also tumor cells [110, 111].

Matrix Metalloproteinases

MMPs are secreted or membrane-associated zinc-dependent proteolytic enzymes that dynamically regulate tumor angiogenesis through multiple pathways. MMPs (viz., MMP-2 and MMP-9) are dramatically upregulated in response to tumor microenvironmental conditions (e.g., hypoxia) and play an important role in the activation of the angiogenic switch [112]. By participating in ECM degradation, MMPs not only open space for de novo capillary formation [113] but also promote vascular sprouting through unmasking cryptic ECM epitopes that can induce a proangiogenic endothelial phenotype by ligating $\alpha_v\beta_3$ integrins. These processes typically occur in a spatially well-coordinated manner and ultimately control the directionality of new vessel formation [114] (Fig. 8.3). Furthermore, MMPs are critical to the release of proangiogenic factors (e.g., VEGF, IL-8) from ECM confinement [115]. Hence, they function as molecular regulators of soluble factor delivery that induce not only the release but also the activation of ECM-sequestered proangiogenic stimuli [114]. In this capacity, MMP-9 seems to play a particularly important role as it is functionally linked to VEGF mobilization and VEGF-R2 signaling and as it induces the recruitment of bone-marrow-derived progenitor cells to sites of neovascularization [114].

In addition to modulating cell functions via ECM degradation, MMPs can also enhance tumor angiogenesis by directly modifying cell-surface receptors. For example, MMP-14 mediated proteolytic modification of $\alpha_v\beta_3$ integrins can influence

the subsequent downstream signaling of this receptor by activating focal adhesion kinase [116]. Conversely, MMPs can also inhibit angiogenesis by generating matrix fragments with antiangiogenic capacity (e.g., endostatin, tumstatin) [117]. As the generation of these fragments is MMP-type dependent, it is not surprising that broad-spectrum MMP inhibitors lack therapeutic efficacy in preclinical trials. In summary, MMPs clearly play important roles in tumor angiogenesis, and well-defined engineering systems may help to further elucidate the pleiotropic nature of these substances.

8.3.2.2 Engineering Perspective

Mimicry of ECM Structure and Composition

Biomimetic ECMs provide innovative systems to evaluate the mechanisms and effects through which the structure and composition of the ECM regulates tumor angiogenesis (Fig. 8.2b). Due to its bioactive properties and availability, Matrigel™ is commonly used for studying tumor cell behavior in 3D culture [118] and for elucidating signaling pathways involved in tumor angiogenesis [21]. For example, Matrigel™ promotes tumor formation [119], and these differences may be due to upregulation of proangiogenic factors (e.g., VEGF and basic fibroblast growth factor [bFGF]) [19]. However, Matrigel™ is derived from mouse sarcomas, contains growth factors, underlies significant batch-to-batch variation, and does not capture in vivo cell behavior appropriately [120]. Hence, better-defined systems are clearly needed to study 3D interactions with the ECM.

The ECM represents a composite system of fibers embedded within a hydrogel, and synthetic or natural ECM analogs can be used to dissect the relevance of this composition in tumor angiogenesis. To recapitulate the hydrated network, a variety of polymers may be used. In addition to alginate [34] and dextran-based hydrogels [121], hyaluronic acid represents a hydrophilic, nonadhesive material that is naturally degradable and influences angiogenesis in vivo. Its physical characteristics (e.g., degradation, mechanical properties, porosity) can be readily adjusted by methacrylation and subsequent photo-cross-linking, and the resulting polymers enable vascularization similar to fibrin [122, 123]. Alternatively, hydrophilic, synthetic materials including PEG and poly(acrylamide) may be used. PEG is particularly attractive due to its relative ease of functionalization (e.g., with polysaccharides), which provides additional routes for modulating degradation and cross-linking characteristics [124]. The development of self-assembling peptide hydrogels represents another strategy to generate ECM analogs. Such hydrogel scaffolds can be formed by self-assembly from aqueous solutions of peptide amphiphiles, and the resulting nanofibers can be customized to display peptide sequences representative of the ECM surrounding blood vessels (e.g., laminin, fibronectin) or to encapsulate cells and growth factors implicated in tumor angiogenesis [124].

Presentation of Integrin Engagement Sites

In order to study the role of altered integrin signaling in tumor angiogenesis, the engineered models need to provide adhesion sites for integrin binding. While porous scaffolds prepared from traditional biomaterials (e.g., PLGA) predominantly mediate cell adhesion via unspecific protein adsorption [21], a variety of materials have been developed that selectively guide cell adhesion by presenting integrin engagement sites in the form of small immobilized peptides. Covalent coupling of RGD sequences to otherwise nonadhesive matrices such as alginate and PEG renders these matrices bioactive. This has been demonstrated in RGD-modified alginate using carbodiimides chemistry, and culture of tumor cells within these matrices dramatically changes their proangiogenic capacity as compared to nonmodified alginate gels (Fig. 8.1b) [34]. Variation of the ligand density, the particular type (e.g., laminin peptide IKVAV vs. fibronectin peptide RGD), and the conformation (e.g., cyclic peptides vs. linear) of the utilized sequence facilitates further control over the cell responses [125].

The spatial arrangement of the presented adhesion peptides also plays an important role in guiding cell behavior and can be investigated using engineering models. Previous studies have identified that nanoscale adhesion ligand presentation modulates cell migration [126], hence, it may be possible that vascular sprouting is affected in a similar manner. Additionally, soluble angiogenic signaling cues may be altered by these phenomena, since cell adhesion events can activate growth factor receptors independent of ligand binding [127]. To evaluate these potential relationships, 2D hydrogel matrices could be modified to independently and systematically vary the surface density and the spatial distribution of adhesion peptides on otherwise nonadhesive backgrounds (e.g., PEG, alginate) [126, 128]. While such systems are typically generated with a uniform distribution of adhesion peptides, ligand gradients could also be incorporated. This has been demonstrated using RGD gradients covalently immobilized on PEG hydrogels. Such systems could be used to evaluate tumor and endothelial cell behavior during neovascularization [129].

MMP-Responsive Culture Systems

Natural and synthetic ECM analogs provide additional tools to study the role of MMP-mediated scaffold degradation in tumor angiogenesis. For example, Matrigel™ can be degraded by MMPs to allow invasion by both tumor and endothelial cells, and these alterations permit subsequent capillary tube formation [30,130]. To specifically assess tumor-mediated endothelial sprouting into collagen-rich interstitial tissues, vascularized tumor models may be developed using collagen hydrogels. By utilizing cell types that overexpress specific MMP variants in these systems, it will be possible to define which specific MMP isoforms regulate collagen invasion [25]. Additionally, collagen gels can be readily implanted into animal models, thereby permitting analysis of MMP-dependent collagen remodeling during neovascularization in vivo [26].

While collagen gels provide broadly applicable substrates to study cellular invasion, they do not allow for investigation of MMP-dependent release of proangiogenic molecules from their biologic delivery system, since these scaffolds lack growth-factor binding sites. Instead, artificial ECMs can mimic the sequestration, release, and activation of proangiogenic factors in response to cell demand. To this end, PEG copolymers with proteolytic sensitivity and cell-adhesion sites have been developed [131]. Specifically, these hydrogels were modified with RGD- and MMP-responsive peptides in the polymer backbone which were then conjugated to VEGF. When cells migrate into these systems, they release MMPs, which in turn locally degrade the hydrogel causing VEGF release. Importantly, endothelial cells invading these matrices upregulate proangiogenic MMP-2 expression, suggesting synergistic interactions between cell-mediated release of VEGF and angiogenic sprouting.

Engineered culture substrates can also be used to determine how cellular MMP-expression is modulated by physicochemical ECM characteristics, and how these changes affect tumor angiogenesis. For example, maleic anhydride copolymer films coated with fibronectin demonstrate that physicochemical surface characteristics of the polymer substrates affect the anchorage of fibronectin and modulate MMP secretion levels and capillary network formation [132]. Specifically, hydrophilic polymer surfaces led to weak binding and strong lateral reorganization of fibronectin into large fibrils, whereas hydrophobic surfaces promoted the formation of a dense network-like layer of small fibronectin fibrils. These changes had immediate relevance because hydrophilic polymer surfaces promoted MMP upregulation and capillary morphogenesis relative to hydrophobic surfaces. Since fibronectin fibril formation is differentially regulated in tumors relative to normal tissues [133], such systems could allow systematic investigations of how atypical matrix remodeling influences MMP expression and angiogenesis.

8.3.3 Mechanical Stimuli

8.3.3.1 Biological Perspective

Mechanical forces modulate tumor angiogenesis in a multifaceted manner by regulating the proangiogenic capacity of tumor-residing cells, influencing endothelial cell sprouting, and modulating the release of proangiogenic molecules. The signaling that alters cell behavior in response to mechanical stimuli is most commonly transduced by integrins [98, 134, 135]. Specifically, integrin mechanoreceptors link the extracellular environment to the cytoskeleton via focal adhesions, and application of mechanical stress to these contact points on endothelial cells results in altered intracellular signaling, which may be relevant to tumor angiogenesis [98, 135]. The mechanical forces dictating variations in integrin signaling are either generated by the cells directly in response to altered ECM stiffness or imposed upon cells through external mechanical stimulation.

Effect of Matrix Stiffness

Matrix stiffness regulates angiogenesis by controlling the incipient stages of blood vessel formation and by regulating the blood-vessel density in normal as well as tumorigenic tissues. As new vessels sprout, their local ECM is remodeled, which results in increased compliance compared to nonsprouting vessels in the surrounding ECM [98, 136]. This enhanced ECM compliance reduces the proliferative response of vascular endothelial cells to proangiogenic factors [95, 98, 134], which typically results in the termination of sprouting during normal angiogenesis and blood-vessel homeostasis. During tumor angiogenesis, however, this regulatory process is perturbed due to a proangiogenic environment and because of the increased collagen content and ECM cross-linking existing in tumors [137, 138]. As a result, endothelial cells residing in the tumor microenvironment interact with stiffer ECMs, which enables them to exert increased cytoskeletal tension and traction forces [139]. These matrix-mediated increases in cellular force drive tumor vascularization by modulating endothelial cell proliferation and VEGF-receptor signaling [140]. Furthermore, increased matrix stiffness may stimulate tumor angiogenesis by affecting the differentiation of circulating or tissue-residing stem cells, which can also contribute to blood vessel formation [141].

External Mechanical Stimuli

External mechanical stimuli in the tumor microenvironment encompass irregularities in fluid flow dynamics, and these alterations may not only affect cell behavior directly but also modulate the release of proangiogenic factors from their ECM depots [142]. The leaky nature of the tumor vasculature combined with an abnormally collagen-rich ECM leads to elevated interstitial hypertension within transformed tissues [143], which has been correlated with enhanced angiogenesis [144]. Additionally, tumor vessels are nonuniform and irregular, which instigate nonlaminar (i.e., turbulent) blood flow and generally altered fluid dynamics [145]. These changes not only promote endothelial cell proliferation [146] but also induce the production of proangiogenic molecules [147], suggesting that changes in fluid flow may indirectly contribute to new vessel formation.

8.3.3.2 Engineering Perspective

To evaluate the influence of mechanical stimuli on tumor angiogenesis, engineering models must recapitulate the dynamic interactions between substrate stiffness, externally applied force or fluid pressure, and cell behavior (Fig. 8.1c). In addition to providing matrices for 3D cell culture, polymeric scaffolds can be extensively modified in their mechanical properties and further subjected to external mechanical stimulation using appropriately designed bioreactors. Utilizing these combined approaches may reveal a more complete understanding of how mechanoregulation influences tumor angiogenesis.

Control over Matrix Stiffness

Owing to their structural and mechanical similarity, hydrogels are frequently used to study the effects of ECM stiffness on cell behavior. The rigidity of hydrogels can be readily modified by altering cross-link density or water content [148, 149]. For example, alginate gels are typically fabricated by ionic cross-linking of alginate in the presence of divalent cations (e.g., Ca^{2+}) [34] or by photo-cross-linking of methacrylated alginate [149]. By adjusting the ion concentration or degree of alginate methacrylation, it is possible to tune the mechanical properties of these hydrogels to mimic stiffnesses observed in normal or tumorigenic tissues. Importantly, alginate hydrogels can be further modified to present adhesion peptides (e.g., arginine–glycine–aspartic acid, RGD) necessary for cells to detect stiffness via engagement of their integrin mechanoreceptors (Fig. 8.1c) [29, 34]. Another material frequently used to study the consequences of ECM stiffness is the synthetic polymer polyacrylamide (PA) [141, 150]. Given its hydrophilic nature and lack of adhesion sites, PA does not inherently allow for cell attachment and thus is typically coated with a thin layer of collagen. Lastly, fibrin gels can be used to study how mechanoregulation influences tumor angiogenesis. Fibrin is a natural protein-based gel, which allows for intrinsic adhesion and biodegradability. The mechanical properties of fibrin gels are typically controlled by varying its concentration [151]. However, this approach simultaneously changes adhesion peptide density, which may complicate a clear interpretation of results as adhesion peptide density modulates cell behavior independent of matrix stiffness [152].

Recreation of External Mechanical Stimuli

The aberrant interstitial flow characteristic of tumors may modulate the release of proangiogenic factors from their ECM depots, and engineered models of capillary morphogenesis could help to elucidate the underlying mechanisms of this process. For example, embedding endothelial cells into matrices containing either tumor cells or proangiogenic factors, which are further subjected to varying interstitial fluid flows, could be utilized to study the combined effects of chemical and mechanical signaling cues on endothelial cell behavior. The value of this approach has already been realized using endothelial cells in VEGF-binding fibrin gels that were cultured in interstitial flow chambers. These culture models demonstrated that blood vessel formation is regulated by the synergy between interstitial flow and proteolytic VEGF-release from ECM depots. Specifically, interstitial fluid flow contributed to the MMP-mediated liberation of VEGF, thereby establishing VEGF gradients to guide capillary tube formation [153].

Traditionally, the effects of hemodynamic forces on cell behavior have been confined to the study of cardiovascular disease. However, these engineering tools could also be utilized to define adaptive cellular responses initiated by the aberrant blood flow commonly observed in tumors. For example, exposure of confluent cell monolayers to varying shear stresses under laminar or turbulent flow can be accomplished using modified flow chambers [146]. Furthermore, by spiking the culture

media used to generate the shear-stress fluctuations with bone-marrow-derived EPCs, it is theoretically possible to study vasculogenic processes as a function of perturbed blood flow [154]. Lastly, the effects of hydrodynamic shear patterns can also be evaluated using microbioreactor arrays. Such systems are advantageous as they allow for exposure of both 2D- and 3D-cultured cells to variable levels of hydrodynamic shear and further permit high-throughput analysis [155].

Engineering systems can also be used to evaluate mechanoregulatory processes that may result from interstitial hypertension or location of tumors in musculoskeletal tissues. For example, loading chambers have been designed to exert hydrostatic pressure on 3D culture models composed of hydrogels (e.g., agarose [156] and collagen [157]) or solid polymer scaffolds (e.g., PLGA) [158]. These systems have thus far been used to evaluate the response of normal cell types to cyclically applied hydrostatic pressure [156, 157], but they may also be important tools to discover a mechanistic relationship between enhanced pressure or compressive loads and tumor angiogenesis.

8.3.4 Cell–Stroma Interactions

8.3.4.1 Biological Perspective

Tumor angiogenesis is influenced by the dynamic interactions between tumor cells with the surrounding stroma that functions as a connective tissue framework. While normal stroma typically prevents tumor formation and progression, tumor-associated stroma supports these processes by secreting bioactive molecules (e.g., growth factors, ECM, proteolytic enzymes). These signaling factors, in turn, enhance angiogenic and inflammatory processes that further increase tumor aggressiveness [100]. Cell types composing the tumor stroma include fibroblasts, immune and inflammatory cells, and vascular endothelial cells [100]. These cells exchange information with the tumor microenvironment through direct cell-to-cell contact or via paracrine signaling routes. Both of these mechanisms are integrated within the complex and dynamic network of tumor signaling during growth and are believed to contribute to new vessel formation.

Cell-to-Cell Contact

Direct contact between cells is established through cellular junctions including adherens junctions. These multiprotein complexes contain cell adhesion molecules that are essential for normal functions of epithelial and endothelial tissues and are distinct from matrix adhesions. During tumor angiogenesis, adherens junctions are remodeled to enable the influx or efflux of cells, which ultimately enables vascular sprouting and metastasis [159]. For example, tumor cells undergo epithelial to

mesenchymal transition to invade their surrounding tissue, and this transition is accompanied by a loss of E-cadherin that normally maintains cell-to-cell contact in epithelial tissues. Instead, upregulation of N-cadherin occurs, thereby enabling tumor cells to associate directly with the stroma and endothelium [160]. This association not only initiates cancer metastasis but, importantly, also promotes angiogenesis by upregulating the expression of proangiogenic factors [161]. Endothelial cells, on the other hand, are mainly characterized by their expression of VE-cadherin. VE-cadherin mediates homotypic adhesion between endothelial cells, which typically protects their susceptibility to apoptosis and inhibits proliferation [162]. During tumor angiogenesis, VE-cadherin-mediated cell-to-cell adhesion between endothelial cells is weakened, ultimately promoting new vessel formation and transendothelial migration of tumor cells [163].

Paracrine Signaling

Tumor stromal cells are phenotypically distinct from nontumor associated cells of the same type [100, 164–166], and these changes drive tumor angiogenesis by altering many of the microenvironmental conditions conducive to new vessel growth. For example, tumor-associated fibroblasts secrete elevated levels of growth factors that not only modulate endothelial cell behavior but also upregulate stromal cell-derived factor-1 (SDF-1) transcription, which promotes tumor vascularization via the recruitment of EPCs [167, 168]. Tumor-associated fibroblasts can also differentiate into myofibroblasts and consequently assume characteristics of activated smooth muscle cells [100, 169]. These cells enhance the stiffness of the tumor microenvironment through modulation of collagen concentration and cross-linking density, which in turn increases tumor angiogenesis. Similarly, immune and inflammatory cells exhibit enhanced proangiogenic capability when they are associated with tumors. In particular, macrophages and neutrophils increase proangiogenic factor transcription in the presence of tumor cells (e.g., MMPs [170], VEGF, and bFGF [171]). Therefore, it is not surprising that increased vessel formation and density are positively correlated with macrophage number in several primary tumors [164, 172, 173].

8.3.4.2 Engineering Perspective

Conventional approaches to evaluate the effect of cell–stroma interactions on angiogenic signaling involve direct coseeding of different cell types in the same culture dish and indirect coculture in Transwell™ chambers (i.e., a 2D culture system that separates two cell types via a semipermeable membrane). Many of the engineering strategies discussed in earlier sections of this chapter can be used to overcome the obvious limitations associated with these conventional techniques, as cell–stroma interactions frequently lead to changes in soluble factor signaling,

cell–ECM interactions, and mechanical stimuli. The following engineering strategies additionally highlight approaches to evaluate effects mediated by direct cell-to-cell contact and culture models specifically designed to evaluate cell–stroma interactions (Fig. 8.1e).

Control over Direct Cell-to-Cell Contact

Microfabrication techniques offer great promise to investigate the role of cell-to-cell contact on tumor angiogenesis. In particular, microcontact printing or Parylene-template-based patterning techniques allow to seed cells individually or in the presence of cell–cell contact (Fig. 8.1e) [47, 174]. Alternatively, cell–cell junctions can be controlled micromechanically by using micromachined silicon culture substrates with movable and interchangeable parts [175]. These devices enable experimental control over tissue composition, spatial organization, and exposure duration of cell-to-cell interactions. With this approach, it is possible to distinguish the effects mediated by direct cell-to-cell contact from paracrine signaling induced by secreted soluble factors. All of these approaches provide exquisite control over 2D cell–cell interactions, but they may only partially recreate conditions influencing cell–cell interactions at the tissue level. Hence, multiple strategies have been developed to manipulate cell-to-cell interactions in 3D culture. For example, dielectrophoretic forces can create high-resolution 3D cellular structures of tumor or tumor stroma cells within a photopolymerizable hydrogel [176]. Similarly, PEG microwell cultures or collagen-based lithographically defined tissue arrays permit control over the size, shape, and homogeneity of 3D cultures and may be used to recapitulate 3D cell-to-cell contact intrinsic to tumor angiogenesis [177, 178].

Control over Paracrine Signaling

A variety of 3D coculture systems has been developed to assess the importance of multicellular interactions on blood vessel formation. For example, coseeding endothelial cells with mesenchymal stem cells (viz., a cell type that is frequently recruited by tumors) in fibrin gels demonstrates that the latter are required for angiogenic sprouting in stiffer ECMs as they enable matrix remodeling via MMPs [151]. However, these studies were conducted in the absence of tumor cells, whose inclusion in this system may be necessary to more appropriately mimic tumor stroma conditions. In support of this contention, similar studies involving coculture of endothelial cells with prostate cancer cells and/or fibroblasts in sandwiched fibrin–collagen gels suggest that the combination of all three cell types may be necessary to maximize angiogenic sprouting [179]. By further enhancing the complexity of these systems (e.g., by incorporating inflammatory cells), it may be possible to generate a more advanced understanding of cell–stroma interactions and their role in tumor angiogenesis.

Most 3D culture studies use artificial ECMs to evaluate the role of cell–stroma interactions. While these matrices offer advantages of availability and reproducibility, they may not appropriately capture the nature of the tumor stroma ECM that is predominantly secreted by fibroblasts. Stroma-derived 3D ECMs may overcome these limitations not only by providing 3D structural support but also by recapitulating the specific protein and growth factor content inherent to tumor microenvironments. These matrices can be developed by decellularization of fibroblast-deposited ECMs with alkaline detergent treatment and have been shown to regulate the growth and drug-responsiveness of human cancer cells [180]. Experimental evidence further indicates that matrices obtained from tumor-associated fibroblasts recreate tumor-typical structural and molecular cues that induce normal fibroblasts to assume characteristics of tumor-associated fibroblasts [181]. Generating matrices from whole tumors rather than individual cell types (e.g., by using strategies previously applied for cardiac tissues [182]) would be an exciting advancement of this strategy that could reveal new mechanistic insights into how spatiotemporal variations of ECM composition drive tumor angiogenesis.

8.3.5 Metabolic Stress

8.3.5.1 Biological Perspective

Hypoxia

Tumors exhibit decreased O_2 tension (hypoxia) relative to normal tissues, and these changes impact critical cell functions by compromising the replenishment of ATP stores. Hypoxia develops when the boundaries of simple gaseous diffusion are exceeded (roughly 150 μm; e.g., due to excessive cell proliferation or compromised blood vessel characteristics) and forces normal cells to initiate new blood vessel formation to endure these conditions. However, tumor cells are able to survive and even grow under reduced O_2, as they can adapt their signaling pathways accordingly. For example, tumor cells alter their DNA and protein synthesis profile in the presence of hypoxia [183] to promote proliferation and evade cell death, but importantly, they induce pathological angiogenesis. Likewise, EPCs can similarly adapt to hypoxia through decreased reliance on O_2 metabolism, which may further promote new vessel formation [88, 184].

Many of the hypoxia-dependent changes in proangiogenic factor expression (e.g., VEGF and IL-8) are mediated by hypoxia-inducible factors (HIFs). HIFs are heterodimeric transcription factors, which consist of an α and β subunit: HIF-α isoforms (HIF-1α, HIF-2α) are located in the cytosol and typically subjected to degradation in O_2-rich environments, whereas the β subunit (HIF-1β) is insensitive to O_2 and localized to the nucleus [185]. In the presence of hypoxia, HIF-1α is stabilized, which enables the transcriptional activation of hypoxia-response genes by translocating to the nucleus and dimerizing with HIF-1β [183]. Once normoxic

levels of O_2 are restored, HIF-1α is targeted for proteasomal degradation [186, 187], and HIF-mediated transcription ceases.

In tumors, proangiogenic factors are expressed in a very heterogeneous manner, and these fluctuations may be due to microenvironmentally controlled HIF activation. For example, IL-8 is predominantly expressed in the periphery of large tumors, whereas VEGF expression is enhanced in the tumor center [188]. This spatial pattern can be explained by the observation that central hypoxia may be the main regulator of VEGF secretion, while normoxic cell–ECM matrix interactions in the periphery drive the secretion of IL-8 [189]. Alternatively, it may be possible that these differences in VEGF and IL-8 expression are caused by cycling O_2 levels due to perturbed blood flow. Specifically, acute hypoxia stimulates HIF activation in tumor cells, but oncogenic mechanisms may lead to the stabilization of the resulting signaling even under normoxic conditions [190]. Similarly, microenvironmental deficiencies of available iron, a necessary cofactor for HIF-1α degradation, can stabilize HIF and sustain downstream gene transcription [191]. Finally, certain morphogens (e.g., insulin, epidermal growth factor) as well as mutations in tumor suppressor genes (e.g., p53, PTEN) can enable HIF-mediated gene transcription independent of hypoxia [192]. Consequently, microenvironmental conditions may upregulate tumor angiogenesis independent of hypoxia by promoting dysregulation of HIF itself.

Acidosis

Acidosis plays an important role in tumor angiogenesis and may be caused by hypoxia-dependent pathways that influence glycolysis and microenvironmental pH regulation. In the presence of a limited O_2 supply, many cancer cells maintain normal cell functions via enhanced reliance on anaerobic glycolysis [193, 194]. The resulting increase in lactic acid in conjunction with decreased nutrient availability, and limited removal of metabolic waste products, translates into enhanced acidity of the tumor environment as compared to that of normal tissues [195]. Furthermore, increased activity of carbonic anhydrase, which converts carbon dioxide and water to carbonic acid, enhances proton export from cancer cells, and decreases pH buffering capacity of the tumor interstitial fluid also contribute to the acidic microenvironment in which cancer cells reside [196, 197].

Acidosis stimulates the expression of proangiogenic factors in tumor cells via hypoxia-independent mechanisms. Specifically, tumor cells exposed to acidic conditions in conventional 2D culture (pH 6.7–7.1 vs. 7.4) not only exhibit enhanced levels of VEGF and IL-8 mRNA, but the stability of these transcripts also appears to be enhanced at lower pH [198]. In addition to increasing the concentration of proangiogenic factors, microenvironmental changes in pH, furthermore, influence VEGF mRNA splicing. Specifically, acidosis increases the concentration of freely diffusible $VEGF_{121}$ relative to matrix-binding VEGF isoforms, which may have important consequences for the development of proangiogenic factor gradients necessary for endothelial sprouting (Fig. 8.4) [199]. Finally, in vivo experiments

have underlined the importance of tumor acidosis in tumor angiogenesis by revealing that VEGF upregulation is not merely a consequence of hypoxia but rather due to a distinct, acidosis-dependent signaling mechanism [200].

8.3.5.2 Engineering Perspective

Resolving the cellular mechanisms through which hypoxia and acidosis regulate the angiogenic capacity of tumor cells and, ultimately, angiogenesis requires the development of innovative culture models. Tumor cells are typically maintained in buffered culture media at pH 7.4 and O_2 concentrations equal to ambient air (21% O_2). However, physiological tissue O_2 levels are significantly lower (between 2 and 9% O_2) [183], and the pH of tumors varies based on the metabolic activity of its cells. Furthermore, gradients in pH and O_2 (ranging from normoxia to hypoxia or even anoxia) are difficult to achieve through typical 2D monolayer culture. In the following lines, we discuss specific physical sciences-based approaches that help to overcome shortcomings of conventional 2D systems in the specific context of hypoxia. Nevertheless, these systems are broadly applicable and can be easily modified to also enable studies of tumor angiogenesis in response to acidosis.

Control of O_2 Levels in Culture

Tumor engineering strategies offer the opportunity to expose homogeneous or heterogeneous cell populations to spatiotemporally varying levels of O_2. For example, tumor cells cultured within 3D porous PLGA scaffolds autonomously recreate spatial variations in O_2 by developing into peripheral normoxic and central hypoxic niches (Fig. 8.1d) [19]. To evaluate the angiogenic capacity of tumor cells in a nondiffusion-limited 3D culture context, alginate-based, microfabricated tumor models may be invaluable [189]. The dimensions of these systems can be readily adjusted based on the O_2 consumption rates of the respective tumor cell type and subsequent mathematical modeling of the intratumor O_2 distribution. Another emerging strategy to measure tumor cell behavior in response to spatial O_2 variations employs microfabricated polydimethylsiloxane (PDMS) inserts, which can be placed in culture dishes at defined distances from the cells. While these membranes regulate the concentration of O_2 in the culture media through diffusion of O_2 across the PDMS membrane, they are predominantly useful in 2D studies [201]. Stacked, paper-supported, and cell-encapsulating gels can alternatively be employed to analyze molecular and genetic responses of cells as a function of O_2 and nutrient gradients under 3D conditions [202].

Microfluidic systems provide yet another strategy to readily control O_2 availability in cell culture. For example, 3D alginate-based microfluidic scaffolds could allow for precise spatial and temporal delivery of O_2, as well as for recreation of O_2 gradients within the scaffold [88, 203]. Similarly, 3D microvascular tubes consisting of confluent monolayers of human endothelial cells that line channels within tumor

cell-encapsulating collagen gels could be used to study tumor angiogenesis in response to spatiotemporal variations in O_2 perfusion [204, 205]. Such coculture systems may be particularly useful as they allow analysis of endothelial cell behavior in response to O_2-dependent changes of tumor cell behavior within the same system.

Monitoring of O_2 Levels in Culture

Platforms for advanced studies of tumor cell behavior will need to permit in situ monitoring of microenvironmental stress. Traditionally, tumor hypoxia is detected immunohistochemically (e.g., using pimonidazole HCl), but this approach lacks the ability to generate quantitative data [19]. Alternatively, polarographic or optical O_2 probes can be used; however, these insertable probes are of limited use in the tumor microenvironment because of their limited spatial resolution and inability to temporally map discrete O_2 concentrations [206, 207]. Hence, new approaches are required that enable real-time measurement of O_2 on a molecular scale in the tissue itself. To this end, the ability of O_2 to quench phosphorescence of particular luminophores can be exploited [208]. For example, encapsulation of ruthenium-based compounds into silica-based microparticles and incorporation of this system into 3D tumor cultures may allow mapping of O_2 variations in situ [209].

8.4 Summary and Future Perspectives

Antiangiogenic therapies provide promising avenues to treat cancer by targeting endothelial cells rather than tumor cells themselves. However, the clinical success of these treatments has been limited due in part to an incomplete understanding of tumor angiogenesis. Current techniques to study tumor vascularization rely heavily upon in vitro and in vivo models that may not faithfully recapitulate the interactions of human tumors with their environment. Through integration of biomaterials with drug delivery and tissue engineering strategies, the development of innovative, biologically inspired tumor models has emerged to address these shortcomings. These engineering systems can be specifically designed to recreate and study specific cell–microenvironment interactions that control tumor angiogenesis including soluble factor signaling, cell–ECM and cell–cell interactions, mechanical cues, and metabolic stress.

Additionally, engineered models of tumor vascularization may broadly transform studies of cancer stem cells grown in culture. Increasing experimental evidence indicates that many types of cancers are sustained by a distinct subpopulation of cancer stem cells, and these cells frequently localize to perivascular niches. Endothelial cells flanking these niches secrete factors that maintain these cells in a stem-cell-like, undifferentiated state. Hence, it is not surprising that antiangiogenic therapies reduce tumor growth not only by ablating blood vessel density but also

perhaps by decreasing the number of self-renewing cancer stem cells [210]. The tools and strategies highlighted in this chapter will be of immediate benefit to identify the mechanisms and effects that contribute to cancer stem cell development and maintenance.

Finally, biomimetic tumor analogs not only provide highly tunable platforms for fundamental research but can also be used as drug testing platforms. For example, these can be applied in industry for high-throughput testing of novel antiangiogenic compounds or drug targeting strategies. Additionally, engineered tumor models offer the potential for clinical translation and personalized medicine. Incorporation of patient-derived cells into these culture models will allow for comprehensive and predictive testing of patient-specific responses to a particular treatment. Such individualized tumor models could be further enhanced by incorporation into a microfluidic device that mimics multiorgan interactions. In these systems, it would further be possible to test drug toxicity in a pharmacokinetic-based manner, ultimately enhancing patient prognosis [211].

Acknowledgments The authors thank Emily Brooks and Daniel Brooks from Cornell University for their help with the editing of this chapter and acknowledge funding from the Cornell Nanobiotechnology Center (supported by the STC Program of the National Science Foundation under Agreement No. ECS-9876771), the Morgan Fund for Tissue Engineering, NIH (RC1 CA146065, 1U54 CA143876-01), and NSF (graduate research fellowship for SPP).

References

1. Hanahan, D. and R.A. Weinberg, *The hallmarks of cancer*. Cell, 2000. **100**(1): p. 57–70.
2. Carmeliet, P. and R.K. Jain, *Angiogenesis in cancer and other diseases*. Nature, 2000. **407**(6801): p. 249–57.
3. Jain, R.K., *Lessons from multidisciplinary translational trials on anti-angiogenic therapy of cancer*. Nat Rev Cancer, 2008. **8**(4): p. 309–16.
4. Goldmann, E., *The growth of malignant disease in man and the lower animals with special reference to the vascular system*. Lancet, 1907. **170**(4392): p. 1236–40.
5. Folkman, J., *Tumor angiogenesis: therapeutic implications*. N Engl J Med, 1971. **285**(21): p. 1182–6.
6. Kerbel, R.S., *Tumor angiogenesis*. N Engl J Med, 2008. **358**(19): p. 2039–49.
7. Ferrara, N., H.P. Gerber, and J. LeCouter, *The biology of VEGF and its receptors*. Nat Med, 2003. **9**(6): p. 669–76.
8. Coussens, L.M., B. Fingleton, and L.M. Matrisian, *Matrix metalloproteinase inhibitors and cancer: trials and tribulations*. Science, 2002. **295**(5564): p. 2387–92.
9. Hurwitz, H., et al., *Bevacizumab plus irinotecan, fluorouracil, and leucovorin for metastatic colorectal cancer*. N Engl J Med, 2004. **350**(23): p. 2335–42.
10. Sandler, A., et al., *Paclitaxel-carboplatin alone or with bevacizumab for non-small-cell lung cancer*. N Engl J Med, 2006. **355**(24): p. 2542–50.
11. Ferrara, N., et al., *Discovery and development of bevacizumab, an anti-VEGF antibody for treating cancer*. Nat Rev Drug Discov, 2004. **3**(5): p. 391–400.
12. Ebos, J.M., et al., *Accelerated metastasis after short-term treatment with a potent inhibitor of tumor angiogenesis*. Cancer Cell, 2009. **15**(3): p. 232–9.
13. Paez-Ribes, M., et al., *Antiangiogenic therapy elicits malignant progression of tumors to increased local invasion and distant metastasis*. Cancer Cell, 2009. **15**(3): p. 220–31.

14. Eskens, F.A. and J. Verweij, *The clinical toxicity profile of vascular endothelial growth factor (VEGF) and vascular endothelial growth factor receptor (VEGFR) targeting angiogenesis inhibitors; a review*. Eur J Cancer, 2006. **42**(18): p. 3127–39.
15. Jain, R.K., et al., *Lessons from phase III clinical trials on anti-VEGF therapy for cancer*. Nat Clin Pract Oncol, 2006. **3**(1): p. 24–40.
16. Verheul, H.M. and H.M. Pinedo, *Possible molecular mechanisms involved in the toxicity of angiogenesis inhibition*. Nat Rev Cancer, 2007. **7**(6): p. 475–85.
17. Bissell, M.J. and D. Radisky, *Putting tumours in context*. Nat Rev Cancer, 2001. **1**(1): p. 46–54.
18. Eccles, S.A., et al., *Preclinical models for the evaluation of targeted therapies of metastatic disease*. Cell Biophys, 1994. **24–25**: p. 279–91.
19. Fischbach, C., et al., *Engineering tumors with 3D scaffolds*. Nat Methods, 2007. **4**(10): p. 855–60.
20. Fischbach, C. and D.J. Mooney, *Polymeric systems for bioinspired delivery of angiogenic molecules. Polymers for regenerative medicine*. Adv Polym Sci, 2006. **203**: p. 191–221.
21. Zisch, A.H., M.P. Lutolf, and J.A. Hubbell, *Biopolymeric delivery matrices for angiogenic growth factors*. Cardiovasc Pathol, 2003. **12**(6): p. 295–310.
22. Fischbach, C. and D.J. Mooney, *Polymers for pro- and anti-angiogenic therapy*. Biomaterials, 2007. **28**(12): p. 2069–76.
23. Hubbell, J.A., *Biomaterials in tissue engineering*. Biotechnology (NY), 1995. **13**(6): p. 565–76.
24. Dang, J.M. and K.W. Leong, *Natural polymers for gene delivery and tissue engineering*. Adv Drug Deliv Rev, 2006. **58**(4): p. 487–99.
25. Hotary, K., et al., *Regulation of cell invasion and morphogenesis in a three-dimensional type I collagen matrix by membrane-type matrix metalloproteinases 1, 2, and 3*. J Cell Biol, 2000. **149**(6): p. 1309–23.
26. van Amerongen, M.J., et al., *The enzymatic degradation of scaffolds and their replacement by vascularized extracellular matrix in the murine myocardium*. Biomaterials, 2006. **27**(10): p. 2247–57.
27. Vaalamo, M., et al., *Distinct populations of stromal cells express collagenase-3 (MMP-13) and collagenase-1 (MMP-1) in chronic ulcers but not in normally healing wounds*. J Invest Dermatol, 1997. **109**(1): p. 96–101.
28. Hall, H., T. Baechi, and J.A. Hubbell, *Molecular properties of fibrin-based matrices for promotion of angiogenesis in vitro*. Microvasc Res, 2001. **62**(3): p. 315–26.
29. Richardson, T.P., et al., *Polymeric system for dual growth factor delivery*. Nat Biotechnol, 2001. **19**(11): p. 1029–34.
30. Kubota, S., et al., *Anti-alpha3 integrin antibody induces the activated form of matrix metalloprotease-2 (MMP-2) with concomitant stimulation of invasion through matrigel by human rhabdomyosarcoma cells*. Int J Cancer, 1997. **70**(1): p. 106–11.
31. Jain, R., et al., *Controlled drug delivery by biodegradable poly(ester) devices: different preparative approaches*. Drug Dev Ind Pharm, 1998. **24**(8): p. 703–27.
32. Rhodes, C.T. and S.C. Porter, *Coatings for controlled-release drug delivery systems*. Drug Dev Ind Pharm, 1998. **24**(12): p. 1139–54.
33. Kuo, C.K. and P.X. Ma, *Ionically crosslinked alginate hydrogels as scaffolds for tissue engineering: part 1. Structure, gelation rate and mechanical properties*. Biomaterials, 2001. **22**(6): p. 511–21.
34. Fischbach, C., et al., *Cancer cell angiogenic capability is regulated by 3D culture and integrin engagement*. Proc Natl Acad Sci U S A, 2009. **106**(2): p. 399–404.
35. Pathi, S.P., et al., *A novel 3-D mineralized tumor model to study breast cancer bone metastasis*. PLoS One, 2010. **5**(1): p. e8849.
36. Zhang, R. and P.X. Ma, *Poly(alpha-hydroxyl acids)/hydroxyapatite porous composites for bonetissue engineering. I. Preparation and morphology*. J Biomed Mater Res, 1999. **44**(4): p. 446–55.

37. Yeong, W.Y., et al., *Rapid prototyping in tissue engineering: challenges and potential*. Trends Biotechnol, 2004. **22**(12): p. 643–52.
38. Huang, L., et al., *Engineered collagen-PEO nanofibers and fabrics*. J Biomater Sci Polym Ed, 2001. **12**(9): p. 979–93.
39. Yoshimoto, H., et al., *A biodegradable nanofiber scaffold by electrospinning and its potential for bone tissue engineering*. Biomaterials, 2003. **24**(12): p. 2077–82.
40. Shin, H.J., et al., *Electrospun PLGA nanofiber scaffolds for articular cartilage reconstruction: mechanical stability, degradation and cellular responses under mechanical stimulation in vitro*. J Biomater Sci Polym Ed, 2006. **17**(1–2): p. 103–19.
41. Cuevas, I. and N. Boudreau, *Managing tumor angiogenesis: lessons from VEGF-resistant tumors and wounds*. Adv Cancer Res, 2009. **103**: p. 25–42.
42. Holash, J., S.J. Wiegand, and G.D. Yancopoulos, *New model of tumor angiogenesis: dynamic balance between vessel regression and growth mediated by angiopoietins and VEGF*. Oncogene, 1999. **18**(38): p. 5356–62.
43. Metheny-Barlow, L.J. and L.Y. Li, *The enigmatic role of angiopoietin-1 in tumor angiogenesis*. Cell Res, 2003. **13**(5): p. 309–17.
44. Ahn, G.O. and J.M. Brown, *Role of endothelial progenitors and other bone marrow-derived cells in the development of the tumor vasculature*. Angiogenesis, 2009. **12**(2): p. 159–64.
45. Mizukami, Y., et al., *Induction of interleukin-8 preserves the angiogenic response in HIF-1alpha-deficient colon cancer cells*. Nat Med, 2005. **11**(9): p. 992–7.
46. Chen, A., et al., *Endothelial cell migration and vascular endothelial growth factor expression are the result of loss of breast tissue polarity*. Cancer Res, 2009. **69**(16): p. 6721–9.
47. Tan, C.P., et al., *Parylene peel-off arrays to probe the role of cell–cell interactions in tumour angiogenesis*. Integr Biol (Camb), 2009. **1**(10): p. 587–94.
48. Dvorak, H.F., *Vascular permeability factor/vascular endothelial growth factor: a critical cytokine in tumor angiogenesis and a potential target for diagnosis and therapy*. J Clin Oncol, 2002. **20**(21): p. 4368–80.
49. Li, B., et al., *VEGF and PIGF promote adult vasculogenesis by enhancing EPC recruitment and vessel formation at the site of tumor neovascularization*. FASEB J, 2006. **20**(9): p. 1495–7.
50. Ferrara, N. and T. Davis-Smyth, *The biology of vascular endothelial growth factor*. Endocr Rev, 1997. **18**(1): p. 4–25.
51. Dallas, N.A., et al., *Functional significance of vascular endothelial growth factor receptors on gastrointestinal cancer cells*. Cancer Metastasis Rev, 2007. **26**(3–4): p. 433–41.
52. Dong, X., Z.C. Han, and R. Yang, *Angiogenesis and antiangiogenic therapy in hematologic malignancies*. Crit Rev Oncol Hematol, 2007. **62**(2): p. 105–18.
53. Mercurio, A.M., E.A. Lipscomb, and R.E. Bachelder, *Non-angiogenic functions of VEGF in breast cancer*. J Mammary Gland Biol Neoplasia, 2005. **10**(4): p. 283–90.
54. Ono, M., et al., *Biological implications of macrophage infiltration in human tumor angiogenesis*. Cancer Chemother Pharmacol, 1999. **43**(Suppl): p. S69–71.
55. Zlotnik, A. and O. Yoshie, *Chemokines: a new classification system and their role in immunity*. Immunity, 2000. **12**(2): p. 121–7.
56. Mehrad, B., M.P. Keane, and R.M. Strieter, *Chemokines as mediators of angiogenesis*. Thromb Haemost, 2007. **97**(5): p. 755–62.
57. Raman, D., et al., *Role of chemokines in tumor growth*. Cancer Lett, 2007. **256**(2): p. 137–65.
58. Singh, S., A. Sadanandam, and R.K. Singh, *Chemokines in tumor angiogenesis and metastasis*. Cancer Metastasis Rev, 2007. **26**(3–4): p. 453–67.
59. Strieter, R.M., et al., *CXC chemokines in angiogenesis*. Cytokine Growth Factor Rev, 2005. **16**(6): p. 593–609.
60. Belperio, J.A., et al., *CXC chemokines in angiogenesis*. J Leukoc Biol, 2000. **68**(1): p. 1–8.
61. Strieter, R.M., et al., *Cancer CXC chemokine networks and tumour angiogenesis*. Eur J Cancer, 2006. **42**(6): p. 768–78.

62. Koch, A.E., et al., *Interleukin-8 as a macrophage-derived mediator of angiogenesis*. Science, 1992. **258**(5089): p. 1798–801.
63. Yoneda, J., et al., *Expression of angiogenesis-related genes and progression of human ovarian carcinomas in nude mice*. J Natl Cancer Inst, 1998. **90**(6): p. 447–54.
64. Strieter, R.M., et al., *CXC chemokines in angiogenesis of cancer*. Semin Cancer Biol, 2004. **14**(3): p. 195–200.
65. Mestas, J., et al., *The role of CXCR2/CXCR2 ligand biological axis in renal cell carcinoma*. J Immunol, 2005. **175**(8): p. 5351–7.
66. Keane, M.P., et al., *Depletion of CXCR2 inhibits tumor growth and angiogenesis in a murine model of lung cancer*. J Immunol, 2004. **172**(5): p. 2853–60.
67. Holmes, W.E., et al., *Structure and functional expression of a human interleukin-8 receptor*. Science, 1991. **253**(5025): p. 1278–80.
68. Murphy, P.M. and H.L. Tiffany, *Cloning of complementary DNA encoding a functional human interleukin-8 receptor*. Science, 1991. **253**(5025): p. 1280–3.
69. Addison, C.L., et al., *The CXC chemokine receptor 2, CXCR2, is the putative receptor for ELR+ CXC chemokine-induced angiogenic activity*. J Immunol, 2000. **165**(9): p. 5269–77.
70. Heidemann, J., et al., *Angiogenic effects of interleukin 8 (CXCL8) in human intestinal microvascular endothelial cells are mediated by CXCR2*. J Biol Chem, 2003. **278**(10): p. 8508–15.
71. Li, A., et al., *IL-8 directly enhanced endothelial cell survival, proliferation, and matrix metalloproteinases production and regulated angiogenesis*. J Immunol, 2003. **170**(6): p. 3369–76.
72. Inoue, K., et al., *Interleukin 8 expression regulates tumorigenicity and metastases in androgen-independent prostate cancer*. Clin Cancer Res, 2000. **6**(5): p. 2104–19.
73. Li, A., et al., *Autocrine role of interleukin-8 in induction of endothelial cell proliferation, survival, migration and MMP-2 production and angiogenesis*. Angiogenesis, 2005. **8**(1): p. 63–71.
74. Luca, M., et al., *Expression of interleukin-8 by human melanoma cells up-regulates MMP-2 activity and increases tumor growth and metastasis*. Am J Pathol, 1997. **151**(4): p. 1105–13.
75. De Larco, J.E., B.R. Wuertz, and L.T. Furcht, *The potential role of neutrophils in promoting the metastatic phenotype of tumors releasing interleukin-8*. Clin Cancer Res, 2004. **10**(15): p. 4895–900.
76. Waugh, D.J. and C. Wilson, *The interleukin-8 pathway in cancer*. Clin Cancer Res, 2008. **14**(21): p. 6735–41.
77. Shono, T., et al., *Involvement of the transcription factor NF-kappaB in tubular morphogenesis of human microvascular endothelial cells by oxidative stress*. Mol Cell Biol, 1996. **16**(8): p. 4231–9.
78. Nor, J.E., et al., *Up-regulation of Bcl-2 in microvascular endothelial cells enhances intratumoral angiogenesis and accelerates tumor growth*. Cancer Res, 2001. **61**(5): p. 2183–8.
79. Yancopoulos, G.D., et al., *Vascular-specific growth factors and blood vessel formation*. Nature, 2000. **407**(6801): p. 242–8.
80. Shireman, P.K., et al., *Modulation of vascular cell growth kinetics by local cytokine delivery from fibrin glue suspensions*. J Vasc Surg, 1999. **29**(5): p. 852–61; discussion 862.
81. Lee, K.Y. and D.J. Mooney, *Hydrogels for tissue engineering*. Chem Rev, 2001. **101**(7): p. 1869–79.
82. Drury, J.L. and D.J. Mooney, *Hydrogels for tissue engineering: scaffold design variables and applications*. Biomaterials, 2003. **24**(24): p. 4337–51.
83. Jain, R.A., *The manufacturing techniques of various drug loaded biodegradable poly(lactide-co-glycolide) (PLGA) devices*. Biomaterials, 2000. **21**(23): p. 2475–90.
84. Makino, K., et al., *Pulsatile drug release from poly (lactide-co-glycolide) microspheres: how does the composition of the polymer matrices affect the time interval between the initial burst and the pulsatile release of drugs?* Colloids Surf B Biointerfaces, 2000. **19**(2): p. 173–9.

85. Sheridan, M.H., et al., *Bioabsorbable polymer scaffolds for tissue engineering capable of sustained growth factor delivery*. J Control Release, 2000. **64**(1–3): p. 91–102.
86. Shea, L.D., et al., *DNA delivery from polymer matrices for tissue engineering*. Nat Biotechnol, 1999. **17**(6): p. 551–4.
87. Chen, R.R., et al., *Integrated approach to designing growth factor delivery systems*. FASEB J, 2007. **21**(14): p. 3896–903.
88. Choi, N.W., et al., *Microfluidic scaffolds for tissue engineering*. Nat Mater, 2007. **6**(11): p. 908–15.
89. Silva, E.A. and D.J. Mooney, *Effects of VEGF temporal and spatial presentation on angiogenesis*. Biomaterials, 2010. **31**(6): p. 1235–41.
90. Silva, E.A., et al., *Material-based deployment enhances efficacy of endothelial progenitor cells*. Proc Natl Acad Sci U S A, 2008. **105**(38): p. 14347–52.
91. Ehrbar, M., et al., *Cell-demanded liberation of VEGF121 from fibrin implants induces local and controlled blood vessel growth*. Circ Res, 2004. **94**(8): p. 1124–32.
92. Ehrbar, M., et al., *The role of actively released fibrin-conjugated VEGF for VEGF receptor 2 gene activation and the enhancement of angiogenesis*. Biomaterials, 2008. **29**(11): p. 1720–9.
93. Zisch, A.H., et al., *Covalently conjugated VEGF–fibrin matrices for endothelialization*. J Control Release, 2001. **72**(1–3): p. 101–13.
94. Simmons, C.A., et al., *Dual growth factor delivery and controlled scaffold degradation enhance in vivo bone formation by transplanted bone marrow stromal cells*. Bone, 2004. **35**(2): p. 562–9.
95. Kalluri, R., *Basement membranes: structure, assembly and role in tumour angiogenesis*. Nat Rev Cancer, 2003. **3**(6): p. 422–33.
96. Timpl, R. and J.C. Brown, *Supramolecular assembly of basement membranes*. Bioessays, 1996. **18**(2): p. 123–32.
97. Xu, J., et al., *Proteolytic exposure of a cryptic site within collagen type IV is required for angiogenesis and tumor growth in vivo*. J Cell Biol, 2001. **154**(5): p. 1069–79.
98. Ingber, D.E., *Mechanical signaling and the cellular response to extracellular matrix in angiogenesis and cardiovascular physiology*. Circ Res, 2002. **91**(10): p. 877–87.
99. Rak, J., et al., *Mutant ras oncogenes upregulate VEGF/VPF expression: implications for induction and inhibition of tumor angiogenesis*. Cancer Res, 1995. **55**(20): p. 4575–80.
100. Mueller, M.M. and N.E. Fusenig, *Friends or foes – bipolar effects of the tumour stroma in cancer*. Nat Rev Cancer, 2004. **4**(11): p. 839–49.
101. Yuan, F., et al., *Vascular permeability in a human tumor xenograft: molecular size dependence and cutoff size*. Cancer Res, 1995. **55**(17): p. 3752–6.
102. Hynes, R.O., *Integrins: versatility, modulation, and signaling in cell adhesion*. Cell, 1992. **69**(1): p. 11–25.
103. Alghisi, G.C. and C. Ruegg, *Vascular integrins in tumor angiogenesis: mediators and therapeutic targets*. Endothelium, 2006. **13**(2): p. 113–35.
104. Kim, S., et al., *Inhibition of endothelial cell survival and angiogenesis by protein kinase A*. J Clin Invest, 2002. **110**(7): p. 933–41.
105. Stupack, D.G., et al., *Apoptosis of adherent cells by recruitment of caspase-8 to unligated integrins*. J Cell Biol, 2001. **155**(3): p. 459–70.
106. Kim, S., et al., *Regulation of angiogenesis in vivo by ligation of integrin alpha5beta1 with the central cell-binding domain of fibronectin*. Am J Pathol, 2000. **156**(4): p. 1345–62.
107. Kim, S., M. Harris, and J.A. Varner, *Regulation of integrin alpha vbeta 3-mediated endothelial cell migration and angiogenesis by integrin alpha5beta1 and protein kinase A*. J Biol Chem, 2000. **275**(43): p. 33920–8.
108. Clark, E.A. and J.S. Brugge, *Integrins and signal transduction pathways: the road taken*. Science, 1995. **268**(5208): p. 233–9.
109. Soldi, R., et al., *Role of alphavbeta3 integrin in the activation of vascular endothelial growth factor receptor-2*. EMBO J, 1999. **18**(4): p. 882–92.

110. Voest, E.E., *Inhibitors of angiogenesis in a clinical perspective*. Anticancer Drugs, 1996. **7**(7): p. 723–7.
111. Gladson, C.L., *Expression of integrin alpha v beta 3 in small blood vessels of glioblastoma tumors*. J Neuropathol Exp Neurol, 1996. **55**(11): p. 1143–9.
112. Overall, C.M. and C. Lopez-Otin, *Strategies for MMP inhibition in cancer: innovations for the post-trial era*. Nat Rev Cancer, 2002. **2**(9): p. 657–72.
113. Ii, M., et al., *Role of matrix metalloproteinase-7 (matrilysin) in human cancer invasion, apoptosis, growth, and angiogenesis*. Exp Biol Med (Maywood), 2006. **231**(1): p. 20–7.
114. Deryugina, E.I. and J.P. Quigley, *Pleiotropic roles of matrix metalloproteinases in tumor angiogenesis: contrasting, overlapping and compensatory functions*. Biochim Biophys Acta, 2010. **1803**(1): p. 103–20.
115. Bergers, G., et al., *Matrix metalloproteinase-9 triggers the angiogenic switch during carcinogenesis*. Nat Cell Biol, 2000. **2**(10): p. 737–44.
116. Deryugina, E.I., et al., *Processing of integrin alpha(v) subunit by membrane type 1 matrix metalloproteinase stimulates migration of breast carcinoma cells on vitronectin and enhances tyrosine phosphorylation of focal adhesion kinase*. J Biol Chem, 2002. **277**(12): p. 9749–56.
117. Ghajar, C.M., S.C. George, and A.J. Putnam, *Matrix metalloproteinase control of capillary morphogenesis*. Crit Rev Eukaryot Gene Expr, 2008. **18**(3): p. 251–78.
118. Lee, G.Y., et al., *Three-dimensional culture models of normal and malignant breast epithelial cells*. Nat Methods, 2007. **4**(4): p. 359–65.
119. Kratzke, R.A., et al., *RB-mediated tumor suppression of a lung cancer cell line is abrogated by an extract enriched in extracellular matrix*. Cell Growth Differ, 1993. **4**(8): p. 629–35.
120. Zimrin, A.B., B. Villeponteau, and T. Maciag, *Models of in vitro angiogenesis: endothelial cell differentiation on fibrin but not matrigel is transcriptionally dependent*. Biochem Biophys Res Commun, 1995. **213**(2): p. 630–8.
121. Sun, G., et al., *Functional groups affect physical and biological properties of dextran-based hydrogels*. J Biomed Mater Res A, 2010. **93**(3): p. 1080–90.
122. Baier Leach, J., et al., *Photocrosslinked hyaluronic acid hydrogels: natural, biodegradable tissue engineering scaffolds*. Biotechnol Bioeng, 2003. **82**(5): p. 578–89.
123. Khetan, S. and J. Burdick, *Cellular encapsulation in 3D hydrogels for tissue engineering*. J Vis Exp, 2009. (32).
124. Baldwin, A.D. and K.L. Kiick, *Polysaccharide-modified synthetic polymeric biomaterials*. Biopolymers, 2010. **94**(1): p. 128–40.
125. Hersel, U., C. Dahmen, and H. Kessler, *RGD modified polymers: biomaterials for stimulated cell adhesion and beyond*. Biomaterials, 2003. **24**(24): p. 4385–415.
126. Maheshwari, G., et al., *Cell adhesion and motility depend on nanoscale RGD clustering*. J Cell Sci, 2000. **113**(Pt 10): p. 1677–86.
127. Miranti, C.K. and J.S. Brugge, *Sensing the environment: a historical perspective on integrin signal transduction*. Nat Cell Biol, 2002. **4**(4): p. E83–90.
128. Kong, H.J., S. Hsiong, and D.J. Mooney, *Nanoscale cell adhesion ligand presentation regulates nonviral gene delivery and expression*. Nano Lett, 2007. **7**(1): p. 161–6.
129. Guarnieri, D., et al., *Covalently immobilized RGD gradient on PEG hydrogel scaffold influences cell migration parameters*. Acta Biomater, 2010. **6**(7): p. 2532–9.
130. Jadhav, U., et al., *Inhibition of matrix metalloproteinase-9 reduces in vitro invasion and angiogenesis in human microvascular endothelial cells*. Int J Oncol, 2004. **25**(5): p. 1407–14.
131. Seliktar, D., et al., *MMP-2 sensitive, VEGF-bearing bioactive hydrogels for promotion of vascular healing*. J Biomed Mater Res A, 2004. **68**(4): p. 704–16.
132. Pompe, T., M. Markowski, and C. Werner, *Modulated fibronectin anchorage at polymer substrates controls angiogenesis*. Tissue Eng, 2004. **10**(5–6): p. 841–8.
133. Wierzbicka-Patynowski, I., Y. Mao, and J.E. Schwarzbauer, *Continuous requirement for pp60-Src and phospho-paxillin during fibronectin matrix assembly by transformed cells*. J Cell Physiol, 2007. **210**(3): p. 750–6.

134. Ingber, D.E. and J. Folkman, *Mechanochemical switching between growth and differentiation during fibroblast growth factor-stimulated angiogenesis in vitro: role of extracellular matrix*. J Cell Biol, 1989. **109**(1): p. 317–30.
135. Meyer, C.J., et al., *Mechanical control of cyclic AMP signalling and gene transcription through integrins*. Nat Cell Biol, 2000. **2**(9): p. 666–8.
136. Ausprunk, D.H. and J. Folkman, *Migration and proliferation of endothelial cells in preformed and newly formed blood vessels during tumor angiogenesis*. Microvasc Res, 1977. **14**(1): p. 53–65.
137. Paszek, M.J., et al., *Tensional homeostasis and the malignant phenotype*. Cancer Cell, 2005. **8**(3): p. 241–54.
138. Levental, K.R., et al., *Matrix crosslinking forces tumor progression by enhancing integrin signaling*. Cell, 2009. **139**(5): p. 891–906.
139. Reinhart-King, C.A., M. Dembo, and D.A. Hammer, *Cell–cell mechanical communication through compliant substrates*. Biophys J, 2008. **95**(12): p. 6044–51.
140. Mammoto, A., et al., *A mechanosensitive transcriptional mechanism that controls angiogenesis*. Nature, 2009. **457**(7233): p. 1103–8.
141. Engler, A.J., et al., *Matrix elasticity directs stem cell lineage specification*. Cell, 2006. **126**(4): p. 677–89.
142. Lee, K.Y., et al., *Controlled growth factor release from synthetic extracellular matrices*. Nature, 2000. **408**(6815): p. 998–1000.
143. Netti, P.A., et al., *Role of extracellular matrix assembly in interstitial transport in solid tumors*. Cancer Res, 2000. **60**(9): p. 2497–503.
144. Boucher, Y., M. Leunig, and R.K. Jain, *Tumor angiogenesis and interstitial hypertension*. Cancer Res, 1996. **56**(18): p. 4264–6.
145. Shimamoto, K., et al., *Intratumoral blood flow: evaluation with color Doppler echography*. Radiology, 1987. **165**(3): p. 683–5.
146. Davies, P.F., et al., *Turbulent fluid shear stress induces vascular endothelial cell turnover in vitro*. Proc Natl Acad Sci U S A, 1986. **83**(7): p. 2114–7.
147. Resnick, N. and M.A. Gimbrone, Jr., *Hemodynamic forces are complex regulators of endothelial gene expression*. FASEB J, 1995. **9**(10): p. 874–82.
148. West, E.R., et al., *Physical properties of alginate hydrogels and their effects on in vitro follicle development*. Biomaterials, 2007. **28**(30): p. 4439–48.
149. Jeon, O., et al., *Photocrosslinked alginate hydrogels with tunable biodegradation rates and mechanical properties*. Biomaterials, 2009. **30**(14): p. 2724–34.
150. Pelham, R.J., Jr. and Y. Wang, *Cell locomotion and focal adhesions are regulated by substrate flexibility*. Proc Natl Acad Sci U S A, 1997. **94**(25): p. 13661–5.
151. Ghajar, C.M., et al., *Mesenchymal stem cells enhance angiogenesis in mechanically viable prevascularized tissues via early matrix metalloproteinase upregulation*. Tissue Eng, 2006. **12**(10): p. 2875–88.
152. Hsiong, S.X., et al., *Integrin-adhesion ligand bond formation of preosteoblasts and stem cells in three-dimensional RGD presenting matrices*. Biomacromolecules, 2008. **9**(7): p. 1843–51.
153. Helm, C.L., et al., *Synergy between interstitial flow and VEGF directs capillary morphogenesis in vitro through a gradient amplification mechanism*. Proc Natl Acad Sci U S A, 2005. **102**(44): p. 15779–84.
154. Greenberg, A.W., W.G. Kerr, and D.A. Hammer, *Relationship between selectin-mediated rolling of hematopoietic stem and progenitor cells and progression in hematopoietic development*. Blood, 2000. **95**(2): p. 478–86.
155. Figallo, E., et al., *Micro-bioreactor array for controlling cellular microenvironments*. Lab Chip, 2007. **7**(6): p. 710–9.
156. Finger, A.R., et al., *Differential effects on messenger ribonucleic acid expression by bone marrow derived human mesenchymal stem cells seeded in agarose constructs due to ramped and steady applications of cyclic hydrostatic pressure*. Tissue Eng, 2007. **13**(6): p. 1151–8.

157. Wagner, D.R., et al., *Hydrostatic pressure enhances chondrogenic differentiation of human bone marrow stromal cells in osteochondrogenic medium*. Ann Biomed Eng, 2008. **36**(5): p. 813–20.
158. Yang, Y., et al., *Effect of cyclic loading on in vitro degradation of poly(*l*-lactide-co-glycolide) scaffolds*. J Biomater Sci Polym Ed, 2010. **21**(1): p. 53–66.
159. Ebnet, K., *Organization of multiprotein complexes at cell–cell junctions*. Histochem Cell Biol, 2008. **130**(1): p. 1–20.
160. Hazan, R.B., et al., *Cadherin switch in tumor progression*. Ann N Y Acad Sci, 2004. **1014**: p. 155–63.
161. Orr, F.W., et al., *Interactions between cancer cells and the endothelium in metastasis*. J Pathol, 2000. **190**(3): p. 310–29.
162. Cavallaro, U., S. Liebner, and E. Dejana, *Endothelial cadherins and tumor angiogenesis*. Exp Cell Res, 2006. **312**(5): p. 659–67.
163. Voura, E.B., M. Sandig, and C.H. Siu, *Cell–cell interactions during transendothelial migration of tumor cells*. Microsc Res Tech, 1998. **43**(3): p. 265–75.
164. Leek, R.D. and A.L. Harris, *Tumor-associated macrophages in breast cancer*. J Mammary Gland Biol Neoplasia, 2002. **7**(2): p. 177–89.
165. Liotta, L.A. and E.C. Kohn, *The microenvironment of the tumour–host interface*. Nature, 2001. **411**(6835): p. 375–9.
166. Bhowmick, N.A. and H.L. Moses, *Tumor–stroma interactions*. Curr Opin Genet Dev, 2005. **15**(1): p. 97–101.
167. Rasmussen, A.A. and K.J. Cullen, *Paracrine/autocrine regulation of breast cancer by the insulin like growth factors*. Breast Cancer Res Treat, 1998. **47**(3): p. 219–33.
168. Orimo, A., et al., *Stromal fibroblasts present in invasive human breast carcinomas promote tumor growth and angiogenesis through elevated SDF-1/CXCL12 secretion*. Cell, 2005. **121**(3): p. 335–48.
169. Lewis, M.P., et al., *Tumour-derived TGF-beta1 modulates myofibroblast differentiation and promotes HGF/SF-dependent invasion of squamous carcinoma cells*. Br J Cancer, 2004. **90**(4): p. 822–32.
170. Chen, J.J., et al., *Tumor-associated macrophages: the double-edged sword in cancer progression*. J Clin Oncol, 2005. **23**(5): p. 953–64.
171. Lewis, C.E., et al., *Cytokine regulation of angiogenesis in breast cancer: the role of tumor associated macrophages*. J Leukoc Biol, 1995. **57**(5): p. 747–51.
172. Leek, R.D., et al., *Necrosis correlates with high vascular density and focal macrophage infiltration in invasive carcinoma of the breast*. Br J Cancer, 1999. **79**(5–6): p. 991–5.
173. Orre, M. and P.A. Rogers, *Macrophages and microvessel density in tumors of the ovary*. Gynecol Oncol, 1999. **73**(1): p. 47–50.
174. Nelson, C.M. and C.S. Chen, *Cell–cell signaling by direct contact increases cell proliferation via a P13K-dependent signal*. FEBS Lett, 2002. **514**(2–3): p. 238–42.
175. Hui, E.E. and S.N. Bhatia, *Micromechanical control of cell–cell interactions*. Proc Natl Acad Sci U S A, 2007. **104**(14): p. 5722–6.
176. Albrecht, D.R., et al., *Probing the role of multicellular organization in three-dimensional microenvironments*. Nat Methods, 2006. **3**(5): p. 369–75.
177. Nelson, C.M., J.L. Inman, and M.J. Bissell, *Three-dimensional lithographically defined organotypic tissue arrays for quantitative analysis of morphogenesis and neoplastic progression*. Nat Protoc, 2008. **3**(4): p. 674–8.
178. Karp, J.M., et al., *Controlling size, shape and homogeneity of embryoid bodies using poly(ethylene glycol) microwells*. Lab Chip, 2007. **7**(6): p. 786–94.
179. Janvier, R., et al., *Stromal fibroblasts are required for PC-3 human prostate cancer cells to produce capillary-like formation of endothelial cells in a three-dimensional co-culture system*. Anticancer Res, 1997. **17**(3A): p. 1551–7.
180. Serebriiskii, I., et al., *Fibroblast-derived 3D matrix differentially regulates the growth and drugresponsiveness of human cancer cells*. Matrix Biol, 2008. **27**(6): p. 573–85.

181. Amatangelo, M.D., et al., *Stroma-derived three-dimensional matrices are necessary and sufficient to promote desmoplastic differentiation of normal fibroblasts*. Am J Pathol, 2005. **167**(2): p. 475–88.
182. Ott, H.C., et al., *Perfusion-decellularized matrix: using nature's platform to engineer a bioartificial heart*. Nat Med, 2008. **14**(2): p. 213–21.
183. Bertout, J.A., S.A. Patel, and M.C. Simon, *The impact of O_2 availability on human cancer*. Nat Rev Cancer, 2008. **8**(12): p. 967–75.
184. Abaci, H.E., et al., *Adaptation to oxygen deprivation in cultures of human pluripotent stem cells, endothelial progenitor cells, and umbilical vein endothelial cells*. Am J Physiol Cell Physiol, 2010. **298**(6): 1527–37.
185. Pugh, C.W. and P.J. Ratcliffe, *Regulation of angiogenesis by hypoxia: role of the HIF system*. Nat Med, 2003. **9**(6): p. 677–84.
186. Ivan, M., et al., *HIFalpha targeted for VHL-mediated destruction by proline hydroxylation: implications for O_2 sensing*. Science, 2001. **292**(5516): p. 464–8.
187. Jaakkola, P., et al., *Targeting of HIF-alpha to the von Hippel–Lindau ubiquitylation complex by O_2-regulated prolyl hydroxylation*. Science, 2001. **292**(5516): p. 468–72.
188. Kumar, R., et al., *Spatial and temporal expression of angiogenic molecules during tumor growth and progression*. Oncol Res, 1998. **10**(6): p. 301–11.
189. Verbridge, S.S., et al., *Oxygen-controlled 3-D cultures to analyze tumor angiogenesis*. Tissue Eng Part A, 2010. **16**(7): p. 2133–41.
190. Chan, D.A., et al., *Role of prolyl hydroxylation in oncogenically stabilized hypoxia-inducible factor-1alpha*. J Biol Chem, 2002. **277**(42): p. 40112–7.
191. Le, N.T. and D.R. Richardson, *The role of iron in cell cycle progression and the proliferation of neoplastic cells*. Biochim Biophys Acta, 2002. **1603**(1): p. 31–46.
192. Maxwell, P.H., C.W. Pugh, and P.J. Ratcliffe, *Activation of the HIF pathway in cancer*. Curr Opin Genet Dev, 2001. **11**(3): p. 293–9.
193. Boucher, Y., L.T. Baxter, and R.K. Jain, *Interstitial pressure gradients in tissue-isolated and subcutaneous tumors: implications for therapy*. Cancer Res, 1990. **50**(15): p. 4478–84.
194. Vaupel, P., F. Kallinowski, and P. Okunieff, *Blood flow, oxygen and nutrient supply, and metabolic microenvironment of human tumors: a review*. Cancer Res, 1989. **49**(23): p. 6449–65.
195. Tannock, I.F., *Treatment of cancer with radiation and drugs*. J Clin Oncol, 1996. **14**(12): p. 3156–74.
196. Gillies, R.J., et al., *Tumorigenic 3T3 cells maintain an alkaline intracellular pH under physiological conditions*. Proc Natl Acad Sci U S A, 1990. **87**(19): p. 7414–8.
197. Stubbs, M., et al., *Metabolic consequences of a reversed pH gradient in rat tumors*. Cancer Res, 1994. **54**(15): p. 4011–6.
198. Shi, Q., et al., *Regulation of vascular endothelial growth factor expression by acidosis in human cancer cells*. Oncogene, 2001. **20**(28): p. 3751–6.
199. Elias, A.P. and S. Dias, *Microenvironment changes (in pH) affect VEGF alternative splicing*. Cancer Microenviron, 2008. **1**(1): p. 131–9.
200. Fukumura, D., et al., *Hypoxia and acidosis independently up-regulate vascular endothelial growth factor transcription in brain tumors in vivo*. Cancer Res, 2001. **61**(16): p. 6020–4.
201. Oppegard, S.C., et al., *Modulating temporal and spatial oxygenation over adherent cellular cultures*. PLoS One, 2009. **4**(9): p. e6891.
202. Derda, R., et al., *Paper-supported 3D cell culture for tissue-based bioassays*. Proc Natl Acad Sci U S A, 2009. **106**(44): p. 18457–62.
203. Bruzewicz, D.A., A.P. McGuigan, and G.M. Whitesides, *Fabrication of a modular tissue construct in a microfluidic chip*. Lab Chip, 2008. **8**(5): p. 663–71.
204. Fischbach-Teschl, C. and A. Stroock, *Microfluidic culture models of tumor angiogenesis*. Tissue Eng Part A, 2010. **16**(7): p. 2143–6.
205. Chrobak, K.M., D.R. Potter, and J. Tien, *Formation of perfused, functional microvascular tubes in vitro*. Microvasc Res, 2006. **71**(3): p. 185–96.

206. Braun, R.D., et al., *Comparison of tumor and normal tissue oxygen tension measurements using OxyLite or microelectrodes in rodents*. Am J Physiol Heart Circ Physiol, 2001. **280**(6): p. H2533–44.
207. Nordsmark, M., et al., *Measurements of hypoxia using pimonidazole and polarographic oxygen-sensitive electrodes in human cervix carcinomas*. Radiother Oncol, 2003. **67**(1): p. 35–44.
208. Rumsey, W.L., J.M. Vanderkooi, and D.F. Wilson, *Imaging of phosphorescence: a novel method for measuring oxygen distribution in perfused tissue*. Science, 1988. **241**(4873): p. 1649–51.
209. Acosta, M.A., et al., *Fluorescent microparticles for sensing cell microenvironment oxygen levels within 3D scaffolds*. Biomaterials, 2009. **30**(17): p. 3068–74.
210. Calabrese, C., et al., *A perivascular niche for brain tumor stem cells*. Cancer Cell, 2007. **11**(1): p. 69–82.
211. Sung, J.H., C. Kam, and M.L. Shuler, *A microfluidic device for a pharmacokinetic-pharmacodynamic (PK-PD) model on a chip*. Lab Chip, 2010. **10**(4): p. 446–55.

Chapter 9
Microbioreactors for Stem Cell Research

Donald O. Freytes and Gordana Vunjak-Novakovic

9.1 Introduction

One of the goals of tissue engineering is to grow functional tissues in a laboratory setting, either for implantation or use as a testing platform for the study of pathological conditions and drug discovery. To create tissues in vitro using engineering principles, it is necessary to overcome some of the current limitations such as the need for a sufficiently abundant source of cells required to create clinically sized, multicellular tissues. It is also necessary to develop technologies that can maintain the viability and function of such tissues in culture and following implantation [1, 2].

Stem cells can provide an untapped source of cells that can be differentiated into functional and supportive cell types, specific to the formation of a target tissue or organ. Undifferentiated stem cells, and to some extent, their differentiated progeny, require specialized microenvironments which should be tailored to resemble some aspects of the cellular environments found in the native tissue. There is a growing notion that to unlock the full biological potential of stem cells and to harness their capability for tissue formation (in vitro and in vivo) one needs to establish native-like signaling [1–3].

The design of sophisticated cellular microenvironments – with colocalization of constituent cells and the application of biophysical forces mediating tissue development – is rapidly gaining attention of researchers in the fields of stem cells and regenerative medicine. Predictable regulation of cell differentiation and assembly remains a fundamental requirement for studying the developmental processes in tissues and organs. During native development, a complex and functional three-dimensional structure is created as a result of coordinated sequences of events that instruct the cells when, where, and how to differentiate. These

G. Vunjak-Novakovic (✉)
Department of Biomedical Engineering, Columbia University, 622 West 168th Street, Vanderbilt Clinic, Room 12-234 New York, NY 10032, USA
e-mail: gv2131@columbia.edu

S. Gerecht (ed.), *Biophysical Regulation of Vascular Differentiation and Assembly*, Biological and Medical Physics, Biomedical Engineering,
DOI 10.1007/978-1-4419-7835-6_9,

events need to be understood before researchers can use the acquired knowledge to harness the potential of stem cells [1–3].

Some of the critically important biological cues that guide the development of functional tissues include (1) matrix architecture along with the surface topology encountered by the cells, (2) chemical signals (in most cases presented as spatial and temporal gradients surrounding the cells), and (3) combinations of physical factors (hydrodynamic shear, mechanical compression or stretch, and electrical signals) exerted on the cells [1, 2].

To utilize the full potential of stem cells, one or more aspects of the dynamic, three-dimensional native milieu needs to be reconstructed. This provides engineers with the challenge of devising and applying state-of-the-art technologies capable of providing biologically sound, sophisticated "niches" for stem cells, that are equally important for engineering large functional tissue grafts for implantation and in vitro platforms with microtissues. In vitro platforms can be used for the screening of cells, drugs, and biomaterials, and thereby support the development of novel therapies that extend beyond the field of regenerative medicine.

In recent years, tissue engineers are increasingly learning from tissue development and regeneration. Tissue development (from the initial fusion of cells to a fully matured organism) provides them with the blueprints needed to create functional tissues starting from a pluripotent cell stage and ending with a multicellular tissue [1]. In contrast, tissue regeneration describes the responses of mature mammalian tissues employing adult stem cells, progenitor cells, and fully differentiated cells working together to alleviate scar tissue formation or to heal a wound. Both events make use of the ability of certain cells to differentiate into specific lineages to create or repair a tissue. Furthermore, the identification and replication of biophysical forces that are present during tissue development and regeneration provide critical information for designing bioreactors that recreate some aspects of the environments found in vivo. The advanced bioreactors we have today could help better understand tissue formation and ultimately exploit the knowledge gained for therapeutic purposes [1, 2].

Novel cell culture technologies mimic with a constantly improving fidelity the native microenvironments found in vivo while decreasing the volume (and thereby the cost) of the cell and tissue culture media needed [1–20]. The miniaturization of bioreactors is an important step toward achieving accurate control of the biophysical forces exerted on the cultured cells while increasing the throughput of conditions that can be studied. The logic is rather simple and based on the established bioengineering principles for living systems: the shorter the distance, the shorter is the time constant for mass transport and signaling, and the faster and more accurate the environmental control.

Miniaturization of bioreactors also helps minimize the amounts and cost of the media and growth factors, and thereby, allows experimentation with large numbers of variables and sample sizes for increased parameter space and statistical significance. Technologies such as cell patterning provide researchers with precise control over the topology of culture substrate and cell placement.

Spatial distributions of cells and matrix components are critical for proper tissue development and function. Other technologies such as microfluidic platforms have been optimized to operate with small mass transport distances in order to enable precise maintenance of microenvironmental conditions and fast cell responses to external stimuli. Microbioreactors can incorporate shear stresses normally acting upon the cells in contact with flow of body fluids, to more accurately mimic the in vivo biophysical conditions. Also, miniaturized cultured systems can be designed to incorporate electrical field stimulation, another important biophysical stimulus present during physiological function of excitable cells such as cardiomyocytes [1–21].

In this chapter, we focus on current microtechnologies designed to mimic biophysical factors found during tissue development and regeneration and allow researcher to study the effects of such stimuli on the health and function of stem cells, in the context of their self-renewal, differentiation, and phenotype maturation. In general, stem cells are cultured in the three-dimensional context of a biomaterial scaffold, with environmental control and the application of molecular and physical regulatory factors. We describe three established microtechnologies: surface patterning, microfluidics, and electrical stimulation, and how they have been applied to study human stem cells (Fig. 9.1).

9.2 Biological Principles, Engineering Designs

Lessons learned from development can provide an appropriate biological context when designing microbioreactors. Cells in an adult organism, as well as stem cells during native development, are surrounded by multiple cell types and in most cases embedded within a highly specialized extracellular matrix (ECM) [1]. In addition, cells are often positioned closely to a vascular network providing the necessary exchange of nutrients and metabolites necessary for cell growth and maintenance.

Cell types, the structure and biomechanics of the ECM, and the vascular networks surrounding the cells all depend on the tissue type (e.g., load-bearing or metabolic) and state (e.g., development, regeneration, and disease). In all cases, cascades of tissue-specific molecular and physical regulatory factors that change spatially and temporally mediate cell fate and function. Early studies were conducted using standard well plates but the technique has serious limitations that may prevent researchers from conducting experiments under realistic conditions, and measuring readouts that are predictive of cell behavior in vivo [1, 2].

It is obvious that the biological complexity of native cell environment cannot be mimicked under standard cell and tissue culture conditions. Stem cells cultured in a well plate are attached to the growth substrate by one side of its membrane, while the other side of the membrane is exposed to culture medium. Clearly, this is an unnatural and asymmetric situation that is likely to skew cellular responses to both genetic and external signals. Moreover, the periodic change of medium results in

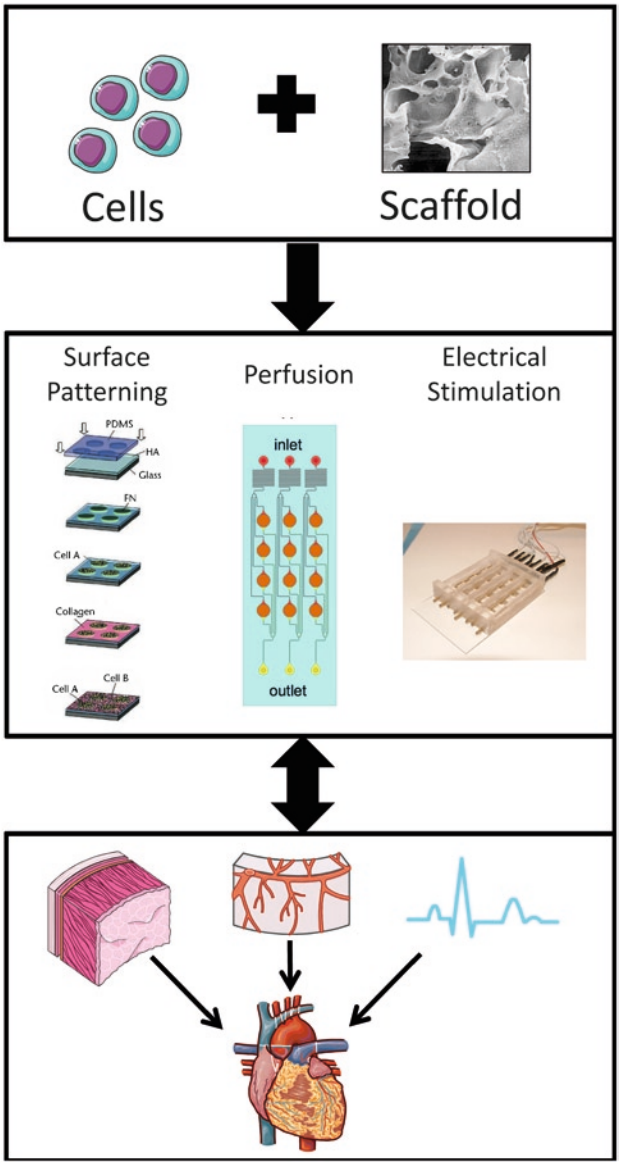

Fig. 9.1 Overall approach to tissue engineering. To unlock the full biological potential of stem cells, it is necessary to establish platforms that recreate native-like environments found in vivo. Current technologies allow the manufacture of microbioreactors able to provide different biophysical stimuli. Properties that can be engineered into microbioreactors include: surfaces with different patterns of molecules, the inclusion of perfusion during culture, and the addition of electrical stimulation during culture. The goal is to recreate environments that are present in the target tissue or organ in order to more accurately study the effects of these environments on the cells of interest. *Middle panel* images taken from Figallo et al. [16], Fukuda et al. [15], and Serena et al. [46]. *Images in the bottom panel* were produced using Servier Medical Art

constantly changing concentrations of molecular species and the depletion of nutrients and growth factors that accumulate during the culture period. Finally, physiological regulatory signals – hydrodynamic, mechanical, and electrical – are absent from static culture.

Taken together, the cell environment in static culture is distinctly different from the dynamics of the actual in vivo environment, imposing limitations to the investigation of stem cell growth and differentiation in vitro. Presumably, if much of the complex interplay of mechanical and molecular factors present in vivo is absent from culture, the cellular responses may be quite different from those expected in vivo, limiting the value, and predictability of data obtained under standard in vitro conditions.

9.2.1 Biomimetics

It is important to utilize biological information to build better systems that help scientists and engineers expand the current knowledge of the events that take place during functional tissue development. A biologically guided approach to the in vitro formation of engineered tissues is considered necessary to direct the three-dimensional (3D) organization of cells (via biomaterial scaffolds) and to establish the conditions needed to instruct the cells to form functional tissue structures (via bioreactors). This approach is based on a premise that cells respond to environmental factors in a predictable fashion and that the in vitro cell function can be modulated by mimicking the factors known to play a role during development and remodeling. In other words, the better we mimic nature during in vitro culture, the better will be our understanding of the biological processes leading to tissue formation and regeneration.

The complex cellular, biochemical, and biophysical mechanisms that take place during tissue and organ formation thus need to be recapitulated when engineered tissues are made in laboratory. This process is limited by the current knowledge regarding the combinations and timing of regulatory factors involved in cell differentiation [1, 2]. Engineers interested in developing microbioreactors for stem cells need to understand how uncommitted cells respond to external and internal signals and stressors and what important cellular biophysical interactions are needed to control cellular behavior.

9.2.2 Bioreactors

One of the most complex aspects of tissue formation that needs to be recreated in the laboratory is the topologically specific and dynamically changing three-dimensionality of tissues. Early methods for cultivating stem cells were restricted to simple two-dimensional (2D) settings, whereas in the physiological milieu, differentiation occurs

in a dynamically changing 3D environment. In recent years, researches have tried to mimic the native environment of stem cells by directing the differentiation of embryoid bodies (EBs) using 3D matrices to enhance the maintenance, proliferation, and differentiation of stem cells [1, 2, 10, 13, 17, 19, 21–23].

The material that provides the best template for the establishment of the three-dimensionality of a forming tissue is the ECM surrounding the cells. The ECM mediates the cell–cell and the cell–matrix communication by providing structural support, attachment sites, and the appropriate cues to direct the cells [1]. The composition, overall architecture, ultrastructure, and biomechanics of the ECM are responsible for the long-range mechanical stability of organized tissues, and the establishment of the appropriate stiffness and elasticity required by resident cells. Overall, the ECM is a dynamic structure that undergoes constant remodeling as part of the natural turnover of the tissues or in response to injury or a pathological state. To better understand the cell behavior in a 3D environment of the ECM, the biochemical and biophysical properties of the tissue-specific ECM need to be approximated in vitro.

9.3 Surface Patterning for Cell Coculture

Mammalian cells have been cultured in 2D settings for just over 100 years using tissue culture plastics, either plain or coated with extracts of the native matrix, feeder cells, or purified proteins. The use of 2D culture techniques resulted in seminal findings that constitute the bulk of our knowledge about stem cell biology and molecular regulation. Recent studies extended 2D culture to the use of substrates patterned on cell culture surfaces, in studies of cell renewal and differentiation as a function of substrate geometry, composition, and stiffness [23–25]. These types of experiments are pushing the boundaries of the traditional cell culture that has been focused on molecular factors, toward the inclusion of physical regulatory factors. Establishment of the relationships between the acting forces and cellular behavior open a door for new and exciting research with large implications to tissue engineering and regenerative medicine [1].

9.3.1 Adhesive Micropatterning

Modifying the substrate geometry is a relatively simple way of regulating cellular functions. Changes observed on patterned substrates may be used to study the effects of physical characteristics of the ECM (i.e., roughness, alignment, etc.) on cell migration, polarization, and other functions. The organization of topological features has been shown to have dramatic effects on cytoskeletal arrangement and focal adhesions in cultured cells [14]. For example, studies using nanopatterned substrates with varying topologies – both random and regular – promote the elongation of stem cells

and their differentiation into an osteogenic linage when compared with more structured patterns [9, 26]. The guided differentiation serves as an example of how substrate modification can be used to influence cellular function.

The shape and size of stem cell colonies can affect how cells sense biochemical signals and respond to these signals. For example, mammary epithelial cell colonies that were micromolded into collagen gels have been shown to branch out along the path of a diffusible inhibitor secreted by the cells [27]. Size can also help prolong the time of human embryonic stem cells (hESCs) in culture or guide their differentiation [10, 28]. hESCs remain in their undifferentiated state longer when cultured in three dimensional wells of a defined size [10]. The observed dependence on size can be traced back to molecular cues such as the levels of Smadl. Increases in size can be positively correlated with increases of Smadl antagonist growth diffrentiation factor-3 (GDF3). This increase occurs under constant levels of bone morphogenetic protein 2 (BMP-2) and, as a result, the level of pSmad1 decreased, while the numbers of pluripotent cell colonies increased [29].

Micropatterning in two dimensions provides many different ways to control cellular shape without the use of chemical agents. Adhesive proteins can be printed onto a substrate in a variety of sizes and shapes, to force the cells to attach and spread only over the patterned geometry. Such topological control of cell size and shape can be used to direct the cells to switch between apoptosis, proliferation, and differentiation [23, 30]. Current micropatterning technologies allow for the precise control of the contact between cells, thereby allowing researchers to distinguish between the effects of cell–cell contact and remote cell–cell communications. For example, the effects of cell–cell contact and the diffusion of molecules between hepatocytes and supportive stromal cells can be systematically interrogated using micropatterned surfaces [31]. This control can, in turn, allow researchers to determine the minimum amount of time in direct proximity necessary to maintain the hepatocyte phenotype and to optimize the effective diffusion distances of the soluble signals [31].

Another simple way of probing the interactions between two cell populations is the use of binary surface patterning [15]. As shown in Fig. 9.2 (upper panel), a nonadhesive layer is patterned on the substrate and seeded with the first cell type, which will attach only to the adhesive regions. The nonadhesive layer is then turned into an adhesive surface without affecting the cells currently attached. The second cell type is then seeded, and these cells will only attach to the remaining adhesive surface. This method allows for two different cell populations to be patterned in two dimensions with complete control over their size or shape. Cells can be distinguished by morphology or by adding a cell-membrane dye. Patterns can also be used to mimic a specific aspect of the native tissue architecture and the technique can be incorporated in a high-throughput fashion, while maintaining higher control over cell seeding distribution and spatial geometry than using random seeding methods [17].

Precise spatial control over cell adhesion and seeding patterns can be used to study the effects of cell spreading and shape on cell ultrastructure and function. For example, cultivation of mesenchymal stem cells on engineered surfaces

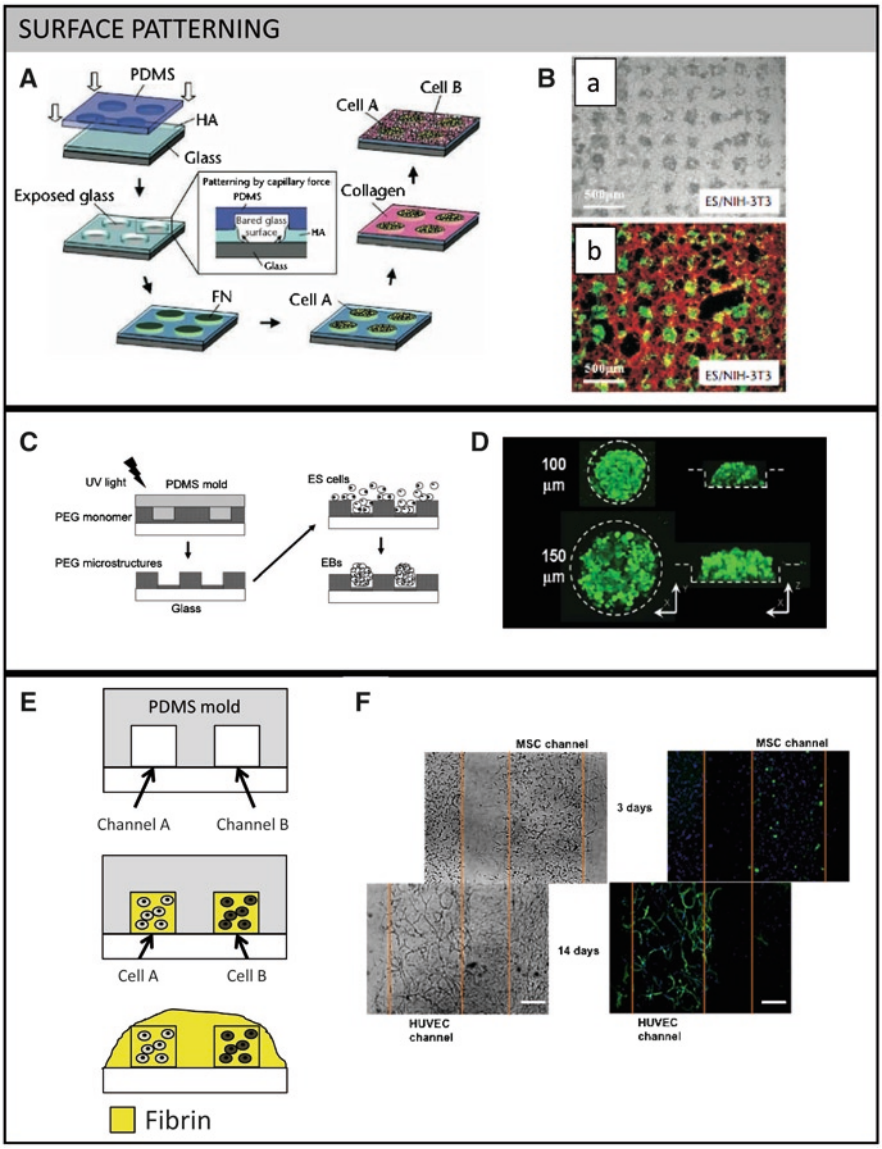

Fig. 9.2 Surface patterning of one or multiple cell types. *Upper panel:* (**A**) Schematic showing the fabrication of a coculture system using capillary force lithography and layer-by-layer deposition. This example uses a layer of hyaluronic acid sandwiched between a PDMS mold and a glass substrate. The wells created by the PDMS mold are coated with fibronectin and the HA surface is subsequently combined with collagen. The different ECM coatings select for different cell types effectively patterning the cells on the glass surface. The images on the *right* show (**B**) the cell culture of ES cells and NIH-3T3 on patterned HA/collagen surfaces (**a** and **b**) where (**b**) ES are stained *green* and NIH-3T3 in *red*. Images obtained from Fukuda et al. [15], pp. 1479–1486. *Middle panel*: (**C**) Schematic representing the fabrication of microwells using photocrossslinkable polyethylene glycol. After creating the microwells, ES cells were seeded onto the surface, allowed

enabled controlled study of shape-induced cell differentiation and cytoskeletal rearrangement [14]. Researchers found that hMSCs cultured on larger patterned islands containing adhesion ligands would preferentially differentiate into an osteogenic lineage, while cultivation of hMSCs on smaller islands resulted in preferentially adipogenic differentiation [32]. Control over cellular shape may thus play an important role in the dynamics of the cytoskeleton, with ultimate effects on overall cellular function. These findings have led researchers to speculate that RohA may regulate stem cell linage commitment and suggested that the size of the patterns could be considered when designing biomaterials for bone tissue engineering applications [32].

9.3.2 Microwells

Researchers have used PolyEthylene Glycol DiAcrylate (PEGDA) microwells to provide control over the size of the EBs, towards more homogenous size distribution in the EB population as shown in Fig. 9.2 (middle panel) [13]. The initial size of EBs was maintained for over 10 days at diameters ranging from 40 to 150 μm. The added homogeneity of size distribution contributed to the homogeneity of ES cell differentiation in EBs. The material also facilitated the removal of the EBs without affecting their size or structure promoting easy analysis, and maintaining their capacity for differentiation [13]. In this sense, the size of EBs can be correlated with a more uniform expression of cell renewal and differentiation markers. In addition, size constraint had a higher effect on self-renewal than on differentiation markers while retaining uniformity [13].

For tissue engineering purposes, the large cell numbers that are sometimes needed can limit the utility of ES-derived cells due to the associated cost and time of cell processing. Modulation of the cellular microenvironment and the restriction of the size of the EB could further help researchers manipulate cells appropriately and obtain larger numbers of cells to accommodate larger experimental groups or to engineer larger tissues. Future work may incorporate other environmental factors such as hypoxia, exogenous cytokines, and the addition of biophysical stimuli.

Fig. 9.2 (continued) to settle, and the arrays washed leaving cells inside the wells. Shown on the *right* are (**D**) confocal laser light microscopy images of the cell aggregates cultured for 5 days inside wells of different sizes. Images obtained from Karp et al. [12], pp. 786–794. *Lower panel*: Schematic (**E**) shows the fabrication of microchannels containing two cell types embedded in a fibrin matrix. A PDMS mold is used to create both channels by allowing the polymerization of the fibrin matrix containing the cells of interest. Once the cells are trapped, the PDMS mold is removed and the two channels are overlaid with additional fibrin. (**F**) Images show (light and immunofluorescence stain: α-SMA – *green* and nuclei – *blue*) the progression of cell sprouting between both channels (500 μm gap), one seeded with umbilical cord endothelial cells and the other with mesenchymal stem cells, after 3 and 14 days of culture. Images obtained from Trkov et al. [21]

9.3.3 Substrate Stiffness

Groundbreaking studies conducted in recent years have demonstrated that cell shape and cytoskeletal tension could be modulated by manipulating the stiffness of the underlying substrate [33]. Cells are sensitive enough to the substrate stiffness that the substrate can direct cell differentiation in a major way. For example, substrates with stiffness closer to the native heart tissue support cardiogenic differentiation of embryonic cardioprogenitors by providing an optimal scaffold for transmitting the contractile work, as opposed to stiffer scaffolds that resemble scar tissue after infarction and do not promote cardiogenesis [33]. The effect of stiffness has been related to cell–matrix interactions via actin-myosin motors. Integrin-based adhesion sites provide resistance to the cellular contraction leading to the recruitment of additional adhesion molecules [25, 34]. Mechanical stresses at the cellular level can also be regulated via cell–cell interactions.

Cells that are confined to a specific geometric shape and size through geometric control of the cell culture substrate proliferate in regions with high traction forces, such as the edges of circles and the corners of rectangles. This feedback loop can have an additive effect to the regulation of multiple cellular functions. Therefore, the stiffness of the substrate alone may direct cell proliferation or differentiation along a specific linage. For example, stiff substrate leads to osteogenic differentiation, medium stiffness substrate supports myogenic differentiation into muscle cells, and soft substrate leads to neurogenesis in adult human stem cells [1, 25, 34].

9.3.4 Microchannels

Miniaturization of bioreactors can also lead to experiments that look at cell–cell and cell–material interactions enabling the identification of important regulatory soluble factors, or any synergy that may result from simultaneous application of two factors [2]. For example, microfabricated structures have been used to study labeled clonal populations of neural stem cells and their progeny to investigate cellular kinetics and cell fate in real time [35]. This approach allowed researchers to track cellular differentiation in a high-throughput manner [2, 35].

A major advantage of microfabrication is the ability to substantially increase the throughput of screening studies. For example, the uses of robotic spotters that dispense and immobilize nanoliter volumes of a specific substrate to create microarrays enable researchers to study cell–matrix interaction in a large parameter space [20]. Synthetic biomaterial arrays can be used to test the effect of numerous combinations of extracellular signals on stem cell differentiation resulting in the development of novel and specialized biomaterials [19, 20]. The same approach can be used with naturally derived ECM molecules that induce and maintain cell differentiation in vitro [36]. Changes in gene expression leading to matrix synthesis and surface marker expression are often associated with cellular morphology, making cellular shape one of the most obvious indicators and regulators of cell function.

Topological features, adhesiveness, and stiffness of the cell attachment substrate can all affect the cell shape and behavior [1, 2].

Even with precise control over spatial cell distributions using micropatterning techniques, the 2D culture does not recreate the 3D environment where the cells normally reside. Soft lithography techniques can be used to generate microarray systems suitable for the study of cell–cell interactions in three dimensions. This is a relatively new technique that allows researchers to approximate the 3D nature of tissues using hydrogel constructs. One approach uses poly(ethylene glycol) methacrylate as a bioresistant, biocompatible material that can form hydrogels after photopolymerization. A small volume of hydrogel is placed on the substrate, followed by the placement of a polydimethylsiloxane (PDMS) mold, which confines the solution within a desired form. The materials are then placed into a chamber and exposed to ultraviolet light to crosslink the hydrogel. The PDMS mold is subsequently removed, leaving behind the hydrogel of the desired pattern [17].

Interactions between two cell types can also be studied using patterning technologies. Functional interactions between human mesenchymal (hMSC) and endothelial cells (hECs) have been explored using a 3D hydrogel encapsulation and microfluidic patterning. This technique allows for a precise control of the distance between the two cells of interest (in the 500–2,000 μm range). The distance separating the cells effectively varied the relative contributions of the heterotypic cell contacts and diffusing signals [21].

As shown in Fig. 9.2 (lower panel), PDMS molds can be used to pattern the 3D hydrogel (fibrin) channels with embedded cells (hMCSs and hECs). After polymerization, the PDMS mold is removed leaving hydrogel channels (with the cells encapsulated) attached to the plastic. Both channels are subsequently encapsulated in another layer of hydrogel to provide uniform and continuous matrix between the cells. Using this technique, bone marrow-derived hMSCs where shown to sprout toward the endothelial cells in a distance-dependent manner. However, the average length of sprouts was not dependent on channel-to-channel distance, suggesting that the chemotactic effects increased the numbers of migrating cells, rather than causing the existing cells to migrate over longer distances. hMSCs also formed long, highly branched, and interconnected tubular structures resembling capillary networks. Interestingly, this was not observed for umbilical cord-derived stem cells, which otherwise show many common properties with hMSCs derived from bone marrow [21].

This study showed marked differences in the localization and relative quantity of α-SMA-positive hMSCs. Staining revealed a well organized and distributed α-SMA expression at sites where endothelial cells and bone marrow mesenchymal cells were in contact, and the expression of α-SMA was not observed elsewhere. Cultures of hECs and hMSCs alone showed no α-SMA expression over 14 days in culture, suggesting that hMSCs derived from bone marrow act as pericytes, with a major role in stabilization of immature vascular networks. The coculture system could be used as a novel platform for the study of vasculogenesis. Precise control over distances and channel dimensions can provide a robust model for studying cell–cell interactions and paracrine effects due to proximity [21].

9.4 Microbioreactors with Perfusion

The maintenance of cellular microenvironment, as well as of spatial and temporal changes of molecular and physical factors, has significant effects on cellular differentiation during tissue development and regeneration. The cellular microenvironment is constantly modified by the degradation of the ECM, deposition of new molecules, secretion of cytokines by the residing cells, and cross-communication between cells via molecular and physical signals. The cell–cell and cell–matrix signaling occur in a 3D environment at different hierarchical levels, ranging from membrane channels (fast signaling over short distances) to complete organs (slower signaling over larger and more complex structures). Each level has its unique readouts that change with developmental stage and tissue maturation.

The microenvironment ("niche") surrounding a stem cell regulates and controls the cell fate and function. The stem cell niche serves as a structural template for cell attachment and tissue development (by providing the scaffolding for the cells), and a logistic template for cell differentiation and assembly (by immobilized and released cytokines that drive cellular functions). Engineering such an environment with biologically meaningful features would help researchers to understand how molecular and physical factors drive stem cell renewal and differentiation and provide the much needed tools required to harness the potential use of repair cells in regenerative medicine.

Cytokines and chemokines can be secreted by the cell itself, by neighboring cells within the same tissue, or by cells in neighboring tissues. Biochemical factors can also be immobilized within the ECM and serve as ligands for cells or can be released from the ECM as degradation products. Secreted or immobilized biochemical factors regulate cell function and tissue development independently or by acting in concert with biophysical signals. The complexity of these processes is further increased by constant changes in regulatory signals and by the effects of additional unknown factors – genetic, molecular, and physical.

Recreating the combined effects of many different types of molecules, at many different levels and timings of application, while maintaining the fidelity of their spatiotemporal occurrence and magnitude, remains a challenging task that cannot be achieved in traditional 2D culture. Recent developments in microarray and microfluidic technologies provide the means to isolate the factors of interest by superimposing other well-defined signals. Although this approach does not capture the complexity of the entire regulatory machinery, it allows researchers to study multiple mechanisms at once. In addition, the miniaturization of the technologies allows for high-throughput experimentation and screening of different combinations of factors, while providing a platform that can help to select the conditions of interest. Furthermore, these platforms could also provide tight control over the cellular environment, leading to better maintenance of cell phenotype and greater control over stem cell differentiation.

Soluble and immobilized forms of regulatory signals in vivo are often presented to the cells in the form of spatial and temporal gradients that directly or indirectly guide morphogenesis. Diffusion and adhesion of molecules provide the necessary gradients needed to drive the selective chemotactic recruitment of cells and the spatial orientation of cells in their positioning into correct anatomical locations. Microfluidic systems can be used to deliver cytokine or chemokine gradients at defined intervals and concentrations. For example, microfluidics have been used to show how neutrophils migrate along an IL-8 gradient highlighting the distinct differences in cellular responses resulting from graduate changes in concentrations. Microfluidic systems have also been used to show that cellular chemotactic responses strongly depend on the shape and magnitude of the concentration gradient profiles.

9.4.1 Microfluidic Systems

Microfluidic systems can provide testing platforms to study how gradients affect stem cell differentiation and to learn how such effects can be harnessed to control their behavior. For example, controlled gradients of growth factors have been used to guide the proliferation and differentiation of neural stem cells in vitro [37]. Other designs of microfluidic system have added an extra level of complexity by using two- and three-dimensional substrates to screen for the synergistic interactions between soluble factors and biomaterials [2]. By incorporating the most current techniques into the design and fabrication of microfluidic systems, researchers are able to mimic, with increasing fidelity, the microenvironments surrounding cells in vivo.

The use of interconnected chambers within microfluidic platforms has been proposed as a technology that allows researchers to study the effects of coculture on cellular behavior and gene expression on a microscale [22, 38]. Interconnected channels allow for the crosstalk among chambers, and subsequently among cells, since the medium flows through each chamber. If no crosstalk is desired, chambers can be selectively isolated with the implementation of an integrated valve system. However, it may be difficult to coat the surface of the chambers or to obtain an evenly seeded surface [16]. These limitations may constrain the usefulness of such devices when recreating in vivo-like conditions.

With the advances in technologies that allow greater precision and accuracy during the fabrication process, it is becoming progressively easier to use microfluidic systems in quantitative studies of cell polarity and signal propagation. Three-dimensional microfluidic systems with controlled molecular gradients have also been explored using collagen, agarose, and alginate as substrates to more accurately recreate the extracellular space [39]. Precise control over the cellular environment in a 3D structure allows researchers to recapitulate with unprecedented sophistication the environment found during tissue formation and enables studies of the mechanisms behind cellular processes.

9.4.2 Microbioreactor Arrays

In general, biomimetic systems with medium perfusion and environmental control (oxygen, nutrients, metabolites, growth factors, pH, and hydrodynamic shear) have great potential for studies of stem cell differentiation. hESCs are certainly the most challenging and highly desired cell source, suitable for use in for small-scale, high-throughput studies, as their culture and expansion require expensive media and reagents making large-scale experimentation financially prohibitive. To alleviate this limitation, researchers have developed multiplexed devices that connect microfluidic platforms with microbioreactors, allowing for quantitative analysis of hESCs cultured in 2D and 3D settings.

Microbioreactor arrays (MBA), hybrids between bioreactors and microfluidic systems, represent a new class of devices that combine the individuality of culture wells with the individual perfusion of medium. MBAs merge the high-throughput character of small well plates with the mechanical and mass transport properties of perfusion bioreactors providing high performance and accurate control over the cellular microenvironment. MBAs share many properties with other microfluidic platforms such as low-medium usage, inexpensive fabrication, compatibility with standard microscopes, and the capacity for high-throughput yield. Also, MBAs allow for the easy translation of existing protocols to the use of liquid handling-robotic systems to further automate the process [2, 16, 18].

hESC culture requirements center around the ability of these to differentiate into any cell lineage, which is the very feature that describes a stem cell and makes it very difficult to control in culture. The differences in serum from batch to batch and the poorly defined constituents within each batch could introduce significant variability making reproducibility more difficult. The environment that dictates the fate and function of hECs is influenced by the local density of the cells, clustering of colonies, and by the uptake and diffusion of factors in the medium. MBAs fill the current need for a platform that can modulate the hESC niche either by manipulating the diffusional layer or by controlling transport and accumulation of factors [18].

There are many different fabrication techniques that can be used to make MBAs as shown in Fig. 9.3 [16]. For example, soft lithography has been used to fabricate a 12-channel MBAs with the footprint of a microscope slide, meeting the following design criteria [16]:

1. A set of independent chambers in each bioreactor, while maintaining high-throughput and low consumption of medium, cells, and substrates.
2. Ability to culture cells in either 2D or 3D settings, for prolonged periods of time.
3. Reproducibility of steady-state levels of cell density, medium composition, oxygen levels, pH, flow regime, shear stress, and mass transport.
4. Accuracy of the environmental parameters, over time, in each well, and from one well to another.
5. Automated quantification of cell proliferation and differentiation using image analysis.

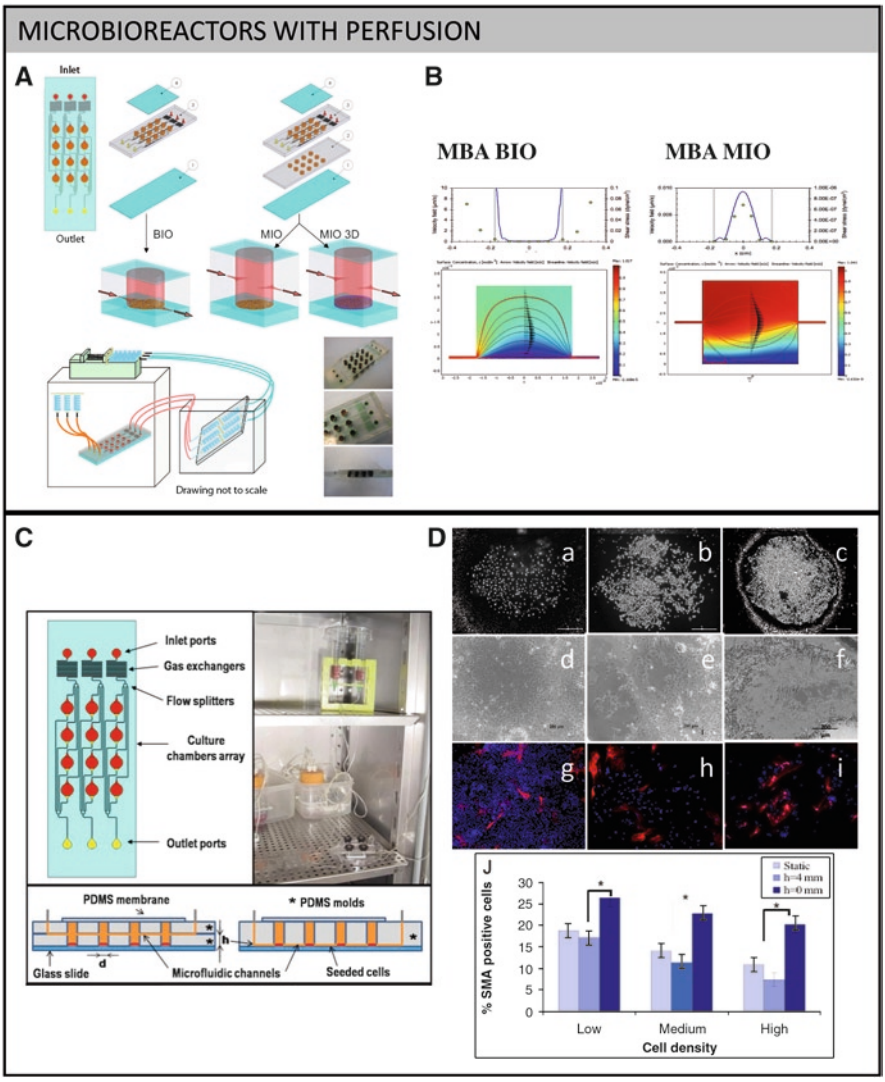

Fig. 9.3 Microbioreactors with perfusion. *Upper panel*: (**A**) Schematic of a microbioreactor array (MBA) arranged in a 4 × 3 array (3.5 mm in diameter, 8 mm vertical, and 7 mm horizontal center-to-center spacing). The array can be made in two configurations: bottom inlet/outlet (BIO) and middle inlet/outlet (MIO). (**B**) Top graphs show the fluid velocity in the plane 50 μm above the cell culture surface (*blue line*) and shear stresses along the centerline (*circles*) for both configurations. *Bottom graphs* show the spatial distributions of oxygen concentrations (*color map*), fluid velocity (*arrows*), and velocity streamlines (*lines*) for both configurations. Images taken from Figallo et al. [16]. *Lower panel*: (**C**) Shows another schematic of a microbioreactor array. It also shows a lateral view to clarify the differences in the configurations available. (**D**) Images show the effect of cell density and transport regime on cell morphology and differentiation. First row (**a**–**c**) shows bright-field images of the culture wells with three different cell densities (60, 160, and 314 cells/well, respectively). The second row and third row show phase contrast and fluorescence images of: static (nonperfused) bioreactors (**d** and **g**), low-shear bioreactor (**e** and **h**), and high-shear bioreactor (**f** and **i**). The graph (**j**) shows the fraction of cells expressing smooth muscle actin (SMA) under these conditions. Images taken from Cimetta et al. [18]

Each channel is 100 μm × 100 μm in cross section and designed to provide the appropriate gas exchange by equilibration of the three inlet streams of medium. The streams are then divided into four equal parts resulting in a 12-chamber culture system. This results in three inlet/outlet ports and three four-way splitters directing the flow with a constant pressure drop and fluid velocity in each chamber. To mimic the ECM surrounding the cells, a photopolymerizing hydrogel can be added to the surface or used to encapsulate the cells. The resulting matrix with a thickness of 200–500 μm is ideal for efficient mass transfer between the cells and the medium flow, while providing three-dimensional scaffolding for the cells [16].

The MBAs can be configured with the inlet and outlets located at the bottom of the device (BIO: *Bottom Inlet and Outlet*) or in the middle plane (MIO: *Middle Inlet and Outlet*) with medium flowing over the cells in a monolayer or encapsulated in hydrogel matrix. By changing the system's geometry (depth of the culture well) and flow regime, the hydrodynamic shear acting on the cells can be modulated over a wide range of values [16].

Modeling of steady-state conditions in the MBAs showed uniform pressure distribution within the chamber and the largest pressure drop occurring at the inlet and outlet. The fluid velocity is also uniform and low among all of the chambers with both configurations operating at low shear (Fig. 9.3, upper panel). There was a clear difference in the fluid velocity and hydrodynamic shear between the two microbioreactor array configurations.

Semiquantitative analyses of the mass transport of oxygen and albumin showed the differences between the two molecules within each configuration. The boundary layer thickness and the mass transport coefficient were lower in the BIO configuration when compared with the MIO. The MIO also showed a diffusion dominated mast transport, while convection played a larger role in the BIO configuration. These differences highlight the flexibility brought by the use of MBAs when it comes to experiments that require fine control over mass transfer properties [16].

hESCs cultured in perfused MBAs were shown to achieve high viability, with the most positive effect on hESCs cultured in a 3D setting, presumably due to enhanced mass transport. MBAs were used to monitor the differentiation of hESCs using live imaging, and automated image analysis routines to track cytoplasmic and nuclear differentiation markers.

In one study, hESCs were differentiated into vascular cells by the addition of vascular growth factor resulting in extensive sprouting and α-SMA expression. A quantitative correlation has been established between the density of hESCs and their differentiation into vascular lineages, based on the expression of smooth muscle actin. Furthermore, hESCs showed higher levels of vascular differentiation in the BIO configuration, consistent with the role of hydrodynamic shear upon stem cell differentiation (Fig. 9.3, lower panel). In all configurations, expression of α-SMA increased exponentially with a decrease in cell density, while the expression of Oct4 was not dependent on cellular density [16].

9.5 Microbioreactors with Electrical Stimulation

The importance of biophysical stimuli on stem cell differentiation has been previously established [40–42, 46]. Electric fields can be found during embryonic development, wound healing, and tissue regeneration in the extracellular space and/or within the cell itself. Electric fields (EFs) play an important role in the spatial and temporal formation of the developing embryo by providing the necessary signals to establish the correct anatomical location of tissues.

Applied electric fields have been shown to influence directional cell migration (galvanotaxis), calcium and sodium ion fluxes, and localization of receptors on the cellular membrane such as epithelial growth factor [43–45]. Electric fields can also promote differentiation of stem cells when applied exogenously during culture, although the exact mechanisms involved are currently unknown.

Recent studies show that human embryonic stem cells respond to electrical field stimulation [46]. This raises an interesting possibility that the differentiation of hES and iPS cells could be mediated by molecular and electrical signals.

The bioreactor for electrical stimulation of human EBs was built on a glass slide for optical transparency using stereolithography into a 4×4 PDMS well configuration (wells measuring 5 mm×5 mm) (Fig. 9.4, upper panel). Electrodes are placed within the chambers 5 mm apart and connected to an electrical stimulator generating a monophasic square wave pulse. EBs were cultured with a field pulse of 1 V/mm and a duration of 1 or 90 s. A nonpolar and nonfluorescent compound that readily diffuses into the cell and rapidly oxidizes into a fluorescent molecule was used to measure intracellular reactive oxygen species (ROS) activity. ROS generation was higher on electrically stimulated EBs than unstimulated EBs with the largest difference observed 5 min after applying the EF (Fig. 9.4, lower panel), and ROS was also increased when the pulse duration was increased from 1 to 90 s [46].

Mouse embryonic stem cells have also been shown to differentiate into cardiogenic and vasculogenic lineages when exposed to EFs [47]. A possible explanation for this effect may be the generation of (ROS) typically generated during the metabolism of oxygen and found to increase during the stimulation of EBs [47]. ROS can inhibit gene expression and affect growth and differentiation of many types of cells. ROS can also activate mitogen-activated protein kinase (MAPK) enhancing angiogenesis via the activation of ERK1,2 and JNK. In addition, ROS has been implicated in the regulation of cardiogenesis and cardiogenic repair via the phosporylation of ERK1,2, JNK, and p38 [48–51].

ROS signaling is an important component that regulates cell proliferation, DNA damage and cell aging, but their production and the mechanisms behind their effects remain largely unknown. Exogenous electrical stimulation does not affect EBs viability even after 4 days in culture. Electrode–electrolyte interface

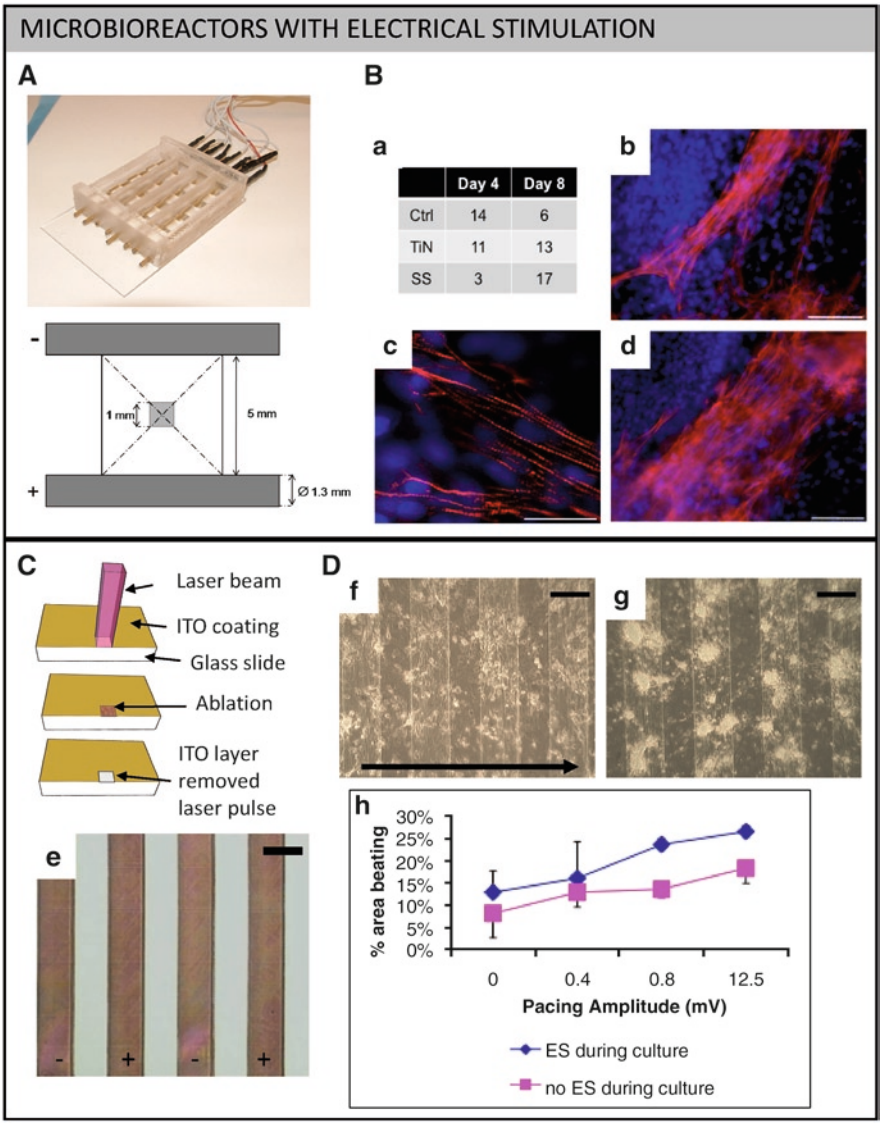

Fig. 9.4 Microbioreactors with electrical stimulation. *Upper panel*: (**A**) Picture and schematic of the mold and PDMS bioreactor with electrodes spaced 5 mm apart. (**B**) The maximum percentage of beating EBs (**a**) that were electrically stimulated at day 4 and 8 with titanium nitride (TiN) or stainless steel (SS) electrodes (controls were not treated). Images show the effect of electrical stimulation on cardiomyocytes differentiation (**b**–**d**) (cardiac troponin T). Taken from Serena et al. [46]. *Lower panel*: (**C**) Schematic of the indium-tin-oxide patterned substrate using laser ablation process. Below is a close-up image of the patterned electrode array (**e**) with 200 μm electrodes and 200 μm spacing in between. *Right panel* shows bright-field images (**D**) of neonatal rat cardiac cells after 4 days of culture with stimulation (**f**) and without (**g**) stimulation (scale bar = 200 μm). *Arrow* shows the direction of the applied field. The graph (**h**) shows the percent area beating per well for cardiac cells cultured with (*blue*) or without (*pink*) electrical stimulation. Images taken from Tandon et al. [5]

characterization found the highest rate of ROS generation using stainless steel electrodes during a 90 s signal and for 4-day-old EBs. This stimulation regime corresponded to EBs incubation in the presence of 1 nM H_2O_2. Spontaneous contractions and expression of troponin T and sarcomeric organization suggested that the EBs differentiated along the cardiac linage as a result of electrical stimulation (Fig. 9.4, upper panel). Electrical stimulation increased ROS production over time, with the highest level found after 8 days of stimulation, suggesting that the effects of electrical stimulation are more pronounced at the earlier stages of development [46].

Gold nanoparticles (20 nm) have been used to promote stem cell differentiation by delivering electrical stimulation in vitro. Culture dishes were continuously coated with fibronectin-coated gold nanoparticles using a layer-by-layer system and seeded with hESCs. Following seeding and culture on the coated surfaces, hESCs were shown to no longer express Oct-4 following electrical stimulation, while collagen type I and CBFA1 (osteogenic markers) expression increased [52]. In separate studies, a modified parallel-plate bioreactor was designed and built to direct current EFs deliver DC to seeded human adipose-derived stem cells [6]. Salt bridges delivered the electrical current and the cells were stimulated continuously for 2 or 4 h at a constant 3 mA under standard culture conditions. Cells were evaluated by morphometric analysis, immunohistochemistry, and RT–PCR analysis.

Cellular orientation began to increase after 2 h of stimulation with cells favoring a perpendicular direction to the applied electrical field. After 4 h of stimulation, the hASCs became highly aligned toward the perpendicular direction with signs of elongation. hASC showed upregulation of CX-43, VEGF, and FGF after 2 h and VEGF and ThB after 4 h [6]. Overall, electrical stimulation favored vasculogenic differentiation as indicated by the upregulation of ThB, VEGF, and FGF. Furthermore, the lack of PPAR-gamma expression suggests that the hASCs may be differentiating down an adipogenic linage. Cells do upregulate Cx-43 during the first 2 h of stimulation but show disassembled gap junctions. After 4 h of stimulation, PNF gene expression was downregulated [6].

Interestingly, DC resulted in disassembly of gap junctions and actin fibers, concurrent with cell alignment and elongation. Given that these cells reorient and migrate in the electrical field as they change their morphology, gap junctional rearrangements could back-regulate the transduction of the electric field stimulus, and cell motility and realignment might mitigate effects from the applied electric field. Longer experiments may provide further insights into cell responses to the DC field in terms of reestablished cell–cell communications and reorganization. Also, treating cells with actin antagonists [54] or gap junctional blockers [53] or studying cell behavior after cessation of electrical stimulation might be an interesting direction of future research.

The development of microscale systems would allow for high-throughput screening of electrical stimulation regimes by varying parameters such as amplitude, frequency, signal duration and shape, and spatial variance [5]. To this end, Indium Tin Oxide (ITO) was shown to provide a viable alternative to traditional electrodes because of its excellent electrical conductivity, optical transparency, and

the ability to be micropatterned on to a surface allowing for better spatial control of the electrical field through the cells. The apparent stability and cytocompatibility of ITO make it ideal for use in microbioreactors and it has already found uses in biosensing, as stimulation and recording electrodes, and electrode arrays for dielectrophoretic cell patterning [5].

A novel and biocompatible microbioreactor array has been described in which the culture surface was micropatterned with ITO resulting in an interdigitated array of electrodes designed specifically for the stimulation of cultured cells (shown in Fig. 9.4, lower panel). Using laser ablation, a microscopy compatible surface with interdigitated ITO electrodes printed on the surface is generated for long-term, microscale stem cell stimulation. Electrical impedance spectroscopy was used to characterize different geometries and regimes and computational modeling of the ITO surfaces showed constant electric fields between the electrodes close to the cells [5].

hASCs culture in the ITO microbioreactor array showed enhanced proliferation, elongation, and reorientation of cells perpendicular to the applied electric field. Also, the cells showed higher number of Cx-43-composed gap junction. Several types of ion channels have been found in hACS that are likely targets of the electrical field: channels for a delayed rectifier-like K^+ current, a Ca^{2+}-activated K^+ current, a transient outward K current, and also a TTX-sensitive transient inward sodium current [6]. Future work should focus on dissecting which ion channels are responsible for the effect of electrical fields on stem cell differentiation [6]. The ability to modulate cell alignment and connectivity by electrical signals would be a valuable tool for tissue engineering applications.

9.6 Summary

The last decade brought about the development of a new generation of culture systems of high-biological fidelity that are finding application in fundamental biological research, engineering of functional tissue grafts, and studies of disease. These engineering designs are inspired by “biomimetics” – an approach that aims to recapitulate in vitro some of the native cellular milieu associated with tissue development and regeneration in vivo.

Ideally, a culture system for human stem cells – embryonic or adult – should provide physical regulatory signals acting in concert with molecular factors, in form of spatial and temporal gradients designed to mimic the cellular environments encountered in vivo. It is clear that highly sophisticated environments, in which cells establish dynamic relationship with matrix and other cells, are enabling the levels of control not achievable in the past.

The microbioreactor platforms described here integrate geometric patterning, medium perfusion, and electrical stimulation with the molecular regulatory factors, within culture settings specifically designed to meet multiple needs of the cultivation of human stem cells. Miniaturization of the individual culture spaces enables experimentation within a large parameter matrix, with sample sizes necessary for

statistical significance, and minimal consumption of cells, substrates, and culture media. These systems, in their present designs and future incarnations, could provide basis for directed differentiation of embryonic and adult human stem cells and the subsequent maturation of cell phenotypes. Most importantly, the "biomimetic" designs of these systems can increase the relevance of cell responses for eventual application in vivo, and thereby enhance translation of fundamental research into regenerative medicine therapies.

Acknowledgements We gratefully acknowledge research support of NIH (R01 HL076485, R01 DE16525 , P41-EB002520 to GVN), and the NIH Postdoctoral Fellowship (to DF, from T 32 HL087745).

References

1. Freytes, D.O., L.Q. Wan, and G. Vunjak-Novakovic, *Geometry and force control of cell function*. J Cell Biochem, 2009. **108**(5): pp. 1047–58.
2. Burdick, J.A. and G. Vunjak-Novakovic, *Engineered microenvironments for controlled stem cell differentiation*. Tissue Eng Part A, 2009. **15**(2): pp. 205–19.
3. Godier, A.F., et al., *Engineered microenvironments for human stem cells*. Birth Defects Res C Embryo Today, 2008. **84**(4): pp. 335–47.
4. Villa-Diaz, L.G., et al., *Microfluidic culture of single human embryonic stem cell colonies*. Lab Chip, 2009. **9**(12): pp. 1749–55.
5. Tandon, N., et al., *Surface-patterned electrode bioreactor for electrical stimulation*. Lab Chip, 2010. **10**(6): pp. 692–700.
6. Tandon, N., et al., *Alignment and elongation of human adipose-derived stem cells in response to direct-current electrical stimulation*. Conf Proc IEEE Eng Med Biol Soc, 2009: pp. 6517–21.
7. Tandon, N., et al., *Electrical stimulation systems for cardiac tissue engineering*. Nat Protoc, 2009. **4**(2): pp. 155–73.
8. Radisic, M., et al., *Cardiac tissue engineering using perfusion bioreactor systems*. Nat Protoc, 2008. **3**(4): pp. 719–38.
9. Oh, S., et al., *Stem cell fate dictated solely by altered nanotube dimension*. Proc Natl Acad Sci USA, 2009. **106**(7): pp. 2130–5.
10. Mohr, J.C., J.J. de Pablo, and S.P. Palecek, *3-D microwell culture of human embryonic stem cells*. Biomaterials, 2006. **27**(36): pp. 6032–42.
11. Khademhosseini, A., et al., *Microfluidic patterning for fabrication of contractile cardiac organoids*. Biomed Microdevices, 2007. **9**(2): pp. 149–57.
12. Karp, J.M., et al., *A photolithographic method to create cellular micropatterns*. Biomaterials, 2006. **27**(27): pp. 4755–64.
13. Karp, J.M., et al., *Controlling size, shape and homogeneity of embryoid bodies using poly(ethylene glycol) microwells*. Lab Chip, 2007. **7**(6): pp. 786–94.
14. Gerecht, S., et al., *Hyaluronic acid hydrogel for controlled self-renewal and differentiation of human embryonic stem cells*. Proc Natl Acad Sci USA, 2007. **104**(27): pp. 11298–303.
15. Fukuda, J., et al., *Micromolding of photocrosslinkable chitosan hydrogel for spheroid microarray and co-cultures*. Biomaterials, 2006. **27**(30): pp. 5259–67.
16. Figallo, E., et al., *Micro-bioreactor array for controlling cellular microenvironments*. Lab Chip, 2007. **7**(6): pp. 710–9.

17. Eng G, Radisic M, and Vunjak-Novakovic G. Controlling cellular microenvironment. *Microdevices in Biology and Medicine*, (Ed. S. Bhatia and Y. Nahmias), Series on Methods in Bioengineering (Editors in Chief M Yarmush and R. Langer), Artech House, Chapter 10, 2009, pp. 211–234.
18. Cimetta, E., et al., *Micro-bioreactor arrays for controlling cellular environments: design principles for human embryonic stem cell applications*. Methods, 2009. **47**(2): pp. 81–9.
19. Anderson, D.G., et al., *Biomaterial microarrays: rapid, microscale screening of polymer-cell interaction*. Biomaterials, 2005. **26**(23): pp. 4892–7.
20. Anderson, D.G., S. Levenberg, and R. Langer, *Nanoliter-scale synthesis of arrayed biomaterials and application to human embryonic stem cells*. Nat Biotechnol, 2004. **22**(7): pp. 863–6.
21. Trkov, S., et al., *Micropatterned three-dimensional hydrogel system to study human endothelial-mesenchymal stem cell interactions*. J Tissue Eng Regen Med, 2010. **4**(3): pp. 205–15.
22. Khademhosseini, A., et al., *Cell docking inside microwells within reversibly sealed microfluidic channels for fabricating multiphenotype cell arrays*. Lab Chip, 2005. **5**(12): pp. 1380–6.
23. Chen, C.S., et al., *Geometric control of cell life and death*. Science, 1997. **276**(5317): pp. 1425–8.
24. Engelmayr, G.C., Jr., et al., *Accordion-like honeycombs for tissue engineering of cardiac anisotropy*. Nat Mater, 2008. **7**(12): pp. 1003–10.
25. Discher, D.E., D.J. Mooney, and P.W. Zandstra, *Growth factors, matrices, and forces combine and control stem cells*. Science, 2009. **324**(5935): pp. 1673–7.
26. Dalby, M.J., et al., *The control of human mesenchymal cell differentiation using nanoscale symmetry and disorder*. Nat Mater, 2007. **6**(12): pp. 997–1003.
27. Nelson, C.M., et al., *Tissue geometry determines sites of mammary branching morphogenesis in organotypic cultures*. Science, 2006. **314**(5797): pp. 298–300.
28. Mohr, J.C., et al., *The microwell control of embryoid body size in order to regulate cardiac differentiation of human embryonic stem cells*. Biomaterials, 2010. **31**(7): pp. 1885–93.
29. Peerani, R., et al., *Niche-mediated control of human embryonic stem cell self-renewal and differentiation*. EMBO J, 2007. **26**(22): pp. 4744–55.
30. Dike, L.E., et al., *Geometric control of switching between growth, apoptosis, and differentiation during angiogenesis using micropatterned substrates*. In Vitro Cell Dev Biol Anim, 1999. **35**(8): pp. 441–8.
31. Evans, A.R., et al., *Laminin and fibronectin modulate inner ear spiral ganglion neurite outgrowth in an in vitro alternate choice assay*. Dev Neurobiol, 2007. **67**(13): pp. 1721–30.
32. McBeath, R., et al., *Cell shape, cytoskeletal tension, and RhoA regulate stem cell lineage commitment*. Dev Cell, 2004. **6**(4): pp. 483–95.
33. Engler, A.J., et al., *Embryonic cardiomyocytes beat best on a matrix with heart-like elasticity: scar-like rigidity inhibits beating*. J Cell Sci, 2008. **121**(Pt 22): pp. 3794–802.
34. Discher, D.E., pp. Janmey, and Y.L. Wang, *Tissue cells feel and respond to the stiffness of their substrate*. Science, 2005. **310**(5751): pp. 1139–43.
35. Tourovskaia, A., X. Figueroa-Masot, and A. Folch, *Differentiation-on-a-chip: a microfluidic platform for long-term cell culture studies*. Lab Chip, 2005. **5**(1): pp. 14–9.
36. Flaim, C.J., S. Chien, and S.N. Bhatia, *An extracellular matrix microarray for probing cellular differentiation*. Nat Methods, 2005. **2**(2): pp. 119–25.
37. Chung, B.G., et al., *Human neural stem cell growth and differentiation in a gradient-generating microfluidic device*. Lab Chip, 2005. **5**(4): pp. 401–6.
38. Thompson, D.M., et al., *Dynamic gene expression profiling using a microfabricated living cell array*. Anal Chem, 2004. **76**(14): pp. 4098–103.
39. Choi, N.W., et al., *Microfluidic scaffolds for tissue engineering*. Nat Mater, 2007. **6**(11): pp. 908–15.
40. Trollinger, D.R., R.R. Isseroff, and R. Nuccitelli, *Calcium channel blockers inhibit galvanotaxis in human keratinocytes*. J Cell Physiol, 2002. **193**(1): pp. 1–9.
41. Mycielska, M.E. and M.B. Djamgoz, *Cellular mechanisms of direct-current electric field effects: galvanotaxis and metastatic disease*. J Cell Sci, 2004. **117**(Pt 9): pp. 1631–9.

42. Djamgoz, M.B.A., et al., *Directional movement of rat prostate cancer cells in direct-current electric field: involvement of voltagegated Na+ channel activity*. J Cell Sci, 2001. **114**(Pt 14): pp. 2697–705.
43. Puceat, M., et al., *A dual role of the GTPase Rac in cardiac differentiation of stem cells*. Mol Biol Cell, 2003. **14**(7): pp. 2781–92.
44. Puceat, M., *Role of Rac-GTPase and reactive oxygen species in cardiac differentiation of stem cells*. Antioxid Redox Signal, 2005. **7**(11–12): pp. 1435–9.
45. Sachinidis, A., et al., *Cardiac specific differentiation of mouse embryonic stem cells*. Cardiovasc Res, 2003. **58**(2): pp. 278–91.
46. Serena, E., et al., *Electrical stimulation of human embryonic stem cells: cardiac differentiation and the generation of reactive oxygen species*. Exp Cell Res, 2009. **315**(20): pp. 3611–9.
47. Sauer, H., et al., *Effects of electrical fields on cardiomyocyte differentiation of embryonic stem cells*. J Cell Biochem, 1999. **75**(4): pp. 710–23.
48. Sorescu, D. and K.K. Griendling, *Reactive oxygen species, mitochondria, and NAD(P)H oxidases in the development and progression of heart failure*. Congest Heart Fail, 2002. **8**(3): pp. 132–40.
49. Sauer, H., et al., *Role of reactive oxygen species and phosphatidylinositol 3-kinase in cardiomyocyte differentiation of embryonic stem cells*. FEBS Lett, 2000. **476**(3): pp. 218–23.
50. Heng, B.C., et al., *Strategies for directing the differentiation of stem cells into the cardiomyogenic lineage in vitro*. Cardiovasc Res, 2004. **62**(1): pp. 34–42.
51. Chen, K., L. Wu, and Z.Z. Wang, *Extrinsic regulation of cardiomyocyte differentiation of embryonic stem cells*. J Cell Biochem, 2008. **104**(1): pp. 119–28.
52. Woo, DG, et. al. *The effect of electrical stimulation on the differentiation of hESCs adhered onto fibronectin-coated gold nanoparticles. Biomaterials*, 2009. 30(29):pp.5631–8.
53. Radisic, M., et al., *Functional assembly of engineered myocardium by electrical stimulation of cardiac myocytes cultured on scaffolds*. Proc Natl Acad Sci USA, 2004. **101**(52): pp. 18129–34.
54. Finkelstein, E., et al., *Roles of microtubules, cell polarity and adhesion in electric-field-mediated motility of 3T3 fibroblasts*. J Cell Sci, 2004. **117**(Pt 8): pp. 1533–45.

Chapter 10
Effects of Hemodynamic Forces on the Vascular Differentiation of Stem Cells: Implications for Vascular Graft Engineering

Rokhaya Diop and Song Li

10.1 Introduction

Vascular tissue engineering is an active area of research because of the need for alternatives to native veins and arteries for vascular surgery. The use of autologous veins for vascular surgery is limited by the availability of healthy blood vessels and poor long-term patency [1]. The drawbacks associated with synthetic and allogeneic grafts include thrombosis, rejection, chronic inflammation, and poor mechanical properties. Synthetic vascular grafts have been constructed from a wide range of biomaterials: polyethylene terephthalate [2], expanded poly-tetrafluoroethylene [3], polyglycolic acid or poly-L-lactic acid [4], silk fibroin [5], polyurethane [6], among others. However, synthetic vascular grafts are associated with a high incidence of thrombosis and occlusion when the diameter of the graft is <5 mm. The development of nonimmunogenic, nonthrombogenic, and mechanically stable vascular grafts requires cell sources that are expandable and scaffold materials that will mimic the structure of native human blood vessels [7]. In this chapter, we focus on potential cell sources for vascular tissue engineering.

10.2 Blood Vessels and Vascular Cells

The wall of blood vessels is made up of three layers. Each of the three layers confers specific functional properties to blood vessels. The innermost layer is a single layer of endothelial cells (ECs), which prevents spontaneous blood clotting in the vessel and regulates the transport between the blood and the tissue. Vascular cells are continuously subjected to mechanical forces due to the pulsatile

S. Li (✉)
Department of Bioengineering, University of California, B108A Stanley Hall, Berkeley, CA 94720-1762, USA
e-mail: song_li@berkeley.edu

S. Gerecht (ed.), *Biophysical Regulation of Vascular Differentiation and Assembly*, Biological and Medical Physics, Biomedical Engineering,
DOI 10.1007/978-1-4419-7835-6_10, © Springer Science+Business Media, LLC 2011

nature of blood flow [8, 9]. Endothelial cell function is regulated not only by chemical signals such as hormones, cytokines, and neurotransmitters, but also by mechanical stimulation (shear stress and mechanical strain generated by blood flow) [10]. In arteries, endothelial cells that line the lumen of blood vessels experience an average fluid shear stress caused by blood flow ranging between 10 and 15 dynes/cm^2 [11, 12].

The medial layer of blood vessels is composed of smooth muscle cells (SMC) and extracellular matrix (ECM) components such as collagens and elastin. The medial layer contributes to the bulk mechanical strength of the vessel as well as its ability to contract or relax in response to external stimuli. SMCs experience very low shear stress of about 1 dyn/cm^2 due to interstitial fluid flow [13]. SMCs in the media layer of the blood vessel wall also experience cyclic mechanical strain due to the pulsatility of blood flow [14]. The outermost layer is composed primarily of fibroblasts and ECM, and has microscopic blood supply as well as nerve [15].

10.3 Potential Cell Sources for Vascular Graft Engineering

Early efforts in the field of engineered vascular grafts utilized vascular cells (vascular SMCs, ECs, and fibroblasts) to recreate structures similar to human blood vessels [2, 16, 17]. The success of this approach is limited in part by the low proliferative capacity of human vascular cells. The isolation and characterization of progenitor cells as well as adult and embryonic stem cells (ESCs) opened new possibilities for engineering tissue-engineered vascular grafts. The advantage of stem cells lies in their ability to replicate indefinitely and to differentiate into multiple cell types. Progenitor cells cannot renew themselves, and usually are more specialized than stem cells in differentiation potential [18]. In this chapter, we discuss endothelial progenitor cells (EPCs), mesenchymal stem cells (MSCs), mesenchymal progenitor cells (MPCs), and ESCs. We review current research on the response of these cell types to hemodynamic forces and their use in vascular graft engineering.

10.3.1 Endothelial Progenitor Cells

EPCs represent a promising source of ECs for synthetic vascular grafts and tissue-engineered blood vessels because they can be easily isolated and possess proliferation potential [19]. EPCs originate from the bone marrow, and can be found in the bone marrow, peripheral blood, or cord blood. Upon stimulation, EPCs are released into the blood circulation and migrate to vascular regions with injured endothelia [20]. In normal adults, the concentration of EPCs in peripheral blood is very low (2–3 cells/mm^3). The concentration of EPCs in cord blood, however, is 3.5 times higher [21]. The controversy about EPCs lies in the fact that there exist multiple

phenotypic definitions for EPCs. In cell culture, there are two phenotypes of EPCs: "early EPCs" and "late EPCs." In addition to cell culture, there exist different methods to identify EPCs by markers such as CD133, CD34, CD31/PECAM-1, and vascular endothelial cadherin (VE-cadherin) [22, 23].

10.3.2 Mesenchymal Stem Cells

MSCs are multipotent stem cells that can be isolated from various adult tissues. Although bone marrow is the most abundant source of MSCs, these cells are also found in muscle, fat, dermis, peripheral blood, and cord blood. MSCs have been shown to differentiate into adipocytes, chondrocytes, osteoblasts, and vascular SMCs [24]. The differentiation of MSCs can be directed by different growth factor combinations. Supplementing the basal culture medium with dexamethasone, ascorbate, and β-glycerophosphate induces differentiation into osteoblasts. Supplementing with TGF-β_3, dexamethasone, and ascorbate induces chondrogenic differentiation while dexamethasone and hydrocortisone will induce myogenic differentiation [25]. Adipogenic induction requires the addition of h-insulin, dexamethasone, indomethacin, and IBMX [26]. There is also evidence that the addition of vascular endothelial growth factor (VEGF) induces differentiation toward an endothelial phenotype [27].

Human MSCs derived from bone marrow can be expanded without losing their multipotency [24]. Although no single cell surface marker for MSCs exists, they are in general positive for STRO-1 (a stromal cell surface antigen), CD105 [endoglin, receptor for transforming growth factor-β (TGF-β) and integrins], CD29 (integrinβ_1), CD44 (receptor for hyaluronic acid and matrix proteins), and CD166 (a cell adhesion molecule), and negative for CD14 (monocyte surface antigen), CD34 (HSC surface antigen), and CD45 (leukocyte surface antigen) [9].

MSCs do not express the major histocompatibility complex II (MHC II) antigens that are responsible for immune rejection. MSCs are therefore a good cell source for allogeneic cell transplantation [28]. MSCs offer a great potential for tissue engineering applications. However, the molecular mechanisms governing renewal and differentiation of MSCs as well as the effects of mechanical stimulation on MSC function are not fully understood.

10.3.3 Embryonic Stem Cells

ESCs are isolated from the inner cell mass of the blastocyst. ESCs are characterized by their unlimited proliferative potential and their ability to differentiate into all cell types of the body [29]. ESCs offer an excellent cell source for tissue regeneration and cell therapy. However, the use of ESCs for tissue engineering applications

depends on our ability to control stem cell proliferation and direct stem cell differentiation [30].

There exist differences between human and mouse ESCs. While human ESCs offer greater clinical applications, the mouse model provides significant insight into human stem cell differentiation and early human development [31]. Murine ESCs proliferate more rapidly than human ESCs in culture. The cell population doubling time is between 12 and 15 h for murine ESCs, whereas the doubling time for human ESCs is between 30 and 35 h [32]. Regardless of the species, all ESCs can maintain their pluripotency or can differentiate into any cell type depending on the culture conditions. Pluripotency makes ESCs an attractive option for tissue engineering applications and cell therapy for human diseases.

In vitro ESCs are cultivated on a feeder layer of embryonic fibroblasts to maintain an undifferentiated phenotype. The addition of leukemia inhibitory factor (LIF) to the culture medium can also prevent the differentiation of ESCs, thus eliminating the need for feeder cells [33]. Several feeder-free culture systems have been developed and are now commercially available. Pluripotent ESCs are characterized by a high expression of endogenous alkaline phosphatase and telomerase. While human ESCs express the surface marker stage-specific cell embryonic antigen (SSEA)-3/4, murine ESCs express the stage-specific embryonic antigen SSEA-1. The maintenance of pluripotency in ESCs requires the expression of transcription factors such as Oct-3/4, Nanog, and Rex-1 [34]. ESC differentiation is initiated in the absence of transcription factor Oct-4 [32], a feeder layer or LIF.

When ES cells are cultured in suspension, they form embryoid bodies and replicate the early stages on embryonic development. These embryoid bodies contain differentiated cells from all three germ layers: the endoderm, ectoderm, and mesoderm [35]. Growth factors, cell-to-cell interactions, and differential access to nutrients all play a role during the differentiation process [36]. Murine ESCs can form both simple and cystic embryoid bodies. Human ES cells can only form cystic embryoid bodies.

Growth factors and chemical compounds are commonly used to direct the differentiation of ES cells. The addition of VEGF to the Flk1-positive cultures promotes endothelial differentiation, whereas mural cells are induced by platelet-derived growth factor (PDGF)-BB [37]. Pancreatic endocrine insulin-expressing cells were derived from undifferentiated ES cells by sequential addition of retinoic acid and sodium butyrate. Meanwhile, sequential addition of retinoic acid and betacellulin (BTC) or activin A yielded neuronal and glial-like cell types [36]. Another approach to direct differentiation is by genetic modification, which includes both the suppression and the overexpression of genes. However, this approach involves the use of viral vectors, which are unsafe for clinical applications [32].

During the process of differentiation, soluble factors, mechanical forces, and ECM all contribute to stem cell fate. To predictably direct ESC differentiation, a better understanding of the effects of each factor is necessary. In this section, we focus on the effects of hemodynamic forces (shear stress and mechanical strain) on stem cell differentiation.

10.4 Effects of Fluid Shear Stress on Stem Cells

Mechanical forces can be converted to biochemical signals which modulate differentiation and proliferation in stem cells (Fig. 10.1). Shear stress is known to activate signaling pathways on the apical surface of the cell through a thin layer of carbohydrate-rich heparan sulfate glycosaminoglycans (HSPGs) known as the glycocalyx [38]. Shear stress is also sensed on the basal surface of the cell through focal adhesions complexes. The mechanical signal is converted to a biochemical signal through focal adhesions, which relay signals to the nucleus in order to induce changes in gene expression [39].

10.4.1 Effects of Shear Stress on Endothelial Progenitor Cells

EPCs represent a promising source of ECs for synthetic vascular grafts and tissue-engineered blood vessels. In 2003, Yamamoto et al. reported that human EPCs isolated from peripheral blood changed their morphology and aligned in the direction of flow after exposure to laminar shear stress (from 0.1 to 2.5 dynes/cm^2). Shear stress also increased the gene expression of EC markers: KDR, Flt-1, and VE-cadherin. In addition, laminar shear stress promoted the proliferation of EPCs by increasing cell density and the percentage of EPCs in G2-M phase. Finally, it

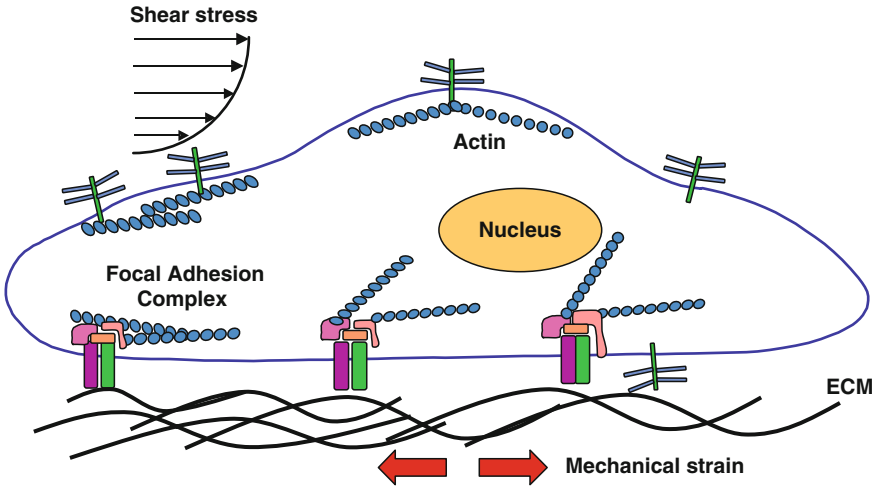

Fig. 10.1 Mechanical shear stress on the apical surface of cells and mechanical strain in ECM are converted to biochemical signals which modulate the differentiation and proliferation of stem cells. Mechanotransduction can be mediated by receptors, membrane, cytoskeleton, and focal adhesions complexes

was noted that shear stress induced the formation of tubular structures in collagen gels. This study demonstrated that EPCs were responsive to laminar shear stress and that shear stress could promote the differentiation of EPCs into mature endothelial cells [40]. A study by Ye et al. demonstrated that shear stress promoted endothelial differentiation of EPCs via activation of Akt. They showed that shear stress increased the expression of endothelial markers, CD31 and von Willebrand factor (vWF), and decreased the expression of progenitor markers, CD133 and CD34, of EPCs [41].

Furthermore, Yamamoto et al. reported that laminar shear stress promoted the differentiation of EPCs toward an arterial EC phenotype. They observed that laminar shear stress increased the gene expression of arterial endothelial markers: ephrinB2, Notch1/3, Hey1/2, and ALK1. In addition, laminar shear stress decreased the gene expression of the venous endothelial markers, EphB4 and NRP2, in a manner dependant on shear stress rather than shear rate. The study concluded that shear stress increased ephrinB2 gene expression by activating the transcription factor Sp1. The mechanism by which laminar shear stress activates SP1 is still unknown [10].

Most recently, Brown et al. showed that late outgrowth umbilical cord blood EPCs (CB-EPCs) were functionally similar to human aortic endothelial cells (HAECs) under flow conditions. CB-EPCs expressed less endothelial nitric oxide synthase protein than HAECs but nitric oxide (NO) levels were not significantly different after exposure to shear stress [19].

Two studies by Yang et al. corroborated the conclusion that shear stress (within physiological range) could improve the antithrombogenic potential of human EPCs isolated from peripheral blood [42]. The group demonstrated that shear stress helped prevent thrombosis by promoting prostaglandin I_2 (PGI_2) secretion and by inhibiting plasminogen activator inhibitor-1 (PAI-1) secretion by human EPCs [43].

10.4.2 Effects of Shear Stress on Mesenchymal Stem Cells

MSCs could be a potential source for vascular tissue engineering. Several studies have shown that MSCs are responsive to fluid shear stress, but the results are not conclusive. While, most studies have focused on differentiation toward the osteogenic lineage [44–46], few studies have concentrated on the effects of fluid shear stress on MSC differentiation into vascular cell types.

Glossop et al. investigated the effects of different profiles of fluid shear stress on mitogen-activated protein kinase (MAPK) signaling pathways. These pathways are known to play an important role in cellular mechanotransduction. It was found that fluid shear stress induced global changes in gene expression. In addition, independent of the magnitude and the duration of exposure, fluid shear stress caused a consistent upregulation of MAP3K8 and IL1B. The study suggests that shear stress activates different MAPK signaling pathways by the induction of MAP3K8 in human bone marrow-derived MSCs (hMSCs) [47].

In another recent study, Bassaneze et al. used a cone plate viscometer system to expose human adipose tissue-derived mesenchymal stem cells (hASC) to a shear stress of 10 dynes/cm^2 for up to 96 h. They reported that fluid shear stress did not induce the expression of EC markers (Flk-1, vWF, and CD31). In addition, no changes in cell morphology and alignment were observed. They concluded that shear stress alone could not induce the differentiation of hASC into endothelial cells. They observed, however, that fluid shear stress stimulated VEGF and nitric oxide (NO) production in hASC [48].

Bai et al. also reported that laminar shear stress alone did not promote the differentiation of rat MSCs toward the endothelial phenotype. A parallel-plate flow chamber system was used in this study. It was found that the addition of VEGF was required to promote endothelial differentiation. Without the addition of VEGF, increasing the magnitude and the duration of cellular exposure to laminar shear stress decreased the differentiation of rat MSCs toward the endothelial lineage. In this study, MSCs were isolated from rat femurs and rat tibias [49].

In a three-dimensional study, however, Dong et al. showed that in vitro shear stress increased the expression of EC markers (PECAM-1, VE-cadherin, and CD34) while decreasing smooth muscle-related markers [smooth muscle myosin heavy chain (SMMHC), smooth muscle α-actin (SMA), and calponin]. In the study, canine MSCs were seeded in tissue-engineered vascular grafts made with polycaprolactone and lactic acid. MSCs were subjected to pulsatile fluid flow in a bioreactor for 4 days [50]. These conflicting results may be due to difference between cell lines and other important factors such as surface topology, surface rigidity, and the composition of the ECM as well as the presence of various soluble factors.

In addition to MSCs isolated from various tissues, there are studies on a cell line C3H 10T1/2 (10T1/2). These murine MPCs are multipotent and have been shown to differentiate into muscle, fat, cartilage, and bone cells [51–53]. In 2005, Wang et al. reported that fluid shear stress could induce C3H10T1/2 cells to differentiate into ECs. In their study, they used a parallel-plate system to expose these cells to a laminar fluid shear stress of 15 dynes/cm^2 for up to 12 h. They observed that laminar shear stress induced the expression of EC markers (CD31, vWF, and vascular endothelial cadherin) both at the RNA and protein levels. Shear stress also induced the uptake of acetylated low-density lipoproteins and the formation of tubular structures on Matrigel. This study also demonstrated that laminar shear stress caused the downregulation of growth factors associated with SMC differentiation [54]. Further studies showed that a laminar fluid shear stress of 15 dynes/cm^2 inhibited TGF-β_1 signaling by downregulating TGF-β_1, TGF-βR, Smad2, Smad3, and Smad4 mRNA production in murine MPCs. The group also found that shear stress caused the upregulation of Smad7 mRNA levels. This study concluded that shear stress could induce differentiation toward the endothelial lineage by suppressing TGF-β_1 signaling in the C3H10T1/2 cell line [55].

Regarding to other lineages, McBride et al. reported that fluid shear stress caused the upregulation of genes associated with the early stages of musculoskeletal development (Runx2, collagen I-a1, Sox9, and collagen II-a1). However, fluid shear stress induced no changes in markers for terminal differentiation such as aggrecan

(chondrogenesis), PPARG-γ2 (adipogenesis), and Osx (osteogenesis). They found that the duration of exposure to fluid shear stress plays a more important role in the differentiation of MPCs than shear stress magnitude. In combination with shear stress, factors such as cell seeding density also plays a significant role in the modulation of gene activity during the early stages of musculoskeletal development [56].

10.4.3 Effects of Shear Stress on ESCs

During embryonic development, ESCs are exposed to mechanical forces, such as cyclic strain and shear stress but much remains to be elucidated about the role of fluid forces in ES cell differentiation [57, 58]. In addition, mechanical factors could be used in combination with biochemical factors to direct ESC differentiation.

Several studies have investigated the effects of fluid shear stress on ESCs. The majority of these studies have focused on the effects of shear stress on VEGF-R2 positive (Flk1$^+$) cells derived from ESCs. The emerging consensus suggests that shear stress induces the differentiation of Flk1$^+$ cells toward the EC phenotype [6, 37, 59–65]. Interestingly, it was also reported that the mere addition of VEGF to the Flk1$^+$ cultures promotes endothelial differentiation, whereas mural cells are induced by PDGF-BB [37].

Illi et al. showed that laminar shear stress of 10 dynes/cm^2 can promote the differentiation of mouse ESCs toward cardiovascular precursors [65]. They found that cardiovascular markers were upregulated up to 24 h after exposure to shear stress: Flk-1, PECAM-1, SMA, smooth muscle protein 22 (SM-22α), myocyte enhancer factor-2C (MEF2C), and sarcomeric actin. It was found that shear stress activated transcription from the Flk-1 promoter. Although the study reported that laminar shear stress caused epigenetic chromatin remodeling at several sites in histones H4 and H3, a causal link between histone modification and genetic reprogramming in ESC has yet to be established. Zeng et al. described that the Flk-1–PI3K–Akt pathway played an important role in the differentiation of mouse ESCs toward ECs [62]. They proposed that laminar flow activated Flk-1 and PI3K–Akt pathway which, in turn, activated the histone deacetylase 3 (HDAC3). HDAC3 deacetylates p53, leading to p21 activation and in stem cell differentiation into ECs. The study also suggested that chromatin modification by HDAC3 might play an important role in the regulation of gene transcription and the process of differentiation.

Yamamoto et al. reported that laminar shear stress (1.5–10 dynes/cm^2) promoted the differentiation of mouse ESCs-derived Flk-1$^+$ cells toward a vascular endothelial lineage [61]. They found that shear stress induced the expression of the vascular EC markers: VEGF receptor-1 (Flt-1), VE-cadherin, and PECAM-1. However, shear stress did not induce the expression of markers for SMCs, blood cells, or epithelial cells. In addition, after exposure to laminar shear stress, Flk-1$^+$ cells were able to form more tubular structures in collagen gel than static controls. Finally, the study proposed that shear stress may promote the proliferation and vascular differentiation of Flk-1$^+$ cells through a ligand-independent activation of

Flk-1. Later, this group found that shear stress plays a role in the arterial and venous endothelial specification in Flk-1$^+$ cells [59]. They postulated that shear stress increased the arterial differentiation of mESCs through the VEGF-Notch signaling pathway. They noted that shear stress increased the expression of EphrinB2 mRNA while decreasing the mRNA level of EphB4 (a venous EC marker). This effect was reversible and depends on the level and the duration of exposure to shear stress. Further, the group showed that shear stress induced a ligand-independent activation of Flk-1 which caused the activation of Notch signaling further downstream.

Interestingly, Adamo et al. showed that exposing Flk-1$^+$ cells to laminar fluid shear stress for 48 h increases the number of PECAM-1-positive cells and enhanced hematopoietic differentiation [63, 64]. They also found that laminar shear stress caused the upregulation of the transcription factor Klf2, a mechano-activated gene in ECs [63, 64].

10.5 Effects of Mechanical Strain on Stem Cells

Cells that reside in the vascular wall experience mechanical strain due to the pulsatile nature of blood flow (Fig. 10.1). Several studies have shown that mechanical strain can induce stem cell differentiation and changes in cell morphology [66–72]. The effects of mechanical strain on stem cell differentiation depend on the several factors which include: magnitude, duration, frequency, whether loading is applied in cycles or in a single step and also the direction in which loading is applied (uniaxial, biaxial, equiaxial, or anisotropic) (Fig. 10.2). In addition, effects may vary if mechanical strain is applied in two dimensions (2-D) or in three-dimensions (3-D). Previous work mainly focused on the effect of mechanical strain on MSCs and ESCs.

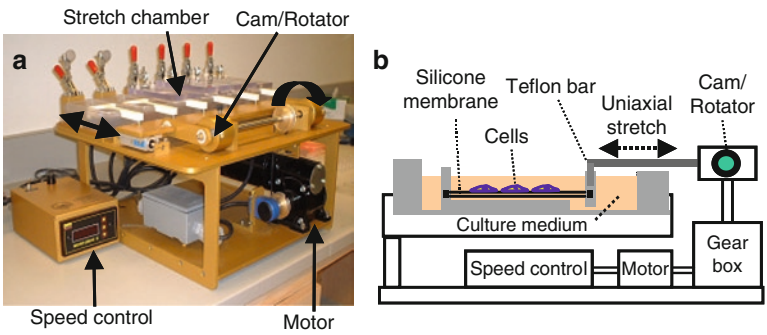

Fig. 10.2 An example of mechanical stretch device. (**a**) A custom-made uniaxial stretching apparatus. (**b**) Schematic drawing of the stretching apparatus. Cells are grown on a silicon membrane. The silicon membrane is stretched in one direction by a Teflon bar controlled by a rotational cam

10.5.1 Effects of Mechanical Strain on Mesenchymal Stem Cells

In 2-D culture systems, tensile strains higher than 3% cause MSCs to differentiate toward a cardiovascular cell phenotype. Notably, it was shown that tensile strains lower than 3% in magnitude induced MSC differentiation toward the osteogenic lineage [48–52]. Although several studies demonstrated that cyclic compression induced chondrogenesis in MSCs of rat and human origin [73–76], Kobayashi et al. showed that compressive strain increased the expression of SMMHC in rat bone marrow stromal cells [66].

Hamilton et al. and Park et al. both demonstrated that uniaxial strain induced early stage marker of SMCs [69, 77]. In addition, Park et al. showed that different modalities of strain had different effects in human MSCs. Cyclic equiaxial strain decreased SMA and SM-22α expression in MSCs as well as SMA in stress fibers. In contrast, cyclic uniaxial strain produced a transient upregulation of the genes for collagen 1, SMA, and SM-22α. The expression of SMA and SM-22α returned to basal levels after the cells aligned in the direction perpendicular to strain. These results suggest that equiaxial and uniaxial strain have differential effects on MSC differentiation [69]. A study by Ghazanfari et al. also demonstrated that cyclic strain promoted the differentiation of MSCs to SMC phenotype without the addition of growth factors.

A newer technique utilizes microgrooves that are oriented parallel to the axis of strain to keep cells aligned in the direction of uniaxial strain [67]. MSCs stimulated with uniaxial cyclic tensile strain on these membranes remained oriented with the strain axis, which led to a decrease in cartilage and bone markers and at least partial differentiation toward a vascular SMC phenotype over the course of several days.

In a 3-D study by Liao et al., human MSCs seeded in collagen, and fibrin gel tubular constructs were subjected to 10% cyclic strain at 1 Hz. Results indicated that cyclic strain increased the gene expression of two smooth muscle markers, SMA and SM-22α, suggesting the differentiation of MSCs into a SMC phenotype [68].

In addition to MSCs, cyclic strain changes the alignment and the morphology of murine MPC line (C3H/10T1/2). After exposure to cyclic strain, the expression of SMA and SMMHC increased significantly both at the mRNA level and at the protein level (compared with static controls) [70].

10.5.2 Effects of Mechanical Strain on Embryonic Stem Cells

Saha et al. described that while cyclic biaxial mechanical strain (>10%) increased the proliferation of human ESCs, it inhibited their differentiation in conditioned medium. This inhibition could not be explained by the secretion of growth factors in the surrounding medium. Interestingly, mechanical strain could not inhibit human ESC differentiation in unconditioned medium. It was concluded that mechanical strain must act synergistically with soluble factors to regulate ESC

differentiation [78]. A follow-up study by the same group showed that the activation of Smad2/3 by TGF-β family ligands is necessary to inhibit ESC differentiation under strain. They hypothesize that cyclic biaxial mechanical strain may induce autocrine or paracrine signaling by increasing the transcription of TGF-β1, Activin A, and Nodal [79].

In the case of mouse ESCs, Schmelter et al. proposed that static mechanical strain induced cardiovascular differentiation by activating reactive oxygen species (ROS) [80]. ROS were generated by membrane-bound NADPH oxidase that was upregulated after exposure to mechanical strain. ROS subsequently initiated intracellular signaling through ERK1, 2, JNK, and p38. These signaling pathways are important in vasculogenesis and in cardiomyogenesis.

More recently, Shimizu et al. showed that cyclic uniaxial strain promotes the differentiation of Flk-1$^+$ mouse ESC toward SMC lineage [58]. They reported a dose-dependent increase in SMC markers, SMA and SMMHC, both at the protein and the mRNA level in response to cyclic uniaxial strain. In contrast, they noted a decrease in the expression of vascular EC marker, Flk-1, and no change in the expression of other endothelial markers.

10.6 Use of Stem Cells in Vascular Graft Engineering

The aim of vascular graft engineering is to create a functional conduit that allows the unobstructed flow of blood. Several options are currently available for vascular replacement. It is not uncommon to use autologous vascular tissue from patients such as the greater saphenous vein or the radial artery. In addition, vascular allografts and xenografts are used but complications often occur due to immune rejection, inflammation, and thrombosis. A promising alternative to autografts and allografts is to create vascular conduits using biocompatible polymer scaffolds and appropriate stem cells.

In early attempts to engineer vascular conduits, vascular cells (SMCs, ECs, and fibroblasts) were seeded onto scaffolds or into hydrogels to recreate structures similar to human blood vessels [2, 16, 17]. However, the use of vascular cells to engineer vascular graft faces several limitations. First, autologous vascular cells have to be harvested from the patient. This requires that the patient is healthy enough to withstand invasive surgery and that the patient has healthy blood vessels to provide a sufficient number of cells. Second, vascular cells harvested from the patient have limited proliferative capacity. Because stem cells can self-renew indefinitely and they have the potential to differentiate into specific cell type in the body, stem cells represent an ideal cell source for vascular tissue engineering.

Several studies have attempted to engineer vascular conduits using MSCs. In an in vivo study, Hashi et al. seeded MSCs in small-diameter vascular grafts made from electrospun poly-L-lactic acid nanofibers [81]. They showed that MSCs had antithrombogenic property and improved the long-term patency of the vascular grafts. After 2 months, MSC-seeded grafts had organized layers of ECs and SMCs

similar to native arteries. Mirza et al. also showed that MSCs had a positive effect on in vivo endothelialization in rats and MSCs partially differentiated into SMCs [82]. Brennan et al. demonstrated that bone marrow mononuclear cell-seeded vascular grafts had 6-month patency in a lamb model [83].

In an in vitro study, Gong and Niklason reported that they had successfully engineered small-diameter vascular grafts from hMSCs seeded in polyglycolic acid (PGA) mesh scaffolds. Using a biomimicing system, they exposed vascular constructs to 5% cyclic strain for up to 8 weeks. They noted that the morphology and histology of the engineered vessel wall was similar to that of native vessels. However, they indicated that more work is necessary to improve the mechanical properties and the endothelialization of the engineered vessels [84]. In a more recent study, Harris et al. demonstrated that adipose-derived mesenchymal stem cells (ASCs) are a potential cell source for vascular grafts. ASCs seeded into vascular grafts differentiated toward a smooth-muscle phenotype as shown by the upregulation of calponin, caldesmon, and SMMHC [85]. Although more work needs to be done, the studies mentioned above are examples among many that provide strong evidence that MSCs are a promising cell source for vascular graft engineering.

In addition to MSCs, a great deal of research has been dedicated to improving endothelialization in vascular conduits. In early studies, endothelial cells were used to minimize the risk of thrombosis [16, 86–92]. In recent years, however, more attention has being given to EPCs because of their ease of isolation. Several studies have indicated that EPCs can be utilized to create a function endothelial layer for vascular conduits.

EPCs isolated from sheep peripheral blood were shown to provide a nonthrombogenic luminal surface when implanted in decellularized porcine iliac arteries. The EPC-seeded grafts remained patent up to 130 days. Vascular grafts seeded with EPCs remained patent 115 days longer than grafts without EPCs. In addition, grafts exhibited nitric oxide-mediated vascular relaxation comparable to native ovine carotid artery [21]. The ability of EPCs to form a nonthrombogenic surface after implantation into vascular graft was also observed with small-diameter grafts made with microporous segmented polyurethane film coated with gelatin [93].

More recently, EPCs were also used to create a functional EC layer on modified expanded poly-tetrafluoroethylene (ePTFE) vascular grafts [3, 20]. These results suggest that this methodology could be applied in vivo.

In order to improve the performance of vascular grafts, research is now focused on developing strategies to increase the mobilization and homing of EPCs to the inner surface of vascular conduits. These strategies include the use of oligosaccharides [94], peptides [95], and antibodies [96] to attract EPCs to the vascular graft surface in an effort to prevent thrombosis.

In comparison to MSCs and EPCs, there have been fewer studies aimed at creating vascular grafts from ESCs. However, some studies have shown that ESCs offer great potential for vascular graft engineering. A study by Huang et al. examined the vascular differentiation of a mixture of mouse ESCs containing about 30% $Flk1^+$ cells seeded in a microporous polyurethane tube. The compliance of the graft was

similar to the compliance of the human artery. The graft was subjected to a low pulsatile flow mimicking the wall shear stress and circumferential strain presented in the human venous system. The cells on the luminal surface reoriented in the direction of flow. While the cells at the surface became positive for PECAM-1, the cells in the deeper layer became positive for SMA. Results from this study introduced the possibility of engineering a vascular graft containing multiple vascular cell types by using ESCs [6]. The main obstacle in the use of ESCs lies in removing residual undifferentiated cells from the engineered vascular grafts. Residual stem cells inevitably lead to teratoma formation in the host. Another problem lies in the ability to guide the differentiation of ESCs toward the desired cell type with efficiency and reliability. If these difficulties can be overcome, ESCs will become an attractive option for vascular graft engineering.

10.7 Future Directions

There is substantial evidence in the published literature indicating that hemodynamic forces play a critical role in the differentiation of stem cells and progenitor cells toward vascular cell phenotypes. This research has paved the way for the use of stem cells and progenitor cells in vascular graft engineering. However, the mechanisms of how hemodynamic forces and biochemical factors work together to drive cell differentiation need to be elucidated in the future. Although considerable advances have been made in the field of vascular graft engineering, several challenges still remain. More work is needed to control the proliferation and the differentiation of stem cells. In addition, the removal of residual undifferentiated stem cells is a pivotal obstacle which must be overcome to eliminate the risk of teratoma formation. In addition to optimizing strategies for the use of stem cells and progenitor cells, success in vascular graft engineering lies in improving the quality of materials used as scaffolds and the ability to recreate an antithrombogenic endothelial lining on the luminal surface of the graft.

Acknowledgments This work was supported in part by NIH grants HL083900 (S.L.) and 1F31HL087728 (R.D.).

References

1. Galambos B, Olah A, Banga P, Csonge L, Almasi J, Acsady G. (2009) Successful human vascular reconstructions with long-term refrigerated venous homografts. Eur Surg Res; 43(3):256–261.
2. Weinberg CB, Bell E. (1986) A blood vessel model constructed from collagen and cultured vascular cells. Science;231(4736):397–400.
3. Ranjan AK, Kumar U, Hardikar AA, Poddar P, Nair PD. (2009) Human blood vessel-derived endothelial progenitors for endothelialization of small diameter vascular prosthesis. PLoS ONE;4(11):e7718.

4. Roh JD, Nelson GN, Brennan MP, Mirensky TL, Yi T, Hazlett TF, Tellides G, Sinusas AJ, Pober JS, Saltzman WM, Kyriakides TR, Breuer CK. (2008) Small-diameter biodegradable scaffolds for functional vascular tissue engineering in the mouse model. Biomaterials; 29(10):1454–1463.
5. Enomoto S, Sumi M, Kajimoto K, Nakazawa Y, Takahashi R, Takabayashi C, Asakura T, Sata M. (2010) Long-term patency of small-diameter vascular graft made from fibroin, a silk-based biodegradable material. J Vasc Surg;51(1):155–164.
6. Huang H, Nakayama Y, Qin K, Yamamoto K, Ando J, Yamashita J, Itoh H, Kanda K, Yaku H, Okamoto Y, Nemoto Y. (2005) Differentiation from embryonic stem cells to vascular wall cells under in vitro pulsatile flow loading. J Artif Organs;8(2):110–118.
7. L'Heureux N, Dusserre N, Konig G, Victor B, Keire P, Wight TN, Chronos NA, Kyles AE, Gregory CR, Hoyt G, Robbins RC, McAllister TN. (2006) Human tissue-engineered blood vessels for adult arterial revascularization. Nat Med;12(3):361–365.
8. Lehoux S, Tedgui A. (2003) Cellular mechanics and gene expression in blood vessels. J Biomech;36(5):631–643.
9. Park JS, Huang NF, Kurpinski KT, Patel S, Hsu S, Li S. (2007) Mechanobiology of mesenchymal stem cells and their use in cardiovascular repair. Front Biosci;12:5098–5116.
10. Obi S, Yamamoto K, Shimizu N, Kumagaya S, Masumura T, Sokabe T, Asahara T, Ando J. (2009) Fluid shear stress induces arterial differentiation of endothelial progenitor cells. J Appl Physiol;106(1):203–211.
11. Weinberg PD, Ross Ethier C. (2007) Twenty-fold difference in hemodynamic wall shear stress between murine and human aortas. J Biomech;40(7):1594–1598.
12. Fung YC, Liu SQ. (1993) Elementary mechanics of the endothelium of blood vessels. J Biomech Eng;115(1):1–12.
13. Wang DM, Tarbell JM. (1995) Modeling interstitial flow in an artery wall allows estimation of wall shear stress on smooth muscle cells. J Biomech Eng;117(3):358–363.
14. Yang Z, Noll G, Luscher TF. (1993) Calcium antagonists differently inhibit proliferation of human coronary smooth muscle cells in response to pulsatile stretch and platelet-derived growth factor. Circulation;88(3):832–836.
15. Niklason LE. (1999) Techview: medical technology. Replacement arteries made to order. Science;286(5444):1493–1494.
16. Niklason LE, Gao J, Abbott WM, Hirschi KK, Houser S, Marini R, Langer R. (1999) Functional arteries grown in vitro. Science;284(5413):489–493.
17. L'Heureux N, Germain L, Labbe R, Auger FA. (1993) In vitro construction of a human blood vessel from cultured vascular cells: a morphologic study. J Vasc Surg;17(3):499–509.
18. Riha GM, Lin PH, Lumsden AB, Yao Q, Chen C. (2005) Roles of hemodynamic forces in vascular cell differentiation. Ann Biomed Eng;33(6):772–779.
19. Brown MA, Wallace CS, Angelos M, Truskey GA. (2009) Characterization of umbilical cord blood-derived late outgrowth endothelial progenitor cells exposed to laminar shear stress. Tissue Eng Part A;15(11):3575–3587.
20. Allen J, Khan S, Lapidos KA, Ameer G. (2010) Toward engineering a human neoendothelium with circulating progenitor cells. Stem Cells;28(2):318–328
21. Kaushal S, Amiel GE, Guleserian KJ, Shapira OM, Perry T, Sutherland FW, Rabkin E, Moran AM, Schoen FJ, Atala A, Soker S, Bischoff J, Mayer JE, Jr. (2001) Functional small-diameter neovessels created using endothelial progenitor cells expanded ex vivo. Nat Med;7(9):1035–1040.
22. Rafii S, Lyden D. (2003) Therapeutic stem and progenitor cell transplantation for organ vascularization and regeneration. Nat Med;9(6):702–712.
23. Urbich C, Dimmeler S. (2004) Endothelial progenitor cells: characterization and role in vascular biology. Circ Res;95(4):343–353.
24. Watabe T, Miyazono K. (2009) Roles of TGF-beta family signaling in stem cell renewal and differentiation. Cell Res;19(1):103–115.
25. Gang EJ, Jeong JA, Hong SH, Hwang SH, Kim SW, Yang IH, Ahn C, Han H, Kim H. (2004) Skeletal myogenic differentiation of mesenchymal stem cells isolated from human umbilical cord blood. Stem Cells;22(4):617–624.

26. Baksh D, Song L, Tuan RS. (2004) Adult mesenchymal stem cells: characterization, differentiation, and application in cell and gene therapy. J Cell Mol Med;8(3):301–316.
27. Oswald J, Boxberger S, Jorgensen B, Feldmann S, Ehninger G, Bornhauser M, Werner C. (2004) Mesenchymal stem cells can be differentiated into endothelial cells in vitro. Stem Cells;22(3):377–384.
28. Le Blanc K, Tammik C, Rosendahl K, Zetterberg E, Ringden O. (2003) HLA expression and immunologic properties of differentiated and undifferentiated mesenchymal stem cells. Exp Hematol;31(10):890–896.
29. Yu J, Thomson JA. (2008) Pluripotent stem cell lines. Genes Dev;22(15):1987–1997.
30. Godier AF, Marolt D, Gerecht S, Tajnsek U, Martens TP, Vunjak-Novakovic G. (2008) Engineered microenvironments for human stem cells. Birth Defects Res C Embryo Today;84(4):335–347.
31. Nichols J, Ying QL. (2006) Derivation and propagation of embryonic stem cells in serum- and feeder-free culture. Methods Mol Biol;329:91–98.
32. Grivennikov IA. (2008) Embryonic stem cells and the problem of directed differentiation. Biochemistry (Mosc);73(13):1438–1452.
33. Zandstra PW, Le HV, Daley GQ, Griffith LG, Lauffenburger DA. (2000) Leukemia inhibitory factor (LIF) concentration modulates embryonic stem cell self-renewal and differentiation independently of proliferation. Biotechnol Bioeng;69(6):607–617.
34. Cormier JT, zur Nieden NI, Rancourt DE, Kallos MS. (2006) Expansion of undifferentiated murine embryonic stem cells as aggregates in suspension culture bioreactors. Tissue Eng;12(11):3233–3245.
35. Doss MX, Sachinidis A, Hescheler J. (2008) Human ES cell derived cardiomyocytes for cell replacement therapy: a current update. Chin J Physiol;51(4):226–229.
36. McKiernan E, O'Driscoll L, Kasper M, Barron N, O'Sullivan F, Clynes M. (2007) Directed differentiation of mouse embryonic stem cells into pancreatic-like or neuronal- and glial-like phenotypes. Tissue Eng;13(10):2419–2430.
37. Yamashita J, Itoh H, Hirashima M, Ogawa M, Nishikawa S, Yurugi T, Naito M, Nakao K. (2000) Flk1-positive cells derived from embryonic stem cells serve as vascular progenitors. Nature;408(6808):92–96.
38. Tarbell JM, Weinbaum S, Kamm RD. (2005) Cellular fluid mechanics and mechanotransduction. Ann Biomed Eng;33(12):1719–1723.
39. Janmey PA, Weitz DA. (2004) Dealing with mechanics: mechanisms of force transduction in cells. Trends Biochem Sci;29(7):364–370.
40. Yamamoto K, Takahashi T, Asahara T, Ohura N, Sokabe T, Kamiya A, Ando J. (2003) Proliferation, differentiation, and tube formation by endothelial progenitor cells in response to shear stress. J Appl Physiol;95(5):2081–2088.
41. Ye C, Bai L, Yan ZQ, Wang YH, Jiang ZL. (2008) Shear stress and vascular smooth muscle cells promote endothelial differentiation of endothelial progenitor cells via activation of Akt. Clin Biomech (Bristol, Avon);23 Suppl 1:S118–S124.
42. Yang Z, Tao J, Wang JM, Tu C, Xu MG, Wang Y, Pan SR. (2006) Shear stress contributes to t-PA mRNA expression in human endothelial progenitor cells and nonthrombogenic potential of small diameter artificial vessels. Biochem Biophys Res Commun;342(2):577–584.
43. Yang Z, Wang JM, Wang LC, Chen L, Tu C, Luo CF, Tang AL, Wang SM, Tao J. (2007) In vitro shear stress modulates antithrombogenic potentials of human endothelial progenitor cells. J Thromb Thrombolysis;23(2):121–127.
44. Grellier M, Bareille R, Bourget C, Amedee J. (2009) Responsiveness of human bone marrow stromal cells to shear stress. J Tissue Eng Regen Med;3(4):302–309.
45. Li D, Tang T, Lu J, Dai K. (2009) Effects of flow shear stress and mass transport on the construction of a large-scale tissue-engineered bone in a perfusion bioreactor. Tissue Eng Part A;15(10):2773–2783.
46. Knippenberg M, Helder MN, Doulabi BZ, Semeins CM, Wuisman PI, Klein-Nulend J. (2005) Adipose tissue-derived mesenchymal stem cells acquire bone cell-like responsiveness to fluid shear stress on osteogenic stimulation. Tissue Eng;11(11–12):1780–1788.

47. Glossop JR, Cartmell SH. (2009) Effect of fluid flow-induced shear stress on human mesenchymal stem cells: differential gene expression of IL1B and MAP3K8 in MAPK signaling. Gene Expr Patterns;9(5):381–388.
48. Bassaneze V, Barauna VG, Ramos CL, Kalil JE, Schettert IT, Miyakawa AA, Krieger JE. (2010) Shear stress induces nitric oxide-mediated VEGF production in human adipose tissue mesenchymal stem cells. Stem Cells Dev;19(3):371–378.
49. Bai K, Huang Y, Jia X, Fan Y, Wang W. (2009) Endothelium oriented differentiation of bone marrow mesenchymal stem cells under chemical and mechanical stimulations. J Biomech; 43(6):1176–1181.
50. Dong JD, Gu YQ, Li CM, Wang CR, Feng ZG, Qiu RX, Chen B, Li JX, Zhang SW, Wang ZG, Zhang J. (2009) Response of mesenchymal stem cells to shear stress in tissue-engineered vascular grafts. Acta Pharmacol Sin;30(5):530–536.
51. Fischer L, Boland G, Tuan RS. (2002) Wnt-3A enhances bone morphogenetic protein-2-mediated chondrogenesis of murine C3H10T1/2 mesenchymal cells. J Biol Chem;277(34): 30870–30878.
52. Taylor SM, Jones PA. (1979) Multiple new phenotypes induced in 10T1/2 and 3T3 cells treated with 5-azacytidine. Cell;17(4):771–779.
53. Singh R, Artaza JN, Taylor WE, Gonzalez-Cadavid NF, Bhasin S. (2003) Androgens stimulate myogenic differentiation and inhibit adipogenesis in C3H 10T1/2 pluripotent cells through an androgen receptor-mediated pathway. Endocrinology;144(11):5081–5088.
54. Wang H, Riha GM, Yan S, Li M, Chai H, Yang H, Yao Q, Chen C. (2005) Shear stress induces endothelial differentiation from a murine embryonic mesenchymal progenitor cell line. Arterioscler Thromb Vasc Biol;25(9):1817–1823.
55. Wang H, Li M, Lin PH, Yao Q, Chen C. (2008) Fluid shear stress regulates the expression of TGF-beta1 and its signaling molecules in mouse embryo mesenchymal progenitor cells. J Surg Res;150(2):266–270.
56. McBride SH, Falls T, Knothe Tate ML. (2008) Modulation of stem cell shape and fate B: mechanical modulation of cell shape and gene expression. Tissue Eng Part A;14(9): 1573–1580.
57. Bai H, Wang ZZ. (2008) Directing human embryonic stem cells to generate vascular progenitor cells. Gene Ther;15(2):89–95.
58. Shimizu N, Yamamoto K, Obi S, Kumagaya S, Masumura T, Shimano Y, Naruse K, Yamashita JK, Igarashi T, Ando J. (2008) Cyclic strain induces mouse embryonic stem cell differentiation into vascular smooth muscle cells by activating PDGF receptor beta. J Appl Physiol;104(3):766–772.
59. Masumura T, Yamamoto K, Shimizu N, Obi S, Ando J. (2009) Shear stress increases expression of the arterial endothelial marker ephrinB2 in murine ES cells via the VEGF-Notch signaling pathways. Arterioscler Thromb Vasc Biol;29(12):2125–2131.
60. Metallo CM, Vodyanik MA, de Pablo JJ, Slukvin, II, Palecek SP. (2008) The response of human embryonic stem cell-derived endothelial cells to shear stress. Biotechnol Bioeng;100(4):830–837.
61. Yamamoto K, Sokabe T, Watabe T, Miyazono K, Yamashita JK, Obi S, Ohura N, Matsushita A, Kamiya A, Ando J. (2005) Fluid shear stress induces differentiation of Flk-1-positive embryonic stem cells into vascular endothelial cells in vitro. Am J Physiol Heart Circ Physiol;288(4):H1915–H1924.
62. Zeng L, Xiao Q, Margariti A, Zhang Z, Zampetaki A, Patel S, Capogrossi MC, Hu Y, Xu Q. (2006) HDAC3 is crucial in shear- and VEGF-induced stem cell differentiation toward endothelial cells. J Cell Biol;174(7):1059–1069.
63. Adamo L, Naveiras O, Wenzel PL, McKinney-Freeman S, Mack PJ, Gracia-Sancho J, Suchy-Dicey A, Yoshimoto M, Lensch MW, Yoder MC, Garcia-Cardena G, Daley GQ. (2009) Biomechanical forces promote embryonic haematopoiesis. Nature;459(7250):1131–1135.
64. Parmar KM, Larman HB, Dai G, Zhang Y, Wang ET, Moorthy SN, Kratz JR, Lin Z, Jain MK, Gimbrone MA, Jr, Garcia-Cardena G. (2006) Integration of flow-dependent endothelial phenotypes by Kruppel-like factor 2. J Clin Invest;116(1):49–58.

65. Illi B, Scopece A, Nanni S, Farsetti A, Morgante L, Biglioli P, Capogrossi MC, Gaetano C. (2005) Epigenetic histone modification and cardiovascular lineage programming in mouse embryonic stem cells exposed to laminar shear stress. Circ Res;96(5):501–508.
66. Kobayashi N, Yasu T, Ueba H, Sata M, Hashimoto S, Kuroki M, Saito M, Kawakami M. (2004) Mechanical stress promotes the expression of smooth muscle-like properties in marrow stromal cells. Exp Hematol;32(12):1238–1245.
67. Kurpinski K, Chu J, Hashi C, Li S. (2006) Anisotropic mechanosensing by mesenchymal stem cells. Proc Natl Acad Sci USA;103(44):16095–16100.
68. Liao SW, Hida K, Park JS, Li S. (2004) Mechanical regulation of matrix reorganization and phenotype of smooth muscle cells and mesenchymal stem cells in 3D matrix. Conf Proc IEEE Eng Med Biol Soc;7:5024–5027.
69. Park JS, Chu JS, Cheng C, Chen F, Chen D, Li S. (2004) Differential effects of equiaxial and uniaxial strain on mesenchymal stem cells. Biotechnol Bioeng;88(3):359–368.
70. Riha GM, Wang X, Wang H, Chai H, Mu H, Lin PH, Lumsden AB, Yao Q, Chen C. (2007) Cyclic strain induces vascular smooth muscle cell differentiation from murine embryonic mesenchymal progenitor cells. Surgery;141(3):394–402.
71. Song G, Ju Y, Shen X, Luo Q, Shi Y, Qin J. (2007) Mechanical stretch promotes proliferation of rat bone marrow mesenchymal stem cells. Colloids Surf B Biointerfaces;58(2):271–277.
72. Song G, Ju Y, Soyama H, Ohashi T, Sato M. (2007) Regulation of cyclic longitudinal mechanical stretch on proliferation of human bone marrow mesenchymal stem cells. Mol Cell Biomech;4(4):201–210.
73. Pelaez D, Huang CY, Cheung HS. (2008) Cyclic compression maintains viability and induces chondrogenesis of human mesenchymal stem cells in fibrin gel scaffolds. Stem Cells Dev; 18(1):93–102.
74. McMahon LA, Reid AJ, Campbell VA, Prendergast PJ. (2008) Regulatory effects of mechanical strain on the chondrogenic differentiation of MSCs in a collagen-GAG scaffold: experimental and computational analysis. Ann Biomed Eng;36(2):185–194.
75. Campbell JJ, Lee DA, Bader DL. (2006) Dynamic compressive strain influences chondrogenic gene expression in human mesenchymal stem cells. Biorheology;43(3–4):455–470.
76. Huang CY, Hagar KL, Frost LE, Sun Y, Cheung HS. (2004) Effects of cyclic compressive loading on chondrogenesis of rabbit bone-marrow derived mesenchymal stem cells. Stem Cells;22(3):313–323.
77. Hamilton DW, Maul TM, Vorp DA. (2004) Characterization of the response of bone marrow-derived progenitor cells to cyclic strain: implications for vascular tissue-engineering applications. Tissue Eng;10(3–4):361–369.
78. Saha S, Ji L, de Pablo JJ, Palecek SP. (2006) Inhibition of human embryonic stem cell differentiation by mechanical strain. J Cell Physiol;206(1):126–137.
79. Saha S, Ji L, de Pablo JJ, Palecek SP. (2008) TGFbeta/Activin/Nodal pathway in inhibition of human embryonic stem cell differentiation by mechanical strain. Biophys J;94(10): 4123–4133.
80. Schmelter M, Ateghang B, Helmig S, Wartenberg M, Sauer H. (2006) Embryonic stem cells utilize reactive oxygen species as transducers of mechanical strain-induced cardiovascular differentiation. FASEB J;20(8):1182–1184.
81. Hashi CK, Zhu Y, Yang GY, Young WL, Hsiao BS, Wang K, Chu B, Li S. (2007) Antithrombogenic property of bone marrow mesenchymal stem cells in nanofibrous vascular grafts. Proc Natl Acad Sci USA;104(29):11915–11920.
82. Mirza A, Hyvelin JM, Rochefort GY, Lermusiaux P, Antier D, Awede B, Bonnet P, Domenech J, Eder V. (2008) Undifferentiated mesenchymal stem cells seeded on a vascular prosthesis contribute to the restoration of a physiologic vascular wall. J Vasc Surg;47(6):1313–1321.
83. Brennan MP, Dardik A, Hibino N, Roh JD, Nelson GN, Papademitris X, Shinoka T, Breuer CK. (2008) Tissue-engineered vascular grafts demonstrate evidence of growth and development when implanted in a juvenile animal model. Ann Surg;248(3):370–377.
84. Gong Z, Niklason LE. (2008) Small-diameter human vessel wall engineered from bone marrow-derived mesenchymal stem cells (hMSCs). FASEB J;22(6):1635–1648.

85. Harris LJ, Abdollahi H, Zhang P, McIlhenny S, Tulenko TN, Dimuzio PJ. (2009) Differentiation of Adult Stem Cells into Smooth Muscle for Vascular Tissue Engineering. J Surg Res;8:1–9.
86. Jarrell BE, Williams SK, Solomon L, Speicher L, Koolpe E, Radomski J, Carabasi RA, Greener D, Rosato FE. (1986) Use of an endothelial monolayer on a vascular graft prior to implantation. Temporal dynamics and compatibility with the operating room. Ann Surg; 203(6):671–678.
87. Clowes AW, Kirkman TR, Reidy MA. (1986) Mechanisms of arterial graft healing. Rapid transmural capillary ingrowth provides a source of intimal endothelium and smooth muscle in porous PTFE prostheses. Am J Pathol;123(2):220–230.
88. Pasic M, Muller-Glauser W, von Segesser L, Odermatt B, Lachat M, Turina M. (1996) Endothelial cell seeding improves patency of synthetic vascular grafts: manual versus automatized method. Eur J Cardiothorac Surg;10(5):372–379.
89. Lamm P, Juchem G, Milz S, Schuffenhauer M, Reichart B. (2001) Autologous endothelialized vein allograft: a solution in the search for small-caliber grafts in coronary artery bypass graft operations. Circulation;104(12 Suppl 1):I108–I1114.
90. Zilla P, Deutsch M, Meinhart J, Puschmann R, Eberl T, Minar E, Dudczak R, Lugmaier H, Schmidt P, Noszian I, et al. (1994) Clinical in vitro endothelialization of femoropopliteal bypass grafts: an actuarial follow-up over three years. J Vasc Surg;19(3):540–548.
91. Zilla P, Fasol R, Preiss P, Kadletz M, Deutsch M, Schima H, Tsangaris S, Groscurth P. (1989) Use of fibrin glue as a substrate for in vitro endothelialization of PTFE vascular grafts. Surgery;105(4):515–522.
92. Isenberg BC, Williams C, Tranquillo RT. (2006) Endothelialization and flow conditioning of fibrin-based media-equivalents. Ann Biomed Eng;34(6):971–985.
93. Shirota T, He H, Yasui H, Matsuda T. (2003) Human endothelial progenitor cell-seeded hybrid graft: proliferative and antithrombogenic potentials in vitro and fabrication processing. Tissue Eng;9(1):127–136.
94. Suuronen EJ, Veinot JP, Wong S, Kapila V, Price J, Griffith M, Mesana TG, Ruel M. (2006) Tissue-engineered injectable collagen-based matrices for improved cell delivery and vascularization of ischemic tissue using CD133+ progenitors expanded from the peripheral blood. Circulation;114(1 Suppl):I138–I144.
95. Taite LJ, Yang P, Jun HW, West JL. (2008) Nitric oxide-releasing polyurethane-PEG copolymer containing the YIGSR peptide promotes endothelialization with decreased platelet adhesion. J Biomed Mater Res B Appl Biomater;84(1):108–116.
96. Rossi ML, Zavalloni D, Gasparini GL, Mango R, Belli G, Presbitero P. (2009) The first report of late stent thrombosis leading to acute myocardial infarction in patient receiving the new endothelial progenitor cell capture stent. Int J Cardiol;141(1):e20–e22.

Index

S. Gerecht (ed.), *Biophysical Regulation of Vascular Differentiation and Assembly*, Biological and Medical Physics, Biomedical Engineering,
DOI 10.1007/978-1-4419-7835-6, © Springer Science+Business Media, LLC 2011